Binder jet 3D printing with recycled glass fines for circular design applications.

Ella Williams

Thesis submitted in fulfilment of the requirements for the degree of

Doctor of Philosophy

under the supervision of:
Associate Professor Stefan Lie
Roderick Walden

School of Design
Faculty of Design, Architecture and Building
University of Technology Sydney
2026

Certificate of Original Authorship

I, Ella Williams, declare that this thesis is submitted in fulfilment of the requirements for the award of Doctor of Philosophy, in the Faculty of Design, Architecture and Building at the University of Technology Sydney.

This thesis is wholly my own work unless otherwise referenced or acknowledged. In addition, I certify that all information sources and literature used are indicated in the thesis. This document has not been submitted for qualifications at any other academic institution.

This research is supported by the Australian Government Research Training Program.

Signature: Production Note:
Signature removed prior to publication.

Date: 21 January 2026

Acknowledgements

First and foremost, I would like to thank my supervisors, Associate Professor Stefan Lie and Roderick Walden, for the endless support, generosity, and expertise. I am truly grateful for all the thought and time you have devoted to this research and the confidence you have instilled in my abilities.

I would like to thank the Co-Directors of the Materials Ecologies Design Lab, Associate Professor Kate Scardifield and Associate Professor Stefan Lie. Without the space and community of this lab, this research would not have been possible. My appreciation extends to MEDL members Nahum McLean, Ben Styles, and Saul Mazabow for the fun, curiosity, and knowledge they have contributed to the process, alongside the numerous pep talks.

Thank you to Professor Tim Schork, Associate Professor Paul Nicholas, Dr. Jesse Adams Stein, Berto Pandolfo, Associate Professor Mohammed Makki, Professor Daniel Barber, Professor Anna Cristina Pertierra, and Professor Kate Sweetapple, who have all read, listened and engaged with my research over the last four years. Your perspectives and feedback have been invaluable.

Thanks to Dr Christina Houen of Perfect Words Editing for copyediting sections of the thesis after revision, according to the guidelines of the Institute of Editors (IPEd) and the university

Thank you to my friends who have patiently and encouragingly listened to my ramblings about 3D printing, glass and circular design. Your steadfast support has not gone unnoticed. To my sister, thank you for your honesty, humour, and always being in my corner. And finally, thank you to my parents for your love and encouragement. I feel so lucky to have had the opportunity to pursue this.

Table of Contents

List of Figures

Chapter 2: Literature Review

Chapter 3: Methodology

Chapter 4: Preliminary Investigation

Chapter 5: Further Prototyping

Chapter 6: Application

Chapter 7: Discussion & Conclusion

List of Tables

Abbreviations

AM	Additive manufacturing
BJT	Binder jetting
CAD	Computer-aided design
CE	Circular economy
CMC	Carboxymethyl cellulose
DED	Directed energy deposition
DIW	Direct ink writing
DLP	Digital light processing
FDM	Fused deposition modelling
HPMC	Hydroxypropyl methylcellulose
HPS	Hydroxypropyl starch
MRF	Material recovery facility
PBF	Powder bed fusion
RtD	Research through design
SD	Sustainable development
SEM	Scanning electron microscopy
SLA	Stereolithography
SLM	Selective laser melting
SLS	Selective laser sintering
TGA	Thermogravimetric analysis
TPP	Two-photon polymerisation
VTP	Vat photopolymerisation

Abstract

As linear production and consumption practices continue to devastate the environment, the need for industrial designers to develop products and services that prioritise circularity has become increasingly urgent. This research demonstrates how designers can integrate hands-on material and production knowledge into creating circular products. Specifically, it explores how 3D printing can be harnessed to transform the waste stream of glass fines. As glass can be endlessly remelted and formed into objects without impacting the material quality, it has the potential to be a key material in the circular economy. However, comingled, and highly mechanised recycling processes generate the low-value by-product of glass fines. These small particles of mixed glass cannot serve as feedstock for traditional glass production. As a result, they are currently underutilised as road base filler and pipe embedment material, terminal applications that do not take full advantage of the properties of glass.

This research presents a novel material formulation, production process and product application for transforming glass fines via binder jetting. This is an additive manufacturing method where parts are made by depositing a liquid binding agent onto a powdered material. Binder jetting can provide cost-effective customisation and allow for complex geometries to be produced without the need for support material. A four-step production process is presented in which glass fines are combined with a binder, printed, dried and then fired in a kiln. During firing, the binder burns out as the glass begins to fuse together, leaving a fused glass object that can be recycled over and over. Parts which are both waterproof and water absorbent with a porosity of approximately 14.5% can be produced by tailoring the firing schedule. This represents a new method for upcycling comingled glass fines, which maintains the inherent circularity of glass material. Additionally, it represents a method of fabricating complex glass objects that cannot be produced via traditional glass manufacturing methods.

To further demonstrate the potential of the process, a product application in the form of an evaporative cooling screen is presented. Drawing inspiration from traditional porous ceramics used for cooling, this design takes advantage of the porosity created during the binder jetting process. The porous structure allows water to permeate the surface, forming a thin film of water that evaporates and cools the surrounding air. A 1:1 scale demonstrator composed of 16 3D printed tiles illustrates how the material's potential can be harnessed alongside the benefits of binder jetting to create product applications with industrial potential.

This research contributes to the growing field of discourse at the intersection of design, circularity, 3D printing, and materials. It highlights not only the alignment of these fields but also how they can be effectively and holistically integrated. By layering the opportunities of 3D printing with circular strategies and material design practices, each of the domains informs and strengthens one another. As a result, a cohesive material, production process, and application have been developed, all grounded by circularity. This expands the scope of traditional industrial design, necessitating designers who can seamlessly navigate through different domains to embed circularity at all stages, from product development to material and production processes.

1

Introduction

1 Introduction

1.1 Background and Context

The climate crisis continues to escalate, with global emissions reaching an unprecedented high in 2023 (United Nations Environment Programme, 2024a). The prevailing 'take-make-waste' linear economic model significantly contributes to this crisis, with material production accounting for 23% of global emissions (International Resource Panel, 2020). This system, which is heavily reliant on fossil fuels for material extraction and manufacturing, demonstrates a concerning lack of long-term resource management and fosters a consumer culture in which products are discarded once they are no longer deemed necessary (Ellen MacArthur Foundation, 2019). In the last fifty years, material use has increased over three times and continues to grow by over 2.3% per year (United Nations Environment Programme, 2024b). Meaningful efforts to mitigate climate change must, therefore, include the transformation of current manufacturing processes, material choices, and consumption behaviours.

The circular economy (CE) has been positioned as a way forward. Broadly speaking, the CE is a framework for shifting the current linear model into a cyclical flow of products and materials that decouples economic growth from environmental degradation. The aim is to establish a closed loop where theoretically, waste no longer exists and the value of resources is maintained for as long as possible (Den Hollander et al., 2017). In 2013, the Ellen Macarthur Foundation published the first comprehensive report on the circular economy, highlighting the economic value lost from a consumption-based system instead of regenerative resource use (Ellen MacArthur Foundation, 2013; Schandl et al., 2020). Since this publication, interest in the CE has grown rapidly across academia, government and industry. This is reflected by an almost two-hundredfold increase in academic articles (Alcalde-Calonge et al., 2022) alongside the introduction of government policies around the globe, particularly in the European Union (European Commission, 2015) and China (Yuan et al., 2006).

Of specific importance to this dissertation is the role and responsibility of industrial designers in transitioning to the CE. Industrial designers have the power to influence how products are conceptualised, manufactured, consumed and disposed of. It has been claimed that up to 80% of the environmental impact of a product is determined in the design phase, where pivotal decisions around materials, form, functionality, production and maintenance ultimately dictate the product lifecycle (International Resource Panel, 2018). Understanding the impact of these design decisions (something which is only amplified through mass production) has led to the adoption of sustainable design approaches such as ecodesign or green design (Moreno et al., 2016). Whilst a positive step, these approaches have been criticised for being simply "less bad", attempting only to optimise the current system (McDonough & Braungart, 2002). Designing for the CE, on the other hand, asks designers to rethink the entire system, starting with the concept of a "closed loop" of resources (Den Hollander et al., 2017; Dokter et al., 2021). This presents new challenges for designers, requiring more holistic and future-oriented approaches. This includes ways of simultaneously and cohesively addressing multiple stages of a product life cycle, and considering how a product or its use may change over time (Dokter et al., 2021; Sumter et al., 2020).

As a result, the CE concept is expanding the scope of the design process and demanding new design competencies (Dokter et al., 2021; Sumter et al., 2020). One of these areas is the need for industrial designers to develop deeper knowledge of materials and production processes (De Los Rios & Charnley, 2017). As material and production choices are critical in the CE and are intimately tied to the health of our planet, designers who possess this knowledge and can collaborate across disciplines and supply chains are essential. As Bak-Andersen

(2021) argues, a design that is not informed by material realities may look attractive or be conceptually compelling, but it is unlikely to meet sustainability criteria if it was not originally designed with these considerations in mind. This aligns with the emerging field of materials design, where designers across the globe are engaging in hands-on self-production practices, developing materials themselves or adapting them for new fabrication methods (Pedgley et al., 2021). The growing interest in this field is due to both an awareness that the material is an indissoluble part of the design process and a desire to find more sustainable material solutions by discovering and experimenting with alternative sources (Clèries & Rognoli, 2021). In this way, materials design approaches have opened new ways for designers to engage with the CE, giving them greater control and opportunity to embed circularity into the material and production chain.

This approach has been further enabled by the democratisation of digital production technologies such as 3D printing (Rognoli et al., 2015; Romani et al., 2021, 2023). 3D printing (3DP) is the process of joining materials to make parts from 3D model data, usually by the successive layering of material (ISO/ASTM International, 2016). 3DP is not just one technology but refers to a family of technologies all based on the same additive principle, each with its own parameters, advantages, limitations, and associated materials. These range from widely accessible desktop machines to specialised industrial and robotic 3DP technologies. Originally developed in the 1980s, 3DP has quickly evolved from a prototyping tool into a manufacturing method for producing end parts. This shift is due to several distinct advantages of 3DP such as the ability to create complex geometries and cost-effective customisation (Ngo et al., 2018). There are also multiple advantages of 3DP in terms of environmental sustainability, including the generation of minimal waste and the ability to create structurally optimised parts. As such, there are some intrinsic features of 3DP that have seen it widely positioned as an enabler of the CE (Ferreira et al., 2021; Rosa et al., 2020; Sauerwein, 2020).

Several researchers have examined the link between 3DP and the CE (Hettiarachchi et al., 2022; Kravchenko et al., 2020; Ponis et al., 2021; Tavares et al., 2023). They have highlighted several key areas, including how 3DP can facilitate repair and maintenance practices through the on-demand printing of spare parts and can allow for the rethinking of business models with a focus on localisation, customisation and shorter supply chains (Despeisse et al., 2017). Of particular interest to this research is how 3DP can enable the CE through the use of waste materials and by-products. The distributed nature of 3DP allows for the disruption of established material value chains, creating significant opportunity to utilise localised waste (Garmulewicz et al., 2018). Globally, there are examples of designers, architects and manufacturers transforming waste products such as recycled plastics, sawdust and scrap metal into unique products via 3DP. By employing 3DP, the capabilities of the technology can be harnessed to not just 'use up' a waste stream but to open compelling application avenues. The scalability and adaptability of the technology can also contribute to greater industrial transformation, moving beyond the craft-based or experimental scale.

Despite the growing interest in the concept of the CE generally, integration into everyday design and manufacturing practices is far from realised. In fact, if you look around, very few things have genuinely been designed for circularity (Bak-Andersen, 2021). As the role of industrial designers expands to include the development and optimisation of materials and production processes, this presents new opportunities to bridge the gap between concept and practice. Furthermore, the access to and expertise in 3DP technologies that many designers have developed enables scalable and adaptable applications of novel materials to be developed. Whilst the individual role of design, materials and 3DP in the CE are individually recognised, research on the relationship between these elements remains in its infancy (Romani et al., 2021). This dissertation aims to contribute to this conversation by developing a method for transforming a specific waste stream into a circular application using 3DP.

1.2 Research Focus

As described in the previous section, this research sits at the intersection of design, materials, advanced manufacturing and the circular economy. Academic literature in this space largely sits in engineering publications looking at the characterisation of additive manufacturing (AM) materials for the CE rather than an integration of design perspectives and practices (Romani et al., 2021). As a result, there is space for research which bridges this gap, building on emerging material approaches from designers and architects who are harnessing 3DP technologies to develop materials and applications for the circular economy by translating this approach to a specific waste stream. The waste stream of interest in this study is glass fines.

As glass can be endlessly remelted and formed into objects without impacting the material quality, it has the potential to be a key material in the circular economy (Westbroek et al., 2021). However, glass recycling rates are very low, with the global average estimated at 21% (Harder, 2018). Whilst this varies significantly across countries, difficulties in the sorting of glass means a significant portion ends up in landfills. In some countries, such as Australia, the comingled and highly mechanised sorting process creates the low-value by-product of glass fines (Flood et al., 2020). These are small particles of mixed glass broken down and contaminated with other waste streams during the collection and sorting (Schandl et al., 2020). They represent 30% of all recovered glass in Australia, with approximately 193,000 tonnes of glass fines produced in 2018 (Madden & Florin, 2019). Glass fines cannot serve as feedstock for traditional glass production and as a result, they are often sent to landfill or stockpiled (Madden & Florin, 2019).

In recent years, concern over glass fines has emerged and there has been a push to find applications. A report by RMIT in 2019 pinpointed the civil sector as potentially the biggest market for raw glass fines, where they can be used in infrastructure projects as a substitute for sand and aggregate (Flood et al., 2019). This reflects recent industry practices in Australia where glass fines are used in large volumetric scales for road base filler, pipe embedment and concrete aggregate (EPA Victoria, 2019; Flood et al., 2020). While this addresses the issue of stockpiling glass fines, these applications downcycle the material, resulting in an economic loss for glass recyclers. They have also been dubbed ‘terminal uses’ as the glass can no longer be recovered (Schandl et al., 2020). Research into the current applications of glass fines also revealed the need for higher value application avenues to make the waste stream economically viable. Glass is a valuable material with high embodied energy and important properties such as hardness and chemical durability. As such, there is a significant opportunity to further utilise and upcycle glass fines in ways that take advantage of these material properties and allow them to remain recyclable.

This research demonstrates how binder jet 3DP can provide a way forward for glass fines. Binder jetting (BJT) is an additive manufacturing method in which 3D parts are made by selectively depositing a liquid binding agent onto a powdered material (ISO/ASTM International, 2016). This type of 3DP was chosen due to its powder-based nature, which means that minimal additional material processing is required, and it has almost unlimited geometric capabilities with the loose powder acting as support material. This allows for forms to be created that are difficult if not impossible to make in traditional glass manufacturing. The powder-based production also results in opaque parts. Whilst this has been positioned as a significant limitation by some researchers, here it is seen as an opportunity to develop novel material expressions and functionalities, ones that broaden the traditional perception of glass materials. Furthermore, unlike other forms of 3DP, binder jetting does not require high-powered lasers or heating elements, making it a more accessible and widely scalable technology. As a result, the advantages of BJT and 3DP more broadly, including geometric complexity, cost

effective customisation and localised manufacturing, can be harnessed not only to make use of glass fines but also to add significant value to them and open application opportunities.

In the context of the circular economy, this research presents a material formulation, a production process and a potential product application for transforming glass fines via BJT. The development of an application aims to demonstrate the potential of the material and production process, allowing the research to be presented persuasively to both academic and design communities and in a way that could lead to further commercialisation opportunities. This is important, as there is a need to ensure that circular materials and production methods are industrially scalable for more sustainable manufacturing and consumption practices to be achieved. Through extensive experimentation, an evaporative cooling screen is presented as a potential application avenue. Porous ceramic materials have been used to cool spaces for centuries, as the porous structure allows water to permeate the surface, where it creates a thin water film that can evaporate and cool the ambient air. This research applies this principle to the glass fines material, taking advantage of the inherent porosity of parts produced by BJT technologies and integrating the benefits of 3DP to increase surface area for the water to evaporate and allow for site-specific adaptability of the design.

Ensuring legitimate circularity and mitigating green washing is paramount to this research. This is particularly important, as there have been calls for more rigorous assessment criteria to measure the environmental impact of material design projects (Duarte Poblete et al., 2024). To do this, the CE principles of material and product integrity, as discussed by Sauerwein (2020) and den Hollander et al., (2017) will be employed. This refers to the extent to which a material or product remains identical to its original state over time (Den Hollander et al., 2017). Designing for material integrity involves designing and utilising materials in a way that allows for the original properties of the material to be maintained even after recycling (Sauerwein, 2020). This means that the material can be recycled over and over in a closed loop; it is not only about utilising a waste source in one loop where it can no longer be recovered. Designing for product integrity involves any measure that extends the product's life, including designing for durability, emotional attachment and repairability. This thinking will be embedded in the design of the application.

1.2.1 Research Questions

This dissertation is structured around one overarching research question with three sub-questions specific to the interrelated areas of material, production and application.

1. How can recycled glass fines be transformed into a product application using a binder jet 3D printing system that can remain in a closed circular loop?
    a. What are the requirements of a material formulation that remains circular?
    b. What are the manufacturing process steps and parameters?
    c. What product application can be developed that demonstrates the opportunities of the material and production system?

The sub-questions relate to the key areas of material, production and application. They can be seen as the threads that make up the overarching research question; they are intertwined, and one cannot be addressed without the other. A material formulation cannot be developed without a thorough understanding of the method of production. Similarly, the capabilities of the material and production system will inform the application. As a result, all three must cohesively come together and be addressed concurrently. This is a

more holistic and tailored approach where the emergent affordances of the material or production guide the application, ensuring they are well-matched. This avoids problems we have seen with materials such as plastic, where their short-term usage conflicts with their long-lasting nature.

1.3 Research Methodology

A Research through Design (RtD) methodological approach is adopted in this dissertation. This refers to the use of design practices and methods as a way of generating knowledge. As a result, prototyping is presented as the primary data collection method, with three different types of prototypes being employed to generate different types of knowledge (Wensveen & Matthews, 2014). This includes prototypes as vehicles for enquiry where the process of making the artefact is the main research contribution and is documented thoroughly. These are used to iteratively develop elements like printing parameters and material formulations. Prototypes as experimental components which are most akin to traditional scientific experiments are used to test specific hypotheses. These are used in this research to integrate materials science and engineering methods, giving validity to decisions and outcomes of the research. Then finally, towards the end of the research, prototypes as research archetypes are employed to illustrate and showcase the research and the chosen application.

The prototyping is conducted in a serial manner, whereby the knowledge generated from one prototype informs the next (Krogh & Koskinen, 2020). This builds a chain of knowledge in response to the research questions. To ensure that knowledge is captured, all prototypes are rigorously documented in reflective experimental logs, allowing for the capturing, analysis and emergence of knowledge. This RtD methodology is also informed by and tailored to a materials design project. This means that key concepts from this emerging field of design are embedded in the approach. In particular, as in many materials design projects, the material in this research serves as the starting point. Its potential is uncovered through hands-on experimentation, and novel material affordances are identified and harnessed (Barati & Karana, 2019; Karana et al., 2015).

In conducting this research, I draw on my training as an industrial designer in which the skills of prototyping, sketching, CAD modelling and conceptualising are central. I also draw on my expertise and experience as a researcher working at the intersection of materials and advanced manufacturing. Since 2020, I have investigated circular economy applications for a number of waste streams and biobased materials including various recycled plastics, recycled paper, algae biopolymers and oyster shells. This has been both in my role as a research assistant and design practitioner and has enabled knowledge of 3DP technologies, parametric design tools and materials to be developed. This prior experience has also informed the methodology, emphasising the importance of a rigorous visual documentation method to properly capture the complexity of the variables at play. It has also resulted in an understanding that the research questions must be addressed concurrently, with a balancing of priorities and a degree of adaptability.

1.4 Research Contributions

Within the context of the circular economy and the emergence of design approaches that closely integrate material and production knowledge, this research presents a method to transform the abundant yet underutilised waste stream of glass fines into circular product applications using binder jet 3DP. Through the

development and outcome of this process, several theoretical, methodological, empirical and practical contributions are made.

Firstly, the theoretical contribution of the research lies in the thorough and cohesive integration of the fields of design, circular economy, materials and 3D printing. While substantial literature and design examples exist at the intersection of two or three of these areas, there remains limited work that critically examines all four domains together. This research highlights not only why they align but how to effectively integrate them. By layering the opportunities of 3D printing with circular strategies and material design practices, each of the domains informs and strengthens one another. This has allowed for the holistic development of a material, production process and application that is underpinned by circularity. This expands the scope of conventional industrial design, asking designers to engage and embed circularity, not just at the product level, but across the material and production development as well. As a result, this research contributes to discourse that recognises the value of interdisciplinary approaches in tackling complex sustainability challenges.

Furthermore, the research contributes to the methodological development of RtD and materials design projects. As RtD can be criticised for its lack of transparency, and methodologies in materials design are still emergent, this research presents an RtD methodology that is specifically tailored to a materials-based project. This includes the employment of three forms of prototypes and a visual documentation method. The different types of prototypes facilitate the integration of materials science and engineering methods such as thermogravimetric analysis with more conventional design prototyping and iteration. This gives validity to decisions and outcomes of the research whilst still being driven by a designerly eye for application. The visual documentation method echoes this approach, capturing both quantitative data about each prototype and qualitative reflections on the process, results, and opportunities. This allows for the effective merging of the rigour associated with scientific methods—essential for traceable and repeatable material development—with the tacit knowledge or intuition that designers often use subconsciously. As a result, the research also contributes to the ongoing discussion about the role of designers in materials projects. When designers actively engage with materials from the outset of a project, affordances and opportunities that might otherwise be overlooked or mitigated can be identified and skilfully integrated into new potential applications.

The empirical contributions of the research come in the form of the novel material formulation and production process. A four-step production process is presented in which the glass fines are combined with a powdered organic binder, BJT printed, dried and then fired in a kiln. During this firing process, the binder burns out as the glass begins to fuse together, leaving a 100% fused glass object which can be recycled over and over. To validate this circularity, thermogravimetric analysis (presented in Chapter 5) was conducted. This is a widely used thermal analysis technique that monitors a sample's mass as it is heated, allowing for the compounds in the sample to be characterised based on physical or chemical changes. Parts which are both waterproof and water absorbent with a porosity of approximately 14.5% can be produced by tailoring the firing schedule. This represents a new method for the upcycling of glass fines, which allows for them to be used repeatedly, harnessing the inherent circularity of glass as a material. It also represents a new method of fabricating complex glass objects which cannot be produced via traditional glass manufacturing methods.

The practical contribution comes in the form of a product application that harnesses the capabilities of the material and production method. An evaporative cooling screen that utilises the inherent porosity of the BJT parts has been developed for application in outdoor public spaces. This is made up of individual 3D printed tiles, which are assembled into a larger screen. Whilst porosity of parts is often positioned as a barrier to application, as it can impact the mechanical properties of a part, in this research it was seen as an affordance of

the material and production process which could be exploited. A 1:1 scale demonstrator was built using the circular BJT glass fines material with a porosity of approximately 14.5%. This allows for the tiles to absorb water at a similar capacity to unglazed terracotta products which are commonly used in evaporative cooling. By developing an application and demonstrator, the potential of the research can be communicated more effectively and in a manner that resonates with industry. It also enables the generation of further knowledge, in which a better understanding of the real-world constraints involved in designing for new materials and production methods can be established. It is important to note that this is just one potential application avenue for the glass fines material and BJT production system, and other opportunities could be explored in the future.

1.5 Structure of Thesis

This dissertation is structured into seven chapters. Following this introductory chapter, Chapter 2 presents an in-depth review of the literature which underpins this research. It is broken into three sections. Firstly, the circular economy concept and its interaction with the field of design, materials and 3DP technologies is presented. This discussion provides the context and conceptual framework for this research. The next section introduces the material waste stream of glass fines. This includes providing context on glass manufacturing, recycling and the limitations in current applications of glass fines. This discussion highlights the opportunity to find higher value and circular applications for glass fines, something which can be enabled by 3DP. The final section reviews the current state of the art in glass 3DP. The opportunities and limitations of each technology are recognised, allowing for binder jetting to be identified as a technology with significant potential for the use of glass fines. This literature review led to the formulation of an overarching research question with three sub-questions related to the material, production and application.

These research questions are presented in Chapter 3 along with the methodological approach employed in this dissertation. As explained previously, a research through design methodology is applied. This chapter highlights that although RtD is an established methodology, there is no single method for its implementation. As in design practice, design researchers' processes and methods can vary greatly. As a result, this chapter clearly outlines the way RtD is employed in this research, arguing for specific methods and approaches which are relevant to this materials-based project. This includes the types of prototypes used, the documentation methods and ways of evaluating and sharing the research. Although a specific materials design methodology has not been applied, elements of this approach inform the research process; consequently, relevant approaches from the materials design field are also discussed. Finally, a research diagram is presented which encapsulates the methodology and highlights that the research is made up of three interrelated areas; material, production and application, which must come together to address the research question and produce a physical artefact which speaks to both the academic and design communities.

Chapter 4 presents the preliminary experimentation conducted in this research. It starts by introducing previous work which was completed using a robotic paste extrusion system to 3DP with glass fines. The findings and limitations of this previous work are highlighted to clarify the starting point for the research in this dissertation. Based on this, the multi-step production process is introduced; material preparation, printing, drying and firing. Then two stages of experimentation are introduced: finding the printing parameters and finding the binder formulation. These are the initial factors required to establish a process for the BJT of glass fines. In the first stage, printing parameters such as layer height, saturation and drying time are incrementally adjusted to develop a set of stable parameters that allow for the accurate printing and excavation of parts. The

second stage then focuses on optimising the binder formulation by testing several organic binders, before landing on a cold swelling hydroxypropyl starch (HPS). This chapter establishes an understanding of the variables and interrelations between the material and production system.

Chapter 5 presents further prototyping by introducing the final step in the production process, firing. This step is crucial for fusing the glass particles into usable objects and for ensuring material circularity. To validate that the HPS binder burns out during the firing process, a thermogravimetric analysis (TGA) is presented, confirming the circularity of the material. Experimentation into different forms and geometries is then presented. As glass flows when heated, this testing reveals the challenges of shrinkage and slumping of the glass in the kiln. Several typologies are examined to determine which geometries can be predictably fired. Pyramidal truss shapes showed significant potential, due to their self-supporting nature, allowing for lattice forms to be fired with minimal slumping. These lattices mark a breakthrough in recycled glass 3DP, presenting complexities not previously achieved in research studies. However, this testing shows that slumping and shrinkage are scale dependent, preventing the creation of universal rules. Instead, applications must be designed closely with the process to tailor the geometry to that function. While this may seem like a barrier, it is ideal for RtD research and parallels with the customisation capabilities of 3DP and local manufacturing in the CE. As it is known that BJT produces parts with some level of porosity, Chapter 5 concludes with an exploration of this. It is shown that both porous and waterproof parts can be created from glass fines by tailoring the firing schedule. The level of porosity is quantified via an experimental prototype, revealing new opportunities for applications.

Chapter 6 draws on the findings of the previous two chapters and outlines the development of an application that demonstrates the capabilities of the glass fines material and binder jetting process. The porosity achieved and described in the previous chapter led to an interest in whether the material could be used for the evaporative cooling of spaces, as porous ceramic has been for centuries. This harnesses a characteristic of the production process which is often positioned as a barrier. Furthermore, the complex geometries and customisation offered by 3DP can contribute to the functionality of evaporative cooling systems. Contextual information on the importance of finding more passive cooling systems for the built environment is first discussed; this includes a series of design precedents and culminates in the setting out of a design brief. The majority of the chapter then discusses the design development phase, highlighting key issues of slumping, changes in geometric typologies and assembly systems. Ridged geometries based on pyramidal structures were found to produce predictable results that were suited to evaporative cooling systems. This culminated in the development of a final prototype which presents a potential application avenue for the BJT of glass fines.

Chapter 7 concludes the research by presenting a final discussion of the findings. It begins by presenting an overview of the thesis and discussing how the research questions have been addressed. This culminates in a discussion of the theoretical, practical and methodological contributions of the research and an analysis of limiting factors. Finally, future research directions are presented in relation to the material, production, application and impact.

1.6 Conclusion

This thesis demonstrates how hands-on material and production knowledge can be integrated into the design process to embed greater circularity. This is demonstrated by the development of a method to transform the abundant yet underutilised waste stream of glass fines into a circular product application using binder jet 3DP. Employing an RtD methodology and a material formulation, the production method and product application

result in the material potential being leveraged alongside the benefits of binder jet 3DP. This results in not just 'using up' the waste stream but transforming it into a valuable application with industry potential. The application presented is an evaporative cooling screen, which harnesses the porosity inherent to the production process to passively cool spaces. This research contributes to the emerging field of study at the intersection of design, circularity, materials and 3D printing.

2

Literature Review

2 Literature Review

2.1 Introduction

This chapter introduces the context for this research and the relevant literature in the field. The chapter is divided into four sections. Firstly, the circular economy will be discussed as the conceptual framework that underpins this research and its goals. The role of design and 3D printing in the circular economy will be specifically explored. The second section will present the material cycle of glass, with a particular focus on the waste stream of glass fines, which is central to this research. The state of the art of glass 3D printing will then be presented to highlight the limitations and opportunities in the field. The chapter will conclude with a discussion of binder jet 3D printing and its specific opportunity for transforming glass fines into circular applications.

2.2 3D printing a circular economy

Our current linear model of production and consumption is driving the climate crisis. This fossil fuel-reliant system of material extraction and manufacturing, and culture in which products are simply discarded after use, is causing extreme environmental degradation (Ellen MacArthur Foundation, 2019). As highlighted in Chapter 1, the Circular Economy (CE) has been proposed as a way forward. Broadly speaking, the CE is a framework for shifting the current linear model into a cyclical flow of products and materials that decouples economic growth from environmental degradation. The aim is to work towards a closed loop where waste theoretically no longer exists (Den Hollander et al., 2017).

2.2.1 Circular economy overview and definition

The concept of the CE has been gaining momentum since the 1970s (Ellen MacArthur Foundation, 2013). Whilst the term itself is often attributed to environmental economists Pearce and Turner (1989), the general concept emerged from Boulding in 1966 (Geissdoerfer et al., 2017; Ghisellini et al., 2016; Millar et al., 2019). He provided the metaphor of "spaceship earth", a closed system with finite material reservoirs in which a "spaceman economy" based on the cyclical use of materials and lower consumption is needed. This foundational idea was progressively built on by other schools of thought such as cradle-to-cradle (McDonough & Braungart, 2002), industrial ecology (Jelinski et al., 1992) and industrial symbiosis (Chertow & Ehrenfeld, 2012).

In 2013, the Ellen Macarthur Foundation published the first comprehensive report on the CE which outlined the significant loss of economic value that comes with a system based on consumption rather than the regenerative use of resources (Schandl et al., 2020). They identified that implementing the circular economy in Europe's manufacturing sector would result in a material cost saving of $380-630 billion USD (Ellen Macarthur Foundation, 2013). Since this publication, interest in the CE has grown rapidly across academia, government and industry. This is evidenced by an almost two hundredfold increase in academic articles (Alcalde-Calonge et al., 2022) and the introduction of government policies around the world, particularly in the EU (European Commission, 2015) and China (Yuan et al., 2006). Similar enthusiasm has been seen in the business world with companies such as Coca-Cola and IKEA signing up to Elen MacArthur's CE100 companies (Millar et al., 2019).

Despite this attention, there is no universal definition of the CE. In fact, Kircherr et al. (2023), conducted an analysis of 221 definitions of the CE, a repeat of work they initially conducted in 2017. Whilst their original work highlighted a conceptual fragmentation and confusion, something which they argue acts as a barrier to advancement, their 2023 analysis demonstrates both a consolidation in the core elements of the CE and a differentiation as additional studies and narrower topics have emerged. They describe it as "the trunk of the CE tree has strengthened, while various new leaves have appeared" (p.9). This analysis of the current CE discourse resulted in the formulation of the following definition.

"The circular economy is a regenerative economic system which necessitates a paradigm shift to replace the 'end of life' concept with reducing, alternatively reusing, recycling, and recovering materials throughout the supply chain, with the aim to promote value maintenance and sustainable development, creating environmental quality, economic development, and social equity, to the benefit of current and future generations. It is enabled by an alliance of stakeholders (industry, consumers, policymakers, academia) and their technological innovations and capabilities."

This wholistic definition of the CE is used in this research as it includes the core principles, aims and enablers of the CE as discussed in current discourse. In this definition, Kircherr et al. (2023), identify the key aims of the CE as sustainable development and value maintenance. Sustainable Development (SD) is commonly defined as development that "meets the needs of the present without compromising the ability of future generations to meet their own needs" (World Commission on Environment and Development, 1987). Whilst there are many models and conceptualisations of SD (including the UN Sustainability Goals), in general, the concept promotes the balance of three key dimensions of human activity; environmental protection (respecting environmental limits), economic prosperity and social equity (Millar et al., 2019)[1]. The linear economy has been criticised for pursuing economic growth at the expense of the other two dimensions whilst the CE has been promoted as a tool to achieve SD outcomes (Ghisellini et al., 2016; Schroeder et al., 2019; Suárez-Eiroa et al., 2019). Kircherr's (2023) definition specifically emphasises the importance of all three dimensions as the CE has previously been critiqued for favouring economic growth whilst simplifying the environmental effect and failing to consider social impact (Corvellec et al., 2022; Geissdoerfer et al., 2017). It has also been highlighted that circularity does not automatically ensure sustainability, so ensuring the impact on SD is needed.

The above definition also points to the aim of value maintenance. This refers to the retainment of the highest possible utility and value of products, components and materials for as long as possible (Ellen MacArthur Foundation, 2015). In other words, it is about extending the productive life of the resources in order to facilitate additional value extraction (i.e. long term use or reuse of the product) and reduce the value destruction (i.e. waste) (Blomsma & Brennan, 2017). By doing this, it follows that resource efficiency is increased and waste is reduced as fewer new materials and energy are needed (Campbell-Johnston et al., 2020; Reike et al., 2018). It is within this context that (Den Hollander et al., 2017) and Saurwein (2020) argue for the need to preserve "product integrity" and "material integrity". Based on Walter Stahel's Inertia Principle, product integrity refers to the extent to which a product remains identical to its original

[1] It is important to note that the SD concept itself has been widely critiqued, particularly for its vagueness. Nevertheless, the principles of SD are still considered important and as such the notions of respecting environmental limits, social equity and economic prosperity should be addressed in CE definitions (Millar et al., 2019).

state, over time[2]. They explain that maintaining the integrity means maintaining the value, which facilitates a longer productive life, essentially preventing obsolescence. Sauerwein (2020) also emphasises that material integrity indicates that the material retains its original properties even after recycling.

Embedded in Kircher et al.'s (2023) definition are the R principles (also known as R Imperatives or R hierarchies). These are seen as implementation or operationalisation principles for the CE (Campbell-Johnston et al., 2020; Reike et al., 2018). They refer to the variations of the 3Rs; reduce, reuse and recycle, that are found across CE discourse (Reike et al., 2018). The detailed 10R Framework proposed by (Reike et al., 2018) has received attention as it provides a synthesis of the differing R frameworks from across 69 academic papers (see Table 2.1). Reike et al. (2018) argue that this nuanced version of the R principles allows for the highest possible value retention of products and materials across the lifecycle. Embedded in the R Principles is the notion of a hierarchy, with the first R, 'refuse', being the before progressing down the others on the list. This aligns with the concept of value maintenance. Although several authors have highlighted the focus on recycling and recovery options in policy frameworks, these options are actually quite low on the list, representing a significant loss in value (Reike et al., 2018). Some authors also use the terminology of "slowing, closing and narrowing loops", first introduced by Bocken et al. (2016). Slowing refers to the prolonged use and reuse of products, closing involves the reuse of materials via recycling, and narrowing focuses on reducing the resources used to create the product. As such, these can be overlayed on the 10R strategies: R0-R1 relates to narrowing loops, R2-R6 is about slowing, and R7-R9 pertain to the closing of loops.

Building on this, the Ellen McArthur Foundation specifically argues for achieving circularity through two distinct cycles; the biological and technological. They draw on the iconic text Cradle-to-Cradle (McDonough & Braungart, 2002) in articulating the necessity of establishing two distinct material and product cycles. The first is the biological cycle, which involves the use of biodegradable materials that can cascade through multiple applications before they are ultimately returned to the earth via processes such as composting. The second is the technical cycle, wherein materials and products must be kept in circulation through processes such as repair, remanufacturing, or recycling (Ellen MacArthur Foundation, 2013). These cycles can be seen clearly in their now well-known 'butterfly diagram' (see Figure 2.1). As McDonough and Braungart (2002) point out, it is imperative that these cycles are kept separate to ensure the maintenance of value and avoid contamination.

2.2.2 Designers and materials in the CE

It is widely accepted that design has a fundamental role to play in transitioning to the CE (Moreno et al., 2016). It has been claimed that up to 80% of the environmental impact of a product is determined in the design phase as it is here that industrial designers make decisions about materials, production, use, repair and maintenance; ultimately determining the product life cycle (International Resource Panel, 2018). This understanding of the impact of design decisions and the responsibility of designers has over the years led to sustainable principles being integrated into the design process, resulting in approaches such as ecodesign or green design (Moreno et al., 2016). Whilst a positive step, these approaches have been criticised for being

[2] "Do not repair what is not broken, do not remanufacture something that can be repaired, do not recycle a product that can be remanufactured. This 'inertia principle' applies to products and components: replace or treat only the smallest possible part in order to maintain the existing economic value of the technical system" (Stahel, 2010, p. 195).

R-Principle	Description
R0 Refuse	For consumers to buy less. Also for producers who can refuse to use specific materials or designs.
R1 Reduce	Linked to producers, stressing the importance of concept and design cycle, e.g. less material per unit of production (dematerialisation).
R2 Resell, reuse	Second consumer of a product that hardly needs any adaptation and works as good as new.
R3 Repair	Bringing back into working order, by replacing items after minor defects. This can be done peer-to-peer or people in the vicinity.
R4 Refurbish	Referring to large multi-component product remains intact while components are replaced, resulting in an overall upgrade of the product.
R5 Remanufacture	The full structure of a multi-component product is disassembled, checked, cleaned and when necessary replaced or repaired in an industrial process.
R6 Re-purpose	Popular in industrial design and artistic communities. By reusing discarded goods or components adapted for another function, the material gets a new life.
R7 Recycling	Processing of mixed streams of post-consumer products or waste streams, including shredding, melting and other processes to capture (nearly) pure materials. Materials do not maintain any of their product structure and can be re-applied anywhere. Primary recycling occurs B2B, whereas secondary recycling takes place post municipal collection.
R8 Recover	Capturing energy embodied in waste, linking it to incineration in combination with producing energy.
R9 Re-mine	Landfill re-mining.

Table 2.1. *The 10R framework developed by Reike et al. (2018).*
Adapted from Campbell-Johnston et al. (2020).

[Production note: This figure is not included in this digital copy due to copyright restrictions.]

Figure 2.1. *Ellen MacArthur Foundation Circular Economy systems diagram (2019).*
Based on Braungart & McDonough (2002) cradle to cradle concept.

simply “less bad”, attempting only to optimise the current system (McDonough & Braungart, 2002). Designing for the CE, on the other hand, asks designers to rethink the entire system, starting with the concept of a “closed loop” of resources where waste is avoided (Den Hollander et al., 2017; Dokter et al., 2021). This is a significant challenge, requiring a holistic approach whereby the design, production, use and waste phases are addressed simultaneously with greater consideration for how a product or its use may change over time (Dokter et al., 2021; Sumter et al., 2020).

As a result, a body of literature in which various approaches and strategies for designing for the CE has emerged (Bocken et al., 2016; Den Hollander et al., 2017; Moreno et al., 2016). A study by Aguiar and Jugend (2022), evaluates strategies relevant to product design in particular. This study incorporates terminology from Bocken et al. (2016) in identifying five main approaches for designing for the CE as narrowing, regenerating, slowing, closing and informing loops. Various strategies were identified from across literature for each approach. For instance, narrowing, which involves utilising fewer raw materials, includes approaches like lightweighting and modular design. On the other hand, slowing which involves extending the usage of products or materials, encompasses approaches such as designing for emotional durability and facilitating easy maintenance or repair. Design aimed at closing loops involves using products and materials again and includes strategies like selecting materials suitable for recycling and creating designs that facilitate disassembly. Authors have also highlighted that these design strategies are just one piece of the puzzle and there is a need to develop circular business models and systems in conjunction with them (Bocken et al., 2016). For example whilst industrial designers may ensure that a product can be easily disassembled or repaired, if there is no wider system or financial incentive in place to facilitate this, then the circularity of the design is inhibited (Dokter et al., 2021).

As a result, the CE concept is expanding the scope of the design process and demanding new design competencies (Dokter et al., 2021; Sumter et al., 2020). Sumter et al. (2020) outline some of these, including the need for interpersonal competencies around facilitating and managing collaboration between experts and stakeholders and anticipatory competencies around foreseeing the consequences of prolonged use or multiple-use cycles. Of specific interest to this research is the need for industrial designers to develop deeper knowledge of materials and material science as discussed by De Los Rios & Charnley (2017). As the selection and development of materials is critical to the development of the CE, they propose the archetype of a ‘Scientific designer’ who possesses this knowledge and can collaborate in new material developments and concept generation with emerging materials.

This concept aligns with the growing area of materials design. In recent years we have seen the emergence of designers who are no longer satisfied with simply specifying materials and handing over their designs for production but are instead engaging in hands-on self-production practices in which the designers themselves develop the material or adapt it for a new fabrication method (Pedgley et al., 2021). This has become an increasingly recognised area of design that sits at the intersection of design, materials science, biology, arts and crafts and has fostered collaboration across these areas (Barati & Karana, 2019). It is intertwined with Do-it-yourself material approaches, which involve practices of ‘tinkering’ (Rognoli et al., 2015), the interrogation of materiality and the experiential qualities of materials (Karana et al., 2015), and a shift towards material-driven design approaches (Karana et al., 2015; Oxman, 2010). Clèries & Rognoli (2021) write that the growing interest in materials design is due to both an awareness that the material is an indissoluble part of the design process and a desire to find sustainable and circular material solutions by discovering and experimenting with alternative sources. Both of these elements are echoed by Bak-Andersen (2021), who writes that material knowledge is essential to not only improving the design of

physical objects but to closing the gap between sustainable design criteria and the skills needed to implement them, allowing designers to remain in control of their designs and production. She writes;

"A design that is not informed by a material reality may be good conceptually or look attractive in a drawing, but a designer who does not know how to design with materials is in many respects as badly equipped as a chef who does not understand the ingredients for the dish she is preparing. Qualities such as innovation and sustainability are not additives that can be injected into a product at the last minute, meaning that a product not originally designed to fulfil these criteria is unlikely ever to do so." (Bak-Andersen, 2021, p. 163)

Consequently, circularity has become a key aspect of materials design (Bak-Andersen, 2021; Romani et al., 2021). Romani et al. (2021) writes that materials design approaches are prone to implementing closed-loop strategies, particularly as many begin with the creative use of waste resources. This is evidenced in a study by Duarte Poblete et al. (2024), which analysed 31 case studies in material design for the CE. Whilst materials design projects range in scope and size from individual design practices to multidisciplinary research projects, their case study selection criteria resulted in the choice of mostly micro to small size businesses. Through this research, they were able to categorise the case studies into three key areas. The first involves the creation of waste-based materials, encompassing both organic and inorganic streams. For instance, Plasticiet in Italy produces plastic sheets for interiors and furniture using various recycled plastics. The second category focuses on the development of renewable materials sourced from fast-growing and abundant renewable resources such as cellulose and chitin. Some examples in this category overlap with waste-derived materials, such as the work of FruitLeather Rotterdam, which turns discarded fruit into a variety of leather-like materials. The final category consists of biofabricated materials that incorporate living organisms in their production, as seen with Ecovative's Mycelium packaging (see Figure 2.2.). Collectively, these examples highlight the potential for material design in the CE through the innovative utilisation of resources and manufacturing processes.

More speculative or craft-based projects also exist in the materials design landscape, including those that require further development to become commercially feasible and those that are designed as a provocation for audiences. Many projects of this scope have been captured in books by Seetal Solanki (2018) and Kate Franklin and Caroline Till (2018) including work from designer Fernando Laposse, who uses the husks of heirloom varieties of corn to create custom tiling and furniture finishes (Fernando Laposse, n.d.) (see Figure 2.3) or work by designer Tessa Silva who uses proteins from surplus cow's milk to handcraft sculptures and furniture (Tessa Silva, n.d.) (see Figure 2.4). Research centres and universities have also recognised and driven work in this space, including prominent programs and publications from Aalto University in Finland and their ChemArts book, the work of Neri Oxman's Material Ecologies Lab and the EU-funded MaDe (2020) project, which developed and showcased work of young designers working with organic waste materials for the CE. These practices and initiatives have contributed to the emergence of new design methodologies that combine material science and design approaches, which will be further discussed in Chapter 3.

Despite the global activity in this space, there have been calls for clearer definitions and assessment criteria to measure the environmental impact of material design projects accurately (Duarte Poblete et al., 2024). As can be seen from the case studies presented by Duarte Poblete et al. (2024) above, the circularity of the project can sometimes be restricted to simply using a waste material. While this is a positive step, designing for circularity requires a more holistic consideration of multiple life cycles, not just one, particularly if

Figure 2.2. *Mushroom packaging from Ecovative.*
Custom compostable, mycelium packaging made for Treaty. Image: Ecovative.

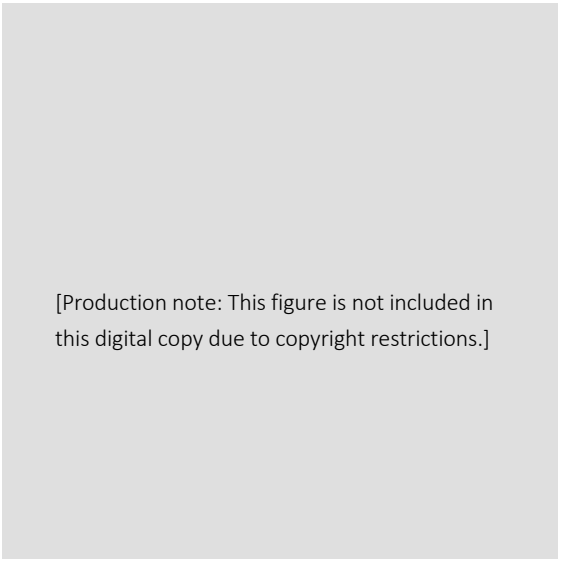

Figure 2.3. *Wall panel with Totomoxtle Corn husk veneer by Fernando Laposse (2019).*
The brightly coloured corn husks are ironed flat and glued onto a paper pulp or textile backing to be used as marquetry for furniture or interior surfaces.
Image: Fernando Laposse.

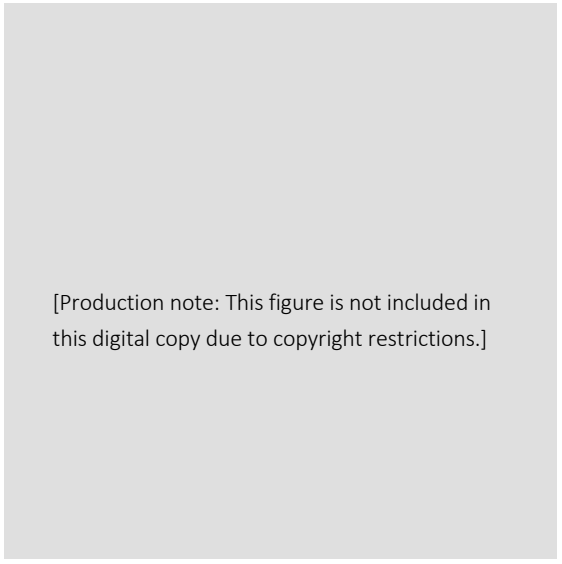

Figure 2.4. *Feminised Protein Loop by Tessa Silva (2024).*
Sculpture made from skimmed milk and calcium carbonate, using a fabric mould.
Image: Tessa Silva.

working with materials in the 'technical' cycle as described by McDonough and Braungart (2002). This also involves understanding user behaviours and establishing systems for high-value material recovery to ensure these life cycles. As a result, composite materials that cannot be separated at the end of life do not represent an ideal circular solution. There is, therefore, room for greater interrogation of the circularity of some materials in this space and further incorporation of CE principles to ensure materials, products and systems that avoid the pitfalls of greenwashing.

Furthermore, whilst there are examples of successful, commercialised products in this field as outlined by Duarte Poblete et al. (2024) (including the Mushroom packaging from Ecovative), these are fairly limited. Just 31 examples were identified worldwide in that research, with varying levels of scale and development within that group. As a result, there is an opportunity for a greater focus on industrial transformation in material design projects for the CE. This means moving beyond the craft-based, experimental scale to developing work that can be picked up by industry and further developed, allowing for greater impact. This requires synergy between engineered material formulations and manipulation techniques to ensure durable, repeatable parts for production. This is where digital fabrication technologies such as 3D printing can play a key role as these technologies are widely scalable and continue to transform the way manufacturers operate, opening opportunities for scalable and adaptable use of new materials for the CE. This research seeks to address these opportunities for enhancing circularity and industry translation through the use of 3D printing technology.

2.2.3 3D printing as an enabler of the CE

3D printing has been widely positioned as an enabler of the CE (Ferreira et al., 2021; Rosa et al., 2020; Sauerwein, 2020). 3D printing is the process of joining materials to make parts from 3D model data, usually by the successive layering of material (ISO/ASTM International, 2016). 3D printing is not just one technology but refers to a family of technologies all based on the same additive principle, yet each with its own parameters, advantages, limitations, and associated materials. These range from desktop technologies which are widely accessible, to specialised industrial and robotic 3D printing technologies. Initially developed in the 1980s, 3D printing has rapidly progressed from a prototyping tool to a manufacturing tool used for end-part production. This is because there are several clear advantages of 3D printing over traditional manufacturing methods, including the fabrication of complex geometries, customisation, freedom of design and minimal waste (Ngo et al., 2018).

3D printing allows for the fabrication of highly complex parts that were previously impractical or impossible to produce using traditional methods (Gibson et al., 2021; Peng et al., 2018). Depending on the type of 3D printing technology there is almost unlimited freedom in the types of geometries that can be printed including complex lattice structures, moving parts and internal componentry; geometries which cannot be achieved with conventional casting or injection moulding. This capability is sometimes described as giving 'complexity for free', as the complexity of the design is not tied to the production costs as the part is generally printed in one step regardless of the geometry (Niaki et al., 2019). This differs from conventional approaches where complex parts may require multiple steps or manufacturing processes and extend the time needed to fabricate the part (Gibson et al., 2021).

3D printing also allows for cost effective customisation of parts. As no moulds or tooling are needed, a series of unique parts can be printed at the same cost as parts that are identical and far more quickly. This is

ideal for industries like aerospace, which demand a limited number of highly complex components, or the medical field, where customised, one-off products are essential. In fact, the manufacturing of in-ear hearing aids has nearly entirely shifted to 3D printing (Ford & Despeisse, 2016). 3D printing is also known for its adaptability, as it allows for easy shifting between different designs or changing circumstances. This provides flexibility in the range of products that can be manufactured, allowing for parts to be printed on demand, reducing inventory waste and meaning that businesses can be highly responsive to market needs at a minimal cost (Ferreira et al., 2021).

Interest continues to grow in how 3D printing can contribute to environmental sustainability, primarily because it offers the potential to save resources (Sauerwein et al., 2019). The additive nature of 3D printing means that minimal waste is generated, especially in comparison with subtractive methods such as CNC milling where parts are made by removing material. The complex geometries that can be printed mean that parts can be structurally optimised to reduce material without compromising mechanical properties (Niaki et al., 2019). Tang et al., (2016) empirically showed that 3D printing can significantly reduce energy consumption and emissions through design optimisation and light-weighting. 3D printing is also known as a distributed form of manufacturing[3] which means that it can promote reconfigured value chains that are shorter, simpler, and more localised (Ford & Despeisse, 2016). As such, there are some intrinsic features of 3D printing that can enable the transition to the CE.

Several studies have recently examined this link (Hettiarachchi et al., 2022; Kravchenko et al., 2020; Ponis et al., 2021; Tavares et al., 2023). Various key areas have been highlighted, including how 3D printing can enable repair and maintenance practices through the on-demand printing of spare parts and can allow for the rethinking of business models with a focus on localisation, customisation and shorter supply chains (Despeisse et al., 2017). This benefit of customisation has also been presented as a way of building stronger personal attachments with users and therefore encouraging product retention (Sauerwein et al., 2019). Attention has also been directed to how 3D printing enables design optimisation and dematerialisation, and how it can facilitate the recycling of both novel and waste materials, including organic and inorganic types (Despeisse et al., 2017). These key areas can be seen in a literature review by Kravchenko et al. (2023) who linked CE strategies with 3D printing benefits (see Table 2.2). Many of these strategies are also echoed in the work of Tavares et al. (2023) and Hegab et al. (2023).

Of particular interest to this research is how 3D printing can enable the CE through the use of waste and by-products. The distributed nature of 3D printing allows for the disruption of established material value chains, creating significant opportunity to utilise localised waste materials (Garmulewicz et al., 2018). Romani et al. (2021) present 74 case studies of projects transforming waste materials using 3D printing within the CE context. They explicitly focus on extrusion-based methods of 3D printing and find examples of a wide range of materials from various recycled plastics to bio-based materials such as algae and starch bioplastics. Ferreira et al. (2021) specifically highlight how industrial symbiosis practices can be facilitated by 3D printing, through the creation of networks in which waste materials are exchanged between different entities. In their work, they highlight five examples including the work of Sauerwein (2020) in which mussel shells, a large waste stream in the Netherlands were turned into a 3D printable material. This material was demonstrated in early applications of a hair piece and lamp shade and could be crushed and

[3] Distributed manufacturing conceptualises a shift from centralised mass production to networks of small-scale, localised production. It is positioned as a promising production model that supports the CE by shortening supply chains and minimising transportation impacts (Van Dam et al. 2020).

CE Strategy	AM Enabling Context	Beneficial Opportunity of AM for CE
Reinvent the paradigm	- Personalised products to enhance consumer attachment - Adding new functions to products	- Product attachment can encourage longer retention - Multifunctionality reduces the need for additional products
Business rethinking and reconfiguration	- New value propositions (e.g. subscription model for customised products and their part replacement and repair)	- Customisation and customer co-creation foster stronger relationships enhancing customer retention and satisfaction - Increased responsiveness to consumer demands.
Reduce impacts in raw material and sourcing	- Utilisation of localised recycled materials as a feedstock for 3D printing - Monomateriality.	- Lower transport and material procurement costs - Reliance on local materials - Greater control over material quality and quantity (monomaterial products aid recycling). - Use of bio-based materials
Reduce manufacturing related impacts	- On-demand production (flexible, made-to-order manufacturing) - Distributed, localised manufacturing - High-precision production without the need for no additional machining tools - Modularity	- Eliminates surplus stock. - Local manufacturing- establishing economies of scope rather than scale; empowerment of local communities and smaller businesses - Shorter supply chains and reduced costs - Reduced material losses and scrap - Late-stage customisation reduces excess inventory.
Reduce impacts throughout the products use	- Optimisation of topology with complex geometries and lightweight structure	- Reduced material demand - Lightweight products can improve efficiency during use
Upgrade	- Adding extra features to a finished product or restyling	- Extends product life and increases customer desirability by adding useful features
Repair and Maintenance	- Rebuilding damaged parts to repair products	- Flexible (value chain independent) operation allows instant production of spare parts or rebuilding the damaged part - Reduction of packaging material and costs - Proximity to customers may encourage repairs
Refurbish or Remanufacture	- Refurbishing individual components of multi-part products - High-precision rebuilding and no additional machining tools - Reverse engineering	- Enables reproduction of failed or outdated parts - Flexible (value chain independent) remanufacturing operation - Reduction of packaging material and costs
Repurpose	- Modifying parts to fit another use context	- Extends the lifespan of parts by adapting them for new applications
Recycle	- Distributed recycling of materials	- Local (decentralised) recovery of waste - Reduction of transport costs - Immediate use of recycled feedstock locally - More control over material quality and quantity

Table 2.2. *Circular Economy strategies supported by AM and the benefits AM brings.*
Adapted from Kravchenko et al. (2023).

reused in multiple lifecycles, addressing the key component of establishing closed loops in the CE (see Figure 2.6).

Romani et al. (2021) highlight that the academic literature in this area is largely situated in engineering publications examining the characterisation of AM materials, with just one example from a design perspective being the work of Sauerwein (2020) mentioned above. This is worth noting as globally, there are numerous examples of design practitioners and businesses transforming waste materials into high-value products using 3DP (see Figures 2.5-2.7). Recycled plastics are the most used material with, notable examples including the Tokyo 2020 Olympic podiums designed by Asao Tokolo which were printed in recycled HDPE that was collected from households around Tokyo (Hahn, 2021) (see Figure 2.7) and the interior of retailer Bottletop in London which was robotically 3D printed in recycled plastic filament produced by Netherlands based company, ReFlow (Arthur, 2017). Sawdust and reclaimed metals have also been transformed into powder-based 3D printable materials by companies Forust (see Figure 2.5) and Continuum, respectively. These examples, strongly link to the practice of materials design discussed in the previous section. Digital technologies such as 3D printing democratise and enable personal fabrication thereby facilitating material experimentation and development by designers (Rognoli et al., 2015).

It is important to note that there are also barriers associated with 3D printing for the CE. These have been outlined by Tavares et al. (2023) and include factors such as the high unit cost of 3D printing, as it is a technology best suited for small batch production, as well as the quality of feedstock and resulting prints, since there is often variation or contamination evident in recycled materials. Sauerwein (2020) also highlights that although 3D printing presents a promising direction for circular manufacturing, it is imperative to ensure that product and material integrity are built into the design and production process. This means that both the product and material remain at their highest possible value, allowing for closed-loop circulation. However, as with the materials design projects discussed earlier, this principle is not always evident in the 3D printing case studies from Romani et al. (2021) or in the work of various design practitioners, where materials (sometimes composites) are presented without clear end-of-life strategies. Whilst the characteristics of 3D printing align well with circularity- especially in leveraging new materials and waste streams- there is limited research on how to integrate these aspects effectively, particularly from a design perspective. This study aims to address that gap.

2.2.4 Critiques of the CE

To accurately align this research with the circular economy framework it is important to acknowledge some of the critiques of this concept. Firstly, as highlighted above, the CE has been criticised for the lack of universal definition and 'conceptual fragmentation' (Korhonen et al., 2018). As the concept emerged from a symbiosis of academia, consultancy, advocacy and policymaking, the CE concept has been pulled in different directions to fulfil differing interests e.g. complexity has been reduced for communication purposes or the building of a business case (Reike et al., 2018). As a result, even the way the CE is described ranges from a 'new business model' (Ghisellini et al., 2016), an 'economic system' (Kirchherr et al., 2023) to a 'material and energy flow model' (Korhonen et al., 2018; Millar et al., 2019). This causes problems as it is difficult to accumulate knowledge if one actor sees CE implementation as purely recycling but others consider it to be the 10Rs (Blomsma & Brennan, 2017; Kirchherr et al., 2017, 2023). Taking this further, some authors have signalled that without clarification and scrutiny, the CE is at risk of becoming an

Figure 2.5. *Binder jet 3D printing of recycled sawdust by Forust.*
Ceiling fan propellers printed in a recycled sawdust and bio-epoxy resin composite.
Image: Forust.

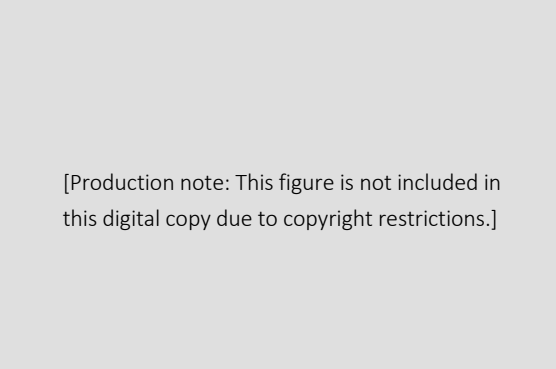

Figure 2.6. *3D printed lampshade in reprintable mussel shell material (Sauerwein., 2020)*

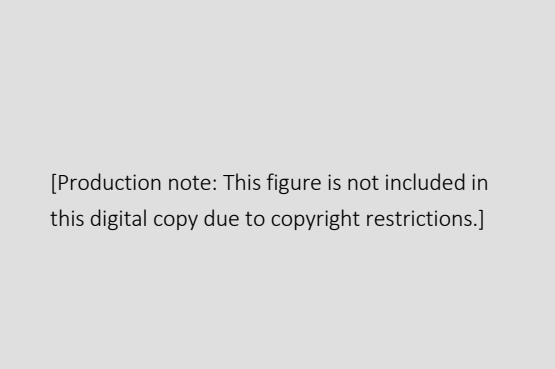

Figure 2.7. *Tokyo 2020 Olympic podiums, 3D printed in recycled HDPE plastic.*
Design by Asao Tokolo. Image: Dezeen.

ambiguous and idealistic buzz-word that lacks clear boundaries and derails actual well-intended efforts to redesign production and consumption (Corvellec et al., 2022; Dzhengiz et al., 2023).

Secondly, whilst a central tenet of the CE is that it is a closed-loop system, there are differing perspectives on whether this is possible. Several authors have spoken to the laws of thermodynamics and entropy as applied to the CE (Cullen, 2017; Korhonen et al., 2018; Millar et al., 2019). Cullen, (2017) wrote that with every loop around the circle, dissipation and entropy are created in the form of losses in quantity (material losses and byproducts) and quality (downgrading and mixing). This means that it is impossible for resources to cycle indefinitely without new materials and energy being inserted into the loop to overcome the losses (Corvellec et al., 2022; Cullen, 2017; Korhonen et al., 2018). Even if renewable energy is used to 'power' this cyclical system, the need for other new resources means that a general reduction in material demand is required (Calisto Friant et al., 2020; Korhonen et al., 2018). As Allwood (2014) wrote, "if demand is growing, the circle cannot remain closed" (p. 446).

This issue of continued growth is perhaps the biggest underlying tension for the CE (Calisto Friant et al., 2020). Whilst CE has been promoted as a "win win" for both the environment and economic growth, with the potential to generate upwards of 600 billion euros in Europe alone (Ellen MacArthur Foundation, 2013), the reality of this is unclear. Some authors have highlighted the concept of rebound effects in relation to the CE (Castro et al., 2022; Zink & Geyer, 2017). This refers to when CE activities unintentionally cause an increase in consumption and production, for example when recycling leads to consumers purchasing more disposable products or lowering prices of recycled materials results in producers purchasing and making more products, increasing the overall environmental impact (Metic & Pigosso, 2022; Zink & Geyer, 2017). As such, numerous authors have pointed out that to truly reduce environmental impact, less production and consumption is required and, therefore, not continued economic growth (Korhonen et al., 2018; Zink & Geyer, 2017).

Furthermore, whilst sustainable development is stated as a key objective of the CE, the relationship between these two concepts is not always clear (Corvellec et al., 2022; Geissdoerfer et al., 2017; Korhonen et al., 2018). It has been pointed out that circularity does not automatically ensure an environmentally beneficial solution as evidenced by the rebound effects discussed above. Until recently, the social dimension of the CE, including labour practices, education, safety, and factors such as consumption habits, lifestyles, and ownership, has also been largely ignored (Leipold et al., 2023; Mies & Gold, 2021; Valencia et al., 2023). As Corvellec et al. (2022) points out, the CE has potential to bring a 'socially positive footprint' but could also make life worse for many. With this in mind numerous authors have highlighted the importance of monitoring and measuring circularity in relation to SD (Corona et al., 2019; Elia et al., 2017; Kristensen & Mosgaard, 2020). This aligns with the discussion in the previous section regarding the need for assessment criteria that accurately measures the environmental impact of material design projects. (Duarte Poblete et al., 2024).

What these critiques largely address is the broad brushing use of the term CE by government, businesses and researchers without interrogation of what that actually means or what it looks like. As a result, the critiques are often concerned with the theory of the CE or its position as a panacea, rather than individual applications of the concept. In fact, authors have acknowledged that more modest, specific applications of circularity are the pathway forward; focusing on an 'actual solution to actual problems" (Corvellec et al., 2022, p. 429). This is because it is clear that for certain materials and products, the application of CE

strategies can have a positive impact. This research highlights the specific material flow of glass fines as one such area with significant application potential for the CE in an industrial context.

2.2.5 Positioning this research

Whilst the CE has been considered by some to be utopian and impractical, it is the absolute nature of this approach that can fuel design solutions. Den Hollander (2017) argues that ecodesign approaches start with the existing system or state and attempt to integrate environmental aspects into the design, therefore only allowing designers to optimise what is already there. In contrast, the CE offers an absolute approach that challenges designers to strive for the ideal state. In doing this, they have the scope to rethink the entire system, expanding the solution space and enabling more opportunities for innovative outcomes (Dokter et al., 2021). With the worsening climate crisis, there is an increasing need to entirely rethink these prevailing systems. As a result, the CE remains a useful—if imperfect—framework in which to situate design research projects despite the mixed definitions and use as a buzzword. Its emphasis on systemic change, value maintenance and material circulation provides a starting point for interrogating and reshaping design practices, even as its limitations warrant ongoing critical engagement.

Furthermore, despite the limits of the CE concept, it is clear that radical improvements can be achieved by reconfiguring our current linear economy to one that is more cyclical (Korhonen et al., 2018). Adopting the CE R-Strategies and considering the whole life cycle of our products and materials can reduce resource use and waste, which will undoubtedly positively impact the environment. As such, this research takes what Leipold et al. (2023) call a 'reformist' perspective of the CE. This viewpoint believes in the potential of the CE to advance a sustainability transformation; however, it also acknowledges that this is only possible if environmental conditions are actually met. This perspective acknowledges that business-as-usual interests (e.g., fossil fuel industry) and potential greenwashing must be overcome and rebound effects, burden shifting, and the continued growth of resource consumption and emissions must be properly addressed. This understanding of the CE signifies a shift from an amorphous and idealised concept to one that is more critically applied in specific contexts where the impact is considered.

As the scope of the CE concept is so large, it is important to acknowledge that this research will not be able to address every element. Instead, the focus will be on the intersection between materials, design, 3D printing and the CE, demonstrating not only the connection between them but the opportunities that exist in this space. To do this, the guiding principles of product and material integrity, as discussed by den Hollander et al. (2017) and Sauerwein (2020) will be employed. To reiterate this refers to the extent to which a product or material remains identical to its original state over time (Den Hollander et al., 2017). Designing for product integrity involves any measure that extends the product's life, including designing for durability, emotional attachment and repairability. Designing for material integrity involves designing and utilising materials in a way that allows for the original properties of the material to be maintained even after recycling (Sauerwein, 2020). This means that the material can be recycled over and over in a closed loop, it is not only about utilising a waste source in one loop where it can no longer be recycled. By maintaining value, it follows that fewer resources are needed.

With this in mind, authors have emphasised the importance of monitoring and assessing circularity (Corona et al., 2019; Elia et al., 2017; Kristensen & Mosgaard, 2020). This, however, is easier said than

done. Whilst some measurement tools and indices[4] have been introduced, there is currently no standardised assessment method for the CE. Other methods such as Life Cycle Assessments (LCAs) and Material Flow Analysis (MFA) from the field of industrial ecology have been applied to the CE (Walzberg et al., 2021).[5] LCAs have a high potential for evaluating the CE at the product and service level and currently appear to be the most comprehensive. However, they are still not entirely resolved with complexities around "open-loop recycling" needing to be addressed (Corona et al., 2019). Furthermore, there is an added challenge when assessing the impact of emerging materials as LCAs in this space can remain theoretical and be insufficiently grounded in the real world (Duarte Poblete et al., 2024).

This presents a crossroads for this research as whilst the need to evaluate the impact of the material, production and application process is clear, the tools to do this are not entirely suitable. As a result, other methods of evaluation need to be employed. This research will align with Corona et al.'s (2019) CE validity requirements and use these as a starting point for evaluation (see below). These requirements cover all three elements of sustainable development; environmental, social and economic to allow for a robust analysis of the circularity achieved.

CE validity requirements
1. Reducing input of resources, especially scarce ones
2. Reducing emission levels (pollutants and GHG emissions)
3. Reducing material losses/waste
4. Increasing input of renewable and recycled resources
5. Maximising the utility and durability of products
6. Creating local jobs at all skill level
7. Value added creation and distribution
8. Increase social wellbeing
(Corona et al., 2019)

Furthermore, as outlined in Chapter 1, this research is situated within a design context. This means that the focus is on the role industrial designers can play in developing more circular materials, products, and production processes. Whilst the role of designers in producing circular products has been well established in literature, an understanding of their role in the other two areas is still evolving. The emergence of Materials Designers and the adoption of 3D printing technologies has established an area of design that focuses on this intersection. However, research in this space often remains in the science and engineering realm or in more exploratory or craft-based design practice. This means that the results of projects often stop at the creation of an exhibitable artefact rather than continuing through to the development of specific industry-relevant applications. This is a missed opportunity for projects to have a wider impact, contributing to industrial transformation by convincingly communicating the opportunities for industry. This is also an area that designers are uniquely equipped to address, bringing an eye for application and the expertise to develop products for market, contributing to CE outcomes.

[4] Examples include the Material Circularity Indicator developed with the Ellen MacArthur Foundation (Goddin et al., 2019) or the Sustainable Circular Index developed by (2017).

[5] LCAs are a standardised method for evaluating the environmental impacts of a product or service throughout its life cycle that have been used for decades (ISO Standard 14040). Recently, they have become one of the most widely applied methods for also assessing circularity impacts. The LCA has also been expanded to LCC (life cycle costing) and S-LCA (social LCA) to provide social and economic evaluation alongside environmental.

2.3 Material Context

2.3.1 Defining Glass

Glass is considered a ceramic material. Clay-based ceramics such as porcelain and stoneware used to make tiles and crockery are just one part of the ceramics landscape. This common understanding of ceramics is based on its earliest origins where clay was extracted from the ground, shaped and fired, resulting in a hard, brittle material now referred to as 'earthenware' (Richerson & Lee, 2018). However, over time we have learnt to synthesise ceramic materials in various chemical compositions and methods. The once important aspect of heating or firing is no longer a requirement and ceramics with a range of properties can be engineered. As a result, a broad (and imperfect) definition has been adopted. The most widely accepted version by Kingery et al. (1976) defines ceramics as simply 'inorganic non-metallic materials'. As stated by Kingery, this definition includes not only materials such as pottery and porcelain but also cement, glass and new materials such as ferroelectrics or magnetic ceramics (Kingery et al., 1976).

Callister & Rethwisch (2018) elaborate that ceramics are mostly compounds between metallic and non-metallic elements such as oxides, nitrides or carbides (compounds of oxygen, nitrogen and carbon, respectively) (2018). For example, some of the most common ceramic materials are aluminium oxide (alumina Al_2O_3) and silicon dioxide (silica SiO_2) (Callister & Rethwisch, 2018). As these definitions can be difficult to work with, especially for someone without a chemistry background, it can be useful to break ceramics into two categories- traditional and advanced. Traditional ceramics have been manufactured for thousands of years and are mostly based on naturally occurring raw materials, particularly silica-based materials such as clays, quartz and feldspars (Heimann, 2010; Kingery et al., 1976). These traditional ceramics can be broken into categories based on application including; structural clay products (e.g. bricks, tiles, pipes); whitewares (e.g. porcelain for crockery, dentures, electrical insulators); cements (e.g. concrete, mortars); refractory materials (e.g. thermal insulators for furnaces); and silicate glass (e.g. bottles, windows) (Pfeifer, 2009). Advanced ceramics are newer carefully engineered ceramic materials s developed with specific properties such as optical or electrical properties (Pfeifer, 2009). They are principally produced from chemically synthesised micro or nano-scale compounds such as alumina or magnesia (Heimann, 2010). This is a growing research field encompassing bioceramics, electronic ceramics, magnetic ceramics and structural ceramics and advanced glass materials (Carter & Norton, 2013; Pfeifer, 2009).

Ceramic materials (with the exception of glass) can be classified as crystalline solids (Barsoum, 2019). This means that they have a 'well-ordered atomic' structure which is periodically repeated (Zanotto & Mauro, 2017). Crystalline solids can be comprised of a single crystal or they can be polycrystalline. Single crystalline solids have a repeated arrangement of atoms that extends throughout the specimen (see Figure *2.8*) (Callister & Rethwisch, 2018). Naturally occurring ceramics such as quartz have a single crystal structure as well as lab synthesised single crystals such as cubic zirconia (Richerson & Lee, 2018). However, the vast majority of crystalline ceramics are polycrystalline, meaning that they are composed of many small crystals or grains with differing orientations (Callister & Rethwisch, 2018). The fabrication of most ceramics from a powder which is subsequently fired at high temperatures, causes the powder particles to fuse forming a polycrystalline ceramic. In ceramics, the grains are typically 1-50 micrometres and visible only under a microscope. The size and shape of the grains, along with other factors such as porosity, describe what is known as the material's microstructure which impacts its properties (Barsoum, 2019).

Figure 2.8. *Atomic structure of cyrstalline, polycrystalline and non-crystalline solids.* Adapted from CDang, Wikimedia Commons.

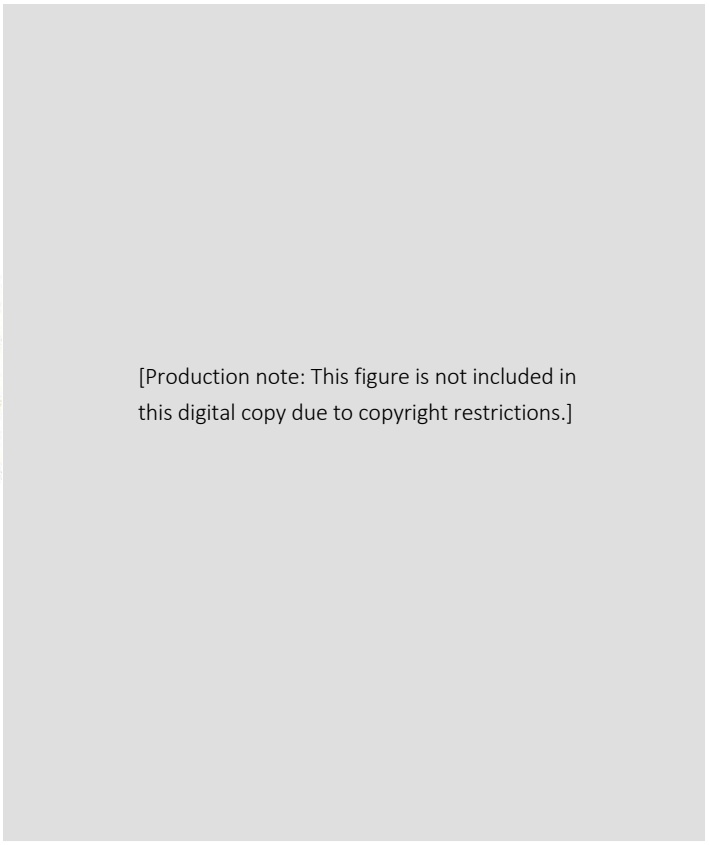

Figure 2.9. *The glass region between the liquid and glassy state (shown as Tm and Tg) is known as the glass transition range.*
Figure from Callister and Rethswitch (2018).

While glass is considered a ceramic, it represents a unique class of ceramics with several distinct properties. To start with, it is considered non-crystalline, meaning it lacks a systematic and regular arrangement of atoms (see Figure 2.8) (Callister & Rethwisch, 2018). This is key to the way it behaves. In particular, unlike crystalline materials, glasses do not have a defined melting point (Varshneya & Mauro, 2019). When a solid crystalline material (e.g. silver) is heated to a liquid state and subsequently cooled, it is abruptly converted back to its crystalline state when the material reaches below the melting point (see the blue line in Figure *2.9*). If a liquid can be cooled below the melting point without crystallisation, a supercooled liquid is attained (see the red line in Figure 2.9). The structure of the liquid will continue to gradually rearrange as it is cooled further, slowly increasing in viscosity. Eventually, the viscosity becomes so great that the atoms can no longer rearrange and instead, the structure of the liquid becomes fixed (frozen in time), creating a glass (Shelby & Lopes, 2005; Varshneya & Mauro, 2019). The atoms are set in a disorderly arrangement typical of liquids and can consequently be softened by reheating. Whilst glass appears solid at room temperature, it is not considered to be a solid or a liquid, instead it is more akin to a 'frozen liquid' exhibiting properties of both (Varshneya & Mauro, 2019).

Understanding this complex behaviour is key to the forming of glass. Like most ceramics, the commercial production of glass begins with powdered raw materials; in almost all cases, this includes silica sand (a crystalline material) and other oxides such as alumina. However, instead of sintering the powders to form a solid, the materials are heated to a temperature where they melt and form a homogenous liquid (Richerson & Lee, 2018). This viscous liquid is then formed into the required shape whilst it is still hot and cooled in a controlled way so that crystals do not form (Richerson & Lee, 2018). Gordon (2006), gives the useful analogy of glass as toffee. Most sugar bought from the shops is crystalline but when it is melted and cooled reasonably quickly, it will form glass or toffee. However, it is possible that the toffee could devitrify, meaning that it abandons the glassy state and crystallises. This often happens when the sugar is heated too quickly. As such, the heating of glass is complex and will be described further in Chapter five.

Contrary to most public perception, glass is not one singular material; there are natural glasses such as obsidian which existed on earth long before human life, glasses such as soda lime silicate used for windows and packaging which have been manufactured for thousands of years, as well as many newer advanced glass materials such as bioactive glasses or metallic glasses (Varshneya & Mauro, 2019). Therefore, many compositions, properties and fabrication methods are associated with glass. The composition is often tailored to meet specific requirements of usage, e.g. strength, opacity. Some of the main glass families that are industrially produced include can be seen in Appendix 1.1. This research is primarily concerned with soda lime silicate, which will be discussed further in the next section.

2.3.2 Soda Lime Silicate Glass

Glass is among the most widely produced materials in the world, with global production reaching 120 million tonnes in 2020 (Hubert, 2019; Sengupta, 2020). Whilst there is a vast array of different types of glass, commercial production is dominated by soda lime silicate, the chosen composition of this research, which makes up 90% of global glass production (Lebullenger & Mear, 2019). Public perception of glass as a singular material that is transparent, lustrous, fragile, and chemically durable largely comes from their experience with soda lime silicate glass (Varshneya & Mauro, 2019). This type of glass has been widely used since ancient times to produce containers, windows and glassware (Hand, 2021). This remains the case

today with soda lime silicate being used for the production of container glass and flat glass, industries which account for 80% of global glass production (Zier et al., 2021).

The widespread use of soda lime silicate glass is due to the availability and low-cost of the raw materials as well as the development of automated fabrication processes (Hand, 2021). As the name indicates, the main components of this glass are soda, lime and silica. Commercially it is made by heating soda ash, which provides the soda (Na2O), limestone which supplies the lime (CaO) and sand which supplies the silica (SiO2) with small amounts of magnesia (MgO), alumina (Al2O3) and other minor ingredients (Furszyfer Del Rio et al., 2022). The composition is approximately 12-16% soda, 10-15% lime and 71-75% silica (Lebullenger & Mear, 2019). These raw materials are heated in a furnace at approximately 1400-1500 degrees whereby they react to form a melt and then a glass upon cooling (see Figure 2.10) (Furszyfer Del Rio et al., 2022). The soda act as a flux, lowering the melting point and viscosity of glass whilst the lime improves the chemical durability (Francis, 2015).

This production process is highly energy intensive, contributing significantly to global carbon emissions. In a paper published in 2021, Westbroek et al. estimate that glass production contributes 86 million tonnes of carbon emissions, equating to 0.3% of worldwide emissions (Westbroek et al., 2021). As demand for glass is expected to continue growing, at the current rate emissions could increase to 107 million tonnes by 2050. The process of melting the raw materials in a furnace accounts for approximately 75-85% of the total energy requirements due to the high temperatures that are needed (Furszyfer Del Rio et al., 2022). These furnaces are operated continuously for years on end, in some cases more than twenty years, as it costs manufacturers too much to turn them on and off (Furszyfer Del Rio et al., 2022).

Whilst soda lime silicate glass has high embodied energy, it can be endlessly recycled without impacting the material quality. It, therefore, has the potential to be a key material in the circular economy. Remelting waste glass greatly reduces energy consumption when compared to producing virgin glass. This reduction is attributed to the lower melting temperature needed to remelt glass and the elimination of process emissions generated from the heating of limestone and soda ash. Westbroek et al. (2021) write that the use of recycled glass reduces energy and emissions from melting by up to 40% compared to virgin glass production (2021). It also avoids the mining of new raw materials and sending glass to landfill where it does not biodegrade. The New South Wales Environmental Protection Agency estimates that for every tonne of glass collected from the kerbside and recycled, the net savings are more than 500kg of greenhouse gases, 2.3 KL of water, over 6 GJ of energy, and approximately a tonne of solid waste to landfill is avoided (EPA NSW, 2010; Schandl et al., 2020).

2.3.3 Glass Recycling in Australia

Glass waste in Australia comes from 3 primary waste streams: municipal solid waste (MSW), commercial and industrial waste (C&I) and construction and demolition (C&D). However, almost 80% comes from the municipal waste stream; meaning domestic settings where it is collected through the comingled kerbside recycling system (Schandl et al., 2020). Generally, councils pay third-party contractors to collect and compact the waste at the kerbside before transporting it to material recovery facilities (MRF). At the MRF, the comingled waste is generally ‘dumped’ on the floor and pushed by mechanical loaders onto conveyor belts for processing (Department of Environment and Energy, 2018). Here, the glass is separated from other recyclable streams, such as paper and metals, creating a mixed glass product that includes tops and

labels (Department of Environment and Energy, 2018). Across Australia, there are 193 MRFS. However, they vary from sophisticated to basic sorting facilities, with many lacking the technical capacity to sort co-mingled municipal waste into high-quality streams (Department of Environment and Energy, 2018; Seadon, 2019). As such, the mixed glass product is generally sent to beneficiation facilities to be processed into the standard required for remanufacturing back into glass. Here the glass undergoes several processes to clean, remove contaminants and sort into colours. These processes require capital-intensive infrastructure, which includes optical sorting technologies that enable the removal of ceramics and other types of glass, such as Pyrex, along with colour sorting. There are only 7 beneficiation sites across Australia, located in Adelaide, Melbourne, Sydney, and Brisbane (Schandl et al., 2020). This means that often heavy glass waste has to be transported from regional centres (Flood et al., 2019).

From this process, glass cullet is created. This refers to glass which is suitable for recycling; it has been sorted into colour and is typically 8mm- 50mm in size (APCO, 2019) (see Figure 2.11). Cullet is purchased from beneficiation facilities by glass manufacturers and used as input to produce new glass containers (Victorian Parliamentary Budget Office, 2019). Currently, recycled input flow is approximately 32% however there is technical capacity to have more than 80% input of recycled glass cullet in packaging manufacture (Schandl et al., 2020). For every 10% of cullet used, the energy saving is 3 and the carbon emission reduction is 5% (Allan, 2019b).

Container deposit schemes (CDS) are also in operation across Australia. These schemes see a deposit added to the cost of the glass container which is then given back to the user if the glass bottle is returned. In NSW this deposit is 10c per bottle. In the 2017-18 financial year it was estimated that approximately 80,000 tonnes of glass packaging was returned and sorted through this avenue (Madden & Florin, 2019). CDS lead to cleaner, higher-quality glass being recycled as it is not mixed with other recycling streams. This also means that the glass can bypass the MRF facility and go straight to beneficiation. As a result, glass from CDS schemes has higher demand and value than glass from the municipal kerbside stream (Victorian Parliamentary Budget Office, 2019).

Whilst the benefits of recycling glass are well documented, recycling rates in Australia remain low. Glass packaging such as bottles and jars makes up approximately 80% of glass consumed in Australia (Schandl et al., 2020). In 2019, the Institute of Sustainable Futures at UTS conducted a life cycle assessment of packaging in Australia on behalf of the Australian Packaging Covenant Organisation. Their research finds that in the 2017-18 financial year, 1.3 million tonnes of glass packaging was consumed in Australia. Although 78% of this number was collected to be recycled and 50% recovered, only 36% was ultimately recycled back into glass packaging (Madden & Florin, 2019). This represents significant losses in the collection and sorting of glass. The low commodity price of recycled glass and the difficulty in recovering it from comingled waste are reasons for the low recycling rate (Department of Environment and Energy, 2018).

It may come as a surprise to the public, who place considerable value on glass as a material, that the economic worth of recycled glass as a commodity is substantially lower than that of plastic. The prices for clean, recycled glass cullet are approximately $70 to $75 per tonne (Schandl et al., 2020; Victorian Parliamentary Budget Office, 2019). This compares to clean PET plastic bales priced at $400-$500 per tonne or $1,000–$1,100 for washed and flaked HDPE plastic (Sustainability Victoria, 2021). The need for significant processing of glass to produce cullet means that beneficiation facilities depend on high volumes, exceeding 1,000 kilotons, to render the process commercially viable (Owens Illinois, 2017). Furthermore, most MRFs do not generate revenue from the mixed glass stream. Instead, they pay an average price of $30

Figure 2.10. *Industrial glass melting furnace.*
Image: Sergofan2015, Adobe Stock.

Figure 2.11. *Glass cullet.*
Image: Saelim, Adobe Stock.

to beneficiation facilities for its removal. Although this expenditure is less than the cost associated with landfilling the material, it means they sort the material at a financial loss.

This lack of economic incentive is exacerbated by the difficulty in recovering glass. Much of Australia has comingled kerbside recycling. Whilst this allows for efficient collection of waste, the highly mechanized system of collection and compaction causes significant glass breakages (Schandl et al., 2020). Once the glass is broken, it is the hardest waste stream to sort and the lowest by value (Flood et al., 2019). It also leads to irretrievable cross-contamination of other recyclable streams; particularly paper grades (Allan, 2019a). As the glass is processed into cullet at MRFs and beneficiation facilities, further breakages occur as it passes through the sorting and cleaning machinery (Madden & Florin, 2019). This results in 20% of glass material being sent directly to landfill from MRF facilities and generates the waste material, glass fines.

2.3.4 Glass Fines

Glass fines are the by-product of the glass recovery process. They are small particles of glass (typically 1-8mm in size) that are mixed in colour and often contaminated by other waste streams (see Figure 2.12). They are unable to serve as feedstock for traditional glass production and are an economic loss when compared to the higher value of cullet (Madden & Florin, 2019). Glass fines are produced at both the MRF stage and beneficiation stage. Due to their low value, they are often sent to landfill or stockpiled (see Figure 2.13). The closure of a glass beneficiation site in Victoria in late 2019 revealed that approximately 120,000 tonnes of mixed glass was stockpiled there. When the site was cleared, most of this glass went directly to landfill, but a small portion was sent to the construction sector (Sustainability Victoria, 2020a, 2020b).

Glass fines are ultimately the result of an ineffective recovery process whereby a recyclable material is systematically broken down and contaminated (Flood et al., 2020;). They are primarily made up of soda lime silicate glass of differing grades, colours and freeze points (Flood et al., 2019). There are often a range of contaminants in the fines, including ceramics, stones, porcelain, plastics, and organics derived from labelling glue or food and drink residue (see Figure 2.14) (Flood et al., 2019).

Globally there are emerging technologies that allow for the sorting and cleaning of glass fines to a state where they could be remanufactured into glass (Flood et al., 2020). These include various optic identification technologies such as X-ray fluorescence and infrared, as well as automatic systems like the Steinert MSort that can sort glass down to 0.5mm particles (Flood et al., 2020; Steinert, n.d.). These technologies are however, still in their infancy. Furthermore, the problem of glass fines is not simply a technological problem, but an economic and logistical one due to the low value of recycled glass as a commodity and the highly complex recycling system in Australia (Flood et al., 2019).

Although this research positions glass fines within an Australian context, it is important to note that the issue is global. The average global glass recycling rate is estimated at just 21% (Baek et al., 2024), with significant variation between countries. For example, the European Union averages around 80%, while the United States lags behind at 34% (Baek et al., 2024).[6] Like Australia, the United States faces challenges in glass processing, leading to a large quantity ending up in landfills. In 2018, 7.6 million tons of glass were disposed of in US landfills, much of which is likely to be considered glass fines.

[6] Figures are based on container glass packaging recycling rates (Baek et al., 2024).

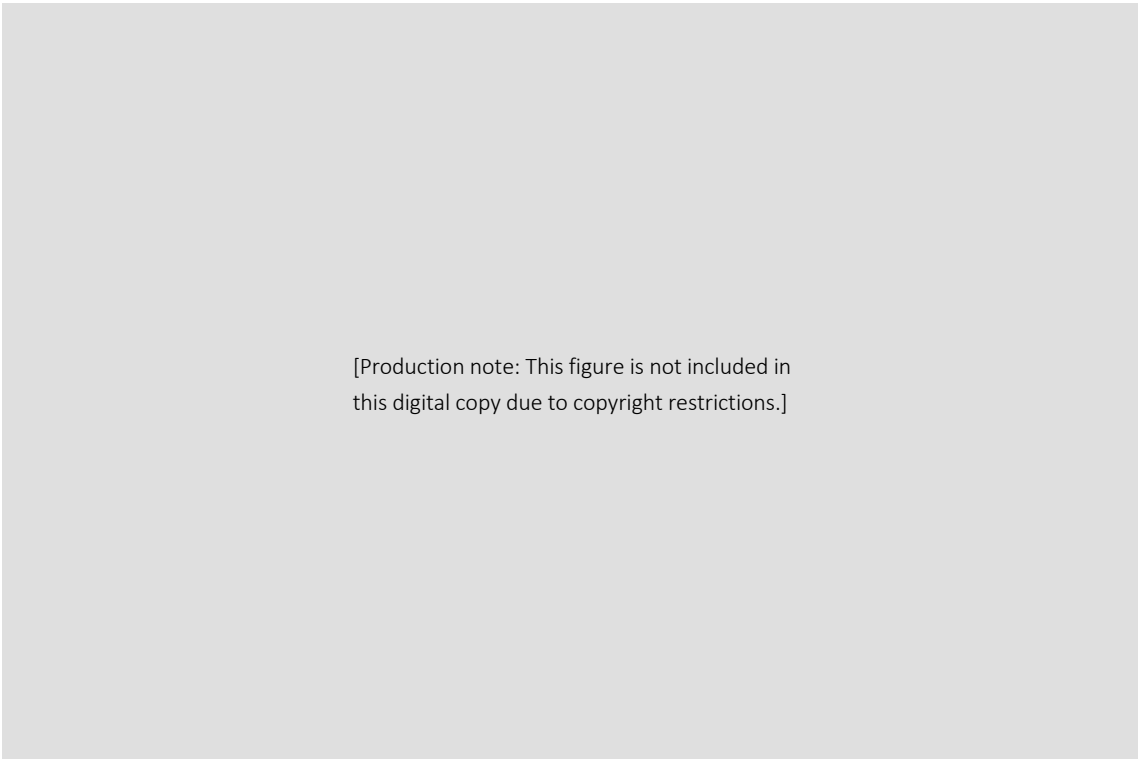

Figure 2.12. *Pile of glass fines awaiting processing at Alex Fraser Group.*
Image: Sand & Stone Magazine (2018).

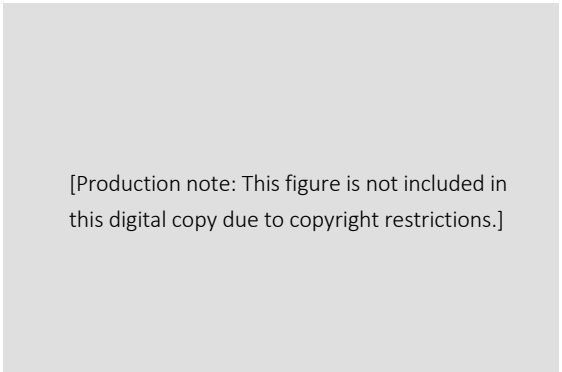

Figure 2.13. *Stockpiled glass fines sitting in 1 ton bags at recycling company Polytrade*
Image: Four Corners episode 2017 (ABC, 2017).

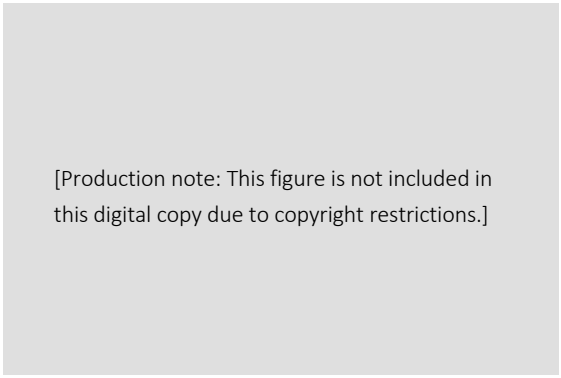

Figure 2.14. *Glass waste in recycling facility.*
Image from Belish, Adobe Stock.

However, even within the European Union—where many countries achieve high glass recycling rates—approximately 8% of collected glass packaging is still downcycled into lower-value products such as glass wool, foam, or construction materials. Additionally, a small portion continues to be sent to landfills (Close the glass loop, 2024). Furthermore, other categories of glass waste, such as flat glass from construction and demolition, or the automotive sector, exhibit significantly higher rates of downcycling into low-value products, with approximately 35%. A further 10% continues to end up in landfills (Bristogianni & Oikonomopoulou, 2023). The reasons for this mirror those seen in Australia, particularly regarding challenges related to collection, sorting, and contamination. As a result, whilst this research focuses on glass fines within an Australian context, mixed waste glass streams, and particularly glass fines, remain a persistent challenge worldwide. This has led to growing international research focused on finding applications for this waste stream. It is worth noting that the term 'glass fines' appears to be largely used within the Australian context, with it being more broadly referred to as 'waste glass' or 'mixed glass' in other regions. For further discussion of global glass recycling streams, refer to work by Baek et al. (2024) and Westbroek et al. (2021).

2.3.5 Applications of Glass fines

There is increasing concern over glass fines and a push to find applications. A report published by RMIT for Sustainability Victoria in 2020 identified over 70 potential applications for glass fines being explored globally. These applications were categorised according to their technological maturity, ranging from experimental to established industry practices, as well as based on the level of processing required, energy intensity and market share. The scope of applications discussed varies from experimental studies on vitrifying glass fines to produce high-voltage electrical insulation, to emerging practices involving the use of raw glass fines in beach replenishment and remediation. For a comprehensive list and analysis, refer to Flood et al. (2019). Out of the 70 applications, nine are classified as mature, indicating that they are recognised as established industrial practices. These are detailed in Table 2.3. The report highlights the civil sector as the biggest market as raw glass fines can be utilised in infrastructure projects as substitutes for sand and aggregate (Flood et al., 2019). This is reflective of current industry practices in Australia, where glass fines are being used in large volumetric scales for road base filler, pipe embedment and concrete aggregate (EPA Victoria, 2019; Flood et al., 2020).

The use of glass fines in road construction has attracted particular attention from government bodies. The first road made from glass fines, recycled soft plastics and asphalt was trialled in Victoria in 2018 (Sustainability Victoria, 2018). Subsequently, roads made from the same material have been built across the country (see Figure 2.15). In 2020, the NSW government released guidelines for Recycled Crushed Glass (RCG) in asphalt and awarded over $735,000 in grants to three projects that aim to unlock new markets for recycled glass in road construction (NSW EPA, 2020). The 2021 National Circular Economy Roadmap released by CSIRO also specifically advocates for the use of glass fines in road construction (Schandl et al., 2020). However, the use of glass fines in road base and asphalt incurs a gate fee of approximately $50-80 for MRF facilities. This fee is higher than the $30 MRFs pay to send mixed glass to beneficiation but lower than the fee to send it to landfill, representing a significant cost to MRF operators (Sustainability Victoria, 2021). Furthermore, Schandl et al. (2020) describe this application as "terminal", meaning that once embedded in roads, the glass fines cannot be recovered, undermining their circularity. Consequently, applications such as this, while reducing landfill accumulation, do not sufficiently address the overarching objectives of a circular economy and therefore represent only a partial or transitional solution.

In 2019 the Alex Fraser Group opened a new type of glass recycling plant that processes glass fines into construction material (Victorian Parliamentary Budget Office, 2019). This plant is additional to the current beneficiation plans in Australia and can process 800 tonnes of glass fines a day into a recycled sand which complies with VicRoads specifications (Alex Fraser, 2019). iQRenew in New South Wales and Re.Group who operate four MRFs across Australia are also processing glass fines into sand for the construction sector (APCO, 2019). This involves removing contaminants such as paper and grading the fines into a range of particles sizes (see Figure 2.16). Further applications of this sand include as water filtration media or as an abrasive material for sandblasting (Department of Agriculture, Water and the Environment, 2021). Whilst this can be seen as a straightforward solution to the stockpiling of glass fines, it represents an economic loss for glass recycling plants as cullet is a far more valuable resource (Madden & Florin, 2019). Furthermore, due to the important properties of glass and its high embodied energy, this can also be seen as a missed opportunity to fully utilise or upcycle the material (Westbroek et al., 2021).

Higher value applications of glass fines are emerging. The Centre for Sustainable Materials, Research and Technology (SMaRT) at the University of New South Wales (UNSW) has developed a process for recycling glass fines into high value building materials using a resin binder (Heriyanto et al., 2018). This research developed into "green ceramics" made predominately from glass fines and textile waste. In collaboration with Mirvac, "green ceramic" tiles, lighting features, bench tops and furniture were presented in a Mirvac apartment (see Figure 2.17) (Mirvac, 2021). Whilst highlighting the commercial viability of utilising glass fines, this material is limited in its circularity as the plastic and glass components are likely to be difficult to separate at end of life. Internationally, there is also emphasis on the utilisation of waste glass in the creation of glass foams as filtration and insulation devices (Bernado et al., 2010; 2007). However, these applications remain relatively unexplored in Australia (Flood et al., 2019). As such, there is significant opportunity to find new methods and applications for the upcycling of this problematic waste material. There is also global interest in the use of waste glass as aggregate in concrete as a sand replacement (Guo et al., 2020; Rashad, 2014). Whilst this addresses issues of finite sand resources, it falls into the same trap as using glass fines in roads, becoming a "terminal" use where the glass can no longer be recovered.

Flood et al. (2020) point out that the economic viability of using glass fines is a key barrier. To overcome this they suggest two approaches; reducing cleaning and sorting costs to make recycled glass competitive with virgin materials, or finding high-value applications that justify the processing expense. The second approach is most relevant to this research, as developing innovative applications is a key role that design can play and one which can be facilitated through RtD approaches and material experimentation. They further highlight the need to align these processing methods and applications with specific end products and markets. This means that glass fines can undergo a level of processing (cleaning, sorting, grading etc.) that is suitable to a specific application. This can support the establishment of a closed loop and allow for investors and businesses to better assess the economic feasibility.

Notably absent from RMIT's report were applications utilising 3D printing technologies. This indicates a gap in current research and an opportunity to transform this material through digital technologies. As discussed in section 2.2.3, 3D printing is often described as an enabler of the circular economy, with many practitioners harnessing its capabilities to transform unconventional or underutilised waste streams. As a result, 3D printing, coupled with material experimentation, could shift glass fines from low-value civil uses towards novel material systems with a strong link to industry.

Application	Description	Production Intensity (Energy)	Market Share (billions)
Civil Water Filtration	Various grades of glass fines can be used as a highly effective alternative to traditional civil water filtration materials. This can be used for stormwater and grey water filtration.	Low	20.3
Glass Ceramic Cooktops	Contemporary electric cooktops used for their low heat conduction to surrounding benchtop	Very High	1.6
Glass Foam Thermal Insulation	Glass Foam can be produced into easily machined thermal insulation blocks and panels. A material that can deal with very high temperatures without combusting or slumping glass foam insulation has numerous applications in the construction and industrial sectors.	High	1.7
Glass Foams for Drainage Aggregates and Screenings	As a very light weight material Glass Foam Aggregates and Screenings provide drainage industries with significant advantages (and transportation cost savings) and offer an alternative to scoria and volcanic stone aggregates	High	1.7
Glass Microsphere Fillers	Applicable to a wide range of industries including paint, plastic and abrasives manufacture	High	2.9
Glass Sand Abrasives	Glass sand is already available as a medium for abrasive industrial applications such as sand blasting	Low	1.7
Line Marking	Glass fines can be added to road paints to denote bicycle and bus lanes and for general line marking. As a paint additive, it provides a low cost and highly durable medium.	Low	20.3
Pipe Embedment	A lightweight alternative to wet sands and rock screening.	Low	20.3
Road Base Filler	Used to pack and level out the ground below a road when compressed	Low	20.3

Table 2.3. *Mature applications of glass fines.*
Adapted from Flood et al. (2019)

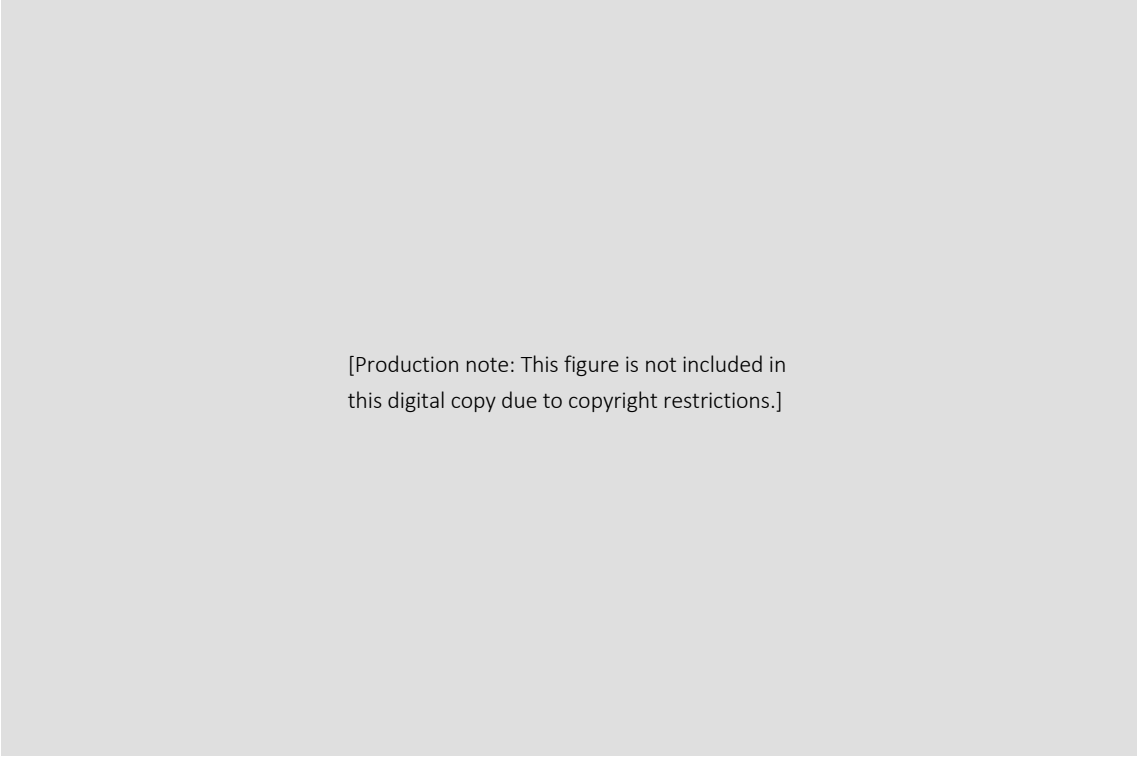

Figure 2.15. *Road built with recycled glass fines and plastic bags in South Australia.*
Image: Onkaparinga Now (2018).

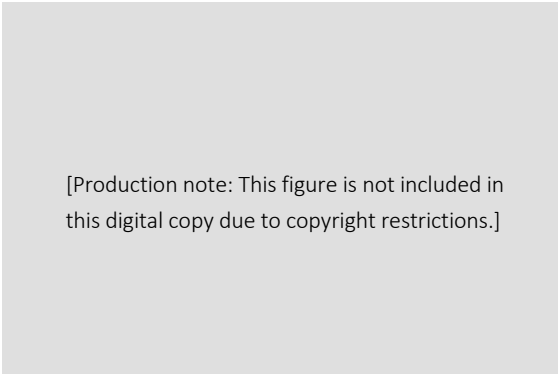

Figure 2.16. *Recycled glass sand produced by iQRenew (formally Envirosand).*
Fine grade (0.5 - 1.0 mm)
Image: Envirosand.

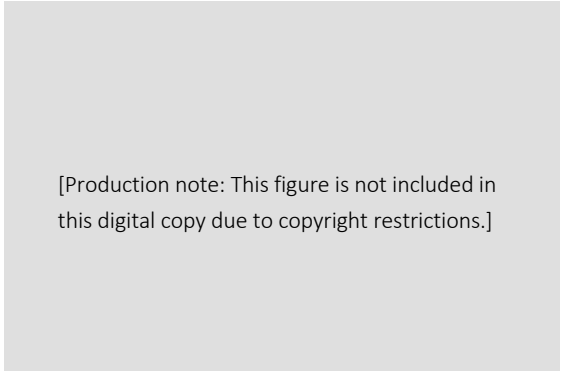

Figure 2.17. *Green Ceramic produced by UNSW's SMaRT Lab (2021).*
Showcased in Mirvac apartment.
Image: Mirvac.

2.4 Fabrication Context

2.4.1 Glass 3D Printing State of the Art

There is increasing discourse around 3D printing with glass. Glass is one of the most important high-performance materials with thermal and electrical insulation properties, optical transparency and excellent mechanical, chemical and thermal resistance (Kotz et al., 2017). However, conventional industrial manufacturing of glass is limited to symmetric and predominantly flat geometries with manual artisanal work required for more complex geometries (Moore et al., 2020). As a result, the 3D printing of glass can open up manufacturing and application possibilities, enabling the creation of previously unachievable forms. The use of glass in 3D printing has only developed more recently due to the high processing temperatures and high hardness properties (Zhang et al., 2022). Unlike 3D printing with polymers, metals and ceramics, glass 3D printing is not yet widely commercially available, and most of the developments remain in the research space.

Progress in glass 3D printing has occurred across a range of technologies including material extrusion, vat photopolymerisation, directed energy deposition, powder bed fusion and binder jetting. The following literature review is grouped based on 3D printing technology. Although the composition of glass used in this research is soda lime silicate, the literature review of glass 3D printing has been expanded to include a range of glass compositions due to the limited range of research on soda lime silicate glass. 3D printing using recycled glass will also be discussed in the final section.

2.4.2 Material Extrusion

Material extrusion refers to the 3D printing process in which material is selectively dispensed through a nozzle or orifice (ISO/ASTM International, 2016). Within this there are two key technologies: Fused Deposition Modelling (FDM) and Direct Ink Writing (DIW). Both of which have been utilized in the 3D printing of glass.

Fused Deposition Modelling (FDM):

The FDM printing of glass involves heating the glass to a molten state and extruding it through a nozzle which moves in the x-y plane. The molten glass is deposited on a print bed and cools to form a thin layer. The print bed then moves downwards, allowing for the next layer to be printed on top (see Appendix 1.2) (Zhang et al., 2021). This process is analogous to conventional desktop 3D printing where molten plastic is deposited layer by layer.

3D printing studio Micron E.M.E (previously Micron3DP) and the Mediated Matter research group at MIT both pioneered glass FDM systems in 2015 (Klein et al., 2015; Krassenstein, 2015). At MIT molten soda lime glass was extruded at 1010°C inside a build chamber set at 480°C (see Figure 2.18). Parts were annealed by slowly decreasing the build chamber temperature to 20°C (Klein et al., 2015). This process was later refined and demonstrated at architectural scale with the 3D printing of a set of 3-metre tall glass columns presented at Milan Design Week 2017 (Inamura et al., 2018). This was the first and so far, only demonstration of large-scale glass 3D printing. Whilst allowing for the creation of complex geometries in optically transparent glass, this method had limited resolution as the smallest nozzle diameter used was 10mm. Micron E.M.E on the other hand demonstrated printing at a much smaller resolution, with layer

heights of 0.1mm compared to MIT's 4mm (see Figure 2.19). They extruded soda lime silicate glass at 850°C as well as the more resilient borosilicate glass used in some Pyrex products at 1640°C (Jackson, 2016; Krassenstein, 2015). This work led to a collaboration with crystal company, Swarovski, where objects such as vases and candleholders were created in 'printed crystal' (Aouf, 2017). Little information is given on the material or fabrication process. Whilst the process appears to be successful, the company has struggled to pinpoint a market and have tabled the commercialization of the technology (Sher, 2018).

In 2021, an Australian based start-up, Maple Glass launched the first commercial material extrusion 3D printers which can use virgin and recycled soda lime glass filament sourced from glass blowing waste (Maple Glass, 2022). Molten glass is extruded from a nozzle in a heated chamber at a minimum layer height of 0.25mm (see Figure 2.20). Likely due to commercial sensitivity, information on the system workings and temperatures used is limited. Currently, applications remain preliminary, with the printing of decorative forms and vases. However, a collaboration with RMIT's Architecture Tectonic Formation Lab resulted in the printing of complex geometries in a façade prototype, representing a possible direction forward.

As the high temperatures needed to extrude soda lime glass are energy intensive and difficult to process, researchers have investigated using other glass compositions. Baudet et al. (2019) utilized an FDM printing process in their 3D printing with chalcogenide glass (see Figure 2.22). This glass was chosen for its low transition temperature and ease of synthesis and processing as well as unique infrared optical transmission properties. They extruded the glass on a modified commercial 3D printer at approximately 330°C, far lower than that of MIT or Micron E.M.E. Similarly, Zaki et al. (2020) tested an FDM method with phosphate glass, which they were able to extrude at 470°C on to a build plate at 320°C using lower temperatures than those needed for soda lime silicate. Both Baudet et al. (2019) and Zaki et al. (2020) prove the feasibility of FDM printing with their respective glass types and discuss potential applications in various optical products, including optical fibre preforms. Despite this, both projects only produce simple, low-fidelity shapes, indicating that process refinement is likely needed to achieve an application.

A different approach to FDM glass 3D printing was proposed by Mader et al. (2021) using a thermoplastic silica nanocomposite. This material is printed using a modified desktop 3D printer and subsequently converted into transparent glass through debinding (the removal of the binder) and sintering at a peak temperature of 1320°C. The material was originally developed for injection moulding but modified for use in FDM printing and is presented as a more accessible form of 3D printing with glass. The authors discuss applications such as design, lighting, jewellery, customised laboratory containers and microfluidic reactors. It is important to note, however, that the high temperatures and sacrificial thermoplastic binder likely make this a process that has a significant environmental impact.

Whilst there are some promising developments in the FDM printing of glass, this 3D printing technology has several limitations, particularly in terms of geometric complexity. As the 3D printing of support structures has not yet been achieved, overhangs and internal features are unable to be printed. The level of detail is also constrained by the nozzle size, limiting the types of geometries that can be printed. Furthermore, the high processing temperatures are not only energy intensive but also make it difficult to accurately control the flow of material (Zhang et al., 2021). Whilst the use of recycled glass via this 3D printing method has been achieved and has great potential, there would likely be significant difficulties in using glass fines. As glass fines are made up of varying grades of soda lime silicate with different melting temperatures the extrusion of these at a single temperature would be challenging.

Figure 2.18. *Glass FDM printed objects from MIT by Kein et al. (2015).*
Image: MIT, Chikara Inamura.

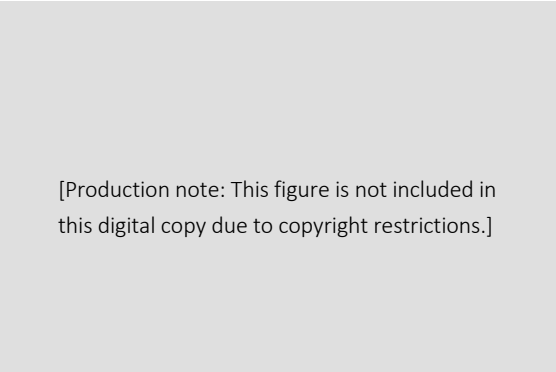

Figure 2.19. *Complex geometries printed in soda lime glass by Micron E.M.E.*
Image: Micron 3DP.

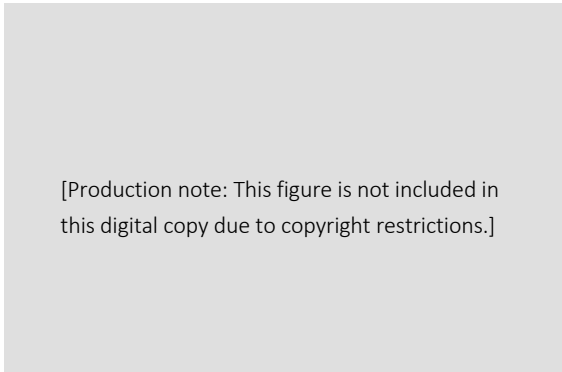

Figure 2.20. *Maple Glass – the world's first commercial glass 3D printer.*
Image: ANU.

Direct Ink Writing (DIW)

Direct ink writing is another form of material extrusion 3D printing of glass which has emerged more recently. Leading research in the DIW of glass is a team based at the Lawrence Livermore National Laboratory. They have developed a two-stage 3d printing process using shear-thinning inks with microscopically dispersed glass particles. These inks are extruded through a nozzle layer by layer, rapidly solidifying upon printing. The 3D printed part is then dried and sintered to produce the final glass components (Nguyen et al., 2017). The team is focused on the application of this technology in optical components, and have developed a series of printable silica, silica titania and germania silica formulations that have allowed for the tuning of the glass refractive index and allowed for the printing of two separate inks from the same nozzle by controlling the ink rheology (see Figure 2.23) (Destino et al., 2018; Dudukovic et al., 2018; Dylla-Spears et al., 2020; Sasan et al., 2020).

Most recently, they have developed a DIW method that allows for the printing of glass with a gradient refractive index. They do this by using a nozzle with an active mixer that combines silica nanoparticles and varying concentrations of titania during the printing process. As the part is printed, the concentration of titania is altered to change the refractive index and produce the gradient. This is expected to open possibilities in terms of controlling the glass composition and associated optical and material properties in three dimensions (Dylla-Spears et al., 2020).

This is a highly technical glass 3D printing process that is still in its infancy. While the application potential is promising, the relevance to this thesis is limited, as the glass particles used in the ink must be processed to the nanoscale and glass compositions tightly controlled. The mixed nature of glass fines, combined with the impracticality of refining them to the nanoscale, makes them an unsuitable feedstock for DIW.

2.4.3 Vat Polymerisation

Increasing attention is being paid to vat photopolymerisation (VTP) methods of glass 3D printing. VTP refers to the 3D printing process in which a liquid photopolymer in a vat is selectively cured by light-activated polymerisation (see Appendix 1.3) (ISO/ASTM International, 2016). Stereolithography (SLA), digital light processing (DLP) and Two-Photon Polymerisation (TPP) are types of VTP that are currently being investigated for glass 3D printing. The difference between these techniques comes in the way the liquid photopolymer is cured.

Similarly, to DIW, the VTP of glass is a multi-step process, involving the printing, debinding and sintering of the final part. They are also alike in their highly engineered nature where glass nanoparticles of specific compositions are dispersed in a liquid. In VTP these liquids are photocurable resins which are ecologically harmful. As such, the relevance to this dissertation is limited. However, as VTP is heralded as the most promising glass 3D printing technology by some researchers, the following section will provide an overview of the current landscape (Zhang et al., 2021).

Stereolithography (SLA)

SLA is known as the original 3D printing technology, patented by 3D Systems in 1986. An ultraviolet laser beam is used to solidify the photocurable liquid point by point, layer by layer to build a part (Zhang et al., 2021). The parts are then typically heat-treated to remove the binder and sintered into the final glass piece.

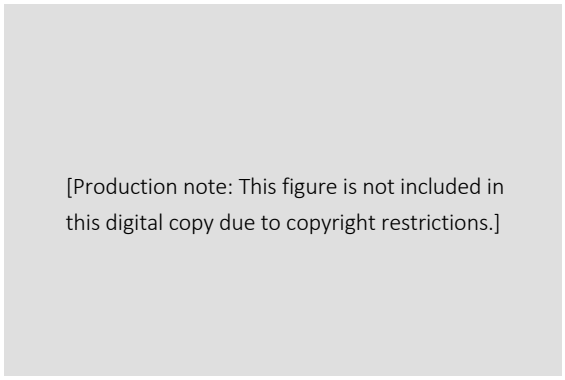

Figure 2.21. *Borosilicate Glass 3D print (Zaki et al., 2020).*

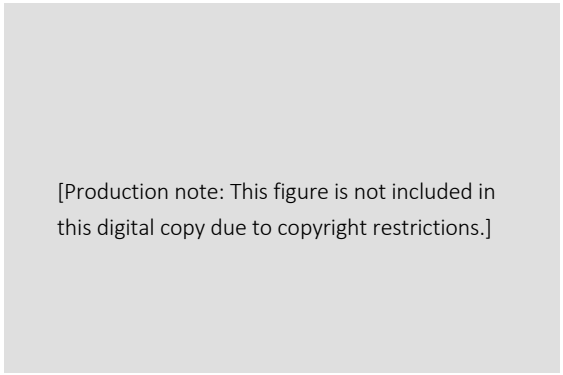

Figure 2.22. *Chalcogenide glass 3D print (Baudet et al., 2019)*

Figure 2.23. *DIW samples with gradient index silica-titania glass (Dylla-Spears et al., 2020).*

SLA processes have allowed for the fabrication of highly transparent and precise glass parts with low surface roughness (Xin et al., 2023). The first and possibly most influential SLA 3D printing of glass was by Kotz et al. (2017). They created a UV curable solution containing pure glass quart (SiO_2) nanoparticles. After printing, parts were sintered 1300°C to burn off the polymer and densify the glass print. Non-porous, complex geometries with the optical transparency of commercial fused silica glass were created (see Figure 2.24). They investigated shapes at both the macro and microscale, applying it to the fabrication of high-resolution microfluidic devices (see Figure 2.25). They further investigated the doping of the 3D printed glass parts with various metallic salts to create different coloured glasses.

Liu et al. (2018a) developed this process further, with a focus on improving the efficiency of the technique. They developed a top-down SLA system rather than the bottom-up system used by Kotz et al (2017). This is a much faster technique which is generally considered to be more reliable (Redwood et al., 2017). By also adopting a heat treatment step their process took one third of the time. They advanced the work by doping the SLA-printed glass with rare earth ions through a solution impregnation method; this occurred after the debinding phase when the glass was porous but before sintering (Liu et al., 2018b) This produced a photoluminescence effect, emitting red, cyan, and blue light when activated by a 254 nm lamp. They also created a space-selective doping method, which allowed for the creation of a multicolour luminescent glass object, opening potential for the design of shape and function in single glass devices (see Figure 2.26).

These key works reflect the potential of glass 3D printing via SLA, particularly regarding the complexity and detail that can be achieved. However, they also underline the need for highly controlled material compositions and the current limitations of scale. The heterogeneity of the recycled glass fines, combined with the significant volume of the waste stream, indicates that other 3d printing techniques would be more suitable.

Digital Light Processing (DLP)

SLA has a slow speed due to the point-by-point approach. Comparatively, DLP allows for the immediate solidification of an entire layer using a digital light projector screen which flashes an image of the entire cross-section- fusing the liquid together (Redwood et al., 2017). Typically the same 3D model requires 60 minutes to print via DLP but 9 hours to finish by SLA (Zhang et al., 2021). This whole layer curing technique also improves the surface profile and roughness (Xin et al., 2023). More studies have been reported using this technology rather than SLA, largely due to the cost of an SLA machine being much higher than DLP machines (Xin et al., 2023)

Some of the most influential work in this space comes from Cooperstein et al. (2018) and Moore et al. (2020). Cooperstein et al. (2018) developed a DLP process utilising a photocurable sol-gel formulation that does not include dispersed silica particles. This approach allowed for parts with controllable density and refractive indices to be produced. On the other hand, Moore et al. (2020) developed a DLP technique that relies on the phase separation of liquid resins to create high resolution glass parts (see Figure 2.27 and Figure 2.28). The phase separating resins can be controlled through UV light and allow for multi-scale porosities to be created, opening up the functionality of glass components. Both studies demonstrated the fabrication of high transparency, precise and complex forms.

Some researchers have focused on the use of DLP processes to specifically produce optical fibres. Chu et al. (2019) were the first to do this. As with the SLA techniques, glass nanoparticles were dispersed in a photocurable resin to print the cladding of the optical fibre. Once printed the core was fabricated and the

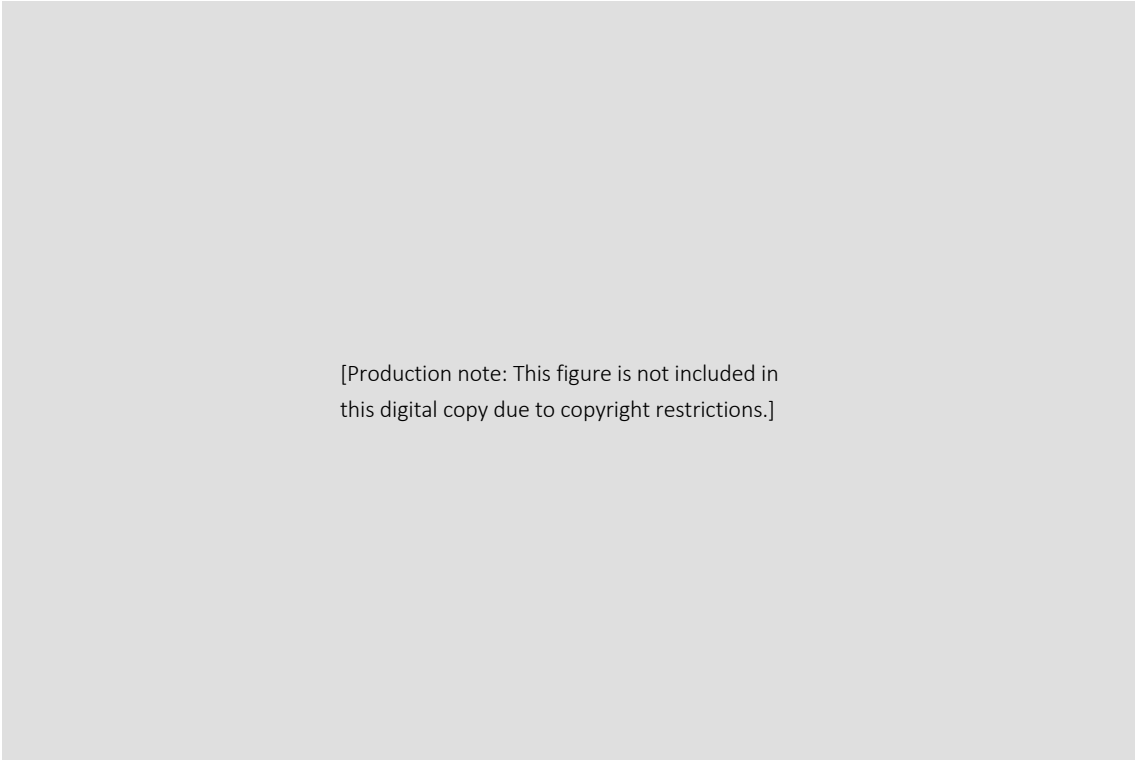

Figure 2.24. *3D printed structure in fused silica via SLA produced by Kotz et al. (2017).*
A polymerised composite is SLA printed and turned into fused silica glass through debinding and sintering.

Figure 2.25. *Microfluidic chip 3D printed in fused silica glass via SLA (Kotz et al., 2017).*

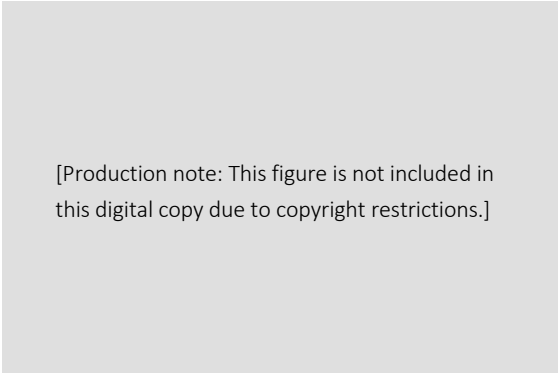

Figure 2.26. *3D printed multicolour luminescent glass produced by Liu et al. (2018b) via SLA.*

part went through a thermal debinding process to remove the polymer. Finally, the optical fibre was drawn. The authors discuss that whilst there is significant scope for improving the transparency of the fibre this process presents potential for fabricating optical fibres which are not constrained by the labour-intensive lathe process. Similar to other VTP processes, optimising the size and uniformity of glass nanoparticles is crucial for the success of this method.

Two-Photon Polymerisation (TPP)

Two-Photon Polymerisation (TPP) is a micro- and nano-scale VTP technology. The UV laser in SLA is replaced with a femtosecond laser which allows for higher resolutions and smoother surfaces to be created (Kotz et al., 2021; Zhang et al., 2022). Kotz et al. (2021) produced a series of fused silica components with tens of micrometre resolution through TPP printing and subsequent thermal debinding and sintering (see Figure 2.29). Colombo & Franchin (2021) built on this work, printing silica glass components with nanometre resolution. This area of glass 3D printing represents an emerging field with application potential in optics, photonics, microfluidics and biomedical applications (Kotz et al., 2021).

All three VTP methods of glass 3D printing can be utilised to produce highly accurate and complex transparent glass parts. As a result, they are often positioned as the most promising method of glass 3D printing. However, the need for nano particles of silica presents a barrier to using recycled glass of any kind, especially glass fines. Furthermore, the use of sacrificial petrochemical-based UV resins makes these methods especially detrimental to the environment. For this reason, other 3D printing methods are more appropriate for the transformation of glass fines.

2.4.4 Directed energy Deposition

Directed energy deposition (DED) is a 3D printing process in which focused thermal energy (often a laser) is used to fuse wire or powdered materials by melting them as they are being deposited (ISO/ASTM International, 2016). This method has been widely used in 3D printing with metal materials but remains in its infancy in 3D printing with glass with minimal development in recent years (Xin et al., 2023).

The first example of glass DED was Luo et al. (2014). They used a wire fed process in which a 1mm borosilicate glass rod was melted and fused directly to previous layers of glass using a CO_2 laser. They produced single-track wide walls that could be post-processed to achieve transparency. They later built on this work by identifying the optimal parameters for this process which would allow for walls with a flat top profile to be built (Luo et al., 2015). They also measured the optical transmission of these pieces and found that after polishing, they were of equal transparent to pieces that were cast in a furnace. Luo et al. (2017) later published a doctoral thesis in which soda lime glass, fused quarts and borosilicate glass types were tested using a DED technique.

Developing the work further, von Witzendorff et al. (2018) presented a study that demonstrated the feasibility of using DED to produce quartz glass components for medical applications. They utilized a glass filament/fibre which was fed at an angle of 25-60° to the laser where it was melted and fused to the previous layer (see Figure 2.32 and Figure 2.31). They envision applications of complex hollow glass structures such as artificial kidneys. The work of Luo et al. (2014, 2017) and von Witzendorff et al. (2018) show the feasibility of this method of glass 3D printing with a variety of glass compositions, however only

Figure 2.27. *Various 3D printed glass objects produced via DLP by Moore et al. (2020)*
Transparent and dense object with high geometric complexity.

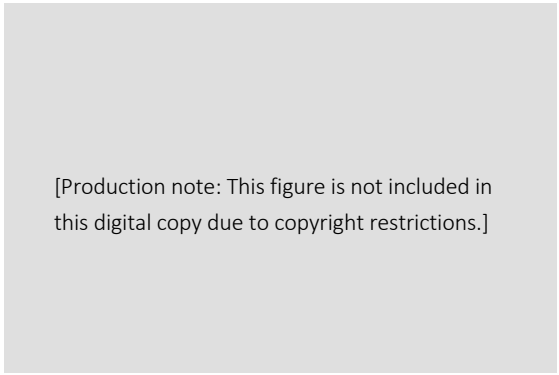

Figure 2.28. *Glass 3D printed object at different stages of fabrication process (Moore et al., 2020).*
Left to right: printed and aged, pyrolysed and sintered.

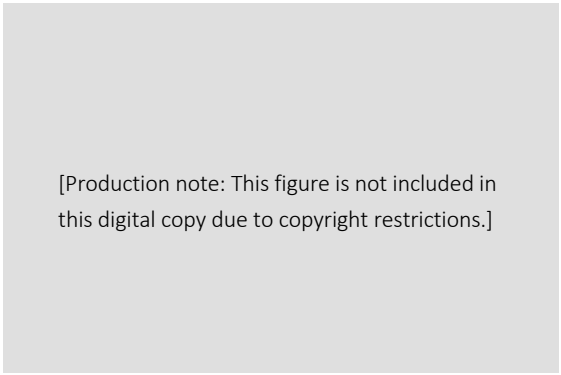

Figure 2.29. *3D printed microscale glass objects produced via TPP by Kotz et al. (2021).*
Scale bar represents 0.5mm.

Figure 2.30. *Powder fed DED method of printing onto a glass bottle substrate (Spirrett et al., 2021).*
3D printed using soda lime silica glass.

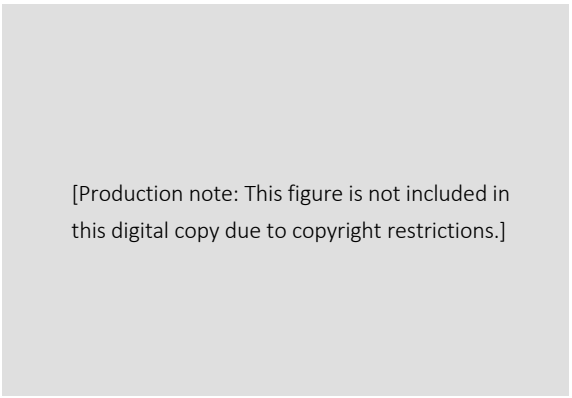

Figure 2.32. *DED printed quartz glass cylinder (von Witzendorff et al., 2018).*
20 mm cylinder diameter.

Figure 2.31. *DED printing process by von Witzendorff et al. (2018).*

rudimentary structures, often with low accuracy have been produced. In a recent doctoral thesis, Spirrett (2021), demonstrated a DED method using glass powder. Soda lime silicate powder was fed through a Teflon powder feed hose and melted using a laser. This process was explored with an industry partner for the specific application of glass bottle décor and is still in the early stages, only achieving single layer structures (see Figure 2.30).

Currently, DED research only uses virgin glass however there is potential for recycled glass to be used in the future. Recycled glass rods could be fabricated as is done for Maple Glass's FDM machine or recycled glass powders could be utilised in the DED process presented by Spirrett (2021). It may be possible for glass fines to even be utilised as feedstock here. However, even if recycled glass was used, the high-powered CO_2 lasers used in DED are energy intensive. Limits to geometric complexity like those associated with FDM printing also exist; overhangs and internal geometries are unachievable, and intricate parts have not yet been achieved. For this research, access to DED technologies is also a barrier, as this equipment is often high in cost or custom-built and can require significant infrastructure to ensure safety and maintenance.

2.4.5 Powder bed fusion

Left out of some discussions on glass 3D printing are powder-based methods. An obsession with the optical transparency of glass has seen these methods overlooked. In their review, Zhang et al. (2022) leave out technologies that do not provide transparent results. This devalues glass, overlooking its potential as a ceramic with high durability and chemical resistance. Furthermore, in the case of glass fines, the mixed colours and grades of soda lime silicate mean that turning them into a transparent glass is impossible to achieve without extensive processing. As a result, powder printing methods have the potential to utilise glass fines, particularly as soda lime glass is often the chosen type of glass used in this technique.

Powder bed fusion is a 3D printing process in which thermal energy is used to selectively fuse powder particles in specific regions on a powder bed (see Appendix 1.4) (ISO/ASTM International, 2016). Selective Laser Sintering (SLS) and Selective Laser Melting (SLM) are two types of powder bed fusion 3D printing which have been explored with various glass materials. A layer of glass is spread across the print bed and a high energy laser beam is used to melt (in the case of SLM) or partially melt (in the case of SLS) the powder according to the required layer geometry. The workbench then moves down, and another layer is spread on top. Density is frequently discussed in powder bed fusion glass printing, as incomplete densification of glass powders leads to light scattering, resulting in the opaque parts. (Klein et al., 2015).

Klocke et al. (2004) appear to be the first to utilise an SLS process in the 3D printing of glass. They use borosilicate glass due to its low thermal expansion properties and tested a range of printing parameters in the fabrication of 20 x 20 x 10mm cubes. They were able to find suitable parameters for the fabrication of porous glass parts with 48.6% of the theoretical density. However, a major drawback was the formation of cracks, assumed to be a result of thermal shock – the rapid change in temperature caused by the laser. Applying thermal post-processing at 700°C helped reduce these cracks and slightly enhanced the density to 54.4%. Despite this, the tests were still of low fidelity and did not provide a convincing demonstration of SLS 3D printing for glass.

Several years later, Fateri & Gebhardt (2015) built on this process, finding parameters that could produce soda lime silica parts with 93% material density, smooth surface, and no crystallinity. Parts continued to be opaque and had similar hardness to conventionally fused silica. They presented a variety of geometries,

including domes, intersecting rings, and square matrices, to demonstrate how the technique could be utilised in various applications, such as jewellery and prototyping (see Figure 2.33 and Figure 2.34). They produced a further conference paper on the SLM glass 3D printing of jewellery (Fateri & Gebhardt, 2014).

Datsiou et al. (2019, 2021) also presented research on a powder bed fusion technique using soda lime silicate. They noted that whilst the parts printed via this technique are opaque, there are several applications where the complex geometries and chemical stability that are achieved are useful; they particularly explored the applications in continuous flow reactor and structure catalyst applications. They evaluated the mechanical and physical properties of the parts finding that they were approximately 10% porous however the pores appear to be fully enclosed. They found that the flexural strength is significantly lower than standard float glass. As such, further work needs to be done to improve the mechanical properties. This work presents the most advanced geometries in powder bed fusion of glass to date (see Figure 2.35). However, the surface quality and accuracy is still poor.

A more novel approach to powder bed fusion of glass is Marcus Kayser's work, Solar Sinter. Aiming to raise questions about energy consumption and material usage, Kayser utilised sunlight and sand to produce glass objects in the desert. A large lens was used to focus a beam of sunlight at a box of sand mounted beneath it (see Figure 2.36 and Figure 2.37). This created temperatures between 1400-1600 degrees Celsius, hot enough to melt the silica sand and build the glass shapes layer by layer (Etherington, 2011; Kayser, 2011). Whilst an interesting and effective design project, this is of course not a feasible manufacturing method.

Powder bed fusion printing with glass remains limited to virgin material. This is unfortunate, as the use of recycled glass, especially recycled soda-lime silicate, appears feasible. Nevertheless, the process requires further refinement. While some degree of geometric complexity has been demonstrated, printed components typically exhibit limited dimensional accuracy and poor surface quality. Additionally, issues such as pores and cracks, which can form during printing, have been identified as significant challenges that need addressing (Xin et al., 2023). The technique can also be energy-intensive and expensive due to the operation of high-powered lasers. Like DED printing methods, this acts as a further barrier to utilisation in this research with glass fines.

2.4.6 Binder Jetting

Binder jetting is similar to powder bed fusion but utilises a liquid bonding agent rather than thermal energy. The liquid bonding agent is selectively deposited onto a bed of powder to join the particles together (see Appendix 1.5) (ISO/ASTM International, 2016). Once printed, the parts are excavated from the powder bed and post-processed, usually by sintering in a kiln to fuse the glass particles together. This technique of 3D printing was one of the first to be applied to glass as it overcomes the challenges of high melting temperatures and high viscosity (Klein et al., 2015). BJT is also a low energy form of 3D printing (not requiring high powered lasers of heating elements) that allows for highly complex geometries to be made without the need for support material. The accuracy of glass parts has been demonstrated to be far superior to some FDM, DED and powder bed fusion methods.

However, like powder bed fusion, BJT of glass produces opaque parts due to the incomplete densification of the glass powders (Nguyen et al., 2017). The focus on transparency in glass 3D printing has meant that little research has been conducted into this method since the early testing.

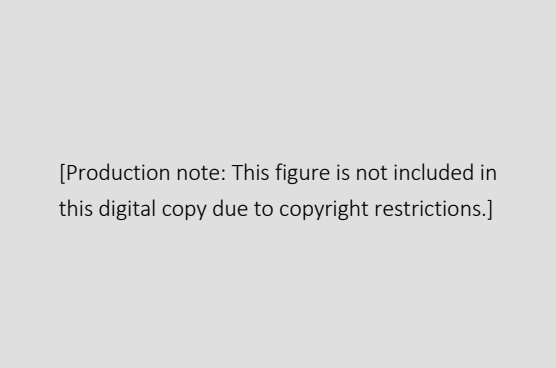

Figure 2.33. *Dome geometry fabricated using glass SLM process (Fateri & Gebhardt., 2015).*

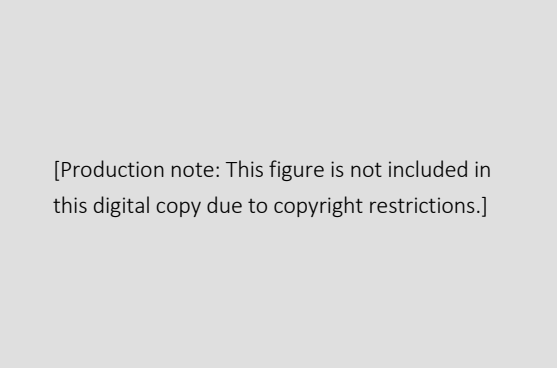

Figure 2.34. *Demonstrative bone artefact fabricated using glass SLM process (Fateri & Gebhardt., 2015).*

Figure 2.35. *Gyroid lattice structures in 3D printed glass using an SLM process (Datsiou et al., 2015).*

Figure 2.36. *Solar Sinter, Marcus Kayser, 3D printer (2011)*
A custom 3D printer used for the in-situ SLS of silica sand. Image: Kayser Works.

Figure 2.37. *Solar Sinter, Marcus Kayser, Print in Progress (2011)*
SLS print in progress, a large lens was used to focus a beam of sunlight onto the silica sand. Image: Kayser Works.

This represents a missed opportunity, as it overlooks the valuable properties of glass beyond transparency. It also ignores potential functionalities and material expressions that can be achieved by harnessing the technical capabilities of BJT. As a result, this research treats the opacity of BJT parts not as a limitation but as an opportunity for new design, aesthetic and functional exploration in glass materials, one that can expand perceptions of traditional glass materials and their applications.

Marchelli et al. (2011) pioneered a method of glass BJT. They mixed powdered maltodextrin into glass powder and developed a water, alcohol and food colouring liquid bonding agent. Using a commercial binder jetting machine (ZCorporation 310), layers of the glass and maltodextrin mixed powder were spread across the print bed and the liquid binding agent was selectively deposited to build objects layer by layer before excavating the part and post processing it. They tested two postprocessing techniques, infiltrating the part with paraffin wax and kiln firing. The wax infiltration technique is used widely in binder jetting to densify the parts. This improved the strength and surface finish of the parts. In the post processing via kiln firing, two methods were utilised; a direct firing processes where the object was placed directly on the kiln shelf; and a 'settering' process where the object was submerged in an inert powder, such as alumina. The settering process allows the inert powder to support the glass structure as it is being fired as the glass will start to slump and flow when it reaches a certain temperature in the kiln. This is the only seminal paper on glass 3D printing that utilises both virgin and recycled glass, with complex forms printed in both (see Figure 2.39 and Figure 2.38).

Marchelli et al. (2011) also outline preliminary experimental data on shrinkage, porosity, and density of binder jetting with recycled glass powder. They find that when fired at 760°C, the porosity of the part reached a minimum of 0.36 percent, demonstrating that the 3D printed recycled glass can approach a fully dense structure. They also discuss the significant anisotropy of the shrinkage with up to 23% difference in shrinkage between the z axis and x-y axes. The research only provides documentation of the sintering of cube shapes- more complex geometries that are presented in the paper remain unfired (Figure 2.40). This research originated from the Solheim Rapid Manufacturing Lab at Washington University, which has worked extensively in binder jetting with novel materials. They have published various recipes and processes on their Open3DP blog, including this experimentation with recycled glass. They adopt a more engineering-focused approach to the materials rather than exploring potential applications (Dunn, 2017).

Furthermore, Marchelli et al. (2011) claim that this research directly led to 3D printing bureau Shapeways, releasing a recycled glass 3D printing option (see Figure 2.41). However, lack of consumer demand, resulted in Shapeways ceasing this option in 2012 (just two years later). Since then, there has been no development of this technology either in literature or industry. It is hypothesised that the absence of any discussion or demonstration of application is the reason for this. Along with the difficulty in knowing how to design for the system as designing for anisotropic shrinkage is a particular barrier. In the service offered by Shapeways it also appears that parts are tack fused in a kiln, meaning the glass particles stick together but are not fully fused into a dense, waterproof object. This could mean they are fragile and porous, a further barrier to application. Arlotti & Knor (2015) filed a patent for a version of binder jetting with glass powder. The patent was initially filed in 2010, around the same time as Marchelli et al.'s (2011) work was published and was accepted in 2015 with the binder jet 3D printing company ExOne as the assignee. Their invention outlines a binder jetting process which is used to form the initial glass part. It is then sintered in a bed of inert powder with high flowability to support the form as the glass slumps in the kiln – essentially the settering process outlined by Marchelli et al. (2011). They present two examples of objects that could be made via this process (see Figure 2.42) a vase and a tile both with ornate, intricate details.

Figure 2.38. *Binder jet 3D printed artefact using virgin glass by Marchelli et al. (2011).*
Complex geometry with high accuracy, pre firing or wax infiltration.

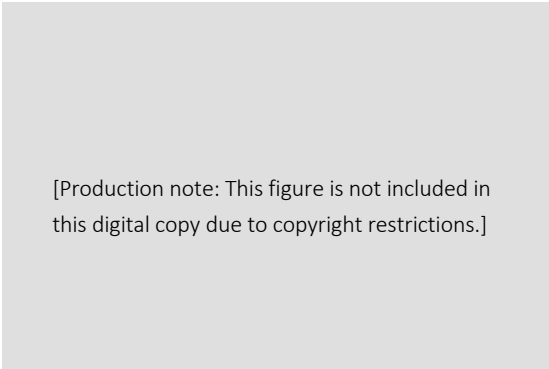

Figure 2.40. *Sintering tests conducted with binder jet recycled glass samples by Marchelli et al. (2011).*
30mm cubed samples reveals anisotropic shrinkage. Sample on the far right was fired at 760 degrees Celsius, achieving 99.64% density.

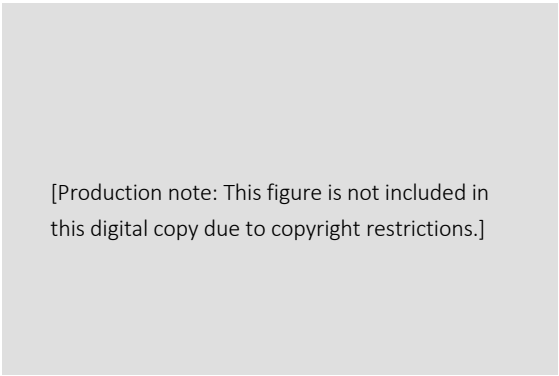

Figure 2.39. *Binder jet 3D printed artefact using recycled glass by Marchelli et al. (2011).*
An identical file to the example above was printed however the recycled glass part shows coarser resolution due to increased particle size and layer thickness.

Figure 2.41. *Complex geometry produced by Shapeways glass 3D printing service.*
Part does not appear to have undergone post processing. Image: Shapeways.

Figure 2.42. *3D printed glass vase printed by Shapeways and presented in Arlotti & Knor's patent (2015)..*
The vase was hand painted with leaded glass enamels. Image: Shapeways.

More recently, Cho et al. (2020) investigated the influence of powder characteristics on the shrinkage of binder jet printed glass structures. They utilized a commercial binder jet printer to build hollow cube structure with an open top and sintered them in a kiln. They compared glass frits and glass beads, finding that spherical glass beads were the closest to isotropic shrinkage.

Marchelli et al. (2011) established a strong precedent for the use of recycled glass powders in binder jetting. Although it is presumed that a relatively pure form of recycled glass was used in their testing, glass fines could most certainly be employed here as minimal additional material processing would be required. The ability to build parts at room temperature eliminates distortions, shrinkage, and cracking typically caused by thermal stresses during printing (Gibson et al., 2021). Given the variation in glass compositions present in glass fines, room-temperature processing is likely advantageous for achieving more consistent printing outcomes. Additionally, printing at ambient conditions enhances the accessibility and scalability of BJT, as it removes the need for costly sealed chambers or laser-based thermal systems. The technology is also recognised for its ability to rapidly produce complex geometries (Mostafaei et al., 2021). In BJT, the surrounding powder bed supports the printed part throughout the process, reducing geometric constraints and eliminating the need for support structures (Du et al., 2020). Although some researchers have positioned part opacity as a barrier, this viewpoint overlooks new material aesthetics and functionalities that can be explored. As such, this strong academic foundation, combined with the technological advantages of BJT, highlights the significant potential for the upcycling of glass fines via this method. However, as indicated by the above studies, successful application will depend on understanding and implementing the right post-processing strategies. Addressing this will be a central focus of the present research.

2.4.7 Recycled Glass 3D Printing

The conducted literature review revealed that recycled glass 3D printing generally is extremely limited. Other than the two examples mentioned previously; Marchelli et al (2011) utilizing recycled glass powders in their binder jet printing and the Canberra based start-up Maple Glass using recycled glass filament in their FDM machines; there is very little research in the area. Recycled glass printing literature focuses almost entirely on composite materials, particularly concrete and polymers.

Using waste glass in concrete production enables the replacement of river sand, an over-exploited natural resource, and promotes the utilisation of abundant waste glass (Liu et al., 2022a). This approach is suggested as a means to enhance the sustainability of concrete production. Whilst this has been explored in cast concrete production as mentioned in Section 2.3.5 of this literature review, it has only recently been investigated for the 3D printing. Key studies have been conducted by Ting et al. (2019, 2021), Cuevas et al. (2021) and Liu et al. (2022a) with a focus on the different properties of the material. Ting et al. (2019, 2021) investigated the rheological and mechanical properties of 3D printed concrete containing different ratios and grades of recycled glass whereas Lui et al. (2022) investigated the microstructure and flexural strength of 3D printed concrete that contained 50% recycled glass and 50% river sand. Cuevas et al. (2021) on the other hand, investigated the thermal properties, incorporating expanded thermoplastic microspheres as well as glass particles to develop a light weight concrete.

Another area of research is the recycling of glass fibre composite materials via 3D printing. Rahimizadeh et al. (2019) investigate the viability of using glass fibre from reinforced waste turbine blades. By reclaiming

the short glass fibres from the waste blades and mixing them with the common thermoplastic printing material PLA, they create a new composite material for FDM printing. A series of mechanical tests were conducted to compare recycled glass fibres with virgin glass fibres. The results revealed that materials made with recycled glass fibres exhibited specific modulus and tensile strength values that were 18% and 19% higher, respectively, than those reinforced with virgin fibres. This is attributed to the fact that the surface of the recycled fibres were partially covered in epoxy which improved the bonding between the PLA and glass fibres. Several similar papers have been produced from the Polytechnic University of Milan in which shredded polymers containing glass fibres were remanufactured using 3D printing (Mantelli et al., 2019, 2021; Romani et al., 2020). In their most recent work glass fibre reinforced wind blades were shredded and combined with a UV curable acrylate resin which allowed for the UV assisted direct ink writing of the material (Mantelli et al., 2021).

Sander et al. (2020) explored the possibility of making stainless steel and recycled glass composites through SLM 3D printing. This is a previously unexplored avenue. They utilised glass powder waste, exploring the upcycling of this material whilst simultaneously investigating how it may allow for the reduction in cost, density (the density of glass is less than three times that of stainless steel) and the creation of unique physical properties. Their initial experimentation revealed that the glass powder did not remain in its original amorphous structure but transitioned to a crystalline phase, bonding to the stainless-steel matrix. The mechanical strength of the composite was inferior to that of SLM prepared stainless steel, but the authors believe there may be application areas that warrant further research into this space. Whilst these composite materials represent a potential avenue for utilising glass fines, they like many of the other current applications or glass fines, impede circularity, as recovering them would be difficult if not impossible.

Of most relevance to this research is an approach presented by Thomsen et al. (2020). Recycled glass powder is mixed into a paste and robotically extruded (see Figure 2.44). The paste formulation comprises of flour, water and glass, creating a clay like consistency. Ceramic stains are also added to colour the glass. Parts are sintered at 950°C and the flour burns away leaving a porous part. This method was used to prototype a series of tiles with varying patterns (see Figure 2.45). However, the parts incurred cracking and foaming in the kiln and require refinement in terms of accuracy in order to find application. This work was later developed by investigating a range of binders and exploring different aesthetic opportunities (Sparre-Petersen & Hnídková, 2023). Whilst compelling artefacts were produced, the work is aimed at the artistic glass field rather than industrial application (see Figure 2.45). There are further concerns over the circularity of the material as the final binder is a Titebond glue that may leave residue in the firing process.

This method is similar to work conducted by the Material Ecologies Design Lab at the University of Technology Sydney, where this thesis is situated. In 2020, a robotic paste extrusion system was developed for the 3D printing of glass fines. Greater resolution and a firing temperature of almost 200°C lower was achieved. This work became the precursor to this dissertation and will be discussed in detail in Chapter 5.

This review of recycled glass 3D printing literature reveals a significant gap. Most work focuses on using recycled glass in various 3D printed composites, just three examples have been found that use only glass or process the prints to a glass state. There is, therefore, significant opportunity for research into recycled glass 3D printing.

Figure 2.43. *3D printed glass fines on blown glass fines forms by Sparre-Petersen & Hnídková (2023).*
The glass fines material was blown into forms with a dark greenish brown colour that appears black when the glass is thick. The 3D printed object is preheated in a kiln before being attached to the blown shape and the fused object annealed.

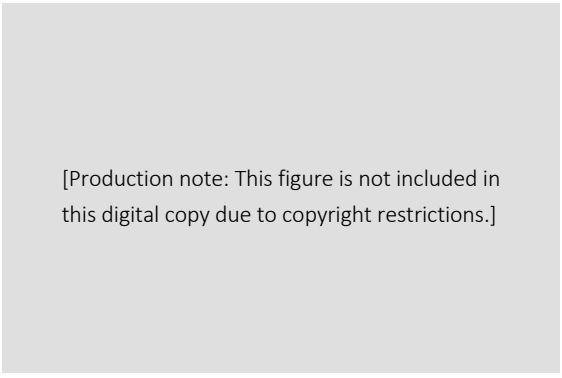

Figure 2.44. *Robotic material extrusion system for the printing of glass fines paste by Thomsen et al. (2020).*

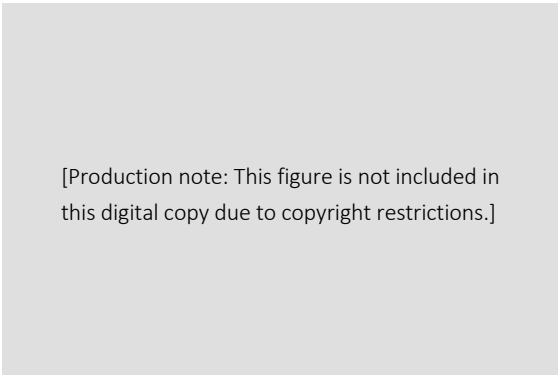

Figure 2.45. *Final 3D printed tile made from glass fines by Thomsen et al. (2020).*

2.5 Material and production positioning

As glass can be endlessly remelted and formed into objects without impacting the material quality, it has the potential to be a key material in the circular economy. However, not only is the glass recycling rate very low in Australia, the comingled and highly mechanised sorting process creates the low value by-product of glass fines. These small particles of mixed glass represent 30% of all recovered glass in Australia. The construction industry has begun to find use for them as sand and aggregate replacement in roads and pipe embedment projects. Although this represents a solution to the stockpiling of glass fines, these applications downcycle the material, representing an economic loss for glass recyclers. Glass is a valuable material with important properties such as hardness and chemical durability. As a result, there is significant opportunity to develop higher value applications of glass fines. Such applications will also provide opportunities to overcome the economic barriers of utilising glass fines as a waste stream.

3D printing can provide a way forward. By harnessing the capabilities of 3D printing, particularly in terms of complex geometries, customisation and localisation, new applications can be envisioned. These applications can not only 'use up' glass fines but take advantage of the unique properties of glass and extend their use. To understand the current state of the art in glass 3D printing, a literature review was conducted. Whilst there is limited research using recycled glass, the use of virgin glass is a growing field as it can allow for previously unachievable forms to be created. This has been developed across a range of 3D printing technologies, including fused deposition modelling, directed energy deposition, vat photopolymerisation, direct ink writing, powder bed fusion and binder jetting. Each of these technologies has associated benefits and limitations.

Fused deposition methods which extrude molten glass layer by layer were pioneered by MIT and Micron DP. They received great attention due to the creation of complex forms in optically transparent glass. Several researchers further built on their work, developing extrusion systems for different glass compositions. The only example of the material extrusion of recycled glass is by the aforementioned start-up Maple Glass that utilise recycled glass filaments. Accuracy and geometric complexity are limited as support structures cannot be used. This type of glass 3D printing can also be energy-intensive due to the high temperatures needed to melt and anneal the glass. As such, few applications for this type of 3D printing have been explored, mostly remaining in the decorative arts space.

Vat photopolymerisation methods have been heralded by some researchers as the most promising due to the highly complex, accurate and transparent results. Generally, glass nanoparticles are dispersed in a liquid photopolymer, which is cured by light-activated polymerisation. The use of highly controlled compositions of nano-sized glass presents a barrier to the utilisation of recycled glass via this method. This is also the case for direct ink writing methods of glass 3D printing. Furthermore, the use of sacrificial petrochemical-based photopolymers is environmentally detrimental. The relevance to this dissertation is therefore limited.

Directed energy deposition methods of glass 3D printing have also been presented. However, existing research focuses solely on virgin glass, despite the possible application of recycled glass filaments and powders with this technique. The outcomes so far have been limited, producing only rudimentary shapes with low accuracy. Furthermore, the use of high-energy lasers presents a significant obstacle to broader application.

Powder based methods of glass 3D printing have received less attention due to the opaque nature of the parts they produce. Although for optical applications these methods are unsuitable, this disregards numerous other applications where material properties such as the high durability and chemical resistance of glass are highly

beneficial. Additionally, it overlooks new aesthetic possibilities and functionalities that can be explored. Furthermore, in the case of glass fines, the mixed colours and grades of soda lime silicate mean that turning them into a transparent glass would be impossible to achieve without extensive processing. This means that products made from glass fines are likely to be opaque regardless. As a result, powder printing methods have been identified as offering significant potential to utilise glass fines.

There are two types of powder-based 3D printing methods, powder bed fusion and binder jetting. Several researchers have demonstrated the printing of soda lime silicate and various other glass compositions via powder bed fusion. However, the process needs extensive development as parts are generally lacking accuracy and have poor surface quality. Binder jetting on the other hand, has been used to 3D print complex and accurate parts in both virgin and recycled glass. This is the only 3D printing method, other than FDM that has been used to print in recycled glass. Marchelli et al (2011) pioneered this method using a maltodextrin binding agent and proposed several postprocessing options including sintering of the glass in a kiln to produce a dense glass object. This research led to 3D printing bureau Shapeways offering a glass binder jet option in 2010. However, just two years later the option was ceased due to a lack of consumer demand. Since then, there has been little development of this technology either in literature or industry. It is hypothesised that an absence of discussion or demonstration of application is the reason for this as well as difficulty in knowing how to design for the system and account for shrinkage of glass parts in the kiln. Although it is presumed that a purer form of recycled glass was used in Marchelli et al's (2011) testing, glass fines could be employed here.

This literature review has revealed that whilst extensive literature exists on the 3D printing of virgin glass, there is extremely limited research in the 3D printing of recycled glass. Most work focuses on the incorporation of recycled glass in various 3D printable composites which limit the circularity of the material in the long term. There is therefore significant opportunity for further development of recycled glass 3D printing and in particular the investigation of glass fines as the feedstock. The analysis of virgin glass 3D printing has allowed for binder jetting to emerge as the most suitable technology for using glass fines. This is due to the high accuracy and complexity it provides along with lower energy and ability to use a non-uniform recycled feedstock. This research builds on the work of Marchelli et al. (2011) by employing glass fines and developing potential application avenues.

2.6 Conclusion

This chapter has presented and analysed the literature relevant to this research. The chapter began by introducing the Circular Economy as the conceptual framework that underpins the work. The overall concept of the CE was discussed, along with its relevance for designers, potential for 3D printing technologies and critiques. The next section, introduced the material waste stream of glass fines, providing context on glass manufacturing, recycling and the limitations in current applications of glass fines. This allowed for the opportunity to find higher value applications for glass fines to be clearly identified, something which can be enabled by 3D printing. The final section reviewed the current state of the art in glass 3D printing. The opportunities and limitations of each technology were recognised, allowing for binder jetting to be identified as a technology with significant potential for the use of glass fines. This is due to its powder-based nature, complex geometric capabilities, scalability and accessibility. This literature review led to the formulation of an overarching research question with three sub questions related to the material, production and application. These will be presented in the next chapter.

3

Methodology

3 Methodology

3.1 Introduction

This chapter introduces the methodology employed in this research. Based on the findings of the literature review, one overarching research question has been formulated, with three sub questions. These relate to the three interconnected areas of material, production and application. As highlighted throughout this dissertation, neither one of these areas can be suitably addressed without the other. To answer these research questions, a Research through Design (RtD) methodology has been employed. This chapter will begin by providing the background and context of RtD before discussing four key areas: the role of prototyping, how the researcher moves through the project, documentation methods, and ways of evaluating the research. These areas will be discussed in relation to how they are employed in this research, thereby presenting a specific and tailored RtD methodology which is ultimately enacted through iterative and evaluative cycles of prototyping. This methodology is also informed by thinking from the field of materials design. Whilst materials design methodologies are not employed in their entirety, certain elements will be discussed in relation to this research. A summary and research diagram will then be presented as a visual representation of the methodology, followed by the limitations of scope and information on navigating the experimentation sections of this project.

3.2 Research Questions

This dissertation is structured around one overarching research question with three sub-questions specific to the interrelated areas of material, manufacturing and design and application. To address these questions, a RtD methodology has been designed and applied.

1. How can recycled glass fines be transformed into a product application using a binder jet 3D printing system that can remain in a closed circular loop?
    a. What are the requirements of a material formulation that remains circular?
    b. What are the manufacturing process steps and parameters?
    c. What product application can be developed that demonstrates the opportunities of the material and production system?

3.3 Research Through Design

This dissertation adopts a research through design methodology (RtD). RtD refers to the use of design practices and methods as a way of generating knowledge. Historically, design and research have been viewed as very distinct practices. Design has been viewed as an industrial practice or craft where activities such as prototyping are used to develop new commercial products. On the other hand, research has been seen as an academic practice of experimentation and reflection which aims to produce new knowledge (Stappers & Giaccardi, 2017). Yet design and research are surprisingly related, particularly in their aims to create something new by building on what is already known (Stappers & Giaccardi, 2017). As design has entered the academic sphere through university faculties and PhD courses, this view of research and design as separate endeavours has shifted significantly and much discussion around the use of design to produce knowledge has been presented. RtD is the term that has been given to this. Whilst RtD is now an accepted methodological approach to research, much debate around the specific terminology, models and practices continues.

The term RtD was initially coined by Christopher Frayling in 1993. In a small working paper, Frayling described three categories of research in design; research into art and design, research for art and design and research through art and design (Frayling, 1993). The first category refers to a traditional approach to research in which historical or theoretical perspectives about design are presented. This is often based on archival research and the external study of specific objects, phenomena or history in design. The second category refers to when the research and thinking is embodied in the artefact and is, therefore, not verbally communicable. By Frayling's own admission, this is a 'thorny' concept, and the term was later repurposed to mean research done during the design process to inform the design of the object (Findeli, 2008).

It is the third category however that gained the most traction. Frayling's explanation of research through art and design, which was later shortened to research through design (or RtD), is the closest to actual design practice, whereby design activities such as prototyping are undertaken to generate knowledge. Amongst others, he gives an example of relevance to this research; the work of Micheal Row, who studied the colourisation and patination of different metals. Row's RtD dissertation resulted in a series of replicable methods of achieving specific colours and effects in metals as well as a series of exhibited designed artefacts made using the recipes. Frayling states that this work takes a problem outside of design and uses design methods and practices to address it (Frayling, 2015). Whilst Frayling's initial definitions continue to be critiqued, especially for their choice of terminology and lack of clarity, he opened the door for the argument that design practice can generate communicable knowledge (Herriott, 2019; Jonas, 2007; Krogh & Koskinen, 2020).

Since this publication, extensive transformation has occurred in RtD. As described by Stappers & Giaccardi, (2017), four 'pockets of energy' in the discourse emerged in the UK, US, Netherlands and Scandinavia. The HCI community in the US became particularly prominent. In 2007, Zimmerman et al. built on Frayling's work in the context of interaction design. Similarly to Frayling, they emphasise that the designer's role in RtD is not making a commercially viable product but making a knowledge contribution. They describe how this is achieved by integrating knowledge from other disciplines (namely engineering, anthropology and behavioural science) and applying it to the construction of an artefact which will transform the world to a preferred state. Through this process, knowledge is produced which can be fed back into those three disciplines, such as technical opportunities for engineers or behavioural impacts that can be discovered through further research of the artefact in use. They also highlight that the artefact becomes a design exemplar that can act as a conduit to communicate knowledge with industry. In later work they provide the succinct definition that will be adopted in this research: RtD is 'a research approach that employs methods and processes from design practice as a legitimate method of inquiry' (Zimmerman et al., 2010, p. 310).

The authors cited above along with many others have contributed to several methodological questions in RtD. These questions range from the type of knowledge that is generated (Krogh & Koskinen, 2020) to the communication and documentation of that knowledge (Pedgley, 2007). There have also been calls by some authors to formalise the methodology with explicit methods and criteria (Zimmerman et al., 2010) whilst others have instead advocated for the need to embrace the diversity of approaches (Gaver, 2012). Some authors have proposed new terminology such as 'constructive design research' (Koskinen et al., 2011) whilst others have argued that the differences between RtD and traditional research methodologies are minimal (Herriott, 2019). Whilst these debates are still in flux, most authors acknowledge that the central aims of RtD are the same: to generate knowledge by employing design methods.

What is important to note is that although RtD is now a well-established methodological approach, there is no singular method by which RtD is conducted. As in design practice, design researchers' activities, methods and processes vary greatly. As such, RtD is often positioned as an overarching methodological framework that is characterised by a diversity in approaches. Whilst this contributes to the richness of the research culture, it can be confusing when attempting to align a project with RtD and requires researchers to develop their own specifically tailored RtD methodology. As a result, the following sections will discuss how this dissertation operationalises RtD by addressing the key areas of the prototyping, how the researcher moves through the project, documentation methods and ways of evaluating the research.

3.3.1 Prototyping

One thing agreed upon in RtD literature is that prototyping and making are central to this methodological approach (Stappers & Giaccardi, 2017). The use of prototypes in typical design practice is well documented, defined by Houde and Hill as 'any representation of a design idea, regardless of medium' (Houde & Hill, 1997, p. 369) with the four broad purposes of: evaluation and testing; understanding the user; idea generation and communication among designers (Lim et al., 2008). However, Koskinen & Frens (2017) highlight that these 'design or industrial prototypes' differ from 'research prototypes' in their definition and function. They highlight that 'research prototypes' are used to test a theory and generate knowledge rather than test product viability or commercialisation. When reviewing seven RtD projects, Stappers & Giaccardi (2017) found that each project included a series of prototypes which were produced as steps in generating knowledge about the research problem. However, they explained that the role of these artifacts varied, the way they were constructed varied and the way that they were placed in relation to earlier knowledge varied. This emphasises that there is no one way of utilising prototypes in RtD and so it is important to be clear about how prototypes will be used in this research.

Prototyping is the primary data collection method that will be utilised in this study. Drawing on the work of Wensveen & Matthews (2014), this prototyping will occur in three forms to fulfil different purposes and ultimately answer the research question. These roles include the process of prototyping as a vehicle for inquiry, prototyping as an experimental component and prototyping as a research archetype.

The process of prototyping as a vehicle for enquiry will be the primary type of prototyping used. This refers to when the process of making the artefact is the main contribution to the research rather than the artefact itself. The making process is documented, analysed, and written up as a research contribution. Wensveen and Matthews (2014) give the fitting example of a doctoral project in which the student aimed to establish new ways of producing Hellenistic and Roman mosaic glass. To develop this, they engaged in extensive experimentation with glass-making practices. As such, the method of conducting the research and the result of the research were both a new practice of making glass. The same thinking can be applied to this dissertation, where the prototyping process of 3D printing with glass fines is both the method and object of the research. Therefore, prototypes as vehicles for enquiry will be a key data collection method. The knowledge built through making these prototypes, such as the impact of certain printing parameters or binder formulations, will be documented, analysed and presented (according to the method outlined in section 2.3.3). Figure 3.1 shows an example of a prototype as a vehicle for enquiry, where the process of making the objects is the generator of knowledge and not the artefacts themselves.

Figure 3.1. *Experiment 6.02, an example of prototyping as a vehicle for enquiry.*
The process of making the printed glass parts generated knowledge.

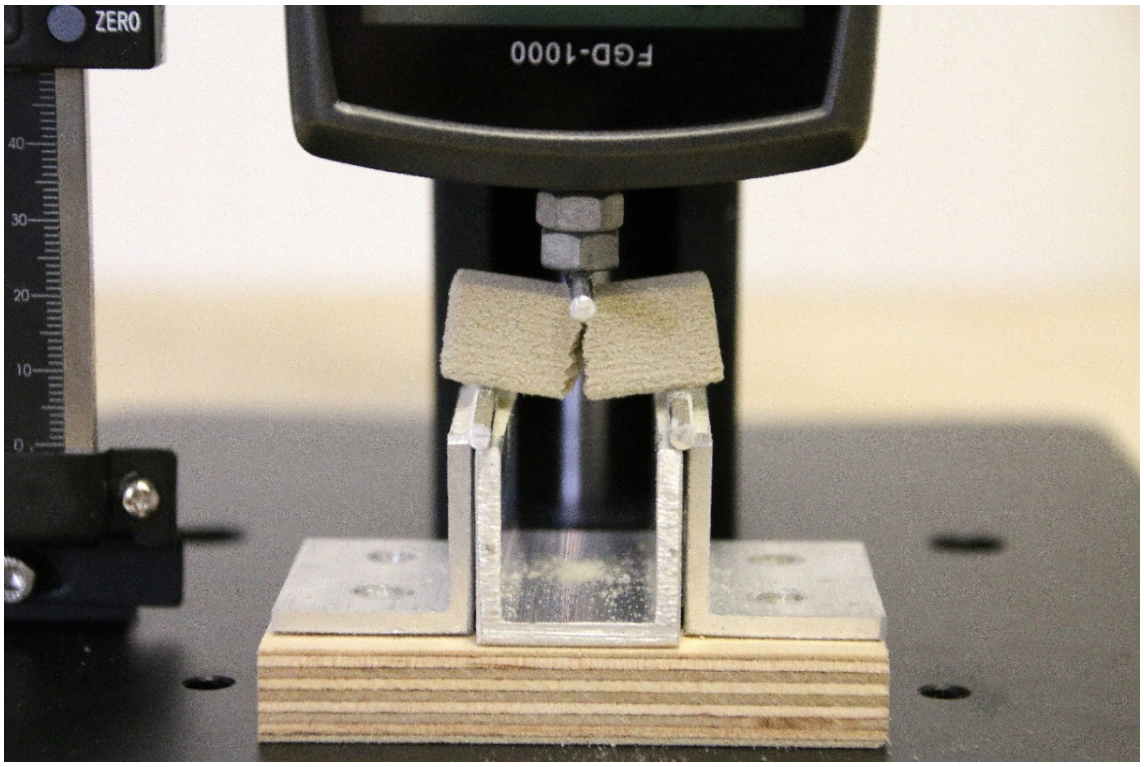

Figure 3.2. *Flexural strength testing of 3D printed parts, an example of prototyping as an experimental component.*
This testing was conducted to verify the adhesive strength of different binders.

Prototyping as an experimental component is most akin to traditional scientific research, where prototypes are constructed to test specific hypotheses. In these cases, the prototype usually physically embodies the hypothesis (i.e. a specific form or function) and is then subjected to testing (e.g. usability or material tests). In this type of prototyping, the design of the experiment or testing is equally as important as the construction of the prototype itself. In this dissertation, prototypes as experimental components are utilised in testing and verifying specific material properties and processes. For example, Figure 3.2 shows flexural testing, which was performed to assess the adhesive strength of different binders used in the printing. It is important to note that these prototypes do not necessarily produce publishable scientific data but can be used to provide information on the best avenue for the research.

Prototypes as research archetypes will also be used. This is where prototypes are used to demonstrate the research; they are physical embodiments of research concepts. These prototypes are primarily illustrative, representing a concept with broad application but that needs specific examples to demonstrate its full potential. This is particularly relevant in this research, as whilst there are numerous possible applications of the material and production system, the thorough investigation and presentation of a specific application allows for the full potential of the research to be communicated. These kinds of prototypes are also often referred to as demonstrators, which are defined as application-led investigations that enable the research to interface with real-world constraints (Thomsen & Tamke, 2009). This definition highlights that through the development of this type of prototype, significant knowledge is also generated. This dissertation will use prototypes as research archetypes to showcase one potential application of the material and production process. These prototypes will be used to gain feedback and ultimately exhibit the work undertaken in this dissertation.

To summarise, these three types of prototyping enquiries: prototyping as a vehicle for inquiry, prototyping as an experimental component and prototyping as a research archetype, will be used to generatively build knowledge in pursuit of the overarching research question. Prototyping as a vehicle for enquiry is conducted throughout the project through iterative experimentation with material formulation, print settings and firing schedules. At points during this process, prototypes as experimental components will be used to verify specific assumptions or hypotheses (e.g. which binder is strongest). To signal this change in the type of experimentation, sections of the document which present prototypes as experimental components have been visually signalled using a light grey page background. As the application potential of the material and production process becomes more apparent, a prototype as a research archetype will be developed to demonstrate the results and potential of the research. Employing all three forms of prototyping is crucial to the methodological approach as it allows for designerly experimentation to be combined with scientific validation and technological feasibility.

3.3.2 Moving through the project

Whilst prototyping is defined as the core means of inquiry in RtD, it is often not articulated how these experiments are carried out in a journey or chain of building knowledge (Krogh et al., 2015). In RtD literature, several authors have discussed the relationship between ‘experiments’, mostly prototypes or sketches, and the ‘program’, which refers to the overarching aim of the research (Brandt & Binder, 2007; Koskinen et al., 2011; Redström, 2011). In this view, the ‘program’ acts as a foundation or frame for

carrying out a series of 'experiments' (Redström, 2011).[7] Stappers (2007) represents this thinking diagrammatically in the 'Research Spiral' seen in Figure 3.3 (Stappers, 2007; Stappers & Giaccardi, 2017). In this image, the central arrow signifies the project's overarching goal ('the program') while the spiral represents iterative prototyping activities that advance toward this goal. The sprisal also symbolises the generative and evaluative cycle involved in prototype development — an idea or prototype is generated, and the outcomes are assessed to push the project forward. In this research, the central arrow is the overarching research question. Iterative prototyping cycles are designed to address the three sub-questions relating to material, production and application, ultimately leading to a realisation of the central research question.

To be more specific about how these iterative prototyping cycles will occur, the work of Krogh and Koskinen is valuable. First published by Krogh et al. in 2015 were five typologies of how designers 'drift' in RtD projects. This concept of 'drifting', initially described by Redstrom (2011), refers to how design researchers move through and between experiments. Krogh & Koskinen (2020) explain that design researchers do not 'drift' accidentally like driftwood but intentionally and controlled, like a car in a rally. They argue that this is a methodic practice which occurs in five patterns or typologies (see Figure 3.4), ranging from 'accumulative', in which in-depth knowledge is developed around a precise topic through experiments which each study a specific variable, to a more explorative 'probing' approach in which a diverse range of experiments are conducted to discover or unpack a less defined research area (Krogh & Koskinen, 2020).

Two types of drifting are evident in this research: serial and expansive. The serial typology is most familiar to designers and is used the most in this research. This refers to design experimentation in which the knowledge generated from one experiment is integrated into the subsequent experiment, evolving as they are conducted. This typology is particularly evident in the early experimentation in Chapter 4 in which prototypes sequentially build on each other by adjusting the production parameters and material formulation step by step. Expansive drifting is also evident. This typology is defined by a broadening of knowledge which best resembles geographers mapping new areas. Unlike serial experiments, this is not based on a linear trajectory but takes a more open approach to investigating different areas and ideas. In this research, expansive drifting is most evident when different geometric forms are being investigated. Seemingly unconnected forms and different approaches to designing for the glass material are presented in order to broaden understanding about what is possible. These points of drifting result from evaluating and reflecting on the results of experiments; they are not illogical jumps but a reframing or adjusting of goals.

Whilst other disciplines may see drifting as a problematic concept, signifying inconsistency or illogical jumps, Krogh and Koskinen argue that this is a hallmark of design practice. It indicates that a designer can continually learn from findings, adjust or reframe their actions and pursue alternative opportunities to arrive at a high-quality and relevant outcome (Krogh et al., 2015). Key moments of drifting will be documented and explained to allow for the research decisions and outcomes to be traceable and transparent (this will be further discussed in the next Section 3.3.3).

[7] Brandt & Binder (2007) discuss how this aligns with professional design practice, where the 'program' is the design brief provided by a client and the 'experiments' are the prototyping and design activities used to respond to successfully to this brief.

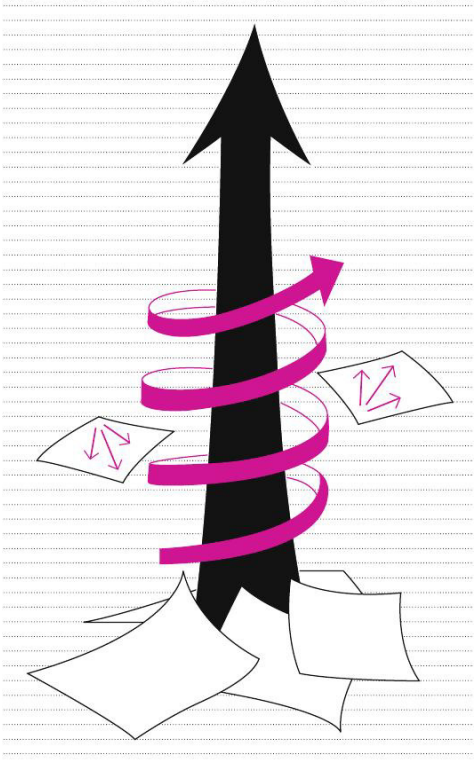

Figure 3.3. *Research Spiral by Stappers (2007).*

ACCUMULATIVE	COMPARATIVE	EXPANSIVE	SERIAL	PROBING
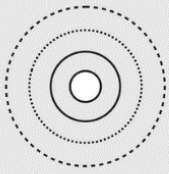	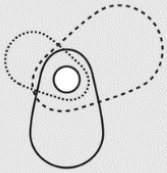	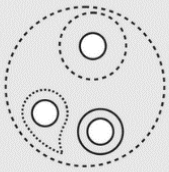	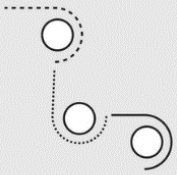	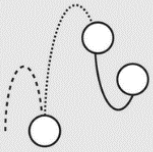
Keyword **Depth, stacking**	Keyword **Acknowledging complexity**	Keyword **Broadening, extending**	Keyword **Systematising local knowledge**	Keyword **Illogical, artistic, impact oriented**
Author **Frens**	Author **Ross, Fogtmann, Wu**	Author **Dindler, Trotto**	Author **Lynggaard, Bang**	Author **Busch, Worbin**

Figure 3.4. *Five typologies of drifting by Krogh & Koskinen (2020).*

This pursuit of a high-quality outcome, an application or a 'success', is the reason for most drifting. Design researchers are rarely satisfied with reporting on a singular 'failed' experiment but will adapt and pursue the research goal until a satisfactory outcome is achieved. It is for this reason that much of the experimentation is grouped into 'sets' of prototypes rather than singular experiments.

Each set of prototypes has an overarching aim, yet multiple experiments are conducted to find a satisfactory outcome before reporting on the results. For example, in finding preliminary printing parameters to produce basic shapes, six individual experiments were conducted which consecutively build on one another. By the sixth test, these preliminary settings have been determined and the key findings from across the six experiments are reported on (see Section 4.6.1). The individual findings of each experiment can be found in the Appendix. This is done for cohesion and clarity of the written document.

3.3.3 Documentation

A significant concern in RtD discourse has been around documentation. It has been pointed out by Zimmerman et al. (2010) that systematic and rigorous documentation can be lacking in RtD projects. This is problematic as documentation is critical to capturing and translating the generated knowledge, allowing the project to be seen as a scholarly activity rather than pure design practice (Bardzell et al., 2016; Sadokierski, 2020). Pedgley (2007) argues that RtD projects require 'systematic and effective methods for capturing and analysing own design activity, so that the resultant data may be used as a credible evidence base' (2007, p. 480). He argues that this 'methodological transparency' through documentation is essential due to the 'autobiographical' nature of design processes and how human conditioning can influence design acts. As Pedgley (2007) points out, in practice 'designers draw on tacit knowing and intuitive decision-making' a 'designerly way of knowing' that evolves over time (Cross, 2007). Whilst this is highly valued in practice (Schön, 1992), these types of subjective insights are problematic in RtD. It has been argued that these insights must be made explicit and communicable to be considered research (Herriott, 2019).

The difficulties surrounding documentation are likely due to the nature of the projects themselves; What is the best way to capture iterative experimentation? Insights from self-reflection and peer critique? Decisions driven by tacit knowledge? Or more broadly, how is it best to document a dynamic process where the research goals and design objectives may change and morph along the way (Bardzell et al., 2016; Sadokierski, 2020)? Due to the complexity of these questions, only a few models have been presented in RtD discourse. The most prominent of these likely include Pedgley's design diary (2007), Gaver's annotated portfolios (2012) or Dalsgaard & Halskov's digital Process Reflection Tool (2012) . Whilst each have their place, the diversity of RtD approaches means these methods are not widely agreed upon or relevant to every project.

Bardzell et al. (2016) point out the role of reflection in documentation. The act of documenting in RtD is not merely the capturing of data or facts; it is a generative act that 'talks back' to the researcher, allowing for reflection, evaluation and analysis. This is supported by Mäkelä & Nimkulrat, (2018), who elaborate by presenting the argument that documentation facilitates two steps of reflection, as coined by influential academic Schon: reflection in action and reflection on action (1992). They explain that when design researchers engage in critical documentation, they consciously reflect on experiences during the process of designing or prototyping (reflection in action) and on experiences after the process (reflection on action).

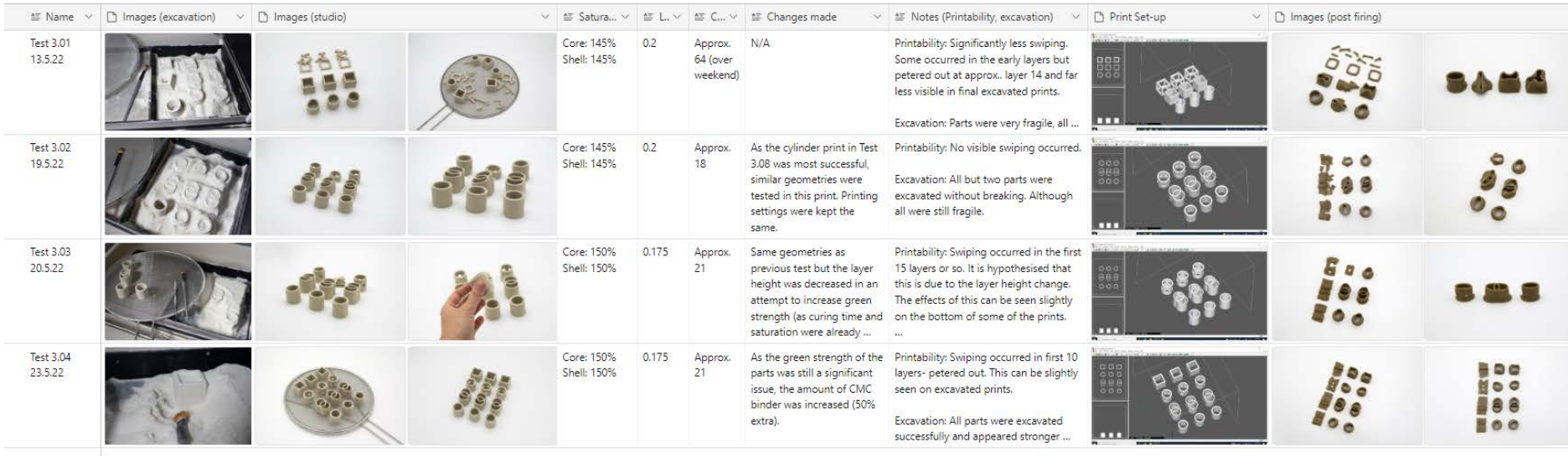

Name	Images (excavation)	Images (studio)	Satura...	L..	C...	Changes made	Notes (Printability, excavation)	Print Set-up	Images (post firing)
Test 3.01 13.5.22			Core: 145% Shell: 145%	0.2	Approx. 64 (over weekend)	N/A	Printability: Significantly less swiping. Some occurred in the early layers but petered out at approx.. layer 14 and far less visible in final excavated prints. Excavation: Parts were very fragile, all ...		
Test 3.02 19.5.22			Core: 145% Shell: 145%	0.2	Approx. 18	As the cylinder print in Test 3.08 was most successful, similar geometries were tested in this print. Printing settings were kept the same.	Printability: No visible swiping occurred. Excavation: All but two parts were excavated without breaking. Although all were still fragile.		
Test 3.03 20.5.22			Core: 150% Shell: 150%	0.175	Approx. 21	Same geometries as previous test but the layer height was decreased in an attempt to increase green strength (as curing time and saturation were already ...	Printability: Swiping occurred in the first 15 layers or so. It is hypothesised that this is due to the layer height change. The effects of this can be seen slightly on the bottom of some of the prints. ...		
Test 3.04 23.5.22			Core: 150% Shell: 150%	0.175	Approx. 21	As the green strength of the parts was still a significant issue, the amount of CMC binder was increased (50% extra).	Printability: Swiping occurred in first 10 layers- petered out. This can be slightly seen on excavated prints. Excavation: All parts were excavated successfully and appeared stronger ...		

Figure 3.5. *Excerpt of experimental log entries in Airtable.*
Images of the process and final prototypes are integrated with data on the print parameters and notes analysing the results.

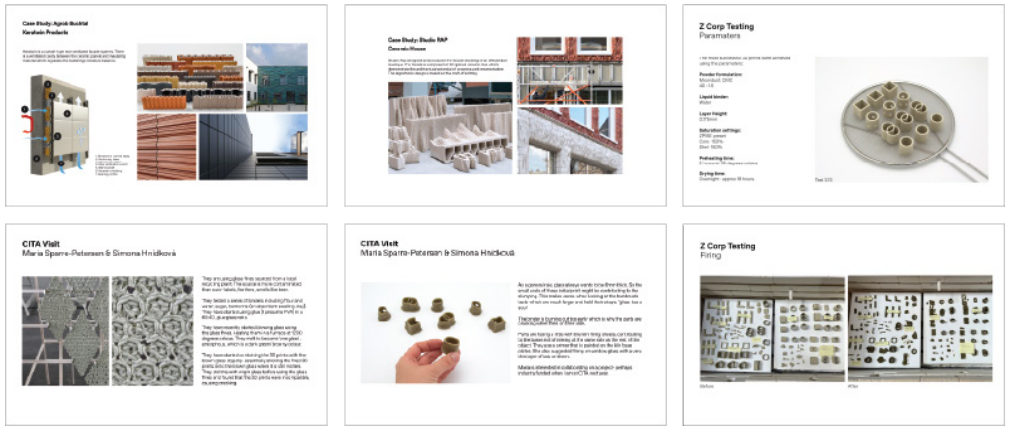

Figure 3.7. *Excerpt of digital slides.*
Containing peer critique, contextual anchors and testing. This is used as both a tool for reflection and documentation of progress and a way of sharing updates with supervisors and peers.

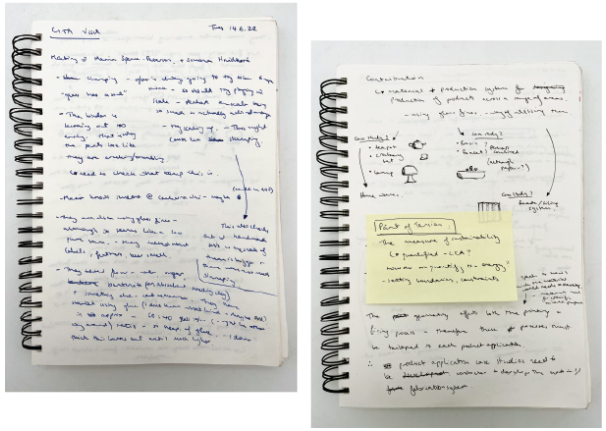

Figure 3.6. *Ongoing design diary.*
Captures reflections, peer critique and reframing of the research direction.

This allows for both learning through making to occur and helpful evaluation and analysis that can lead to new ideas or directions.

Sadokierski (2020) provides a comprehensive set of documentation guidelines for RtD researchers that captures many of these concepts. The documentation methods for this research are drawn from this work. She explains that critical and rigorous documentation practices in RtD aim to convincingly demonstrate how original and transferable knowledge has emerged through practice. The primary method of documentation utilised in this dissertation is a reflective experiment log. For each prototype, a log is created which records the aim, process and reflections. These are dated and archived chronologically. The logs are created using the online platform Airtable, which allows for multiple mediums and aggregations of the data to be added and rearranged (see Figure 3.5). As such, high-quality photographs, text and videos are integrated into the logs. The visual nature of this documentation method is particularly useful for materials-based projects, as it allows for clear capturing of material qualities and results.

This process of documenting also facilitates continued reflection on action and records any insights that may have resulted from reflection in action, allowing for the next prototyping experiment to be formulated. Relevant literature is also incorporated if required to aid in the explanation and analysis of specific results. As stated in the previous section, the written experimentation chapters present many of the prototypes in 'sets' rather than as singular experiments. This allows for the primary findings that have driven the research to be cohesively communicated whilst incremental findings from each prototype can be found in the Appendix.

Sadokierski also suggests three other methods: documenting and reflecting on peer critique; capturing and analysing contextual anchors such as literature or case studies which inspire a design process; and progressively creating overview maps which 'map the big picture' of the research. Although these are less formally incorporated into the research documentation, these methods are present in a handwritten design journal (see Figure 3.6) and an ongoing series of digital slides (see Figure 3.7). Critique from supervisors, colleagues and external researchers is integrated with case studies of existing work and planning of research directions. Similarly to the experimental logs, these documentation tools allow for continual reflection and evaluation of the research. Knowledge gathered from these sources is integrated with the experimental logs to form the basis of the written experimentation chapters.

3.3.4 Evaluating and Sharing

Various authors have discussed evaluation criteria for RtD projects, giving differing perspectives on what constitutes 'good' RtD (Brandt & Binder, 2007; Gaver, 2012; Prochner & Godin, 2022; Zimmerman et al., 2007). As with the other discussion areas in this chapter, there is no widespread consensus. Zimmerman et al. (2007) and Prochner & Godin (2022) have put forward clear guidelines, whilst Gaver (2012) has argued that normative standards could inhibit diversity in RtD and in turn stifle a thriving research culture. While Gaver's points are valid, it is difficult to see how either of these guidelines would inhibit diversity, given their lack of prescriptiveness and the clear room to interpret, adjust and extend the guidelines to fit a particular RtD project. As such, Zimmerman et al's (2007) guidelines will underpin the research agenda to ensure quality of outcome. They will be used at seminal points or interactions to frame the direction and evaluate the current state, and they will be used when describing the contribution and outcomes of this research.

In their writing, they specify four lenses for evaluating design research contributions:

1. Process- The process of an RtD project must be documented clearly and in enough detail that it could be reproducible by others. This further speaks to the 'traceability' or 'transparency' of the research contribution; as Brandt & Binder (2007) write, RtD 'involves a traceable genealogy, an intervention in the world and the articulation of an argument for others to engage with' (Brandt & Binder, 2007, p. 3).
2. Invention- The contribution must be novel; a unique integration of various knowledge which addresses a specific situation. Literature must be used to situate the concept.
3. Relevance- The work must be framed in terms of the real world and the preferred state the project attempts to achieve. If science researchers emphasise validity, design researchers emphasise relevance. This further speaks to a general applicability of the research in the real world and creating a positive impact (Prochner & Godin, 2022).
4. Extensibility- The contribution must be usable as a basis for new research, which means that it is documented and communicated in a way that other researchers can leverage and build upon it.

Evident in these guidelines is the dual audiences that RtD speaks to. As Krogh and Koskinen point out, design researchers aim to do work that design practitioners will 'understand, respect and take seriously' (Krogh & Koskinen, 2015, p. 121). This means that design researchers are accountable and speaking to the RtD community and design practitioners. As Krogh and Koskinen acknowledge, juggling these two audiences is difficult. It means that the project must have an 'eye for generalisability' and 'an eye for applicability', the dual striving for knowledge and effect (Stappers, 2007). It also must demonstrate a rigour in the process as required by the research community, and in the aesthetic and functional sensibility required by design practitioners. These dual audiences also mean that the research contribution will be shared, not only via formal academic publications, including this dissertation, but also through exhibition and online platforms, whereby the designed artefacts and prototypes will be exhibited alongside documentation of the process.

3.4 Materials Design

This research also sits within the emerging field of materials design. As discussed in Chapter 2, in recent years, materials skills and hand-making processes have regained importance in design, with a growing group of designers who are no longer satisfied with simply specifying materials and are instead engaging with material experimentation and self-production (Pedgley et al., 2021). This has become a well-recognised area of design that sits at the intersection of design, materials science, biology, engineering and crafts, and has fostered collaboration across these areas (Barati & Karana, 2019). The RtD methodology outlined in the previous section has been tailored to a materials-based project, and as a result, key concepts from this field have informed the approach. Whilst specific materials design methodologies have not been enacted, some key concepts from the field are evident in this methodology.

Hands-on material manipulation has long been integral to design, with artisans crafting unique artifacts for centuries. However, the introduction of industrial processes created a divide between intent (design) and making (production), leading to an emphasis on theoretical knowledge of material properties and processes rather than hands-on involvement (Pedgley et al., 2021). The materials design field has rejected this approach; instead of designing a specific product or function and forcing a material to fit, the material itself is the starting

point of the design process and its potential is uncovered through hands-on experimentation. This establishes a two-way exchange between material and designer, establishing an exploratory and practical design process rather than a more theoretical one (Ferreira et al., 2025). These concepts were embedded in a methodology developed by Karana et al. (2015) called material driven design (MDD). This approach aims to understand and integrate both the technical and experiential qualities of a material to unlock meaningful user experiences and design potential. This is an approach which considers our experiences of materials beyond their utilitarian value. Whilst the MDD methodology has not been adopted in its entirety in this dissertation, this is seminal work in the materials design field which positions the material as the explicit starting point in the design process and highlights the importance of hands-on experimentation by designers.

As such, the importance of material explorations or 'tinkering' practices are fundamental in materials design. This is an explorative practice in which designers interact with the material, engaging in cycles of creation and evaluation (Karana et al., 2015). This process allows for an in-depth understanding of the material attributes and constraints to be formed, which is necessary to design with a material effectively. This practice of tinkering is embedded in what Rognoli et al. (2015) call DIY materials. These materials are produced through individual or collective self-production processes. They can be entirely new or modified versions of existing materials, often created using techniques invented by the designer themselves. This DIY approach has been enabled by the democratisation of production technologies, such as 3D printing and wider access to information about manufacturing processes. They describe how the approach is characterised by 'learning by doing' in which designers test, re-test and adjust materials and production processes. This approach to material experimentation is embedded in this research, particularly in the form of prototypes as vehicles for enquiry.

Barati and Karana (2019) articulated the contribution of design to material development projects, highlighting that this contribution goes beyond simply 'coming up with' application ideas. Instead, they demonstrate how designers contribute to both the final application and development process by harnessing the material form, functionality and experience (the emotions, meanings and actions it elicits), and by unlocking novel material affordances. The concept of affordances is well discussed in design theory and broadly refers to the possibilities for action that are offered by a product or environment. In this context, the material affordances are described as 'what a specific material has to "offer"' in the collaborative process (Barati & Karana, 2019, p. 116). The authors state that through skilful engagement, designers perceive, invent, and exploit novel material affordances, which contribute to the process of material development, not just the product outcome. They explain how these affordances can arise through spontaneous discovery, where unexpected results or accidents occur, and through the invention of new techniques, or modification of existing ones. They provide the example of the Polyfloss machine, which repurposes a fairy floss machine to process plastic into lightweight foam materials. This takes advantage of the affordances of plastic to discover new methods of recycling it.

Barati and Karana (2019) also point to the way materials design practices break certain norms around manufacturing and material choices, with many examples of design activity that exploits what are often considered undesirable characteristics or materials. They highlight the work of Menges and Reichert (2012), who harness the often undesired swelling properties of wood to create moisture-responsive forms. This designerly practice of perceiving and exploiting material affordances is embedded within this dissertation, guiding the material, production and application development.

A key element of materials design projects (and RtD projects generally) is the integration of knowledge from various fields. This often takes the form of cross-disciplinary collaboration, but is also facilitated by the growing accessibility of fabrication tools and open exchange of information regarding manufacturing processes (Rognoli

et al., 2015). This is evident in a material-driven design methodology presented by Ribul et al. (2021) which draws on materials science and design processes. In their methodology, specifically developed for textiles, they outline three phases: exploration, translation, and activation. The exploration phase is grounded in materials science, with tests conducted to identify interventions and benchmark the process. The translation phase merges material science and design, validating and visualising the findings. The final activation phase is rooted in design, drawing on the insights from the first two stages to inform a design vision and application prototyping. The experimentation in this dissertation is structured into three chapters (Chapter 4-6) which largely align with the stages of experimentation, translation and activation. Chapter 4 focuses on understanding and developing a workable production process and material, Chapter 5 begins to validate and explore how these findings could manifest and Chapter 6 develops a design application.

The RtD methodology outlined in Section 3.3 is informed by and tailored to a materials design project. As such, relevant approaches from the field of materials design have been highlighted and discussed in relation to how they inform this research. The key concepts which have been drawn on are the centrality of the material, the processes of experimentation and self-production, the identification and harnessing of novel material affordances and the three stages of testing highlighted by Ribul et al. (2021). It is important to note that the temporal orientation of this work differs from many materials design methodologies. Methodologies such as MDD and DIY materials typically operate within speculative timeframes (10-20 years), whereas this research is aligned with a nearer-term horizon (0-5 years). Consequently, the emphasis is placed on more practical industrial and design applications, requiring an approach that combines designerly experimentation with scientific validation and technological feasibility.

3.5 Summary and Research Diagram

This dissertation adopts an RtD methodological approach that is primarily enacted through iterative and evaluative cycles of prototyping. As this project is focused on materials, approaches from the field of materials design are also evident in the methodology. Consequently, design practices such as prototyping, sketching, and 3D modelling, together with systematic material experimentation, will be employed to generate knowledge that guides the development of a material, production process and application.

Prototypes will be the primary means of data collection in this project. Drawing on the work of Wensveen & Matthews (2014) they will be utilised in 3 specific ways;

2. process of prototyping as a vehicle for inquiry- the process of making the prototype is the main research contribution and is documented thoroughly (i.e. 3D printing parameters, binder formulations).
3. prototyping as an experimental component- prototypes are constructed and then used in an experiment to test a specific hypothesis (i.e. material strength).
4. prototyping as a research archetype- prototypes developed as demonstrators of the research (i.e. façade cladding components made from 3D printed glass fines).

These prototypes will be structured in a series of iterative ‘experiments’ that will become steppingstones towards the overarching research goal. This ‘serial’ typology of moving through an RtD project means that the knowledge generated through one prototyping experiment will be used to frame the direction of the subsequent one (Krogh & Koskinen, 2015). The methodological approach can be seen in the research diagram in Figure 3.8.

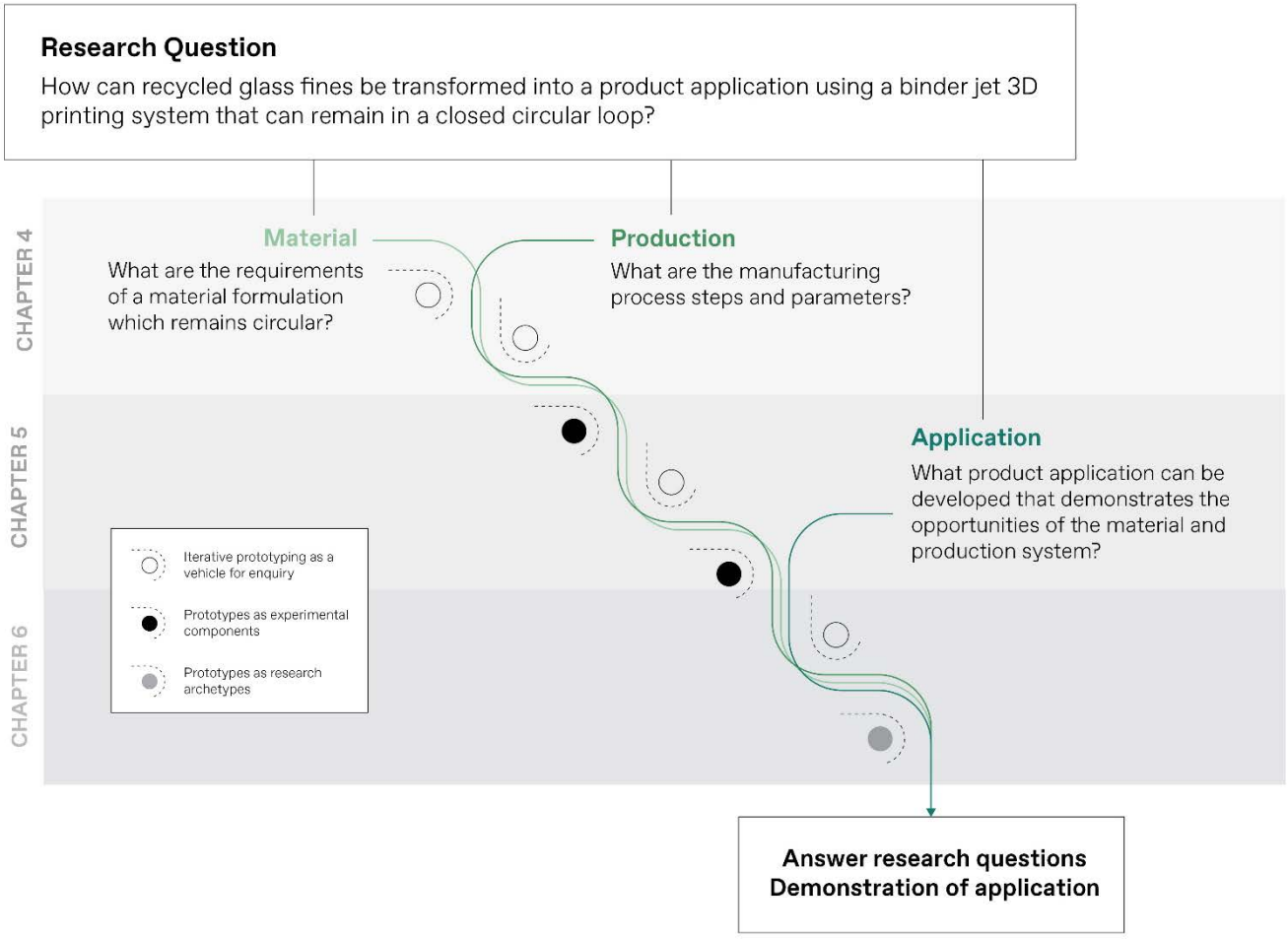

Figure 3.8. *Research Diagram*
Different types of prototypes are employed in a chain of building knowledge. The three key threads of the research questions, underpin and guide this prototyping. At the beginning of the research, the prototyping is focused on material and production. As the material properties and the capabilities of the production system become clearer, potential applications emerge and these can begin to drive the research.

In this research diagram the iterative prototyping is depicted in the same style as the 'serial' experimentation presented by Krogh & Koskinen (2020), as a series of cascading circles. The directional outline around the circles demonstrates how knowledge is fed from one prototype to the next in pursuit of the overarching research goals. It is important to note that whilst elements of 'expansive' drifting are also evident in the research, the findings from these prototypes are still ultimately fed into the next. The prototyping enquiries follow a cascading path made of three threads representing the three sub-research questions relating to the material, production process and application. These three areas overlap and are interconnected with each impacting the other. At the beginning of the research, prototyping enquiries focused on the glass fines material and BJT production system are conducted. As the material properties and production capabilities emerge, potential applications can be explored and begin to drive the research.

These prototyping inquiries will be documented thoroughly via reflective experimental logs integrating text, images and video (Sadokierski, 2020). These are used to capture important information about the inquiry; aim, method, results and analysis and facilitate reflective practice that allows for ideas to emerge and be captured (Bardzell et al., 2016). Further documentation practices including analysis of contextual anchors such as case studies and literature, peer critique, and continual re-examining of the overarching design goal will be captured in a written journal and digital slides.

The RtD contribution will be evaluated according to guidelines set by (Zimmerman et al., 2007). The process will be clearly documented with enough detail to be reproducible by others. The contribution will be a novel integration of various knowledge that addresses a specific situation. The work will be framed in terms of the real world and the preferred state the project wishes to achieve. Furthermore, the contribution will be usable as a basis for further research by others. This research will further be structured around speaking to two audiences; RtD community and design practitioners. This means that new knowledge will be built and presented in a traditional thesis and will be presented in the form of a designed product application.

3.6 Limitations of Scope

This dissertation will generate a method of transforming glass fines using a BJT system into a product application which highlights the capabilities of the material and production system. Only one application will be demonstrated in this research. This will act as a demonstrator of the material and production process, allowing for interfacing of the research with real-world constraints (Thomsen & Tamke, 2009). There are other possible application directions which will be discussed but not realised.

This research will demonstrate a method of the BJT of glass fines, it will not be the only possible method and will leave room for further experimentation and testing. As this is an RtD project, the focus is on developing and optimising the production process and material formulation for the specific application. It is not on empirically optimising 3D printing settings such as particle size distribution which is commonly seen in engineering and science-based binder jetting literature. As such, the material and production will remain in a proof-of-concept stage.

An important element of the project is that the material must remain circular. This means that any binders need to fully burn out during the firing process, leaving pure soda lime silicate glass which could be returned to a regular recycling stream or be crushed and reused in the same BJT production system. As a result, only

organic binders such as starches and cellulose will be used. Furthermore, the infiltration of parts using resins is a common post-processing method used in BJT literature to give parts increased strength and density. This use of resins and other plastics creates composite materials where the components cannot be separated at the end of life, often meaning that perfectly recyclable materials are sent to landfill. As such, firing the parts in a kiln will be the only post processing technique employed in this research as it will allow for strong parts to be created without the need for petrochemical based materials.

3.7 Navigating this project

Like many RtD and materials design studies, this project is complex and multifaceted. Developing a circular material, production method and potential application involves investigating numerous interconnected parameters ranging from print settings to firing schedules and binder ratios. As a result, there are a number of prototyping enquiries that must be conducted to address specific elements and variables in order for the overarching research aims to be achieved. Whilst this is common in RtD, the sheer number of parameters in this research, can make it difficult to understand how these individual investigations connect to the broader aims and arc of the research. To address this, several signposting techniques have been used in this document to guide the reader through the project.

Firstly, Figure 3.9 has been included to show how the Research Diagram connects to the prototyping activities and the Airtable documentation. This figure shows that for every prototyping enquiry, a number of individual experiments are conducted and documented to address the specific aims. As explained in Section 3.3.2, these individual experiments are performed sequentially, building on one another until satisfactory conclusions or results are achieved. Following that, a new prototyping enquiry with different objectives is initiated. These enquiries are always driven by the central research questions. Although not every individual experiment is included in the main body of this thesis, the full Airtable documentation is available in the Appendices.

Secondly, research diagrams have been included at the end of each experimentation chapter (Chapters 4, 5 and 6). These provide a summary or snapshot of the prototyping enquiries discussed and indicate where in the journey of answering the research questions we are. The diagrams resemble the one in Figure 3.8, showing which research sub-questions have been addressed as well as incorporating images and annotations to clearly communicate the prototyping enquiries. Consequently, these diagrams serve as reference points or a timeline of the research, enabling the reader to easily consult and understand the progression of the study. Thirdly, Section 4.4 introduces a diagram outlining the key parameters and variables involved in this project. It is referenced throughout the document to help readers understand the goals of various prototyping investigations. This is important as there are numerous variables—related to material, production, and application— which interact and influence one another in this research.

Finally, hyperlinks are present throughout the document to allow the reader to move between the Appendix, where a large amount of the experimental documentation is located, and the main text, and to click easily between each Figure. As explained in Section 3.3.1, segments of the document which present prototypes as experimental components have been visually signalled using a light grey page background. This highlights to the reader that there is a change in the type of experimentation, from qualitative designerly enquiry to quantitative scientific methods. These techniques aim to make it easier for the reader to navigate the complexity of this project effectively.

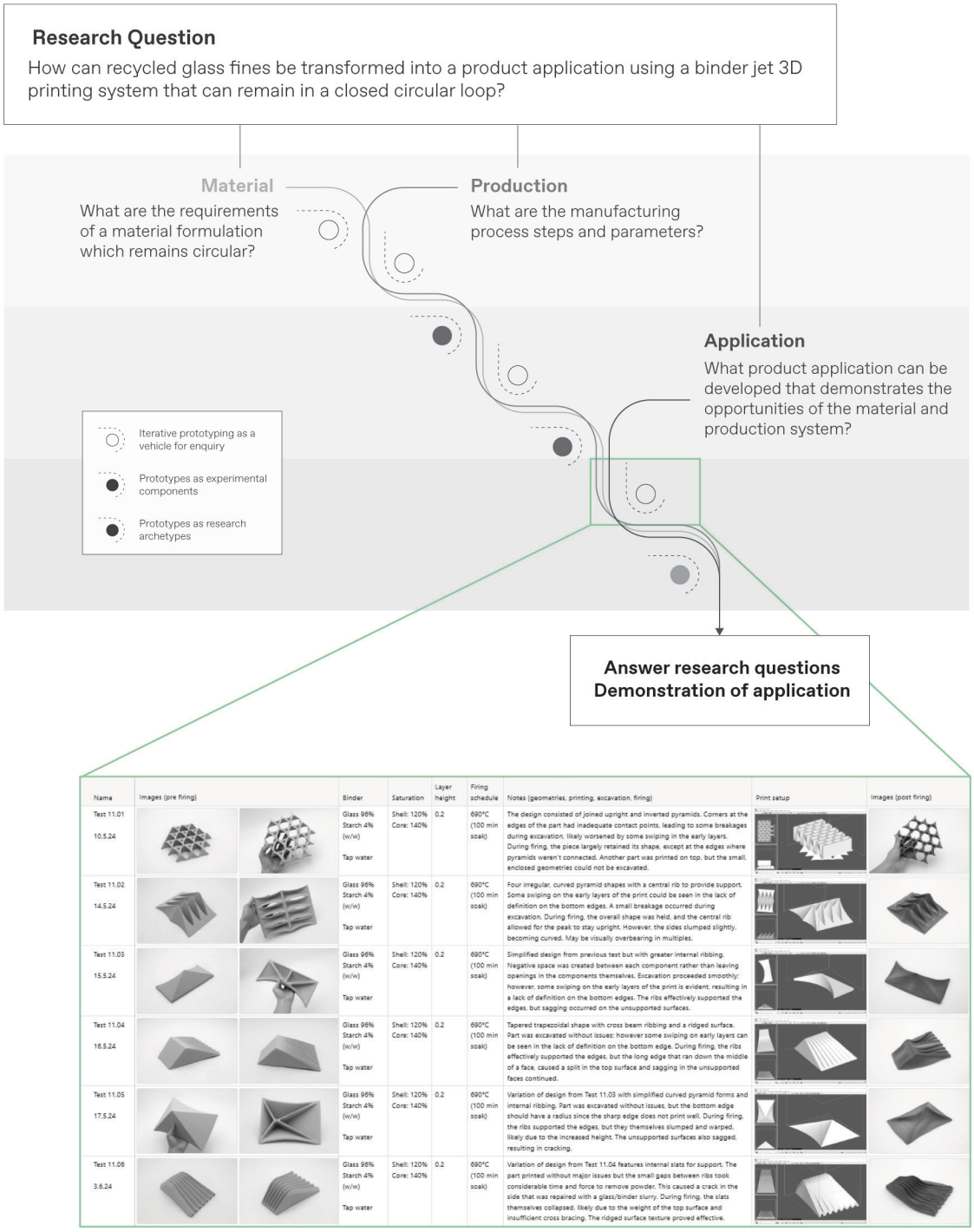

Figure 3.9. *Relationship between prototyping enquiries, individual experiments and overarching research goals.* Each prototyping enquiry is conducted in pursuit of the overarching research questions. Within each prototyping enquiry, a multitude of individual experiments are conducted and documented in an Airtable.

3.8 Conclusion

A Research through Design methodological approach will be adopted in this dissertation. Whilst this chapter has highlighted the diversity in approaches and differing views in the RtD community, it has also defined and argued for the specific approaches that will be utilised in this project. Prototyping will be the primary data collection method used with three different types of prototypes being employed; prototyping as a vehicle for inquiry, prototyping as an experimental component and prototyping as a research archetype (Wensveen & Matthews, 2014). The prototyping will be conducted in a serial manner whereby the knowledge generated from one prototype will inform the next. All prototypes will be rigorously documented in reflective experimental logs, which allow for the capturing, analysis and emergence of knowledge. The research diagram demonstrates how the prototyping enquiries systematically build on each other in pursuit of the research goals. The diagram also highlights that the research is made up of three interrelated areas; the material, the production process and the application which must come together to address the research question and produce a physical artefact which speaks to both the academic and design communities.

4

Preliminary Investigation: Material Formulation and Print Settings

4 Preliminary Investigation: Material Formulation and Print Settings

4.1 Introduction

This dissertation is structured around one overarching research question with three sub-questions specific to the interrelated areas of material, production and application:

1. How can recycled glass fines be transformed into a product application using a binder jet 3D printing system that can remain in a closed circular loop?
    a. What are the requirements of the material formulation?
    b. What are the manufacturing process steps and parameters?
    c. What product application can be developed which demonstrates the opportunities of the material and production system?

To answer these questions, experimentation in the form of prototyping has been conducted. This chapter will present the process and findings of the first stage of prototyping which focuses on developing the material formulation and print parameters. As the starting point of the experimentation was defined by previous work done with glass 3D printing, the first section of this chapter will briefly outline this prior work. Background information on the material and binder jetting production system will then be discussed, including the results of a scanning electron microscopy (SEM) analysis of the glass fines. The bulk of the chapter will then discuss this first phase of prototyping, starting with a series of manual tests which were conducted by hand. By the conclusion of the chapter, workable material formulation and set of print parameters will be presented. These will be tailored in the following chapters to suit a specific application.

4.2 Previous Work

Prior to this dissertation, we demonstrated the 3D printing of glass fines using a robotic paste extrusion system. This was a multi-step fabrication method in which a recycled glass powder was mixed into an extrudable paste, printed, dried, and then fired in a kiln. During the firing process, the binder burns out and a 100% fused glass object remains (see Figure 4.1). This multi-step method was chosen to avoid the need for high temperatures and specialised equipment as seen in the case of MIT or Maple Glass' extrusion systems (discussed in Chapter 2), making it a more accessible method to transform glass fines via 3D printing.

Developing an extrudable glass paste in which the binder could burn out was crucial for ensuring the circularity of the material. To establish this, existing techniques utilised in crafted glasswork were investigated. One such technique is Pâte de Verre which translates from French to 'pastes of glass'. Popularised in the Art Nouveau period in France, it involves grinding glass into a powder and combining it with a binding agent, typically gum Arabic or sodium silicate, to make a malleable paste that is spread into a mould and fired in a kiln (Hollister, 1988; Ørvik & Stewart, 2022). Adding metal oxides to impart colour is a key element (Cummings & Stewart, 2013; Vande, 2008). Depending on the desired effect, the glass can either be fired to a temperature in which the glass particles are tack fused, giving a sugar-like quality or can be fired into an amorphous state, giving a solid cast glass piece through which light can penetrate (Stewart, 2010). Leading Pâte de Verre expert, Max Stewart, writes that using an organic glue is crucial as the glue must burn away in the kiln without leaving any residue. In

his work, he found that inorganic or plastic-based glues, including wallpaper pastes that contain fungicides can leave a black residue. For our research, this is significant as it could impact the circularity of the material.

More modern iterations of the Pâte de Verre technique utilise the cellulose derivatives, methylcellulose (MC) and carboxymethyl cellulose (CMC) as the binding agent (Cummings, 2009; Ørvik & Stewart, 2022). MC and CMC are water-soluble derivatives of cellulose that are widely used in food and cosmetics. Sources high in cellulose such as wood biomass can undergo a series of physical and chemical treatments to obtain a range of cellulose-based derivatives (Kaarianen et al., 2020). To attain MC and CMC, natural cellulose is modified through an etherification. CMC is the most widely used cellulose derivative, acting as a thickener, , binder and stabiliser in diverse applications including paper making, textile processing and drug formulations (Heinze et al., 2018). CMC is usually purchased as a powder and when combined with water it forms a thick sticky liquid, depending on the ratio of water to CMC used (Jernegan, 2009). The use of CMC in glass fusing was also demonstrated in glass artist and writer Richard La Londe's 'liquid glass line' method (La Londe, 2006). It is now also a fairly common ingredient among ceramicists who use it to turn powdered glazes into a brushable medium (Jernegan, 2009; Kline, 2018). As a result, it is widely available at many ceramic suppliers. Despite this, CMC has yet to be utilised for the 3D printing of glass powders, let alone recycled glass fines. Therefore, we experimented with CMC as a binder for the paste extrusion of glass fines.

Through extensive experimentation, a recipe for an extrudable glass fines paste was developed. The paste needed to flow under pressure yet maintain its shape without collapsing once printed. To do this CMC (tylose) powder was hydrated in water to form a 6% solution. This creates a slippery, jelly-like consistency. Micro-fibrillated cellulose (MFC) was then dispersed through the solution. MFC is another product made via the physical and chemical processing of natural cellulose. It is essentially a mixture of cellulose fibrils in water, which appear as an interconnected web of nanoscale fibres (Herrick et al., 1983; Kaarianen et al., 2020). This was added to the 3D printing paste as MFC dispersions exhibit thixotropic properties, meaning that when force is applied to MFC, the viscosity decreases allowing for it to flow more easily, yet when the force is taken away the original viscosity recovers (Mewis & Wagner, 2009; Turbak et al., 1983). This is useful when printing pastes as it means that the paste can be deposited easily yet hold its shape once printed. A 10% dispersion of MFC was mixed with CMC and a small amount of water in a food processor at high speed for 30 minutes. This binder solution was then mixed by hand with the glass fines to form a dough-like paste. Various geometries were printed using a modified commercial Cerambot extruder mounted on a UR10 Universal robot (see Figure 4.1). These were left to dry and fired in a conventional kiln to form a fused, waterproof object (see Figure 4.2).

Whilst the developed material and extrusion method shows potential for upcycling glass fines, the system has significant limitations. These include accuracy, geometric complexity, and print size due to the consistency of the paste material which can deform or collapse when certain heights or geometries are printed and a lack of support structures. This drastically reduces application potential. Furthermore, paste extrusion can be unreliable and volatile due to clogging, air bubbles and changes in uniformity. Therefore, the powder-based 3D printing system utilised in this research addresses these limitations, allowing for highly accurate complex geometries to be more reliably produced. Several critical elements from the previous work were adopted in this research. These include the multi-step printing and firing process, the firing schedules developed to fuse the glass particles in the kiln and the use of cellulose binders. These elements were starting points for the experimentation in this research but developed and shifted as new knowledge was discovered.

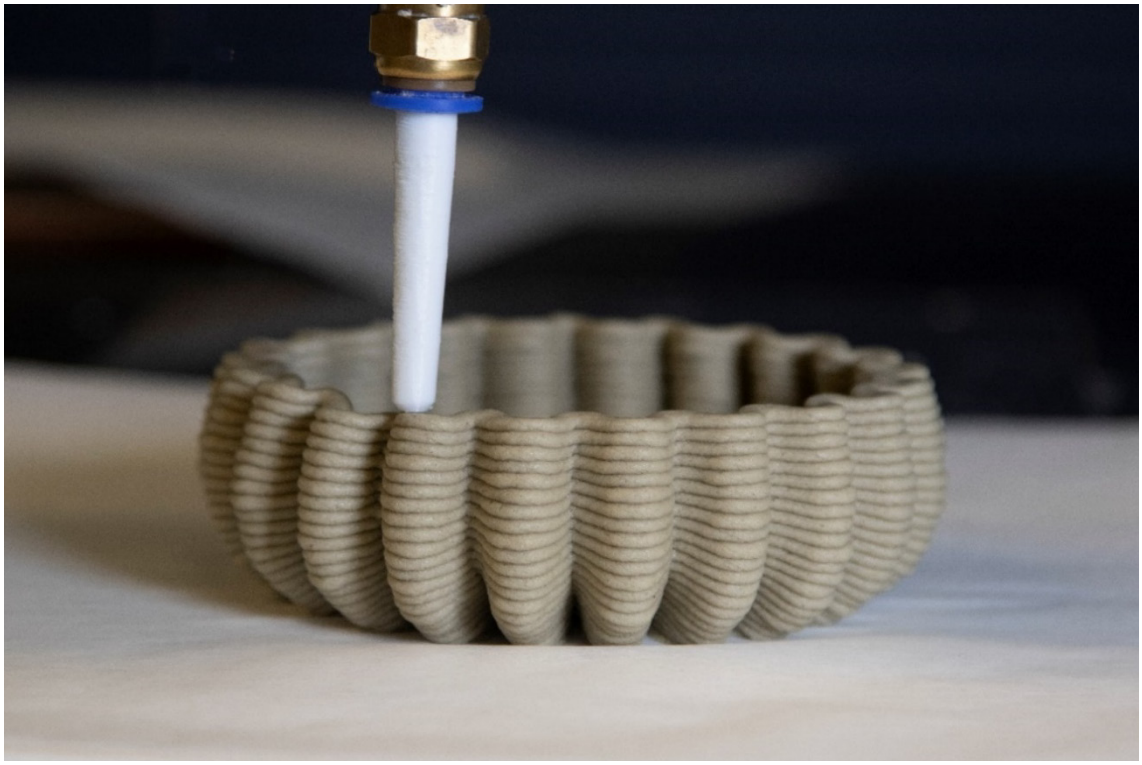

Figure 4.1. *Robotic 3D printing of glass fines material.*
Robotic material extrusion of glass fines paste using a CMC and MFC binder.

Figure 4.2. *Robotically extruded glass fines samples post firing.*
Different tones reflect the different level of fusing with the lighter parts remaining porous and the darker pieces being fully fused

4.3 Material Background: Glass fines

Glass fines were obtained from a Queensland company called Envirosand. Envirosand processes glass fines from recycling centres across Brisbane, removing contaminants such as metal tops and plastics and grinding them down into different powder grades (Norris, 2022). The grade of powder used for this project is called moondust which has a particle size of 75 - 150 um (see Figure 4.3). This is the smallest grade offered by Envirosand and was chosen as it was the closest to the particle sizes typically used in binder jet 3D printing of ceramics which according to Du et al. (2020), is from 0.3um to 355um based on the minimum particle-sized used by Miyanaji et al. (2016a) and the maximum particle-sized used by Meininger et al. (2016). These glass fines are mainly sourced from container glass (jars and bottles). However, they include a mixture of both colours and grades of soda lime silica, which means that the composition of the glass and associated properties (although similar) differ across the powder. This is significant as the composition of the glass will impact the temperature at which it softens and melts. Partway through the research, Envirosand was purchased by another recycling operator called iQRenew, and processing was moved to the Central Coast of New South Wales.

The particle size and shape (morphology) of the powder feedstock significantly impacts the BJT printing process and the characteristics of the final part. BJT literature highlights that the particle size and shape (morphology) determine the flowability of the powder, the packing density and the sinterability of the part (Mostafaei et al., 2021). Flowability refers to the ability of the powder to flow freely (Butscher et al., 2011). It is crucial in creating uniform, smooth layers and therefore a homogenous internal structure of the parts (Du et al., 2020). Powder packing density refers to how a network of particles is arranged and their maximum contact (Mostafaei et al., 2021). This is an important parameter in BJT as it determines the density of the printed part which is known to affect the strength during excavation and the shrinkage and deformation caused by the sintering process (Gibson et al., 2021; Mostafaei et al., 2021).

The relationships between the powder characteristics, the printing process and the final properties of the part are incredibly complex, and compromises often must be made. For example, larger particles generally have better flowability than small particles (Butscher et al., 2012). This is because as the diameter of the particle decreases, interparticle forces and friction increase, preventing free flow behaviour and encouraging agglomeration (Diener et al., 2021). This was seen in a study by Sun et al. (2017), whereby powder with a particle size between 0-25 um was difficult to spread into a thin layer, causing dislocation between layers and powder adhering to the roller. However, smaller particles generally exhibit better packing density than larger particles, which is desirable in BJT as it improves resolution and surface quality. High packing density has also been found to aid in the sintering of the part and positively impact the final mechanical properties (Du et al., 2020). As a result, a compromise in the particle size must be found, such that the powder still exhibits flowability whilst maintaining a suitable packing density[8].

4.3.1 SEM Analysis

To better understand the powder properties of the glass fines, a scanning electron microscopy (SEM) analysis was undertaken. SEM is a widely used method for visualising a material's microstructure,

[8] Also note that whilst large powder particles have better flowability than smaller particles, they can also cause powder bed instability as the coarse particles will not pack as tightly and can shift when a new layer is deposited (Butscher et al., 2012).

topography and composition (Kathirvel et al., 2022). It is a type of electron microscope that uses a focused beam of electrons to scan the material's surface, allowing for a magnification of up to one million times (Jaidka et al., 2022). The SEM analysis revealed that the moondust powder is irregular and angular in morphology (see Figure 4.4). In ceramic BJT this can pose some challenges as highly irregular particles are generally considered to have lower flowability than their spherical counterparts and lower tap densities (Du et al., 2017, 2020; Gildenhaar et al., 2011). Tap density refers to the density of a powder that has been tapped to settle in a container (ASTM International, 2022a; Du et al., 2020). However, during printing, powders are slightly compressed by a counter-rotating roller when spread across a thin layer. The counter-rotating roller aids in the flowability of the powder and the slight compaction aids the packing density of the irregular powders, meaning that irregular powders can and are still utilised in BJT (Lv et al., 2019; Mostafaei et al., 2021). In fact, one study by Suwanprateeb et al. (2010) found that irregular hydroxyapatite powder had a higher packing density due to friction between the particles which restrained them from flowing between each other and instead were tightly compressed by the roller.

The SEM analysis also confirmed that the glass fines feedstock contains a mixture of particle sizes, making it a multimodal powdered feedstock. In ceramic BJT both monomodal and multimodal distribution of particle sizes are utilised (Lv et al., 2019). Monomodal distributions are those in which a single particle size is present whereas multimodal distribution contains a mix of different particle sizes. Typically multimodal distributions are made by mixing several monomodal powders (Du et al., 2017). Using a multimodal powder can increase packing density as the larger particles assure flowability while the fine powders fill voids between large particles (Mostafaei et al., 2021). This can also decrease shrinkage during sintering and increase the surface quality of a print (Lanzetta & Sachs, 2003; Zhao et al., 2022).

In BJT literature, the preparation of powders is often optimised to encourage flowability and high packing density. Several methods can be utilised, including sieving and grading the powders or granulation. Granulation is where the raw powdered particles are glued together into larger granules using a binder. This has been demonstrated in several studies (Chumnanklang et al., 2007; Du et al., 2021; Miao et al., 2020; Suwanprateeb et al., 2010). Despite these existing methods, the glass fines in this research will be used as is. This is to minimise any additional variables, streamline the production process and minimise energy usage. The experimentation will demonstrate how to work with these properties of the glass fines.

4.3.2 Safety

When conducting materials-based experimentation, particularly with new or unconventional materials and production systems, it is critical to have health and safety protocols in place prior to the work beginning. This is particularly significant for this research as working with glass powders can pose health and safety risks. It is important to note that glass fines are a non-crystalline form of glass, meaning that they do not cause silicosis- unlike crystalline forms of silica (Merget et al., 2002). The glass fines used in this research are also considered to be non-hazardous according to criteria provided by Safe Work Australia (Envirosand, 2019; iQRenew, 2022). Regardless, it is still advised to have safety measures in place when working with amorphous glass powders as if inhaled they can cause respiratory irritation and prolonged, repeated exposure can lead to lung damage. Eye and skin irritation can also occur if glass powders are not handled correctly (Envirosand, 2019).

Figure Error! No text of specified style in document**..1.** *Glass fines, moondust grade.*
Processed glass fines used in this research. Moondust grade powder (75 - 150 um) Sourced from Envirosand in Queensland Australia and later iQRenew, in New South Wales, Australia. Image from Envirosand (n.d.).

Mag = 49 X
Pixel Size = 2.270 um

Mag = 465 X
Pixel Size = 240.3

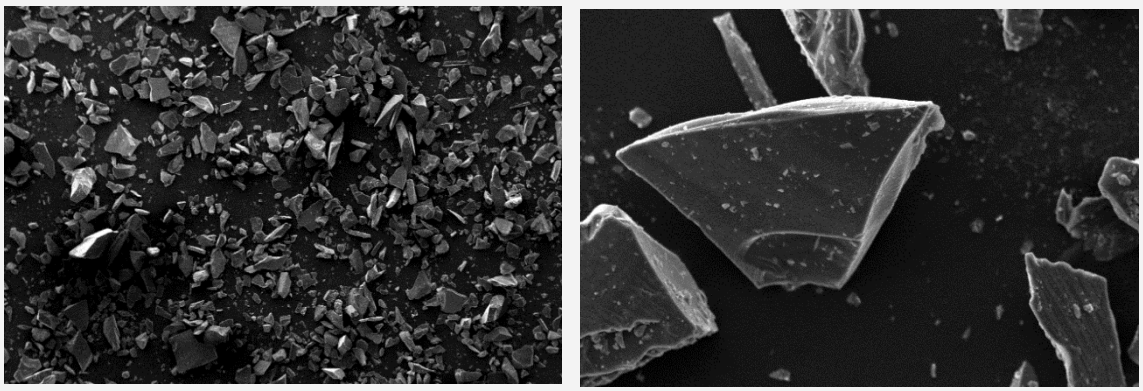

Figure 4.4. *SEM analysis of glass fines conducted in this research.*
Two images from the SEM analysis of the glass fines (moondust grade). These revealed that the powder is irregular and angular in morphology and confirmed that a range of particle sizes are present.

As a result, risk assessments and safety precautions were put in place in line with the with the Safety Data sheets provided by Envirosand and iQRenew. These included the wearing of personal protective equipment and ensuring that dust particles were adequately contained. A half-mask respirator fitted with gas, vapour and particulate filters which comply with the standard AS/NZS 1716:2012 (Standards Australia & Standards New Zealand, 2012) is worn, alongside a lab coat, safety goggles, and enclosed shoes when handling the glass fines material or unfired samples. Printing is conducted in a dust extraction tent where a vacuum is used to create negative pressure to ensure that dust does not escape. A large downdraft table is also used to extract and filter fine particles from the air while excavating prints. It is important to note that BJT printing with ceramic powders and sands has been widely practised for decades. As a result, many of these safety protocols are standard practice in industry and academic settings that use BJT technologies.

The effectiveness of the dust extraction tent and down-draft table in containing dust particles was confirmed through airborne contaminant testing. The monitoring of inhalable and respirable dust was conducted in accordance with AS 3640-2009; Workplace atmospheres - Method for Sampling and gravimetric determination of inhalable dust (Australian Standards, 2009) and AS 2985-2009; Workplace atmospheres - Method for sampling and gravimetric determination of respirable dust (Australian Standards, 2009). The testing was conducted by the external company Getex Pty Ltd. For both inhalable and respirable dusts, the results were below the workplace exposure standards for airborne contaminants outlined by Safe Work Australia (2024).

Research projects utilising glass powders and binder jet production systems should undertake comprehensive risk assessments in accordance with their respective national and institutional regulations. This practice is crucial for ensuring responsible research conduct.

4.4 Production Background: Binder Jetting

As was explained in Chapter 2, Binder Jetting (BJT) is an additive manufacturing method in which 3D parts are made by selectively depositing a liquid binding agent onto a powdered material (ISO/ASTM International, 2016). A commercial BJT machine called a Z Corporation 310 printer (Z Corp) was used. This is a discontinued model which unlike current binder jet 3D printers, allows for non-propriety powders and binders to be used. This makes it suitable for the prototyping of novel materials such as glass fines. These printers are often used by researchers experimenting with new materials because of their flexibility and accessibility (Dunn, 2017). It is important to note that using these machines does not compromise the transferability or reproducibility of this research, since the fundamental operating principles and machine parameters are consistent with newer models. Consequently, the material formulation and production process can be adapted to newer machines in the future. Furthermore, as Z Corporation machines were originally the industry standard for BJT printers, they continue to produce high-quality parts when properly maintained. Two Z-Corp 310 binder jet printers were acquired for this research (see Figure 4.5).

To 3D print an object using a Z-Corp machine, a 3D model is first created using CAD software. In this study, all 3D models were designed in Rhinoceros and Grasshopper. This enabled the creation of parametric models that could be easily modified based on experimental results, while also supporting the development of complex forms. The CAD model is then uploaded to the ZPrint application. The part is positioned within the build volume, print settings are configured, and the software automatically slices the 3D model into layers, based on

the selected layer height (0.15-0.2mm in this study). The printing process then commences. Figure 4.6 depicts a typical binder jet 3D printer. The powder supply is located in a bed next to the print bed. The feed platform moves up to the desired layer height, and the powder is spread across the build platform in a thin layer using a counter-rotating roller. The inkjet print head then deposits the liquid activator in the required geometry onto the powder layer in the print bed. Once the binder is deposited, the build platform moves down by the set layer height, ready for the next layer of powder to be spread (Ziaee & Crane, 2019). As the build progresses, the layers combine to form a 3D object that is encased in a box of powder. This part is known as a 'green' body.

BJT is a multistep additive manufacturing process, the printing process is just one step in producing final parts. Typically, there are 4-5 steps in the BJT process. The first step involves the preparation of the raw materials. There are two main methods for this, jetting in place where the binder is combined with the liquid printing solution or powder-binder premixing where the powdered binder is mixed into the feedstock powder (Butscher et al., 2012; Du et al., 2020)[9]. This research employs a premixing process to prevent potential nozzle clogging that can occur in jetting in place approaches. To achieve this, a separate printing liquid that activates the binder in the powdered feedstock is also required. This is typically a water-based mixture which sometimes contains alcohol and/or glycerine (Du et al., 2017; Marchelli et al., 2011; Solis et al., 2019).

The next step is the printing itself, described above. The third step is drying. The aim of this is to strengthen the green body so that it can be excavated from the powder bed without breakages. Even when the adhesion of the binder is good, the strength of these parts is low (Lv et al., 2019). For metal binder jet 3D printing the printed parts are the consistency of wet clay before this curing step but after are similar in strength to a piece of chalk (Mostafaei et al., 2021). In ceramic BJT literature, this is sometimes referred to as a curing step and can vary from letting the parts dry in the print bed at room temperature for a number of hours (Marchelli et al., 2011; Suwanprateeb et al., 2010), to removing the entire print volume and placing it in an oven[10] (Gonzalez et al., 2016; Miao et al., 2020) to more complex processes such as vacuum drying (Zhao et al., 2017).

After this, a debinding step is sometimes undertaken. This involves thermally decomposing or burning out the binder, typically at 600-800 degrees Celsius, leaving what is known as a brown part (Du et al., 2020). This step is not used in this research. The final step in BJT is usually a sintering or infiltration process (Lv et al., 2019). As the mechanical properties of most green parts produced by BJT (no matter the material and binder adhesion) are insufficient, several post processing steps are available. In ceramic BJT literature, this post-processing step is most commonly sintering. This is where parts are heated to a high temperature (often just below the melting point) in order to create a dense body (Du et al., 2020).[11]

The success of the BJT process and the characteristics of the final product are greatly affected and highly sensitive to the properties of the powdered feedstock and printing parameters (Chen et al., 2022). A significant body of knowledge on the parameters and variables for BJT has been built across various materials. Despite the extensive research, few universal rules exist. Instead, considerable experimentation and fine-tuning of variables is necessary to develop tailored systems for each material, BJT machine, and application.

[9] Premixing can be done in a wet or dry state. In dry mixing, the feedstock and binder are combined as dry powders. Wet mixing is often called 'precoating'. The ceramic powder and binder are combined with a solvent to form a slurry, which is then dried (often spray-dried) and sieved to form the powdered feedstock (Chumnanklang et al., 2007; Suwanprateeb et al., 2010). Wet pre-mixing can produce a more evenly mixed material but requires more processing steps (Du et al., 2020).

[10] A range of 35 degrees to 200 degrees was found in literature (Gonzalez et al., 2016; Miao et al., 2020).

[11] Other techniques used to densify the final part include infiltration or isostatic pressing. However, these can compromise geometric accuracy, heat resistance, biocompatibility and material composition (Du et al., 2020; Lv et al., 2019).

Figure 4.5. *Two Z Corp 310 binder jet printers acquired for this research.*
The two printers were set up in a dust extraction tent to contain work with the glass powders.

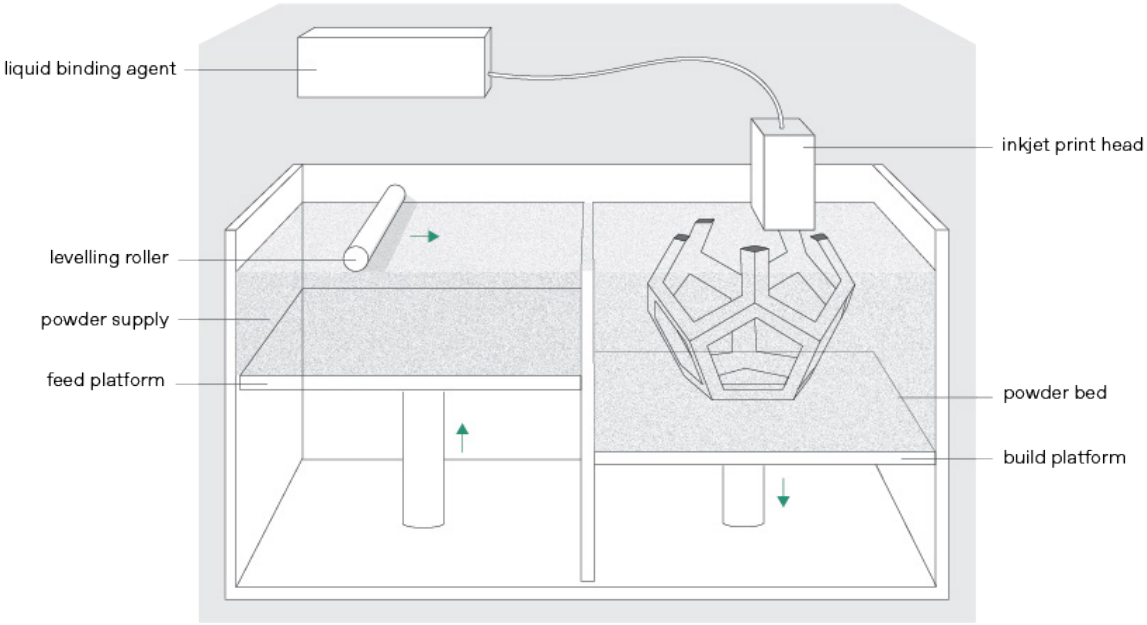

Figure 4.6. *Diagram of a typical binder jet 3D printer.*
Adapted from Additively.com (n.d.)

This research employs a four-step production process to create pieces from glass fines: (1) material preparation, (2) printing, (3) drying, and (4) firing. Figure 4.7 depicts this process and highlights key parameters influencing each production stage. It also highlights critical parameters in the material and application aspects of this research that affect the production steps. For example, the material formulation (type and ratio of binder) directly influences print settings such as saturation and layer height (these will be explained further in the next section), and the scale and types of geometries have a direct impact on the drying step. This diagram illustrates the complexity and interconnectedness of these parameters and will be referenced throughout the experimentation chapters to aid the reader in understanding the aims of different prototyping enquiries. It is important to note that the glass fines material and the steps in the firing process remain fixed throughout the research (indicated by the grey boxes). This chapter will cover the development of the first three production steps and their associated variables; the final firing step will be covered in the following chapter.

4.4.1 Print Parameters

There are three main print settings which can be adjusted and which impact the quality of the final printed part. These include binder saturation, layer thickness and orientation of the parts. Other parameters affect the printing process, including roller speed and the drying time between layers. These cannot be adjusted on the ZCorp 310 machine so will remain in the default settings.

Binder saturation refers to the amount of binder deposited onto each layer in print. This is made up of two values, the shell and core saturation. When a print is uploaded to the ZPrint software, each layer of the part is divided into a shell and core region (see Figure 4.8). A higher saturation value is applied to the shell, ensuring the part has enough strength whilst optimising printing time (Castilho et al., 2015; Lv et al., 2019). It is important to ensure the saturation levels are correct as low saturation, results in more fragile green parts as there is insufficient adhesion between the particles. However, high saturation results in bleeding, in which the binder liquid spreads out of the required area, compromising accuracy (Du, Ren, et al., 2020).

Layer thickness is simply the height of each layer of powder, typically ranging from 15 to 300 μm (Mostafaei et al., 2021). Smaller layer thicknesses improve resolution and surface finish but increase printing time. The possible layer thickness depends on the size of the powdered particles. Several differing rules for layer thickness have emerged in literature. Some studies state that the layer height must be at least greater than the largest particle size, whilst others recommend twice or at least three times the particle size (Du et al., 2020; Mostafaei et al., 2021). There is also a relationship between saturation and layer height. If the layer height is increased, the saturation may also need to be increased to penetrate through the whole layer; otherwise delamination may occur, meaning the layers will come apart (Chen et al., 2022).

The orientation and placement of parts in the print bed is also a key variable. The build orientation refers to how parts are aligned with respect to the x,y and z axes of the build volume (Mostafaei et al., 2021). Figure 4.9 demonstrates how the same rectangular prism can be oriented in multiple directions. The orientation of the part can impact both the accuracy and mechanical strength. Lv et al. (2019) write that due to the unlimited forms that can be printed, it is difficult to propose universal rules. However, it is generally accepted that parts oriented vertically will be weaker than ones aligned horizontally due to the smaller contact area between successive layers (Asadi-Eydivand et al., 2016).

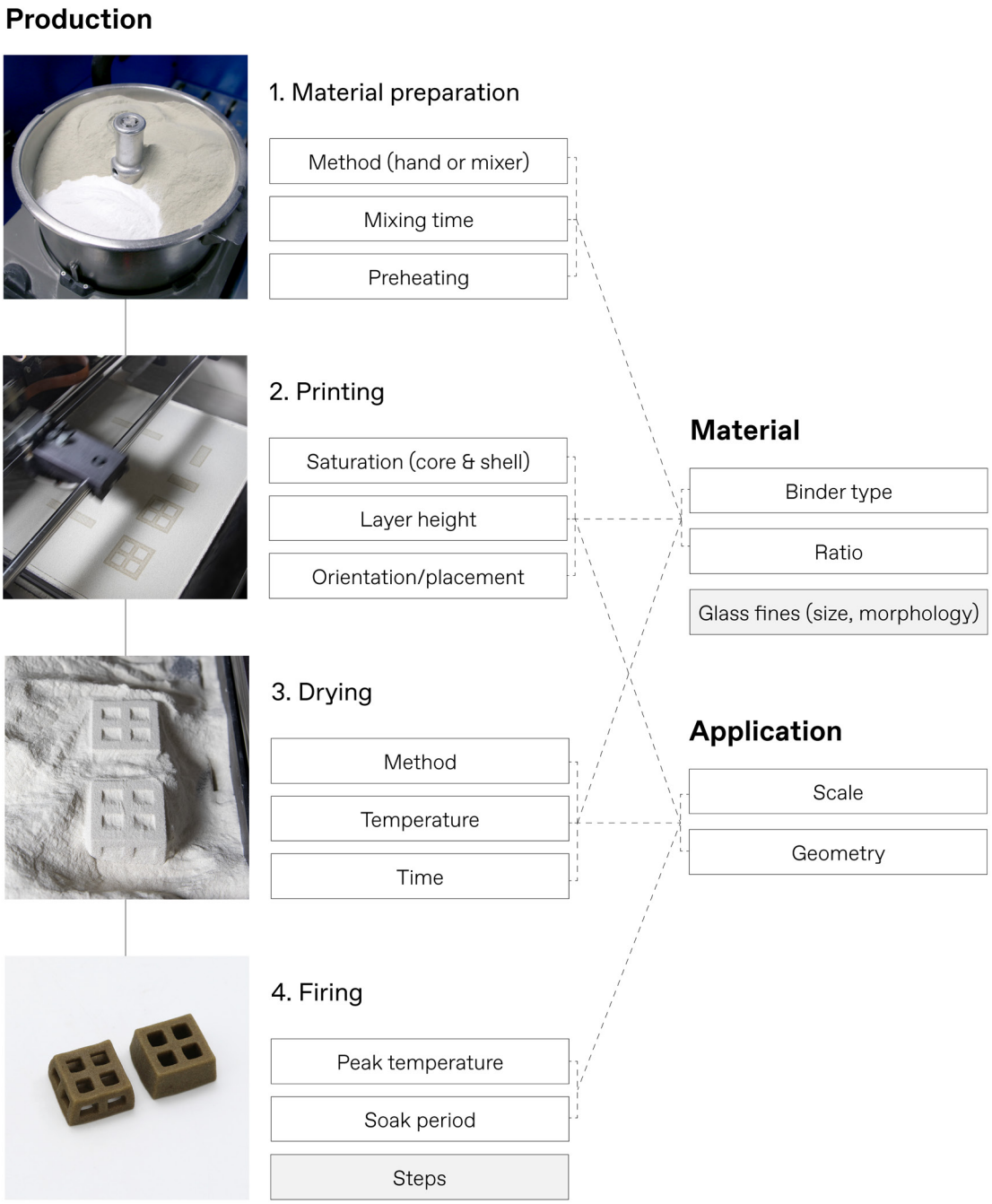

Figure 4.7. *Production steps and parameters*
The four-step production process of (1) material preparation, (2) printing, (3) drying and (4) firing and the key parameters impacting each step. The critical parameters associated with the material and application elements of this research are also shown, with dotted lines highlighting which variables are interconnected (where changing one variable may affect another). For example, the geometry and scale of the application will impact the method (air dry or oven heating), temperature and time required for the drying step. The grey boxes for the firing steps variable and glass fines indicate that these are fixed and not modified during this research.

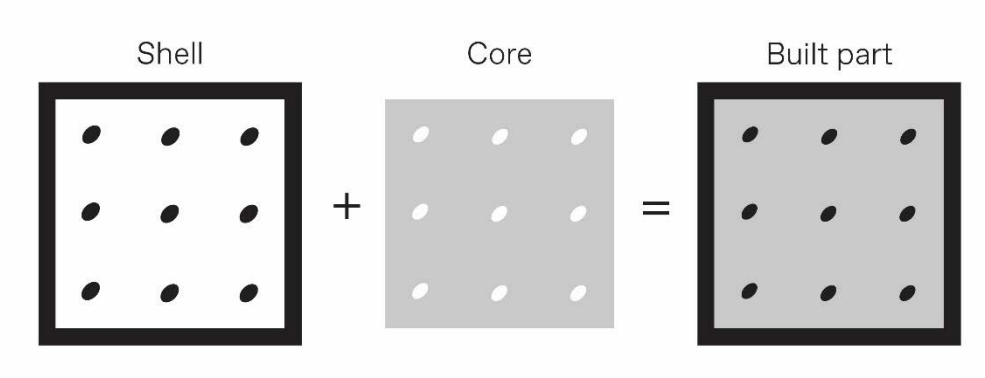

Figure 4.8. *Binder saturation is made up of two values; the shell and core.*
Each layer of the 3D print is divided into a shell and core region. Diagram adapted from Castilho et al. (2015)

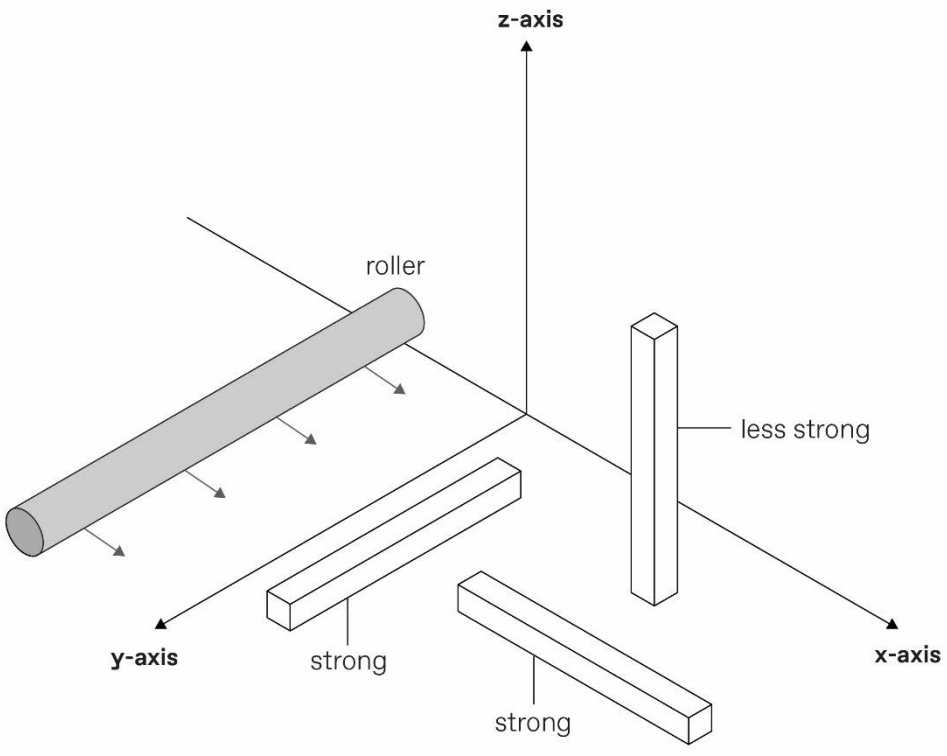

Figure 4.9. *Different orientation options of a rectangular prism.*
The strength and printing of parts differs according to their placement and orientation in the print bed. Diagram adapted from Z Corporation (n.d.).

4.5 Manual Testing

Given the success of CMC as a binder in the paste extrusion of glass fines, this was the first binder tested in developing the material formulation for binder jetting of glass fines. Prior to utilising a commercial binder jet 3D printer, preliminary manual tests were performed. These expanded on the 'spritz tests' conducted by Marchelli et al. (2011) in which the powder mixture is placed in a petri dish and sprayed with a liquid binder activator. The goal is to assess the compatibility of the powder, binder, and activator. According to the authors, the ideal outcome is a thin yet rigid shell forming on the first powder layer. However, since glass does not absorb water like other ceramic powders, achieving this effect is more challenging. As a result, a more comprehensive testing method was developed.

Glass fines were mixed by hand with CMC powder. A cylindrical container with a wooden base was created to simulate the build chamber. A tamping tool that fit tightly into the container was also made. This would be used to level out the powder, like the roller on a conventional BJT machine. A layer of the glass and CMC powder was added to the container. The first layer was larger to prevent the part from sticking to the base. The powder was levelled out by lightly swirling the container and packed down using the tamping tool. A guide was then attached to the bottom of the tamping tool and lightly pressed into the layer of powder. Following the guide, a small syringe was used to deposit water onto the powder. A new layer of powder was then placed on top of this and tamped down without the guide attached. This process was repeated until the glass powder was approximately 40mm high (see Figure 4.10).

Various ratios of glass fines to CMC powder were tested, along with the amount of powder used for each layer. Several basic shapes: discs, cylinders and donuts were created and left to dry. Once dry, the samples were fired in a kiln at 760°C. This temperature was chosen based on our previous extrusion-based work as the lowest temperature at which parts become waterproof. The compatibility of glass fines with the CMC binder and water as the activator was verified. It was found that adding approximately 2.5% CMC to moondust (w/w) was a suitable formulation and that approximately 24g of powder per layer allowed for a part to be formed and excavated. The samples also fired as expected, forming fused glass objects (see Figure 4.11 and Figure 4.12).

This test verified the powder, binder and activator combination that could then be tested on a commercial binder jetting machine. It is important to note that this test does not provide information on print parameters or the final ratio of binder to powder as the simulated parameters differ significantly on a commercial machine. For example, the amount of activator that is deposited and its accuracy is difficult to control using a syringe by hand, meaning that larger layers of powder are needed in these tests to not oversaturate the part. The pressure applied by tamping the powder also potentially compacts the powder more than a conventional BJT machine would, making a stronger and denser part than could be expected on a conventional machine. As such the ratio of binder to powder will act only as a starting point for testing on a Z Corp machine.

Figure 4.10. *Method of conducting manual binder tests.*
(1) tamping down first layer of powder, (2) pressing guide into powder layer, (3) depositing liquid activator, (4) adding new layer of powder, (5) removing part from powder bed, (6), brushing off (depowdering) part.

Figure 4.11. *Various fired samples from manual testing (2020).*
Three rudimentary shapes formed during the manual testing, fired in a kiln to 760°C.

Figure 4.12. *Close up of image of sample from manual testing (2020).*

4.6 Finding printing parameters

The first stage of experimentation focused on determining suitable printing parameters and production steps for the BJT of glass fines. Two 'sets' of prototypes were completed using the CMC binder and water activator, which were found to be compatible in the manual testing. The first set investigated simple shapes such as a rectangular prism and the second set explored more complex geometric shapes. The first set included six individual experiments, and the second set included four. The printing parameters of layer thickness and binder saturation were a key focus as well as the drying time needed before excavating the parts (see Figure 4.7 for an overview of the production parameters). The overall findings of each 'set' are reported on, notes on each individual experiment can be found in Appendix 2.

4.6.1 Basic shapes

The aim of this set of tests was to develop preliminary print settings suitable for the BJT of glass fines using a CMC binder. Each prototyping experiment was evaluated using two main criteria. The first was printability, which refers to the occurrence of any defects, printing errors, or issues such as layer delamination during the build process. The second was the success of part excavation. This involved assessing whether the printed components could be depowdered effectively without breakages or compromising fine details.

Six individual experiments were performed (Experiment 1.01-1.06). Based on the manual testing 2.5% CMC was mixed by hand with moondust (w/w) and tap water was used as the liquid activator. Three rectangular prisms and two corner pieces were printed in each experiment (see Figure 4.13 and Figure 4.14). As findings were generated, three parameters were adjusted incrementally. These include the binder saturation which was adjusted in the range of 75%-150% (using the ZCorp ZP15E stock powder setting), the layer thickness which was adjusted from 0.15-0.2mm and the time the prints were left to dry in the bed before excavating which was between 2 and 18 hours. By the sixth experiment, preliminary printing parameters that allowed for parts to be printed with minimal defects and excavated without breakages were determined. The parts printed using these parameters can be seen in Figure 4.15 and Figure 4.16. See Appendix 2.1 for full details.

During this set of experiments two key issues emerged: the importance of drying time and the phenomenon of swiping. The relationship between drying time, saturation and green strength was observed in this set of experiments. As discussed above, a green part is one that has been printed and dried but has not undergone firing. The strength of these parts is important as they need to survive the excavation process without breaking (Mostafaei et al., 2021). The green strength of the first four experiments was insufficient, and parts could not be excavated from the bed without cracking or crumbling apart (see Figure 4.17). At first, it was hypothesised that reducing the layer thickness may increase green strength as literature reports that a thinner layer thickness can lead to higher density parts (Gonzalez et al., 2016; Mostafaei et al., 2021). However, it was found that increasing the saturation had a more significant impact. This aligns with literature indicating that low binder saturation adversely affects the strength of green parts due to inadequate contact between the powder and binder (Du et al., 2017).

The impact of the drying time was also noted. In accordance with BJT literature, in-bed drying was employed in these experiments, simply leaving the parts in the print bed for a specified time before

excavating. It was found that parts left for between 15-18 hours exhibited greater green strength than parts that were only left for two hours- these would break upon excavation (see Experiment 1.04 and 1.05 in Appendix 2.1). This supports existing literature which highlights the necessity of a drying step to ensure complete adhesion before excavation, essentially confirming that the glue must be dry before handling the pieces. Although the precise drying time was not established in this series of experiments, the 15-18 hour timeframe proved sufficient for the parts to dry thoroughly and be excavated effectively. There is also potential to employ other drying techniques, including removing the whole print bed and placing in an oven or dehydrator. It is important to note that the drying time is linked to the saturation settings and the geometry of the parts; as saturation is increased so too must the drying time and as larger parts are printed they will need longer to dry. Therefore, this parameter will likely be adjusted over time.

Furthermore, the accuracy of all six experiments was impacted by swiping. Swiping is the term used by Marchelli et al. (2011), to refer to a layering defect in which the location of a layer is slightly shifted as the roller spreads a new layer of powder on top (see Figure 4.18). The impact of swiping on the excavated prints can be seen in Figure 4.15, where the bottom layers have been displaced. The parts on the right-hand side, furthest from the feed reservoir experienced less to no visible swiping. This phenomenon has been discussed by several authors (Bai & Williams, 2018; Choong et al., 2022; Marchelli et al., 2011; Miyanaji et al., 2018; Rishmawi et al., 2018). It has mostly been reported that swiping results from unoptimised saturation settings, where an excess use of binder prevents the sufficient curing of the current layer before the next is deposited. Some authors have offered alternate explanations; Miyanaji et al. (2018) specify that it occurs due to the inadequate drying of the binder between layers, Marchelli et al. (2011) attribute it to insufficient layer height and excess shell saturation and Rishmawi et al. (2018) highlight that if the rotation of the roller is deactivated during the powder spreading noticeable swiping can occur.

In Choong et al.'s (2022) research, swiping only occurred in the first 3mm of the print and then self-corrected (2022) (see Figure 4.19). This mirrors what was observed in this set of experiments. They highlight that once there is a stable base, the top layers can be accurately formed. As such, it is the force of the roller depositing powder on the unanchored and unstable early layers that causes their displacement. This is similar to the swiping observed in this set of experiments. Choong et al. (2022) propose some solutions. Firstly, they suggest rotating the prints to reduce the points of contact of the roller and printed geometries. Secondly, they design a print fixture, which is essentially a support structure that enhances the stability of the unbound powder. The second approach is like the support structure that can be generated in the ZPrint software. They found that a combination of these two approaches fully mitigated the swiping.

Similarly to Marchelli et al. (2011) the swiping that occurred in these experiments occurred predominantly on the pieces that were closest to the feed reservoir. This could indicate, as suggested by Miyanaji et al. (2018), that the swiping is also a result of insufficient drying time between layers, since those parts closest to the feed reservoir have a shorter drying time than those that are furthest away. Whilst delay times can be set for some BJT printers, this is not an option for the ZCorp 310 and so other methods of mitigation must be tested. Based on these various accounts from literature, it is hypothesised that the swiping which occurred in this set of experiments is due to a combination of the unanchored early layers, higher saturation settings and insufficient drying time between layers. Whilst these higher saturation settings are needed to ensure the green strength of the parts, the strategies suggested by Choong et al. (2020) hold promise. Through the six individual experiments, preliminary BJT printing parameters for the creation of basic shapes using glass fines were determined. These include using a 0.2mm layer height, 145% shell and core saturation and leaving prints to dry for at least 15 hours before excavating.

Figure 4.13. *Excavation in progress for Experiment 1.03 (2022).*
Parts are roughly excavated in print bed before being more closely brushed off over the down draft table.

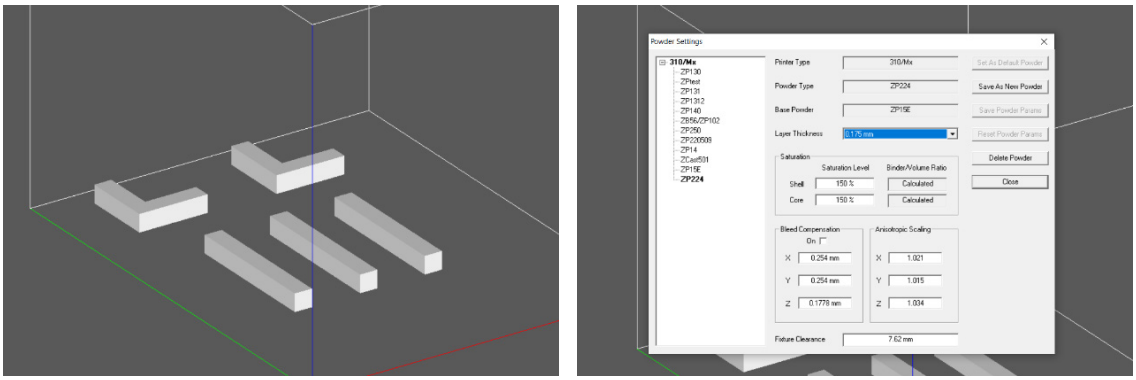

Figure 4.14. *Print layout and settings dialogue box for Experiment 1.01.*
Parts are placed in the middle of the print bed, leaving significant space around each part. The dialogue box shows the print settings used for this Experiment 1.01, including saturation and layer height.

Figure 4.15. *Excavated results from Experiment 1.06.*
Parts from Experiment 1.06 were successfully excavated but ones closest to the feed reservoir experienced swiping on the early layers as evidenced by the excess material at the base.

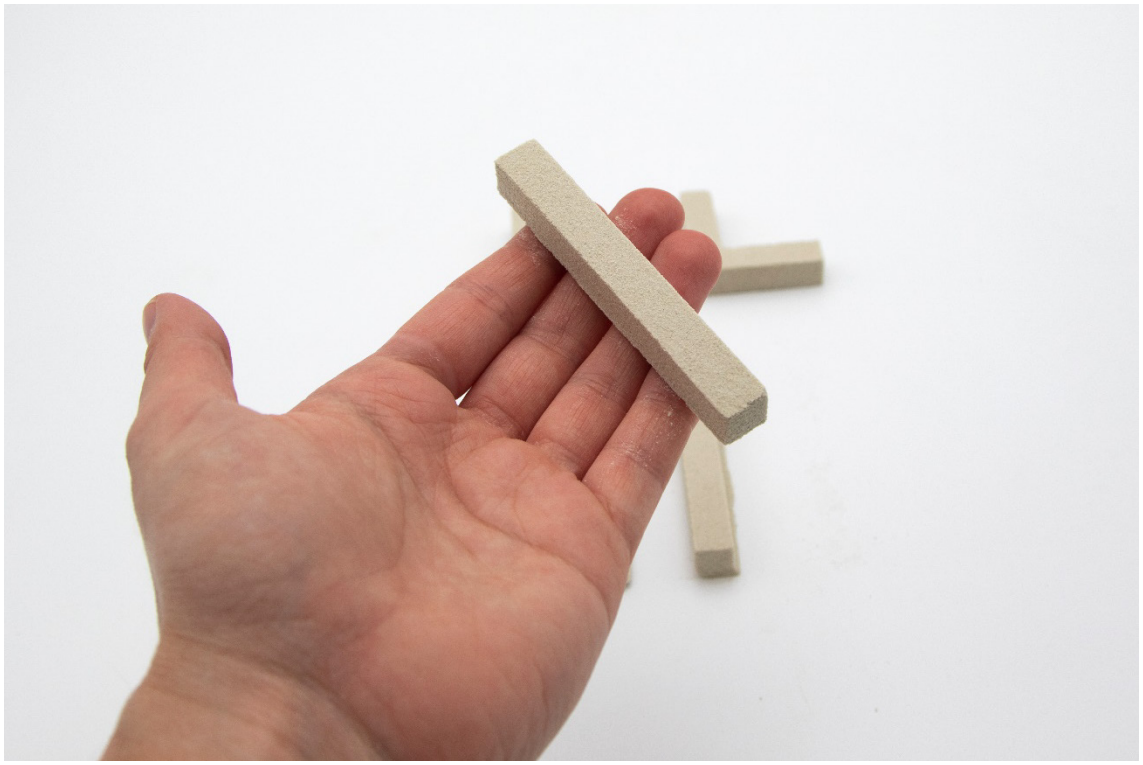

Figure 4.16. *Close-up of excavated rectangular prism from Experiment 1.06.*
This piece was furthest from the feed reservoir and did not exhibit signs of swiping.

Figure 4.17. *Breakages during excavation of parts in Experiment 1.04.*
The breakages are due to insufficient green strength.

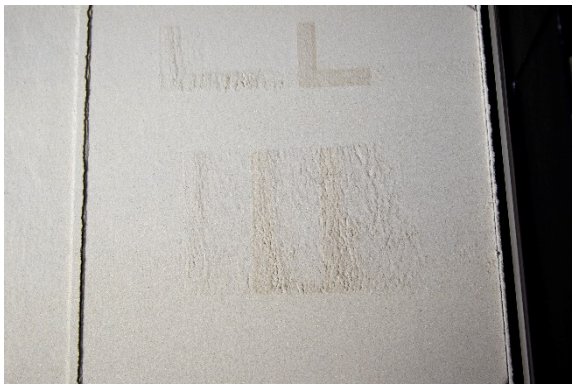

Figure 4.18. *Swiping which occurred during the printing of Experiment 1.05.*

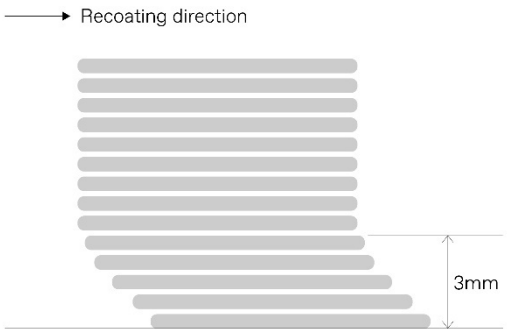

Figure 4.19. *Diagrammatic representation of swiping as reported by Choong et al. (2020).*
Layers in the first 3mm of the print shifted as a new layer of powder was coated. This self-corrected over time.

4.6.2 Geometric shapes

This set of tests aimed to further optimise printing parameters by experimenting with complex geometric forms, while also addressing the previously identified swiping issue. Although several swiping mitigation strategies were found in literature, the work of Choong et al. (2022) was used to inform this set of experiments. Choong et al. (2022) suggested that when a roller contacts a large, printed line rather than a point, the resulting force of transmission is greater and is therefore more likely to shift the layers. Drawing on this, a series of geometric shapes with smaller areas of initial contact were designed. Thus, the aim of this set of experiments was twofold: to assess whether more complex geometric shapes could be accurately printed and excavated using the parameters determined previously, and to examine if swiping occurs on shapes with smaller points of contact. The overarching aim remained the optimisation of print settings.

Four individual experiments were undertaken (Experiment 2.01-2.04). The geometric shapes were adjusted in each experiment, however the overall typology remained similar, investigating thin walls, corner joints, overhangs, cut outs and intersecting parts (see Figure 4.20 and Figure 4.21). Three of each geometry were printed as the previous testing had demonstrated that the print's accuracy can differ across the print bed. Three parameters were incrementally adjusted throughout the four experiments; the core and shell saturation was adjusted between 145-150%, the layer height between 0.175-0.2mm and the concentration of the binder was adjusted between 2.5%-3.75% (w/w). All experiments were left to cure in the bed for at least 18 hours before excavation and tap water was used as the binder activator. See Appendix 2.2 for full details. By the fourth experiment, the parameters had been sufficiently optimised to print these more complex geometries. To do this, the binder concentration needed to be increased by 50%, and the corresponding print settings were adjusted to be 150% shell and core saturation and 0.175 layer height. The parts printed using these settings can be seen in Figure 4.22 and Figure 4.23.

This set of experiments confirmed the link between the geometry and the severity of swiping. By creating parts with smaller contact points with the roller, swiping was significantly reduced, to the point where it was not or only slightly visible on the excavated prints. Despite the improvement, there was still swiping on three of the four experiments for approximately the first 10 layers. As a result, further mitigation strategies could be investigated. It is also important to note that decreasing the layer height from 0.2 to 0.175mm appeared to increase swiping in Experiment 2.03. As such, the relationship between layer thickness and swiping could be examined.

The importance of green strength and its relationship to binder concentration was highlighted in this testing. Breakages occurred during the excavation of the first three experiments, particularly on the bottom half of the prints (see Figure 4.24 and Figure 4.25). The wireframe cube geometry was also abandoned as it was too fragile to be excavated with the corner joints providing minimal areas of contact. As a result, the binder concentration was increased by 50% in the final experiment, allowing for excavation of all parts in Experiment 2.04. This aligns with literature that reports increasing binder concentration can enhance green strength (Chumnanklang et al., 2007). Despite this, the parts printed in Experiment 2.04 remain fragile and must be handled with extreme care. This green strength is likely to be insufficient for larger and more complex pieces to be excavated. Literature provides furthe options for improving this; including increasing the saturation levels to allow more activator to penetrate the vertical and lateral directions of the powder (Miyanaji et al., 2016b). However, Lv et al. (2019) and Mostafaei et al. (2021) highlight that the bonding properties of the binder itself are really the key. It was hypothesised that whilst CMC has adhesive properties, these are not sufficient for the scale and types of geometries which are aimed at in this research.

Figure 4.20. *Excavation of Experiment 2.04.*
Excavation in progress, parts are roughly excavated in the print bed and then brushed off more closesly over the downdraft table.

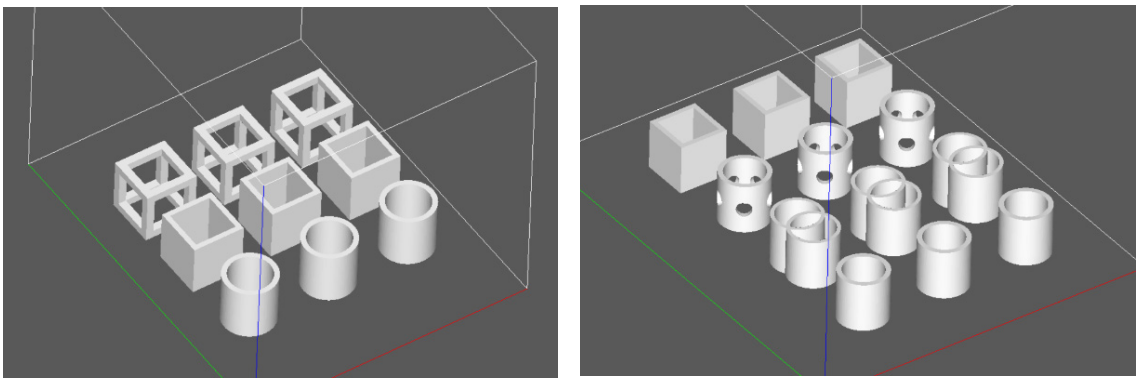

Figure 4.21. *Print layout of Experiment 2.01 (left) and Experiment 2.04 (right).*
The print geometries were adjusted throughout the set of tests but the overall typology remained similar, investigating thin walls, corner joints, overhangs, cut outs and intersecting parts.

Figure 4.22. *Excavated results from Experiment 2.04.*
Parts from Experiment 2.04 were successfully printed and excavated.

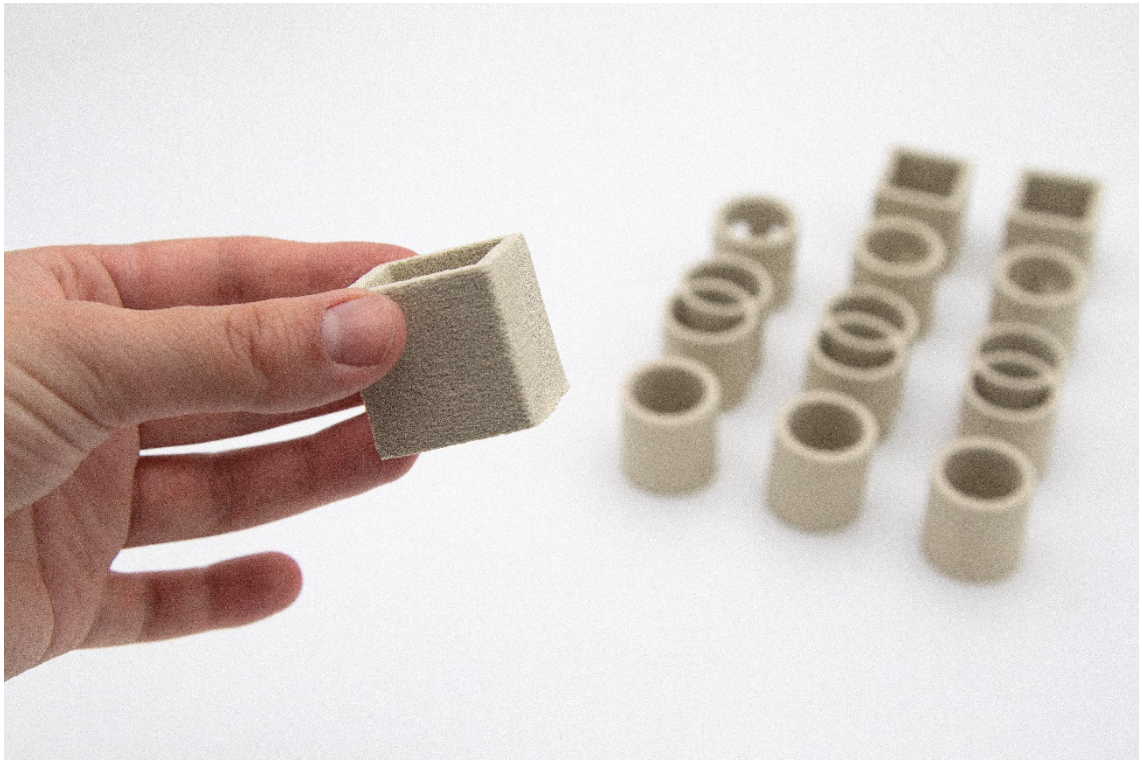

Figure 4.23. *Close-up of cube geometry from Experiment 2.04.*

Figure 4.24. *Breakages that occurred during the excavation of Experiment 2.01.*
Low green strength of parts caused breakages during excavation.

Figure 4.25. *Breakages that occurred during the excavation of Experiment 2.02.*

4.6.3 Summary of finding printing parameters

These two sets of experiments using basic shapes and more complex geometric forms, allowed for preliminary printing parameters and production steps to be determined. These include using a layer thickness of between 0.175 and 0.2mm and a saturation of 145-150% for both the core and shell settings. It was also found that the parts should be left to cure for a minimum of 18 hours before excavating to ensure they are fully dry. These settings are taken forward into the next phase of experimentation.

Whilst a series of geometric shapes which exhibit a certain level of complexity were achieved, issues around swiping and green strength emerged. Swiping was largely overcome by decreasing the points of contact with the roller, however, could be further optimised by rotating the geometry or including a support fixture. Whilst there are options for increasing the green strength, including continuing to increase the concentration and saturation, it was hypothesised that other binder materials with stronger adhesive properties may be more effective. As a result, the next series of prototyping enquiries looks at optimising the binder formulation.

4.7 Finding the Binder Formulation

The fragility of the green parts in the previous testing phase will likely be a barrier to application. The low green strength will make more complex and larger-scale objects challenging to excavate. Therefore, this phase of experimentation aims to optimise the material formulation by investigating different binder types and ratios (see Figure 4.7 for an overview of the production parameters). This was done through three sets of experiments. The first set included five individual experiments that looked at using other cellulose derivatives that may have greater adhesive properties. The next set, made up of three individual experiments, looks at binders more commonly used in ceramic BJT literature, specifically modified starch binders. The final set takes the form of an experimental prototype, employing a scientific method to compare the strength of two binders to verify the best direction. Each prototyping experiment continues to be analysed on its printability and green strength during and after excavation.

4.7.1 Cellulose Binders (CMC and HPMC)

There are a wide range of cellulose derivatives that are known to have adhesive properties of varying degrees. As a level of success had been attained using the CMC and there is a precedent for this group of materials in glass art, it was decided that this set of experiments would investigate another cellulose-based binder but one that was hypothesised to have higher adhesive qualities. Hydroxypropyl methylcellulose (HPMC), is a water-soluble cellulose derivative that has been used as an adhesive in various applications including construction products, paints and drug delivery for over 70 years (Lim et al., 2021). In particular, it has been used in tile adhesives, where it is mixed into the mortar to enhance water retention and workability, as well as to improve adhesion (Petit & Wirquin, 2013). It was hypothesised that using a construction grade of HPMC may provide advanced adhesion properties in the BJT of glass fines. This set of tests, therefore, aimed to determine if using HPMC as a substitute or in combination with CMC would provide greater green strength.

Construction grade HPMC was sourced from Lotte Fine Chemical (Mecellose PMC-40US). Five individual experiments were conducted (Experiment 3.01-3.05). A rectangular prism and a wire frame grid were modelled in CAD. Three of each were printed to assess the change in quality across the print bed (see Figure 4.26 and Figure 4.27). For the first experiment, 3% HPMC was combined by hand with moondust (w/w). A layer height of 0.175mm was used, and the saturation was set to the default 100% for both core and shell, as it was unclear how the new binder would behave. However, both Experiment 3.01 and 3.02 could not be excavated and so the binder was adjusted to 2% CMC and 2% HPMC. It was hypothesised that, as CMC is typically more hydrophilic than HPMC, the green strength of the parts may improve (He et al., 2021). A further two experiments were undertaken (3.03-3.04) in which the saturation was also increased (see Figure 4.26). This increase in saturation caused significant swiping to return. So, for the final experiment (Experiment 3.05) sacrificial geometry was included to delay the time between the jetting of binder and the recoating of the next layer (see Figure 4.28). Increasing drying time between layers is recommended in literature for mitigating swiping (Miyanaji et al., 2018). However, this setting cannot be adjusted on the ZCorp 310 machine and so sacrificial geometry in the form of four rectangular prisms positioned close to the powder reservoir were a makeshift way of testing this. See Appendix 2.3 for full details of this set of experimentation.

In all five experiments, the green strength was found to be insufficient for the successful excavation of all parts. Despite attempts to optimise the production parameters, the parts produced in the final experiment remained very fragile and two of the delay geometries cracked (see Figure 4.29 and Figure 4.30). Overall, the incorporation of HPMC did not appear to increase the green strength. In fact, it is hypothesised that there was a reduction in green strength as breakages occurred in every test iteration (see Figure 4.26). There are likely to be several ways of optimising the use of HPMC as a binder, both in terms of the print settings and the grade of HPMC used. The physical properties of cellulose ethers, such as HPMC, are related to the substitution of hydroxyl groups in the cellulose molecule with methyl and hydroxypropyl groups. The type and number of substitutions directly affect the properties (Lim et al., 2021). The HPMC used in this testing had a low degree of substitution, which may have limited its binding ability. Acquiring a HPMC grade specifically optimised for higher adhesive strength could improve the results.

Swiping re-emerged as a critical issue. Delay geometry was investigated in Experiment 3.05 as a makeshift way of increasing the drying time between layers. This technique had a positive result with swiping occurring on just the first four layers. This was a significant improvement from Experiment 3.04 without delay geometry where swiping occurred on the first 20 layers. The impact of the swiping could also not be seen on the excavated parts in Experiment 3.05. This indicates that the drying time between layers does impact the severity of swiping in the BJT of glass fines. However, it is important to note that drying time will be just one variable impacting swiping. As discovered in the previous testing, the geometry, placement, and contact points with the roller are also factors.

Furthermore, unlike the CMC, this grade of HPMC also has a delayed solubility property, meaning that it can be dispersed in water but will not dissolve immediately; a property designed to mitigate lumps forming. This grade of HPMC will take approximately 20 minutes to dissolve (Lotte Fine Chemical, n.d.). Whilst this is a desirable feature for some applications, it may have inhibited the water from penetrating the layer of powder immediately, causing the liquid to sit on the surface and impacting swiping. It also likely disrupts the binding between the layers during printing. throughout the five experiments, the impact of layer height on the spreading of the powder was also evident. It was observed that using a 0.2mm layer height results in a more uniform and smooth powder spread.

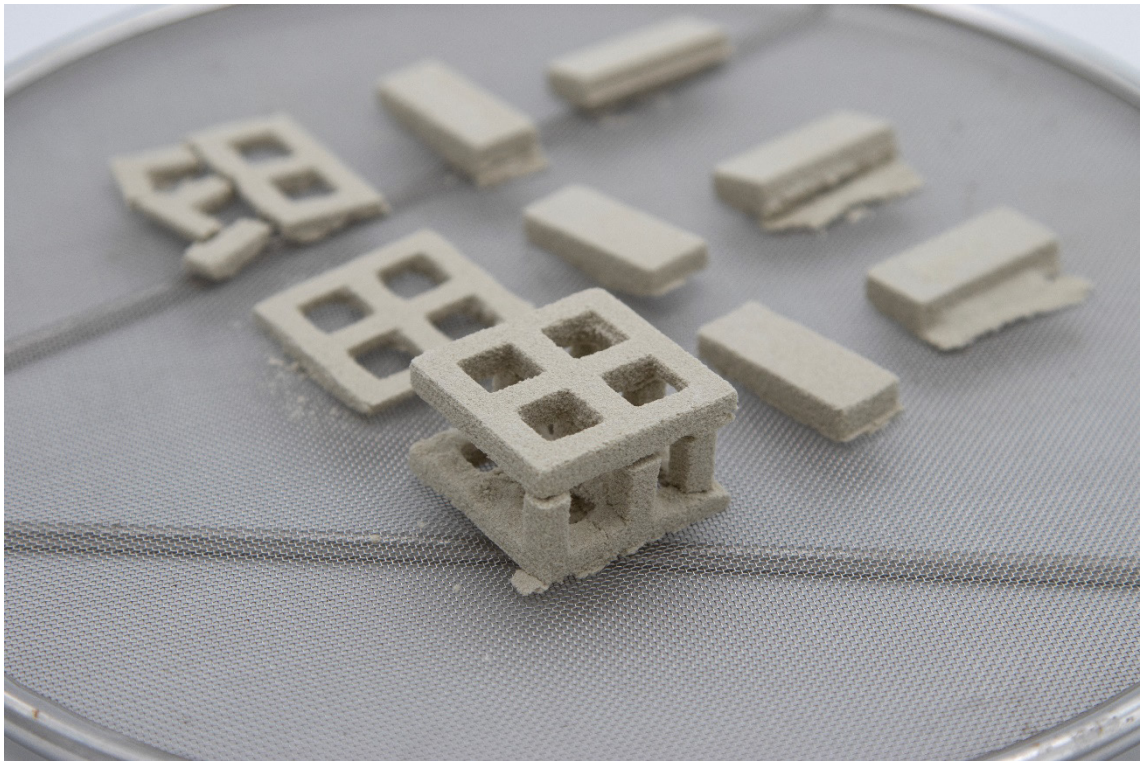

Figure 4.26. *Breakages which occurred during the excavation of Experiment 3.03.*
Low green strength of parts caused breakages during excavation.

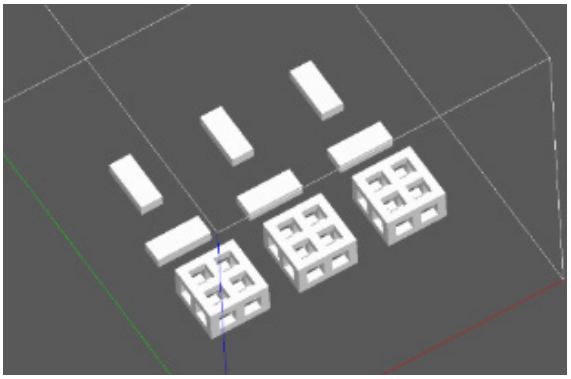

Figure 4.27. *Print layout for Experiments 3.01-3.04.*

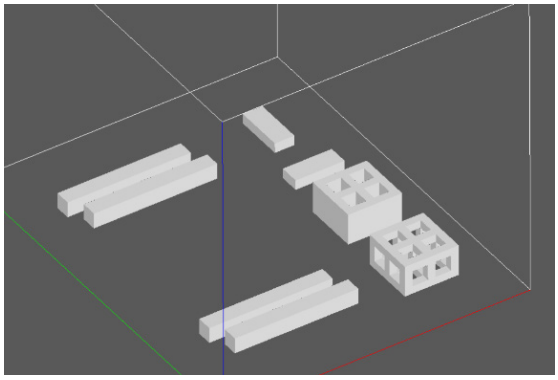

Figure 4.28. *Print layout for Experiment 3.05.*
The print geometries and layout were adjusted to account for the high saturation settings needed for the HPMC binder. Four rectangular prisms were placed on the left-hand side of the print bed as delay geometries.

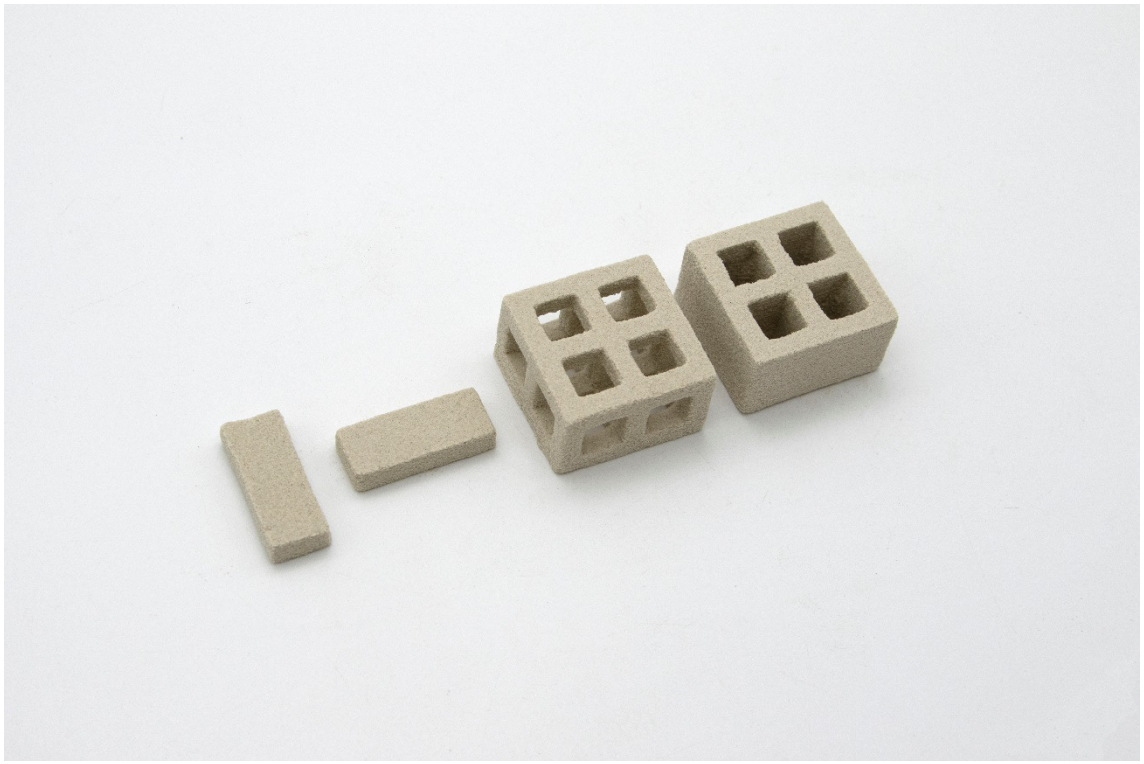

Figure 4.29. *Excavated results from Experiment 3.05.*
Whilst accurate parts were accurately printed and excavated, they remained extremely fragile.

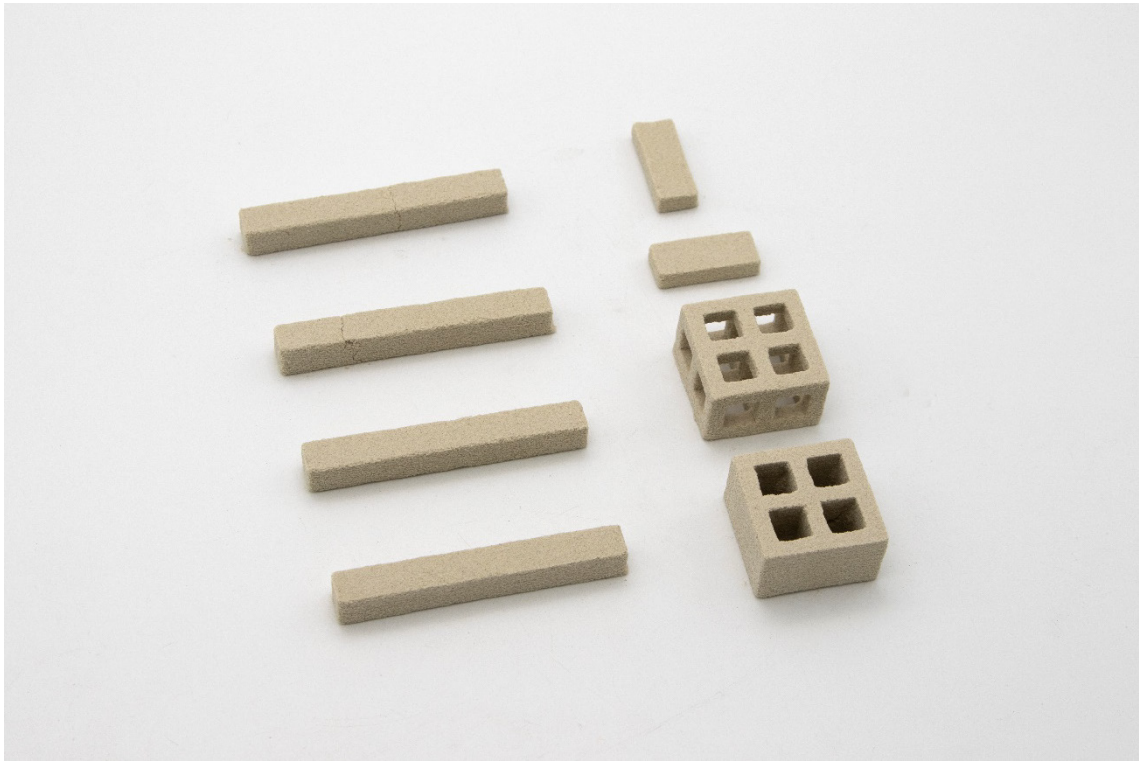

Figure 4.30. *Excavated results from Experiment 3.05 including the delay geometries.*
Two of the four delay geometries cracked during excavation, demonstrating the low green strength.

Considering the particle size of the glass fines at 75 - 150 um and the guidance from BJT literature that the layer height must be at least greater than the largest particle size, if not twice or thrice that size, using a 0.2mm layer height appears to be the most suitable.

4.7.2 Hydroxypropyl Starch Binder (HPS)

Due to the low green strength provided by the cellulose derivative binders and the minimal precedent in BJT literature, other alternatives were investigated. Du et al.'s (2020) literature review found that carbohydrates such as starches are the most common binders in the BJT of ceramics. Although often discussed as a singular material, there are a variety of starches which differ in properties, sources and method of preparation (Zobel & Stephen, 2016). Like cellulose, starch can undergo a range of physical and chemical processes to obtain derivatives with specific characteristics. This material group is known as modified starches (Tharanathan, 2005; Wurzburg, 2016).

One of the key properties which has been modified is the solubility of starch. Regular starches (or native starches) are insoluble in cold water and require heating to dissolve so a pre-gelatinisation modification has been developed (Tharanathan, 2005). Pregelatinised starches (sometimes called instant starches) are essentially precooked and dried to form cold swelling starches, meaning they can dissolve in cold water (Zia-ud-Din et al., 2017). These starches are widely used in the textile and food industry, and function as adhesives in the production of cores and shells for metal casting (Zia-ud-Din et al., 2017). Starches have been used as adhesives for hundreds of years, particularly in fabricating corrugated cardboard, paper bags, adhesive labels and wallpaper pastes (Kennedy & Fischer, 1984). Combining this adhesive property with the pregelatinised modification has led to even further adhesive applications and can make these starches suitable for binders in BJT printing. Since the starch can dissolve in cold water, it will bind the particles together when the liquid activator is deposited.

A pregelatinised hydroxypropyl starch (HPS) was used for this testing. This modified starch has undergone etherification, meaning the hydroxyl groups in the starch molecule are replaced with hydroxypropyl groups (Tharanathan, 2005). Similarly to HPMC, HPS is added to plasters and tile adhesives to increase green strength and sagging of the plaster on the wall (Plank, 2004). It is also used widely in the food industry in which it is designed to withstand high temperatures and extremes of pH and is often used as a stabilising agent (Tharanathan, 2005). Pregelatinised HPS derived from tapioca was sourced from supplier, Ingredion under the name NATIONAL 208. The NATIONAL 208 product is marketed as a food additive which is easily dispersed in liquids and provides excellent resistance to heat, acid and shear (Ingredion, 2021). The manufacturer advised that this ingredient also has strong adhesive properties, exhibiting binding strength similar to another product BONDSTAR PLUS 8000. This product is used in the briquetting industry to create solid bricks of charcoal, gypsum, and steel. It provides suitable compressive strength and shatter resistance on the final briquette products (Ingredion, 2019). This suggests that using this starch as a BJT binder will allow for greater green strength. The NATIONAL 208 product was chosen due to its accessibility and food-safe properties.

The aim of this set of experiments was to determine if using this modified starch binder would increase the green strength of the BJT-printed parts. Before assessing this, the printing parameters needed to be adjusted to account for the behaviour of the new binder. Each experiment was analysed based on printability and green strength. Additionally, the sacrificial delay geometry utilised in the previous set of

tests continued to be assessed. Three individual experiments were undertaken (Experiment 4.01-4.03). 4% HPS binder was mixed by hand with the moondust (w/w). The same geometries and printing parameters from the previous test (Experiment 3.05) were used here to allow for a clear comparison of the printability and green strength to be made (see Figures 4.31-4.33). The binder saturation and binder concentration were adjusted incrementally over the course of the three Experiments. See Appendix 2.4 for full detail.

By the third experiment, suitable printing parameters for the HPS binder had been determined. It was found that saturation settings of 120% core and 145% shell in combination with a binder concentration of 3% (w/w) allowed for the printing and excavation of accurate parts. These parameters were used in Experiment 4.03, pictured in Figure 4.34 and Figure 4.35. The primary finding of these experiments was the noticeable improvement in green strength of the HPS binder over the cellulose derivative binders. Parts could be easily excavated and handled without any crumbling or breakages. This was a significant breakthrough for the research as it represents a binder formulation with potential for printing and excavating larger and more complex geometries.

Furthermore, minimal swiping occurred during these experiments. Zero swiping was observed in Experiment 4.03 and only on the first layer of Experiments 4.01 and 4.02 when the saturation was higher. Using delay geometries to increase the drying time between each layer has continued to be a successful technique. However, it is important to note that this method has two major issues. Firstly, controlling and quantifying the drying time between each layer is difficult, and secondly, the delay geometries occupy space in the printing bed, limiting the scale possible for the primary prints. As the swiping was drastically reduced in these prints, it was hypothesised that the HPS binder absorbs the liquid activator more rapidly than the cellulose derivatives, thus reducing swiping. It was determined that further investigation into swiping with this new binder was necessary to ascertain if delay geometries could be avoided.

Despite the success of Experiment 4.03, it is important to highlight the issue of oversaturation. This is when the binder saturation levels are set too high and the binder liquid bleeds out of the selected area, compromising the accuracy of the part (Du et al., 2020). Oversaturation occurred in both Experiment 4.01 and Experiment 4.02 (see Figure 4.36). In fact, in Experiment 4.01 the oversaturation was so significant that the geometry stuck to the bottom of the printing bed and the holes in the grid pieces could not be excavated (see Figure 4.37). The saturation was reduced in Experiment 4.02, but some oversaturation still occurred with rounding of the internal corners on the grid pieces. In Experiment 4.03, the saturation remained the same, but the amount of binder mixed into the powder was reduced from 4% to 3%. This adjustment allowed for a suitable balance between saturation and binder to be achieved and demonstrates the interconnectedness of these parameters (see Figure 4.7 for an overview of the production parameters). The impact of oversaturation on the accuracy of printed parts is well-established in BJT literature (Du et al., 2017; Lv et al., 2019; Marchelli et al., 2011). However, it is also important to note that higher saturation levels can increase green strength; therefore, finding a balance between mechanical strength and accuracy is crucial (Lv et al., 2019).

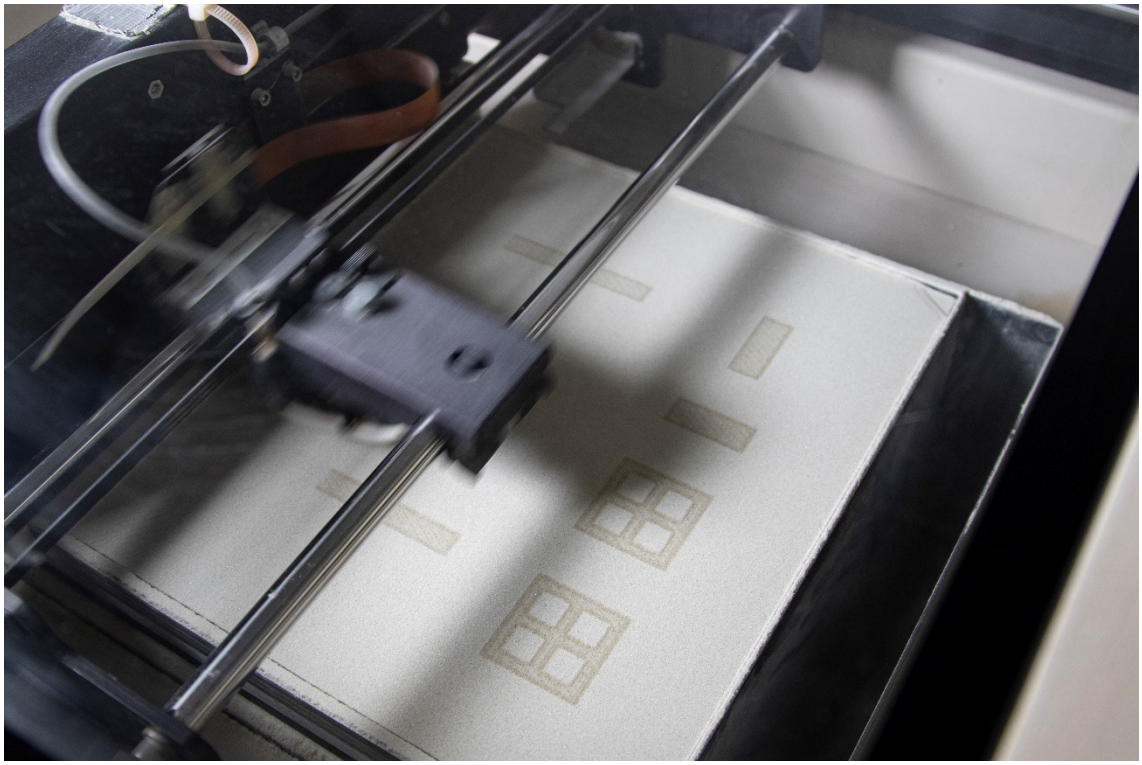

Figure 4.31. *Experiment 4.01 print in progress.*
Four rectangular prisms placed on the left side of the print bed as delay geometries.

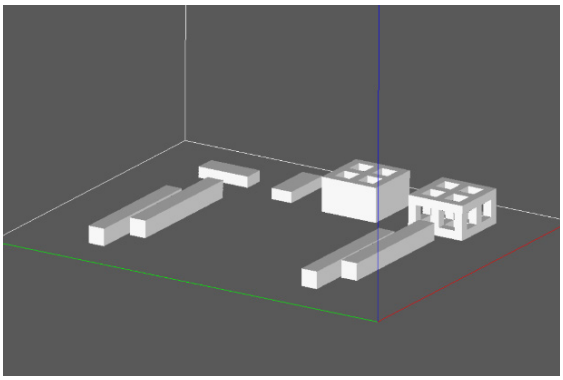

Figure 4.32. *Print layout for Experiments 4.01-4.03.*
Delay geometries placed on the left side of the print bed.

Figure 4.33. *Experiment 4.01 excavation in progress.*
Removing parts from the print bed.

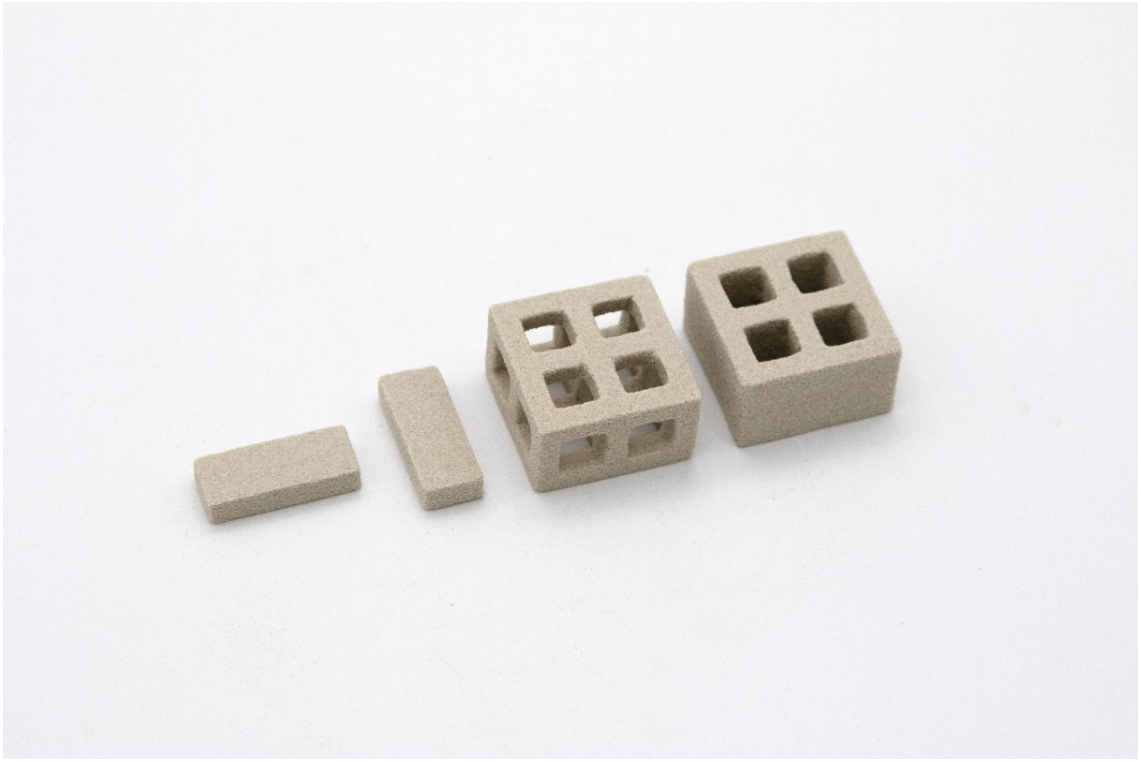

Figure 4.34. *Excavated results from Experiment 4.03.*
Parts with high accuracy and a degree of geometric complexity were able to be printed and excavated. Image does not include the delay geometries.

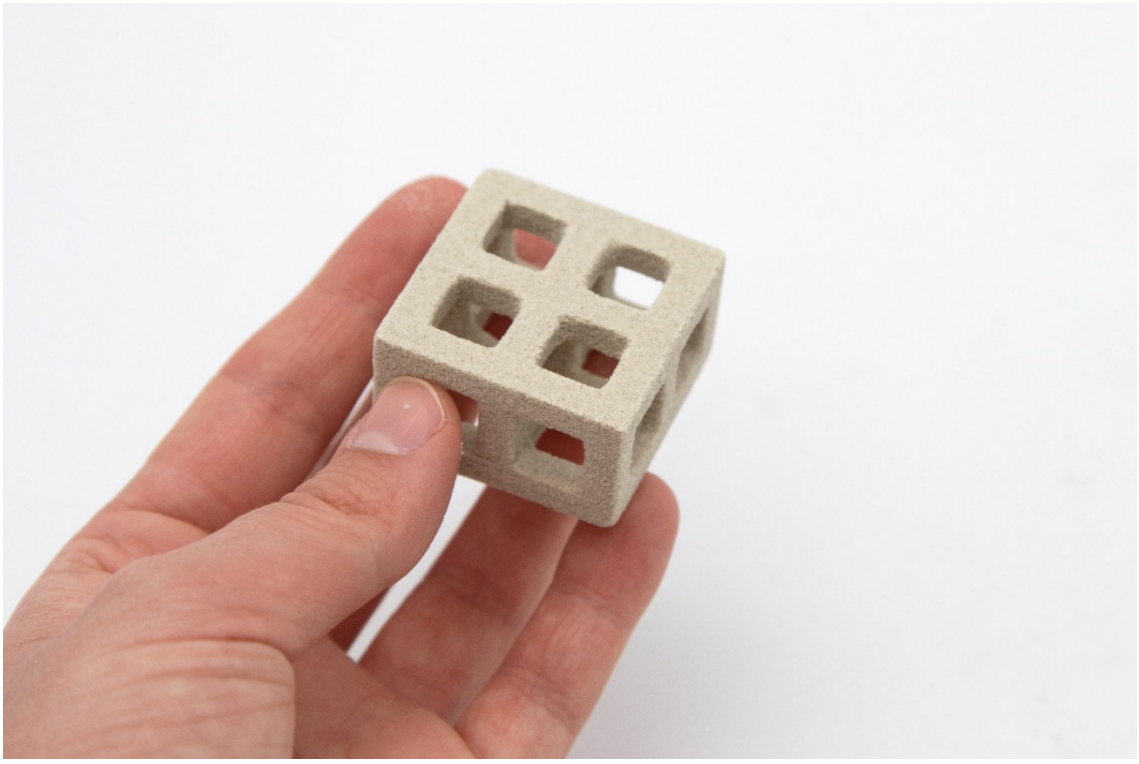

Figure 4.35. *Close-up of excavated wire frame grid from Experiment 4.03.*
The wireframe grid geometry reflects the complexity and accuracy achieved in this Experiment.

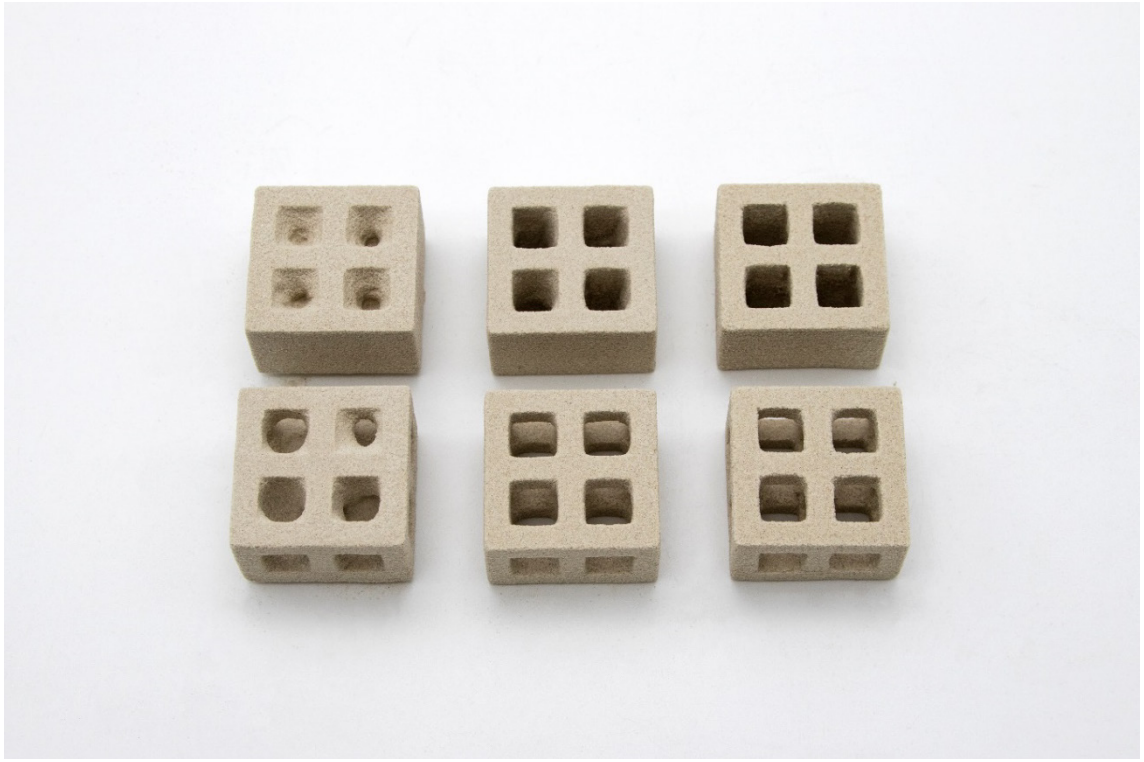

Figure 4.36. *Comparison of effects of saturation in Experiment 4.01-4.03.*
Experiment 4.01 (left) highest saturation, Experiment 4.02 (middle) reduced saturation, Experiment 4.03 (right) optimised saturation.

Figure 4.37. *Oversaturation in Experiment 4.01.*
Significant oversaturation caused the geometry to stick to the bottom of the printing bed and the holes in the grid pieces could not be excavated.

4.7.3 Hydroxypropyl Starch vs Maltodextrin

As stated in the previous section, a range of modified starches have been used in BJT literature. Maltodextrin is one of the most common of these materials. Maltodextrin is also a form of modified starch obtained through the conversion of starch by hydrolysis (Blanchard & Katz, 2016). This is the reaction of breaking the starch structure into simpler sugars. Maltodextrin is defined as having a dextrose equivalent of between 3-20. A dextrose equivalent is the term used to describe the degree of hydrolysis that has occurred, meaning the percentage of the starch that has been converted to sugars (or dextrose) (Castro Gutierrez et al., 2016; Kennedy et al., 1995). Like pregelatinised starches, maltodextrins are cold-water soluble with water-holding and non-hygroscopic properties (Y.-J. Wang & Wang, 2000). Maltodextrin has a wide range of applications, particularly in the food industry (Blanchard & Katz, 2016).

Of relevance to this research is also its application as an adhesive and its widespread use as a binder in the BJT of ceramics (Dewi et al., 2021; Du et al., 2020; Tharanathan, 2005). The only published academic article working with recycled glass in BJT printing used a powdered sugar and maltodextrin binder, in a composition of 80% glass powder, 10% powdered sugar and 10% maltodextrin (Marchelli et al., 2011). Given the strong precedent for using maltodextrin and the absence of prior use for the HPS binder, it was determined that testing should be conducted with maltodextrin. As green strength remains the primary challenge in the BJT of glass fines, a comparison of the green strength between the two is conducted to validate the future use of HPS.

This set of prototypes can be seen as 'prototyping as an experimental component' whereby the prototypes are constructed to test a specific hypothesis (refer to Section 3.3.1). It is specifically used here to determine the best direction for the binder formulation in this research. This type of enquiry is most akin to traditional scientific experimentation and for that reason it is presented under the subheadings of aim, method, results, discussion and conclusion. Elements of the production process have become more precise in this section to aid the validity of the experiment, i.e. the powdered feedstock is mixed using a food processor rather than by hand. A series of preliminary experiments were performed prior to this test to find the print parameters that allowed for accurate parts to be printed and excavated using the maltodextrin binder. The concentration of binder and saturation settings were adjusted to find parameters that would be suitable for both binders to allow for a valid experiment.

Aim:
To compare the green strength of 3D printed glass fines parts produced with a HPS or maltodextrin binder through a 3-point bend (flexural strength) test.

Method:
Moondust was mixed with a powdered binder in a commercial food processor for 15 minutes. 4% binder to moondust (w/w) was used, and water was used as the liquid activator. The tested binders include; HPS (National 208 from Ingredion) and Maltodextrin (DE-18 sourced from Red Spoon Company). A Z-Corporation 310 BJT machine was used to print rectangular prisms in the orientation and layout as seen in Figure 4.38 and Figure 4.39. Extra samples were printed in each binder to allow for breakages and testing of the equipment set-up (see Figure 4.40). A layer height of 0.2mm was used with saturation settings of 120% for shell and 130% for core based on the stock powder ZP15E. Once printed, parts were left in the print bed to dry for approximately 24 hours before being placed in a dehydrator at 60°C for 2 hours.

The green strength of the samples was measured using a 3-point bend test (also known as a flexural strength test). The testing method was adapted from ASTM B312. This is the standard test method for measuring the green strength of specimens compacted from metal powders (ASTM International, 2020). According to Mostafaei et al. (2021), there are currently no formalised standards for this process for BJT parts. This test specifies the use of a 3-pointbend test on a 1.25 × 0.5 × 1.25-inch rectangular bar. Five samples were tested as per ASTM D790-17 (ASTM International, 2017). A testing fixture was manufactured as per the ASTM B312 Transverse Rupture Test (see Figure 4.41 and Figure 4.42).

A Starr digital force gauge mounted on a manual stand was used to conduct the three-point bend tests. The stand uses a mechanical hand wheel that creates 3mm of linear movement for every rotation. A test specimen was placed on top of the test fixture. The wheel was turned on the testing stand until the specimen ruptured. The peak rupture measurement in Newtons was recorded (see Figure 4.41).

Results

As can be seen in Table 4.1 below, the parts printed using the HPS binder exhibited higher flexural strength than the maltodextrin samples. The flexural strength of the HPS samples was approximately 60% higher than those using maltodextrin. Both samples experienced swiping when printed, which is visible in the final parts (see Figure 4.40).

Test Number	Maltodextrin (N)	HPS (N)
1	24.0	35.8
2	17.7	39.7
3	25.0	37.2
4	25.3	39.7
5	20.2	32.6
Average	22.44	37

Table 4.1. *Results for flexural strength of Maltodextrin and HPS.*

Discussion:

As maltodextrin is widely used in BJT literature, the hypothesis was that the maltodextrin samples would have a higher green strength than the HPS ones. However, using these parameters, the HPS samples exhibited approximately 60% greater flexural strength. Drawing from current literature, it is hypothesised that the printing parameters for maltodextrin could be refined further, and that exploring additional types of maltodextrin might enhance its effectiveness as a binder. However, this test validated the use of HPS as a binder for this research, demonstrating that it has the potential to outperform maltodextrin. As a result, the printing parameter for HPS should continue to be optimised rather than pivoting to maltodextrin.

It is important to note that the ASTM B312 standard specifies that a uniformly increasing compressive load at a rate of approximately 90N/min is applied to the sample until a fracture occurs. As the Starr digital force gauge is a manual gauge that uses a mechanical hand wheel, the load rate cannot be as precisely controlled. As such, these results act as a comparative test of binder strength rather than a definitive reading of the flexural strength of the samples.

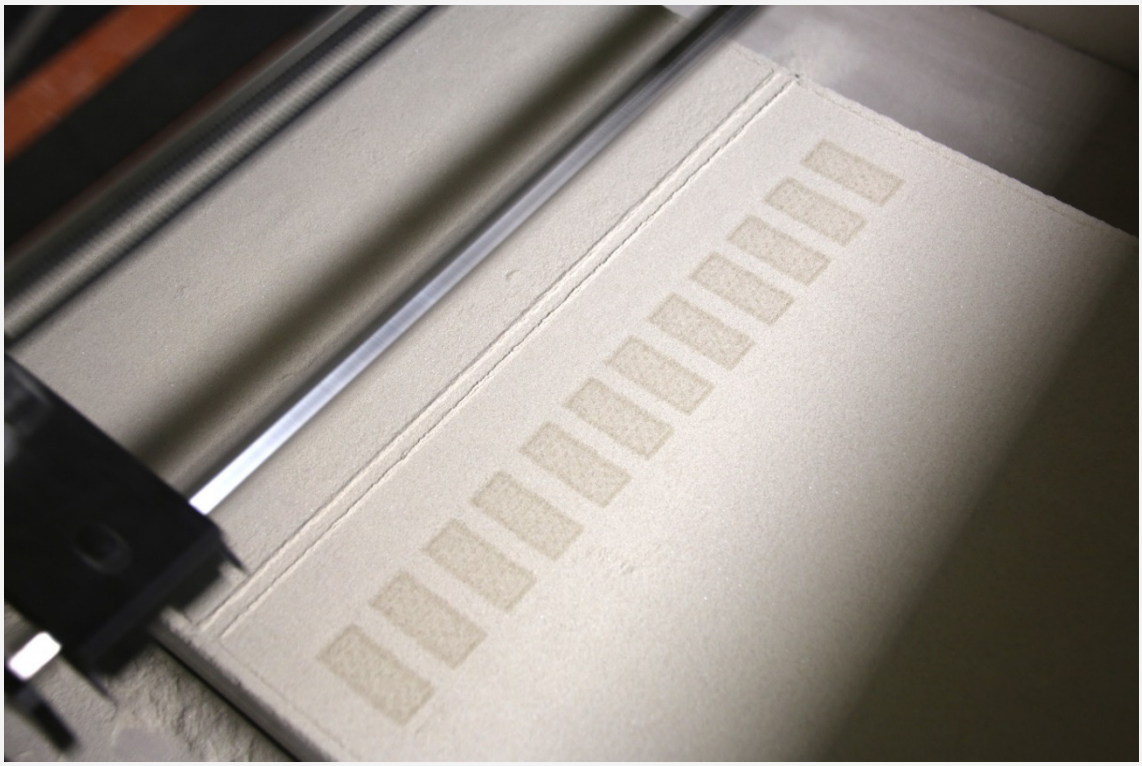

Figure 4.38. *Print in progress for test specimens for the flexural strength testing.*
Extra samples were printed in each binder to allow for breakages and testing of the equipment set-up.

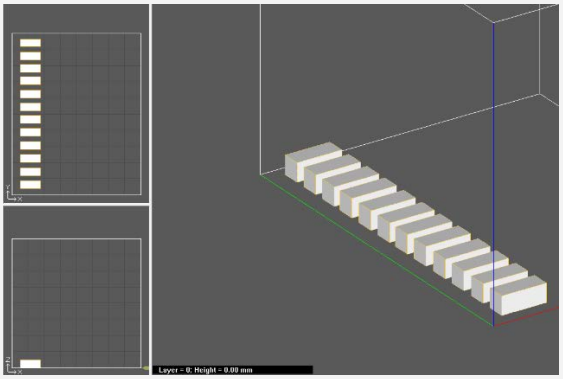

Figure 4.39. *Printing set up for comparative test of HPS and maltodextrin green strength.*

Figure 4.40. *The effect of swiping seen on the excavated test specimens.*

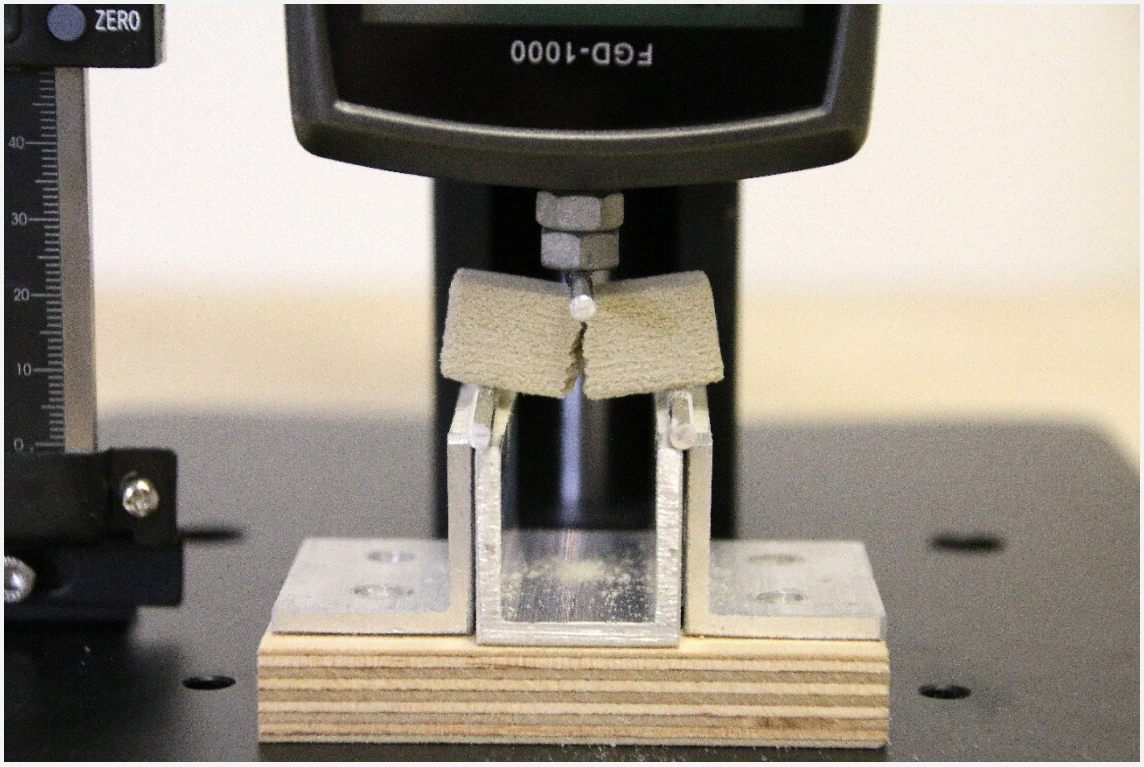

Figure 4.41. *Flexural strength testing in progress.*
The wheel was turned on the testing stand until the specimen ruptured as seen here. The peak rupture measurement in Newtons was recorded

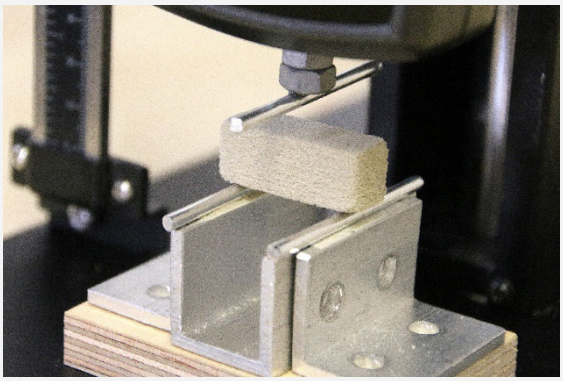

Figure Error! No text of specified style in document.**.42.** *Testing fixture and set-up for assessing the flexural strength of the green parts.*
A Starr digital force gauge mounted on a manual stand with testing fixture.

The swiping that occurred while printing the samples continues to be a challenge. This impacts the dimensional accuracy of the prints (see Figure 4.40). Whilst it is acknowledged that the large flat cross sections lend themselves to swiping, this needs to be investigated further.

This experimental prototype also resulted in a refinement of the material preparation process and drying step. Combining the binder and glass powder in a commercial mixer for 15 minutes and using a dehydrator to ensure the proper curing of the prints before excavating fully is in line with BJT literature and results in a more controlled and repeatable production process.

Conclusion:
The HPS binder produced samples with a higher flexural strength than the maltodextrin under the specified printing conditions. As such, this research will utilise the HPS binder. Further optimisation of the concentration and print parameters should be undertaken to increase the green strength further and reduce the swiping phenomenon.

4.7.4 Summary of finding the binder formulation

This phase of experimentation allowed for a more suitable binder formulation to be determined. The superior green strength provided by HPS, particularly over the cellulose derivatives makes this binder a suitable option. A concentration of 3-4% with saturation settings of 120-130% core and 120-145% shell produced accurate parts that could be excavated and handled without any breakages. These parameters are carried into the next phase of experimentation, which explores geometry, scale and the firing phase of the production process. While these parameters were successful in producing small-scale objects (20mm in height), they will likely need adjustment as the scale and complexity of the shapes increase.

Swiping continued to be a challenge, impacting the printability of the parts. Sacrificial geometries were used to increase drying time between layers. This reduced the occurrence of swiping but is difficult to quantify and takes up significant space in the print bed. As swiping depends on geometry, it will continue to be assessed in the next section as geometries and scale are explored.

4.8 Reflection and conclusion

This chapter has documented and discussed the initial stage of experimentation in the 3D printing of glass fines via BJT. The first section of the chapter provided contextual information on the researcher's previous work to clarify the foundation and starting point of the current study. Information regarding the material background and production background was then presented, including the equipment set-up and an SEM analysis of the glass fines. The second half of the chapter discussed two stages of the experimentation; finding the printing parameters and finding the binder formulation. Figure 4.43 provides a diagrammatic representation of the experimentation in this chapter, including the initial SEM analysis. This diagram is based on the Research Diagram presented in the Methodology (see Section 3.5), utilising cascading circles to depict the sequence of experiments, where insights gained from one experiment guide the next. The circles vary in colour to represent the different kinds of prototypes; transparent circles denote prototypes as vehicles for enquiry, whereas the black circles represent prototypes as experimental components (see Section 3.3.1)

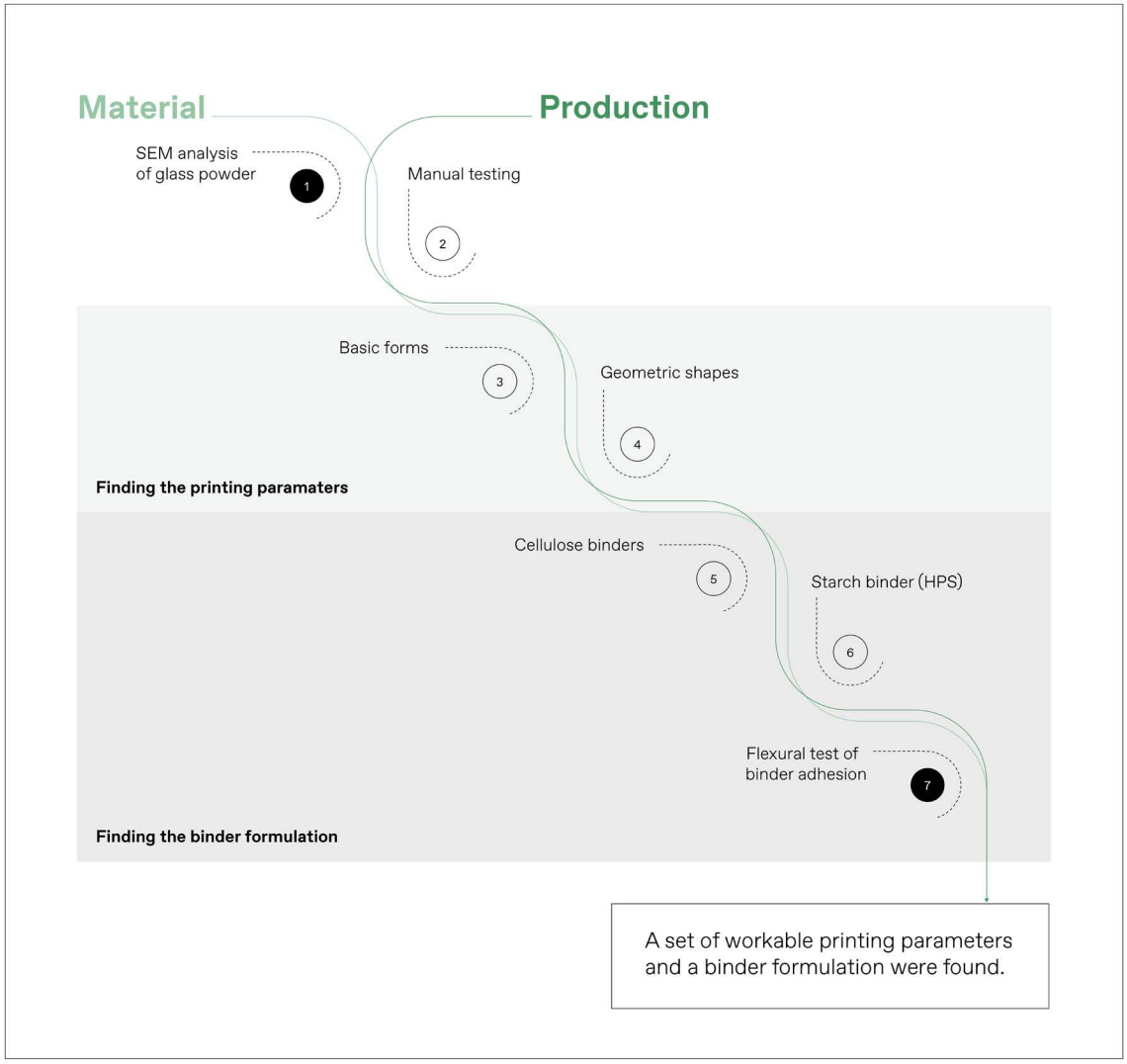

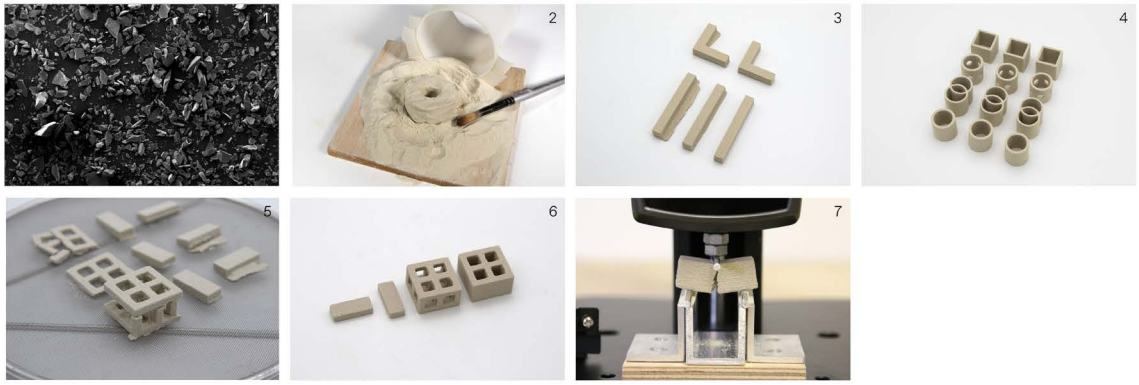

Figure 4.43. *Diagrammatic representation of Chapter 4 experimentation.*
The experimentation in this chapter focused on the material and production threads of the research questions. These questions were addressed through seven sets of experiments, symbolised by the cascading circles. The experiments in the diagram are numbered to correspond with their respective images.

These experiments are informed by the 'threads' of the research. As shown in this diagram, the material and production threads or research questions (a) and (b) are the focus of this chapter. The application has not yet come into play. This is a key component of materials-based design projects, where a certain level of understanding and expertise of the material and production is needed before potential applications can be envisioned. This exploration phase, as Ribul et al. (2021) may describe it, allows for foundational knowledge of material properties and production capabilities to be built that can drive decisions around suitable applications.

The diagram shows that seven groups of experiments were conducted in this Chapter, with some containing multiple individual tests as highlighted throughout the chapter and in the documentation provided in Appendix 2. The experimentation started with the initial SEM analysis, which provided information on the properties of the glass fines material. Manual tests were subsequently carried out to validate the BJT production method and the initial material formulation quickly and cost-effectively. The experimentation then focused on determining the printing parameters, starting with basic forms and moving on to more complex geometric shapes. Parameters such as layer height and saturation were adjusted incrementally to develop a workable method. This testing highlighted the importance of green strength in ensuring that parts could be excavated from the print bed without breaking.

Consequently, the next group of experiments focused on optimising the binder formulation. Initially, cellulose derivatives were tested with limited success before exploring starch derivatives, where the potential of a cold swelling HPS binder was discovered. An experimental prototype was then conducted to further assess the adhesive ability in comparison to another binder option, ultimately determining the suitability of HPS and enabling further refinement of the production process.

Overall, the experimentation in this chapter resulted in the development of a set of stable production parameters and the determination of a suitable material formulation. This allowed for accurate parts with a degree of geometric complexity to be printed and excavated without breakages. Through this experimentation, an understanding of the numerous variables and interrelations between the material and the production system was also developed. Both the material itself and each step of production involve several variables that must be balanced, as changing any one can significantly impact the process. For example, material variables such as particle size and shape impact powder spreading and density (as discussed in Section 4.3.1), whereas the type and concentration of binder are closely linked to saturation levels and drying time (as highlighted in Section 4.7.2). Understanding and accounting for these variables presents a key challenge in materials-based research and underscores the need for a rigorous documentation method through which decisions and results can be traced. Integrating knowledge from materials science and engineering with hands-on experimentation is crucial in developing this understanding. It also aligns with the increasing body of literature in materials design, which advocates for enhanced interdisciplinary collaboration (Duarte Poblete et al., 2023).

When dealing with this level of complexity and variables, it becomes pertinent to make decisions that can contain the research and to begin to fix certain variables where possible. For example, whilst there are numerous material preparation steps for BJT, the dry mixing method was chosen for this research to eliminate any further variables and streamline the production process. Similarly, although several other binders could have been investigated, once HPS was found to provide adequate green strength and accuracy, this became fixed. This approach prioritises the development of workable and stable parameters over the quantification or optimisation of each individual element. This stems from the RtD methodology, where the research is driven by the pursuit of an application alongside this more generalisable knowledge. It also signals the translational role that designers play in materials based research, bridging the gap between emerging materials and

production methods, and real-world applications and industry practices. This perspective does not discount the importance of optimising material or production parameters but speaks to the value of parallel design-led exploration and technical refinement.

As mentioned above, throughout this experimentation, some variables such as layer height and the choice of binder have become fixed. However, it has also become clear that some variables will need to remain open to adjustment or exist within ranges. This is because part geometry and scale, and therefore the chosen application are closely linked with the material and production parameters (see Figure 4.7 for an overview of the production parameters). For example, large-scale parts require longer drying times, whereas saturation settings may need to be adjusted for highly intricate parts.

Whilst a thorough understanding of the printing parameters and material formulation has been built throughout this chapter, at this stage, the printed parts remain small in scale and the final production step of firing has not yet been covered. The following chapter will focus on these elements and will bring in the application thread of the research questions.

5

Further Prototyping: Firing and Exploring Geometries

5 Further Prototyping: Firing and Exploring Geometries

5.1 Introduction

The previous chapter documented the first phase of prototyping, which resulted in a binder formulation and associated printing parameters being determined. The combination of these two elements allowed for the printing and excavation of geometric shapes (approximately 40mm in height max) with a degree of complexity (thin walls, overhangs). However, the final stage of the production process, firing, in which these green parts are fused into usable glass objects, has not yet been covered. This stage of the production process is both crucial and complex. The first section of this chapter will discuss the relationship between heat and glass and the requirements of the firing step employed in this research. This will be followed by 'expansive' prototyping into the geometric capabilities and limitations of this material and production method. The expansive approach draws on the types of drifting outlined by Krogh & Koskinen (2020) in Chapter 3.

A key benefit of using BJT is being able to create geometries from glass that are difficult, if not impossible, to make using traditional glass manufacturing methods. This stage of experimentation will explore novel geometries with a focus on surface textures, lattices and scale. Whilst an eye for application and aesthetic awareness is present throughout this experimentation, the development of an application will be covered in detail in the following chapter. To conclude the chapter, two prototypes as experimental components will be discussed, which are used to verify the properties of the material and its circularity.

5.2 Heat and Glass

As outlined in the previous chapter, a four-step production process is undertaken in this research to create artefacts using glass fines: material preparation, printing, drying and firing. As the mechanical properties of most green parts produced by BJT (no matter the material and binder adhesion) are insufficient, a post-processing step is necessary. In this research, a firing step is employed in which the parts are fired in a kiln to fuse the glass particles together. To accomplish this, it is important to understand the complex behaviour that glass exhibits when heated and cooled. In this section, two key areas of knowledge have been integrated, theoretical materials science research and insights from glass artists and craftspeople who specialise in what is known as the kiln forming of glass.

As discussed in Chapter 2, commercial soda lime silicate glass is formed by melting soda ash, and limestone with silica sand to create a homogenous viscous material. The cooling process is then controlled to prevent crystal formation, resulting in a disordered, non-crystalline atomic structure. This means that glass does not have an exact melting point; instead, it gradually softens when heated, becoming more fluid as the temperature increases. Additionally, this allows glass to be reheated to various temperatures to reform it. This heating and cooling process is, however, quite a complex phenomenon. As shown in Figure 5.1, several key temperatures exhibit specific viscosity characteristics that affect the glass forming process (Callister & Rethwisch, 2018). The gradual softening of glass when heated can be seen in the gentle relation curve between temperature and viscosity (Beveridge et al., 2005). For typical soda lime silica glass, the glass 'melts' at approximately 1450°C, becoming viscous like a thick syrup (Varshneya & Mauro, 2019). The working and softening points represent the highest and lowest temperatures, respectively, at which the glass can be formed (Hand, 2021). For soda lime

silicate this is between approximately 700°C and 1000°C. As glass cools down, stresses form due to the non-uniformity of the cooling (i.e. the outside of the glass begins cooling first) (Varshneya & Mauro, 2019). These stresses can cause the glass to crack or break. It is therefore essential to control the cooling of the glass through an annealing process. This involves holding the temperature of the glass at the annealing point for approximately 15 minutes and then slowly lowering the temperature to the strain point (Varshneya & Mauro, 2019). For soda lime silica the annealing point is approximately 550°C and the strain point is approximately 500 degrees. Once it reaches the strain point it is no longer necessary to slowly cool the glass (Hand, 2021).

These key glass viscosity points provide the theoretical basis for the glass art practice of kiln forming. This refers to a range of techniques for shaping and fusing glass in a kiln; including slumping and casting (Beveridge et al., 2005). In Figure 5.1, the typical working temperatures for different kiln-forming techniques with soda lime silica can be seen. At around 550°C the glass begins to bend or slump under its own weight. Many glass artists harness this to produce work in which glass sheets are slumped over or into moulds. The glass will continue to stretch as the temperature increases due to gravity and its growing fluidity. At as low as 650°C the surface skin of the glass will collapse meaning that the glass will stick to any surface it meets (Cummings, 2001). This means that at this temperature, separate pieces of glass can be fused (or stuck) together. Glass artists employ low-temperature tack fusing and high-temperature full fusing techniques using a range of glass materials including sheets, powders, rods and tubes. Tack fusing will partially fuse the glass, sticking the different layers or particles together but the piece will essentially retain its original shape. The glass melts completely in full fusing, forming an amalgamated piece with rounded edges (Beveridge et al., 2005). See Figure 5.2 for comparison. When heated above approximately 850°C, glass can be cast in a mould. There are a range of methods for this including using glass powders or Pâte de Verre techniques (Cummings, 2001).

Crucial to each of these kiln-forming techniques is not only the temperature of the kiln but the rate and steps at which this temperature is applied. A typical glass firing schedule can be seen in Figure 5.3. As stated above, the heating and cooling of glass must be controlled to avoid thermal shock or devitrification. Devitrification refers to the formation of crystals in the glass. This typically happens when the glass is kept at high temperatures for too long (Cummings, 2001). Devitrification causes transparent glass to become cloudy or translucent and opaque glass to lose its shine (Beveridge et al., 2005). As such, the main goal of a glass kiln firing schedule is to bring the glass up to a temperature at which it will fuse or slump into shape and then return the glass to room temperature without causing internal stresses or devitrification. A successful firing program is the result of the right combination of time and temperature (Beveridge et al., 2005).

Most glass firing schedules contain eight stages (see Figure 5.3). The initial heating phase involves slowly heating the glass from room temperature to just above the strain point. This increase must be slow to avoid any thermal shock. The glass will remain solid until just above the strain point (Beveridge et al., 2005). The pre-rapid heat soak is an optional step designed to even out the temperature in the glass body before the rapid rise stage. Including this step can allow for a faster ascent (Bullseye Glass, 2020). The rapid heat phase involves increasing the temperature to within the working range of the glass as fast as possible to avoid devitrification (Bullseye Glass, 2020). The process soak allows for a brief stabilisation of the glass before a rapid cooling process occurs where the temperature is reduced to the annealing point. As in the rapid heating phase, this must be as fast as possible to avoid devitrification. Once the glass reaches the annealing point it is left to soak for generally 15 minutes (although this depends on the thickness of the glass) and then slowly cooled to the strain point. The final step is the cooling back to room temperature which must be reasonably slow to avoid thermal shock.

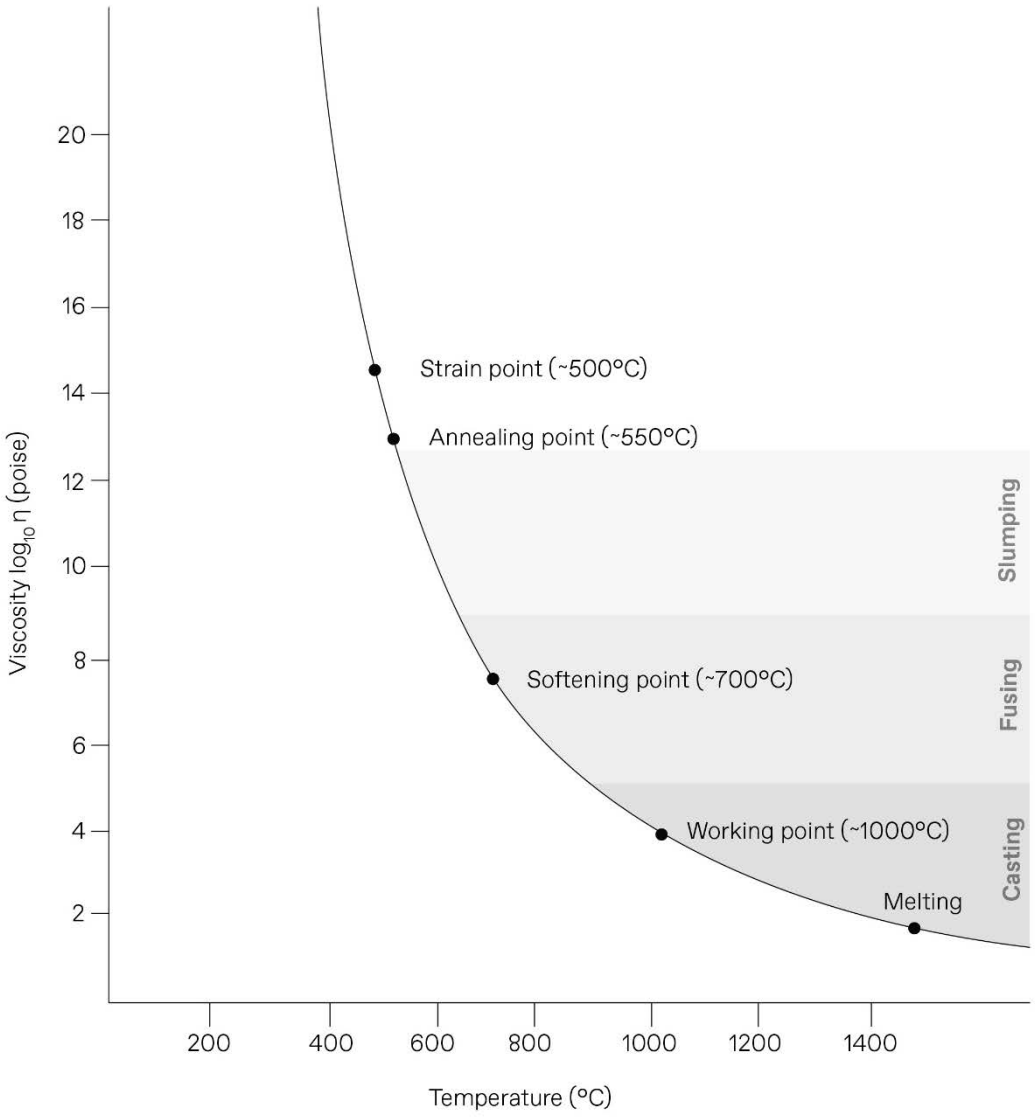

Slumping- At approximately 550°C unsupported glass begins to bend under its own weirght and take up the form offered by moulds.

Fusing- At approximately 650°C individual glass pieces will begin to fuse together. At the lower end of this temperature range parts will be tack fused, at the higher end full fusing will occur.

Casting- At approximately 850°C, glass flows and can be cast in moulds. This can be done with small glass pieces (frit) or using crucibles filled with molten glass which can be poured or unplugged to let flow into moulds.

Figure 5.1. *Changing viscosity of soda lime silicate glass with temperature.*
Image adapted from Varshneya & Mauro (2019), combining kiln forming temperature data from Cummings (2001).

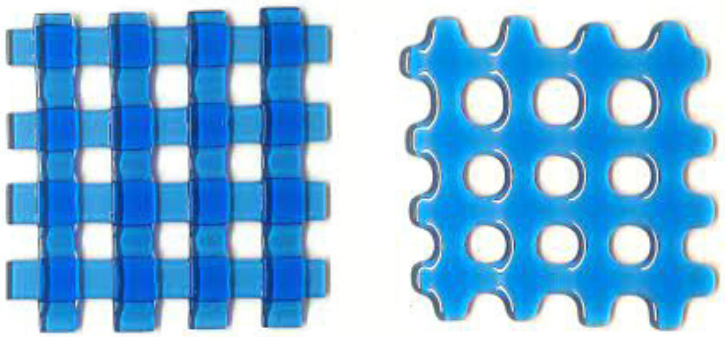

Figure 5.2. *Comparison of tack fused glass (left) and fully fused glass (right) .*
Image adapted from GlassCampus (n.d.).

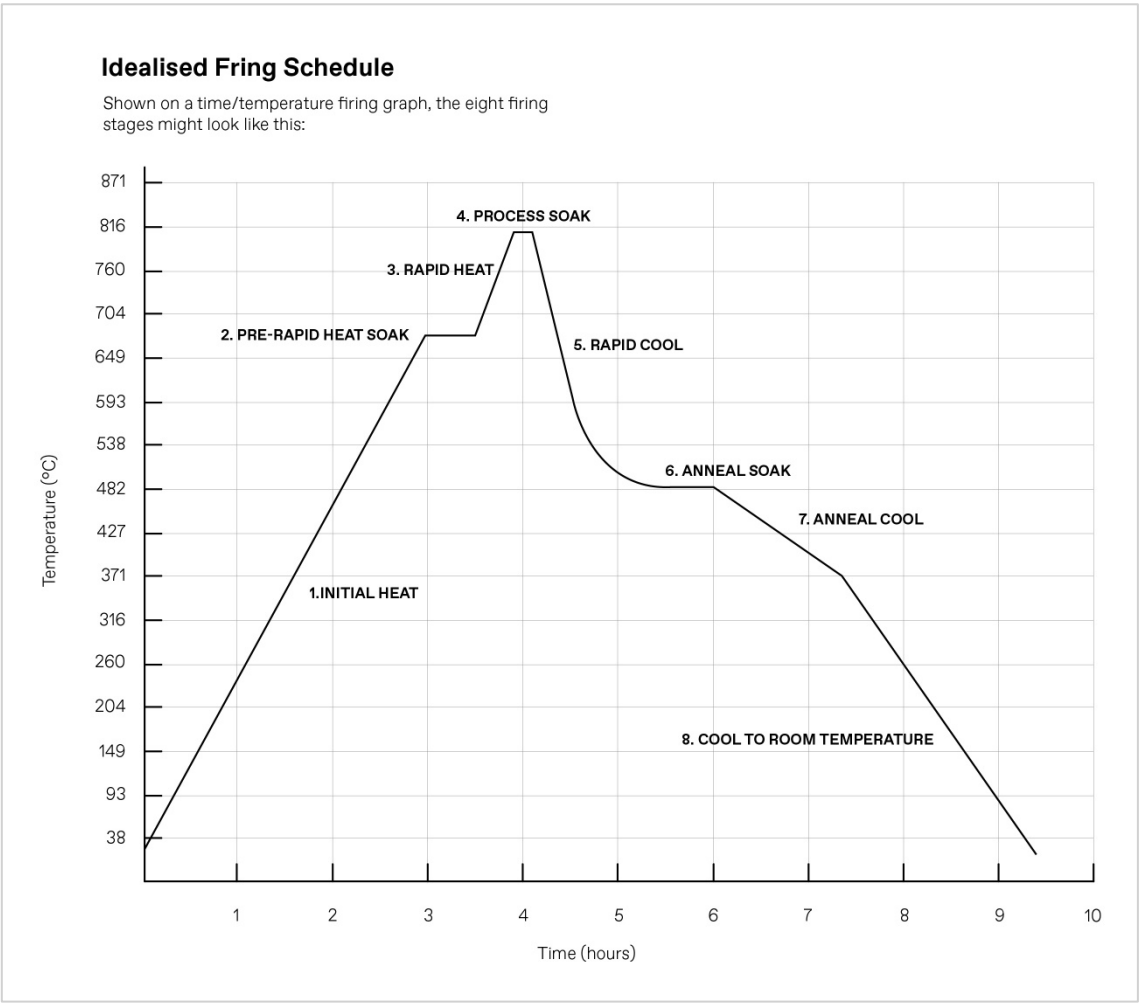

Figure 5.3. *Idealised time/temperature firing schedule for full glass fusing.*
Image adapted from Bullseye Glass (2020).

5.3 Firing Process

The firing process used in this research is comparable to the sintering step found in much of the ceramic BJT literature. This involves heating green parts made of ceramic powders to a high temperature (often just below the melting point) to create a dense body (Du et al., 2020). This is a standard processing procedure for ceramics. However, pre-shaping glass powders into green bodies and subsequent sintering is considerably less common. This is particularly true in industry, where glass is primarily produced through a melt-quenching process, in which raw materials are melted together in a furnace (Liu et al., 2022b). Despite this, the lower temperatures required for sintering and the potential for producing new geometries have prompted investigation (Lin et al., 2015; Rabinovich, 1985).[12]

The sintering process of non-crystalline materials such as glass is referred to as viscous sintering and it takes advantage of the gradual softening that occurs when glass is heated (Rahaman, 2007; Scherer, 2001). During the heating process, the glass particles will start to flow and coalesce, reducing their surface area, much like raindrops merging on a window (Scherer, 2001). Figure 5.4 demonstrates the sintering of two glass spheres via viscous flow. Once the glass cools, it hardens again. This is what occurs during the firing of the green parts printed in this research. However, as previously mentioned, the heating and cooling processes need to be carefully controlled and refined to reduce internal stresses or prevent devitrification.

As with ceramic BJT parts, the printed glass fines parts are inherently porous, so any firing or sintering process causes shrinkage. Typically, some porosity also remains in the part after this firing process (Gibson et al., 2021). Furthermore, although the sintering process enables the glass to fuse, the retained porosity typically prevents the parts from being transparent (Rabinovich, 1985). As glass softens when heated, material slumping—which does not occur in ceramic sintering—affects geometric accuracy and the kinds of geometries which can be produced. Understanding and controlling the slumping is a key element of this research, which will be explored throughout this chapter and the next.

5.3.1 Initial Firing Schedule

The initial firing process used in this research was based on iterative testing conducted during the previous extrusion-based work (see section 4.2). To develop this firing schedule, we collaborated with experienced glass craftspeople to adapt a typical glass fusing schedule to suit our recycled glass 3D forms. We achieved this by gradually altering the peak temperature, soak time, and process steps (refer to Figure 4.7 for an overview of the production parameters). As shown in Figure 5.5, the temperature increases steadily at first, followed by a sharp rise to the peak temperature and an immediate decrease to the annealing point. These events occur rapidly to prevent devitrification. Typically, in kiln working with glass, there is a soak period at the peak temperature to allow for a brief stabilisation of the glass. However, due to the 3D forms, we were advised to omit this step as it would likely cause the parts to slump or deform under their own weight as they started to soften. A soak time of one hour is included at the annealing point before a gradual reduction in heat back to room temperature. High-temperature ceramic kiln paper was placed on the kiln shelf to prevent glass parts from sticking. This firing schedule was used for the experimentation discussed in this chapter and will be referenced throughout.

[12] It is worth noting that the sintering of glass powders is not a new concept, it is almost as old as glass technology itself as glazes which have been used for thousands of years are essentially coloured glass powders that have been sintered together (Rabinovich, 1985).

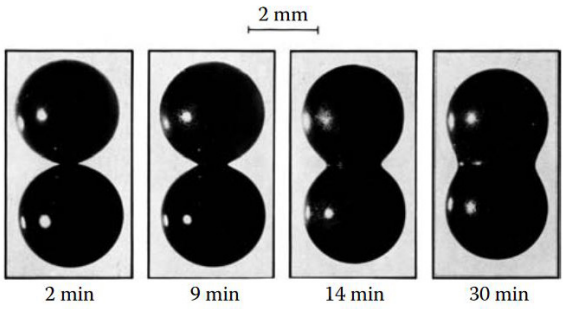

Figure 5.4. *Two glass spheres coalescing during viscous sintering at 1000°C.*
Image from Scherer (2001).

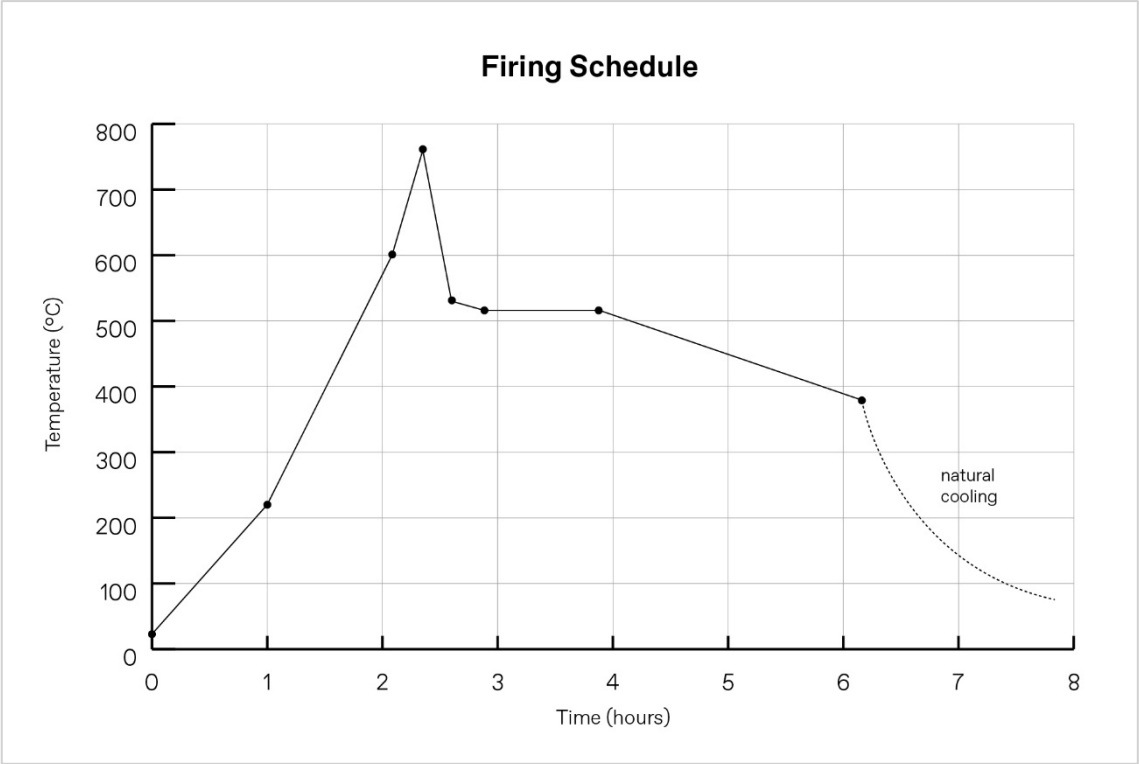

Figure 5.5. *Initial firing schedule.*
This schedule was made up of seven steps with a peak temperature of 760°C.

The aim of this firing schedule was to create fused glass parts that were waterproof. In observational testing of parts fired using this schedule, they appeared waterproof with droplets staying on the rather than permeating through. As a key property of glass is often waterproofness, validating this is important for determining applications that may require water-tightness. This will be explored further in Section 5.7.3.

5.4 Firing and Circularity

Beyond creating fused, usable parts, this firing process has a secondary aim that has not yet been discussed. Crucial to this research is how the firing process can enable the circularity of the material. Creating composite materials or adding binders to a material can pose a barrier to circularity. This is largely due to the difficulties associated with separating the material components, which can be challenging or sometimes impossible, resulting in materials and products being sent to landfill. As a result, it is important to this research and the broader development of circular materials that the recycled glass remains as glass, without compromising the material integrity with any additional materials. It is for this reason that other post-processing steps, such as infiltration, where the porous green parts are filled with a liquid like epoxy, were not pursued. Similarly, for this reason, 'no-bake' binder options such as furan were not pursued (Ziaee & Crane, 2019)

To ensure the binder would burn out during the kiln firing, organic binders have been employed. The concept is that the binder burns away as the glass starts to soften and adhere, enabling the shape to be preserved while resulting in a pure glass object with no binder remaining. This is a common process for BJT of both ceramics and metals. With this in mind, the organic binders tested in the previous chapter were selected based on their theoretical capacity to burn off without leaving any residue or producing toxic fumes. It was also crucial to consider the burn-off temperature of these binders in order to find a balance between this and the softening temperature of the glass, thereby preventing the entrapment of the binder in the glass material as it fused.

In the previous chapter, HPS was identified as the most suitable binder due to the green strength it provided. It was also selected because, theoretically, no HPS binder should remain in the 3D printed glass fines after firing. This is because previous studies have reported that HPS burns off between 290°C and 330°C (Silva et al., 2013). As the 3D printed glass are fired in excess of 600°C, it is highly unlikely that any HPS is remaining in the samples. However, to properly validate this and determine if it is, in fact, just the soda lime silica that remains once the parts are fired, a Thermogravimetric Analysis was undertaken.

5.4.1 Determining Material Circularity: Thermogravimetric Analysis

To determine the material circularity of the 3D printed glass fines, a Thermogravimetric Analysis was conducted (TGA). TGA is a quantitative thermal analysis technique in which the mass of a sample is monitored whilst it is gradually heated (Saadatkhah et al., 2020). Heating causes the sample to undergo physical or chemical changes, allowing for the characterisation of the compounds within the material. These compounds can be identified by examining the temperature at which the changes occur and the heat energy involved in the reaction (Ahluwalia, 2023). TGA is used widely in materials science and chemical engineering for assessing factors such as thermal stability, multicomponent composition, and moisture and volatile content (Saadatkhah et al., 2020). The TGA conducted in this research is considered a prototype as

an experimental component. Consequently, this section is organised under headings that align with the scientific method.

Aim:
To determine the composition of the 3D printed glass fines material after firing and assess whether any binder remains.

Method:
Three powder samples were prepared: (1) a 3D printed sample (fired according to the schedule seen in Figure 5.5), which was crushed into fine powder, (2) glass fines powder only, and (3) glass fines powder combined with 4% HPS (as per the feedstock powder used for printing in this research). All three samples underwent TGA under the following experimental conditions.

All experiments were conducted in a Netzsch STA 449F1 TGA instrument. Approximately 10 mg of samples were placed in an aluminium oxide crucible with a perforated lid. These crucibles are used in TGA because they can withstand high temperatures. Samples were heated from room temperature (approximately 30°C) to 650°C, at 10°C per minute heating rate and held at that temperature for 30 minutes. All experiments were carried out under the 50ml instrument air (80% N_2, 20% O_2) and 10 ml N_2 gas flow. A background experiment under similar experimental conditions was run before the actual sample runs to account for any instrument drift, buoyancy and baseline noises.

Results:
The results of the TGA on the three samples can be seen in Figures 5.6- 5.9. A comparison of the three samples can be seen in Figure 5.6. Figure 5.7 shows the 3D-printed, fired sample. It can be seen that the weight of this sample remains stable throughout the studied temperature range (30°C-650°C). Figure 5.8 shows the glass fines (only) sample. A weight loss of 0.87% occurred up to the temperature of approximately 460°C. After this temperature, the material was stable, and no further weight loss was observed. Figure 5.9 shows the glass fines sample containing starch binder. An overall weight loss of 4.48% was observed. The weight loss began at approximately 210°C with a maximum decomposition at approximately 317°C.

Discussion:
In Figure 5.8 it can be seen that the glass fines (only) sample, represented by Curve 3.1 (purple) in Figure 5.6 experienced 0.87% weight loss up to a temperature of approximately 460°C. This is likely the burning off of a small amount of organic matter or resins. As glass fines are a mixed, recycled material they are known to contain contaminants like this. It has been suggested that thermally heating glass fines in a conventional kiln up to 550°C can provide a way of heat treating them to remove these contaminants (Flood et al., 2019). In their TGA of glass fines, Flood et al. (2019) also suggested that the burn off of this organic matter results in the formations of a primary carbonaceous char between 450-550°C which then fully oxidises at temperature greater than 550°C.

The glass fines and starch sample, seen in Figure 5.9 and represented by Curve 5.1 (black) in Figure 5.6, experienced an overall weight loss of 4.48%. Initial decomposition of 3.58% began at 210°C with a maximum decomposition at 317°C. This likely corresponds with the burn off of the HPS binder. A further decomposition of 0.9% was observed until approximately 480°C at which the weight becomes stable.

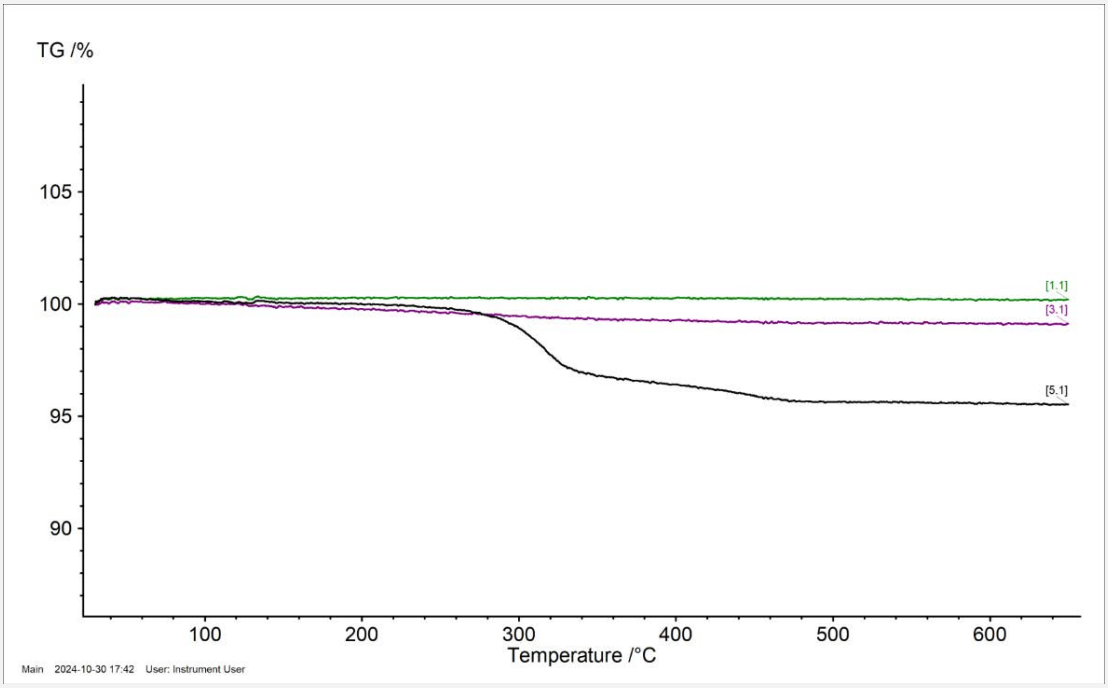

Figure 5.6. *Comparison of TGA results for the three samples.*
Curve 1.1 (green) 3D printed, fired sample; Curve 3.1 (purple) glass fines only sample; Curve 5.1 (black) glass fines combined with HPS binder sample

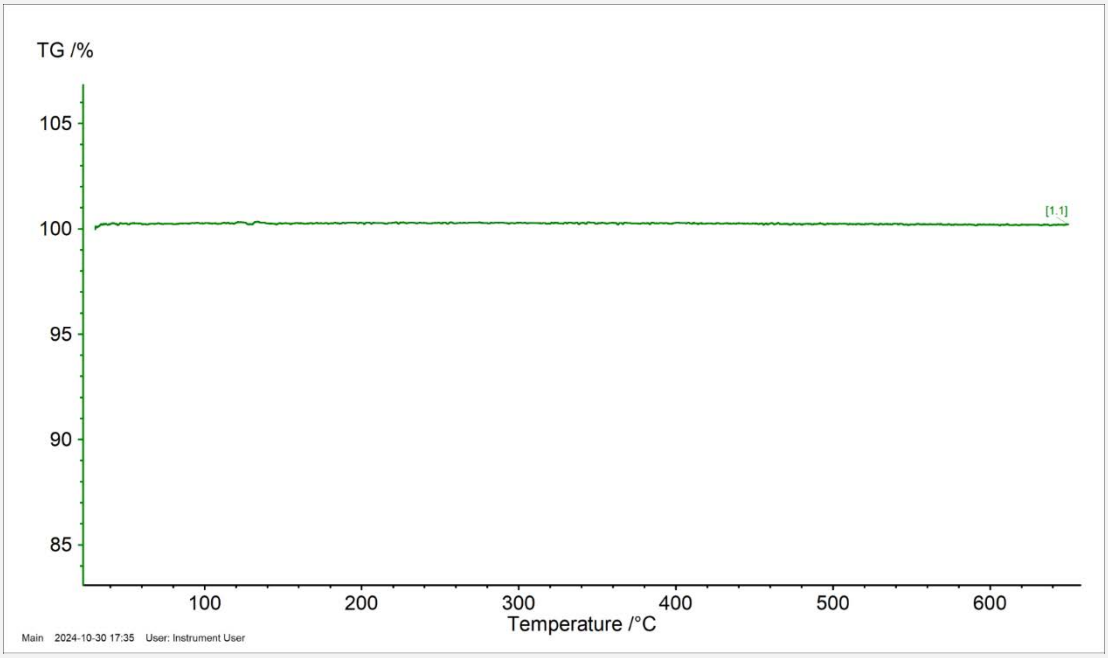

Figure 5.7. *Results of TGA for 3D printed and fired sample.*
No weight loss was observed, reflecting that the binder is no longer present in the material once fired.

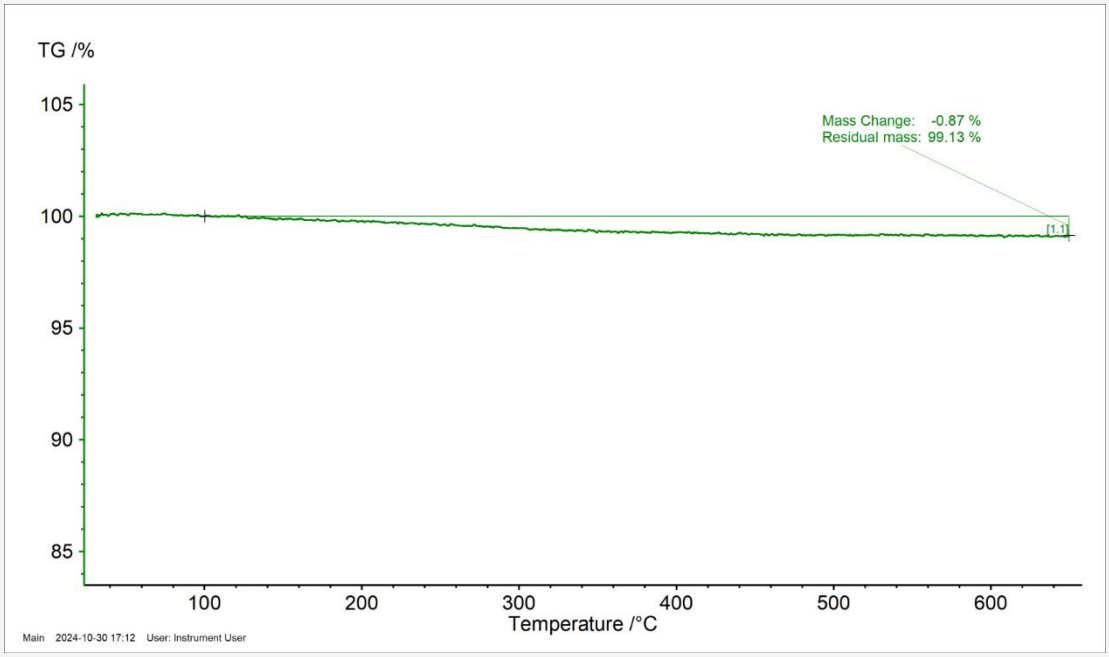

Figure 5.8. *Results of TGA for glass fines (only) sample.*
A weight loss of 0.87% was observed. This is likely the decomposition of organic contaminants.

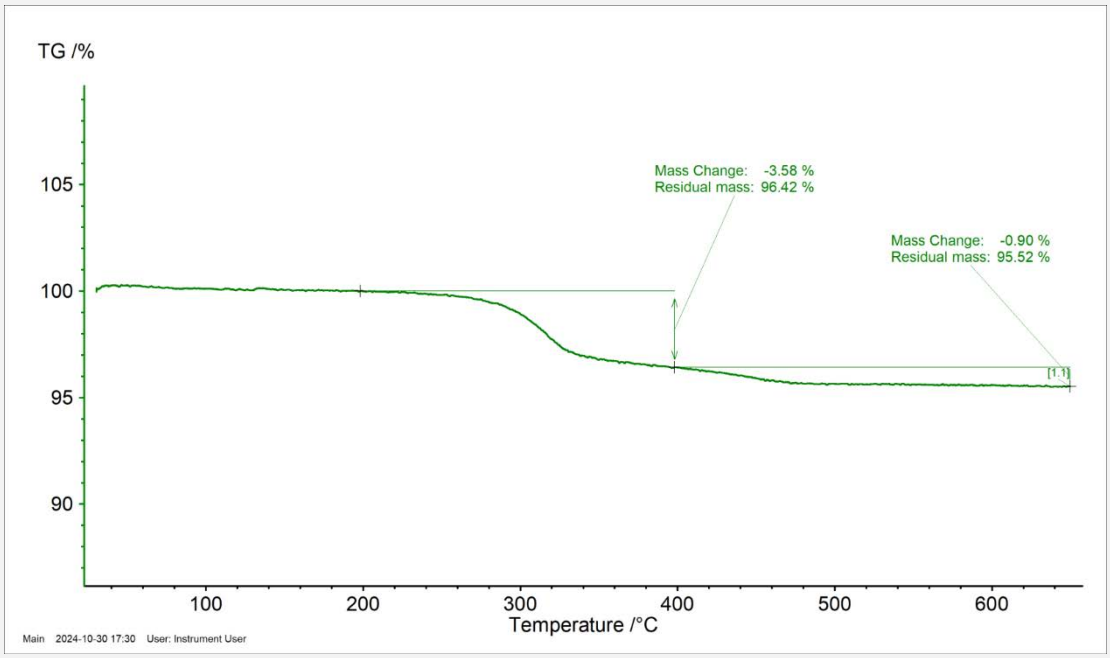

Figure 5.9. *Results of TGA for glass fines combined with HPS binder sample.*
A total weight loss of 4.48% was observed. This is likely the decomposition of the HPS binder and organic contaminants present in the glass fines sample.

Given the results explained above, this is likely the decomposition of the organic matter or contaminants in the glass fines. Due to the presence of these contaminants, it is not possible to determine at exactly what temperature the HPS begins to burn out, but these results are in line with the temperatures observed by (Silva et al., 2013) in which the HPS decomposed between 290-330°C. Slight variations in the amount of contaminants are likely due to the heterogeneity of the glass fines, which is common in recycled materials.

The 3D-printed and fired sample, seen in Figure 5.7 and represented by Curve 3.1 (green) in Figure 5.6, remained stable throughout the studied temperature range. This suggests that no binder remains in the material and that any organic contaminants have also been removed during the firing process. As such, the resulting material consists solely of soda lime silica glass fines, thus preserving the material's integrity and recyclability. This further implies that the part could re-enter the existing glass recycling system.

It is worth noting that even if small amounts of the binder were found to remain in the material, it would not necessarily inhibit the circularity of the material. Parts could be further heat treated as was suggested by Flood et al. (2019) above or could go into a closed loop system. Furthermore, as traditional recycling of glass involves heating cullet in furnaces up to 1500°C, this would result in the burn-off of any remaining residue.

Conclusion:
These results confirm the circularity of the BJT glass fines material after firing. It can be seen that the material remains stable when heated to 650°C, demonstrating that the binder and other contaminants have decomposed during the initial firing process. As a result, this material formulation and production process can facilitate the creation of circular products made from glass fines that can be recycled repeatedly.

5.5 Exploring Geometries

With the preliminary print parameters and material formulation established in the previous chapter, this next phase of prototyping focuses on the firing process and geometries. As glass softens when heated, its behaviour in the kiln significantly impacts the geometries that can be created. This phase of prototyping will explore its potentials and limitations. Additionally, there is a focus on creating novel geometries that cannot be produced using traditional glass manufacturing methods, in order to truly harness the capabilities of the BJT system. Consequently, experimentation with surface textures, lattices, and slumping was conducted. Furthermore, the geometries printed in the previous chapter remained small-scale (a maximum of approximately 40mm in height); these will be scaled up in this chapter.

This stage of experimentation can be divided into four sets of tests, each exploring a different geometric typology. Although each prototype builds upon its predecessor, this approach is more expansive in nature. This means that the focus was on broadening the understanding of the glass behaviour by experimenting with a variety of forms rather than acquiring in-depth knowledge about a single type. This approach was adopted as it places the material and production at the centre of the design process, allowing for potentialities to emerge that can guide the application direction.

5.5.1 Vessels

The first geometric typology explored was vessels. Vessels and cylindrical shapes are commonly linked with glass and ceramic materials. This connection arises from the inherent properties of these materials and their historical role in storing water or goods, along with the forms produced through traditional manufacturing methods like glassblowing or using a pottery wheel. With this context, the goal of this experimentation was to determine whether these types of forms could be successfully printed, excavated, and fired in a kiln. Furthermore, surface textures were investigated, drawing inspiration from organic, woven patterns.

A series of cylindrical forms with parametric wave-like surface textures were modelled in CAD software, Rhinoceros and Grasshopper. The pieces were approximately 77mm in height with an external diameter of 69mm. This represents a significant scaling up from Chapter 4, where the grid pieces were only 20mm in height and 35mm in length and width. Each cylinder features a distinct wave texture, with some incorporating a gradient that fades completely. This makes each part subtly unique while still adhering to the same overall design typology. The customisation of each component is a key capability of 3D printing, as discussed in Section 2.2.3.

The parts were printed in two batches and included the tile pieces discussed in the next section. Experiment 5.01 used the print settings and binder concentration determined in the Chapter 4 (Section 4.7.2). However, during this experiment some swiping was observed in the early layers of the print. As such, the saturation was decreased for Experiment 5.02 to a core saturation of 110% and a shell saturation of 130%. This reduction in saturation appeared to reduce the swiping with only a small amount occurring on the first layer. Parts were left for a minimum of 18 hours before being partially excavated and placed in the dehydrator (see Figure 5.10-5.11). All green parts could be easily handled without breaking and appeared to capture the CAD modelled designs accurately. The excavated prints can be seen in Figure 5.12 and Figure 5.13. All parts were then fired in a kiln following the firing schedule in Figure 5.5.

This experimentation confirmed that the current material formulation and print parameters are suitable for printing vessel shapes of this size and with surface texture details. However, the results of the firing revealed some challenges. When the glass fused in the kiln, it shrunk and warped significantly, with some of the pieces collapsing in on themselves (see Figure 5.14 and Figure 5.15). Whilst some shrinkage is inevitable in BJT, slumping of this level becomes a barrier to reliable and repeatable production process and therefore application. There is potential to optimise the firing schedule to reduce this effect by adjusting steps, temperatures and rates of increase and decrease. The technique of packing glass parts with high-temperature ceramic powders, such as talc or alumina, to support the glass during the firing process could also be considered. This has been demonstrated by some glass artists and literature (Arlotti & Knor, 2015; Ørvik & Stewart, 2022) and will be discussed further Section 6.2.1.1. However, it is important to note that cylindrical forms may not be the ideal geometry for this research due to the slumping of glass during the kiln firing process.

Figure 5.10. *Partial excavation of Experiment 5.01.*
Parts are partially excavated as seen here before being placed in a dehydrator.

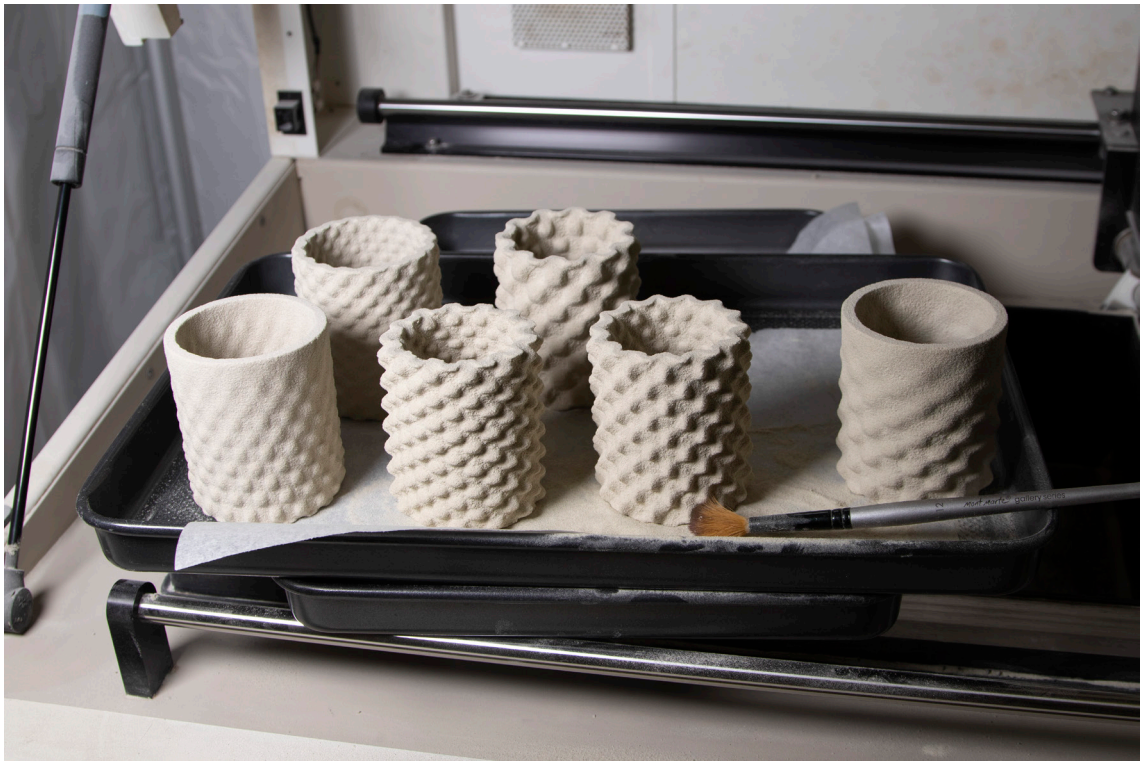

Figure 5.11. *Full excavation of Experiment 5.01 and 5.02.*

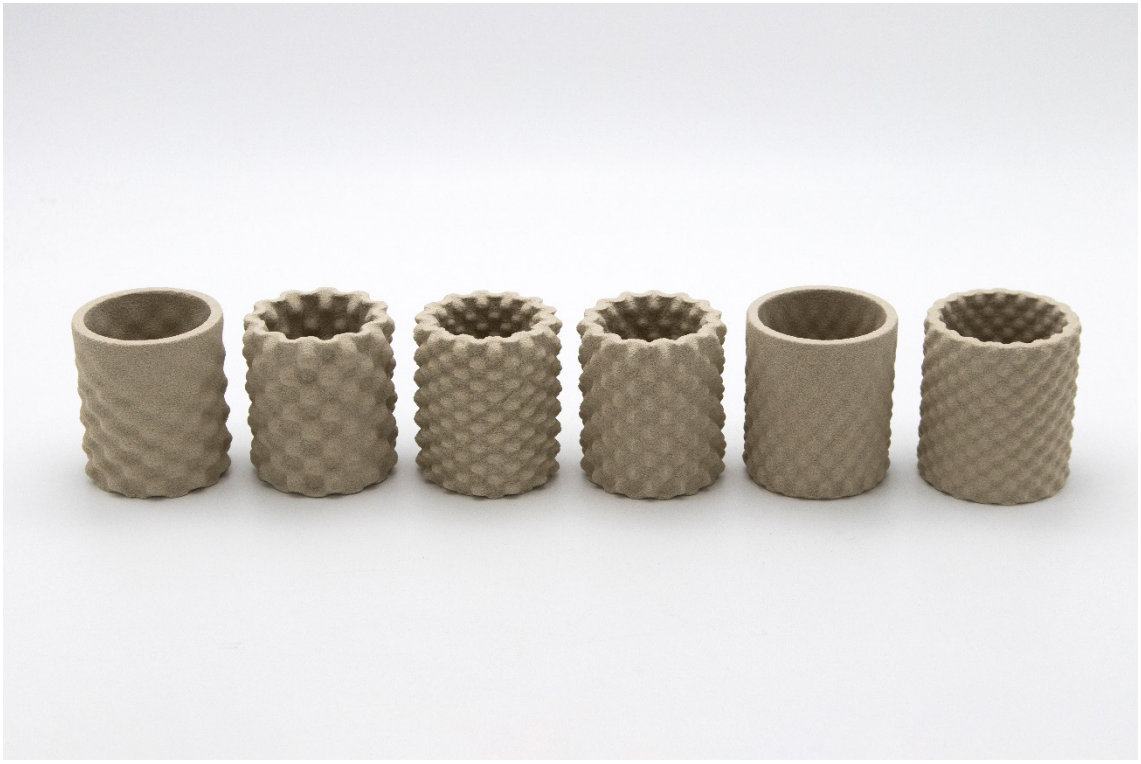

Figure 5.12. *Excavated results from of vessel experimentation (front view).*

Figure 5.13. *Excavated results from vessel experimentation.*

Figure 5.14. *Fired results from vessel experimentation.*

Figure 5.15. *Fired results from vessel experimentation.*

5.5.2 Tiles

The second geometric typology to be explored was tiles. Similarly to the vessel shapes, tiles are widely associated with ceramic and glass materials. Their form is also significantly different to the vessels, allowing for a broadening of understanding of how different geometries behave in the kiln. A series of small tiles were modelled in CAD software Rhinoceros and Grasshopper. The same parametric wave surface textures were applied to most of the tiles, leaving one without. The surface textures differed in fidelity, with some being more detailed and subtle, while others were larger and bolder. The tiles were rectangular, measuring 77mm in height and 69mm in width. The tiles were printed in the same print bed as the vessel shapes discussed in the previous section to maximise the use of the print bed. The tiles were placed on the left-hand side closest to the feed reservoir.

As a result, they were printed using the same material formulation and print parameters outlined above. Since the tiles were placed on the side closest to the feed reservoir, they acted similarly to the delay geometries discussed in Chapter 4 (see Section 4.7.1). This meant that more swiping occurred on the tiles than on the vessel shapes in the first print. However, the decrease in saturation in the second print led to almost no swiping. All tiles were excavated without breakages and could be easily handled. The CAD modelled designs were also accurately captured. The excavated prints can be seen in Figure 5.16 and Figure 5.17 and were fired according to the schedule in Figure 5.5.

Like the vessels, this experimentation confirmed the material formulation and printing parameters while also revealing challenges related to the firing process. The distortion of the tiles was minimal compared to that of the vessels, largely due to them being fired while lying flat. However, there was still some impact on the geometric accuracy. As can be seen in Figure 5.18, the edges tended to pull towards the centre in a non-uniform fashion. There is potential to overcome this by refining the firing process or by accounting for it in the geometry by offsetting the shrinkage in the design. This means that instead of printing tiles with straight edges, they could be convex to counteract the inward pulling that occurs during firing.

The shrinkage of the tiles was also examined. They were found to have shrunk approximately 11% in length (X direction) and 22% in width (Z direction) (see Figure 5.19). This non-uniform (anisotropic) shrinkage has been reported in metal BJT literature, with parts tending to shrink more in the Z-direction than in the XY directions (Marczyk et al., 2022; Miyanaji et al., 2020; Yegyan Kumar et al., 2018; Zago et al., 2021). Whilst in some cases this is due to gravity, anistropic shrinkage can also be due to the differences in particle consolidation both within layers (XY) and between layers (Z). Yegyan Kumar et al. (2018) suggest that there is higher porosity within layers (XY), leading to less shrinkage, while particles in the Z direction tend to coalesce more due to their denser packing. This correlates with what is seen in this experiment. However, it is important to note that, although the tiles were printed standing up, they were fired lying down, as they would have fallen over or slumped significantly (see Figure 5.19). This means that the Z-direction changed between the two steps. Anisotropic shrinkage itself is not a barrier to application and is common across many materials and production methods. It is, however, essential to understand why this occurs and to design parts that account for it.

These tile geometries have potential in terms of creating uniform and predictable forms using this production method. However, they do not take full advantage of the geometric capabilities of BJT and could potentially be manufactured in a more conventional way using a mould.

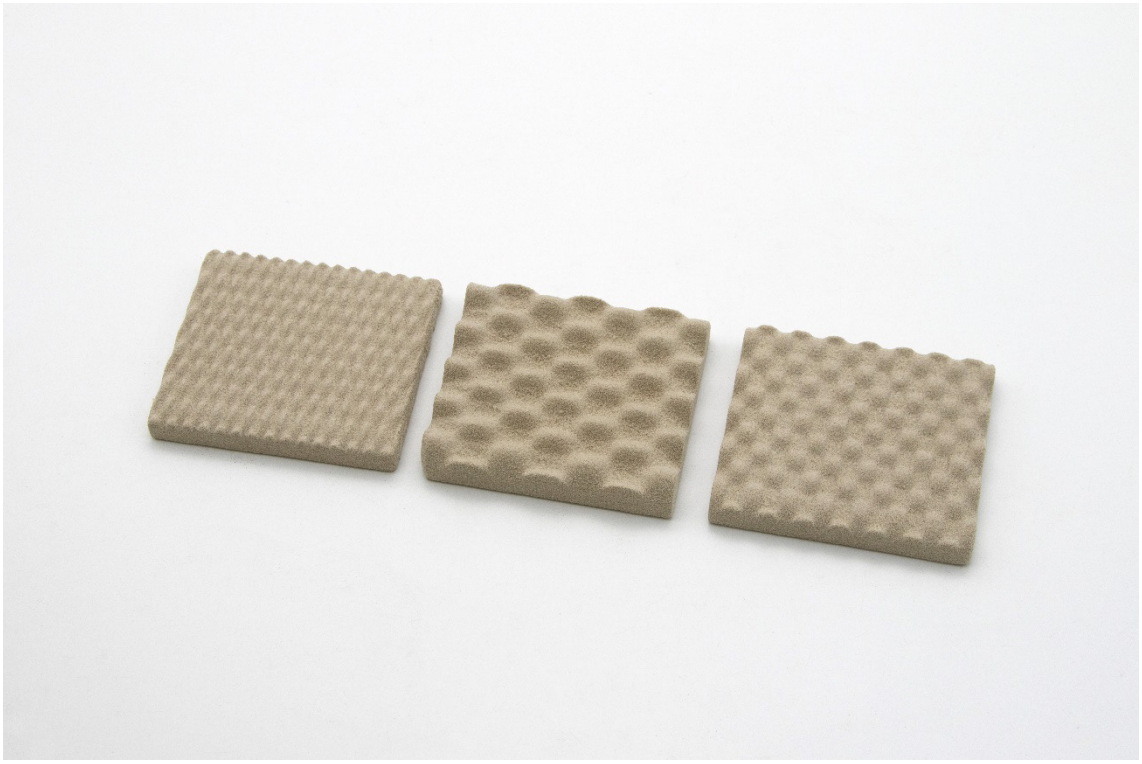

Figure 5.16. *Excavated results from tile experimentation.*

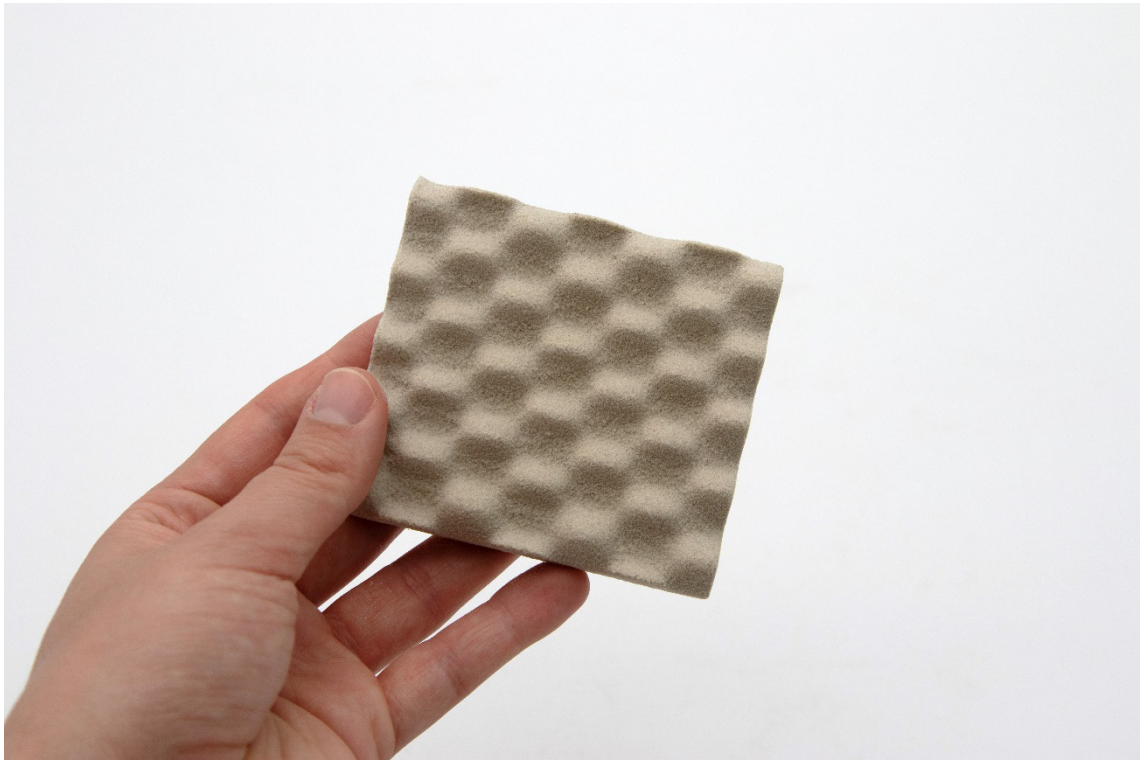

Figure 5.17. *Close-up of excavated tile from experimentation.*

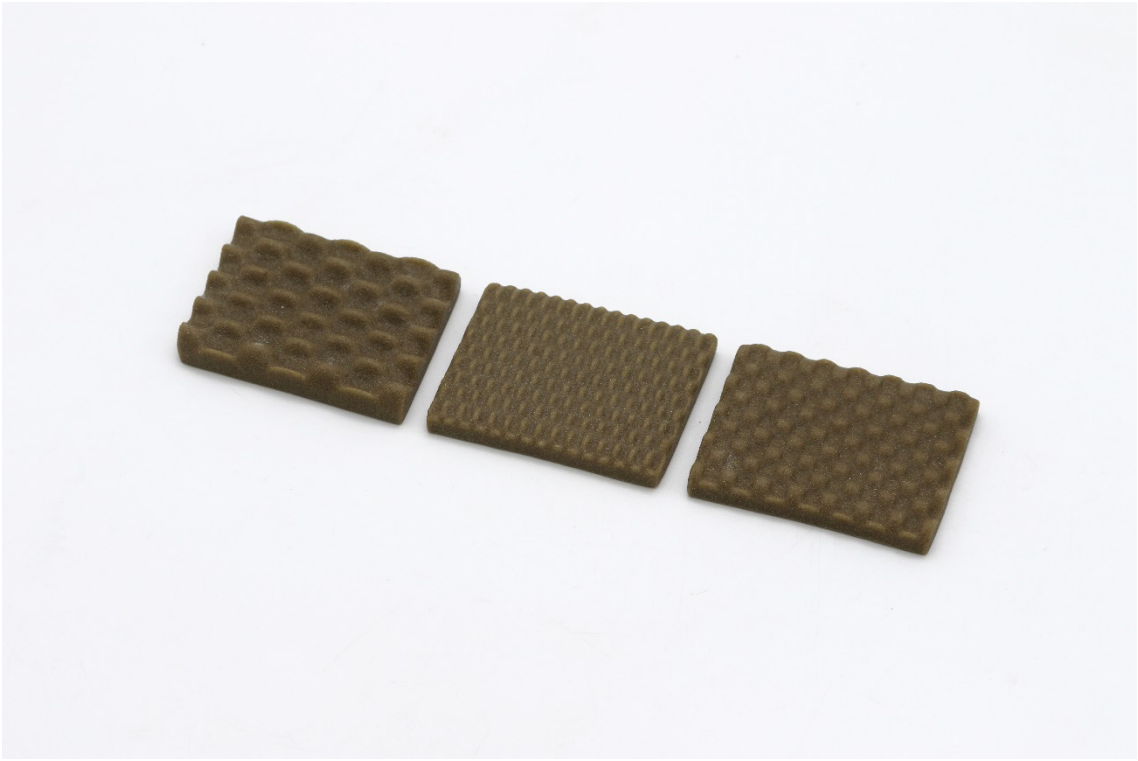

Figure 5.18. *Fired results from tile experimentation.*

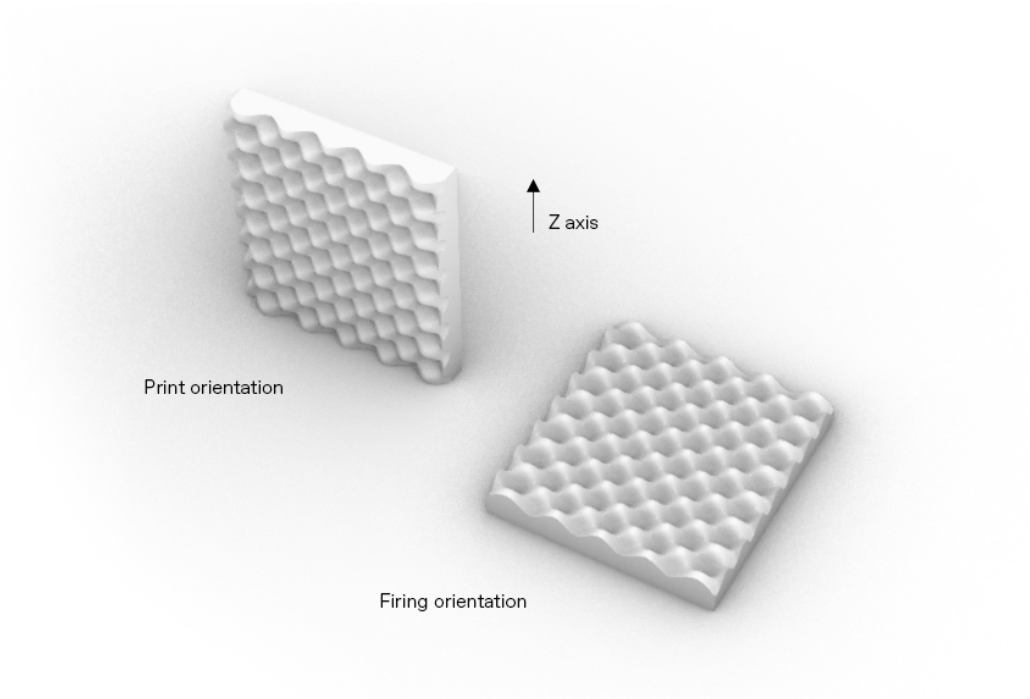

Figure 5.19. *Comparison of print orientation and firing orientation of tiles.*

5.5.1 Layered slumping

Based on the slumping observed during the vessel experimentation, the aesthetic potential of utilising slumping to create forms was explored. This represents a slight sidestep from the more pragmatic testing that has been presented so far. However, it aligns with the RtD methodology where moments of drifting can occur which help to adjust and reframe the project (see Section 3.3.2 for further discussion of drifting).

To investigate this, a multilayered slumped vessel was envisioned. A series of vessel shapes were modelled to fit concentrically within each other, resembling cascading sizes of measuring bowls. The hypothesis was that when fired, they would slump outwards, like petals on a flower. The top of each vessel was angled in different directions to encourage this. Five individual parts were modelled that could be assembled into two multilayered objects before firing. The pieces ranged in height from approximately 78mm to 88mm (see Figures 5.20 - 5.22).

The parts were printed using the same parameters and formulation discussed in the previous section. This includes 3% HPS binder to moondust (w/w), 110% core saturation and 130% shell saturation and 0.2mm layer height. Parts were left to dry in the print bed for a minimum of 18 hours before being placed in the dehydrator. Some challenges were faced during this printing process. Namely, swiping and drying time. All the vessels had closed bottoms, leading to large flat surfaces being printed in the initial layers, which caused swiping. This type of geometry is prone to swiping and should be rotated around the YZ or XZ plane to print the base incrementally and mitigate swiping. Additionally, one of the vessels was positioned inside another due to limited space in the print bed. These pieces, in particular, experienced significant swiping and could not be excavated without breaking (see Figure 5.22). It is hypothesised that insufficient space between each part increased the severity of the swiping, causing the layers to shift and fuse together. This shows that the arrangement of components in the bed affects the frequency and intensity of swiping.

The second issue was the drying time. Parts were left overnight to dry in the print bed; however, when excavating these (to ready them for the dehydrator), they were still damp. As parts increase in size, the time left to dry in the printer needs to be increased or alternate ways of removing the entire print bed and placing it in the dehydrator should be used. This highlights the connection between the key variables of drying (method, time and temperature) and the scale of parts (refer to Figure 4.7 for an overview of the production parameters).

Despite the breakages on two of the five pieces, the remaining parts that were not broken were placed one inside of the other (see Figure 5.20) and fired according to the schedule in Figure 5.5. The fired pieces from this experimentation can be seen in Figure 5.23 and Figure 5.24. The multilayered vessel, slumped significantly creating an interesting abstract form. The pieces were designed with a wide, tapered opening to encourage the pieces to slump outwards, away from the centre. However, the layers primarily slumped to one side with the two outer layers almost folding in half. This technique has the potential to be further developed for creating compelling artistic works or one-of-a-kind design pieces, particularly as the process produces a unique result every time. While this makes the proces compelling, it also renders it unreliable. In the context of manufacturing and industrial design, this unpredictability can be a barrier to practical application. Consequently, this research will focus on identifying and developing forms that can be fired more reliably and predictably.

Figure 5.20. *Excavated pieces from layered slumping experimentation (firing position).*
The three pieces which did not experience breakages were placed one inside the other for firing.

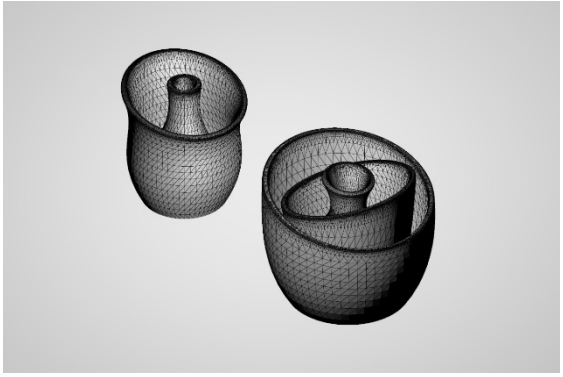

Figure 5.21. *Digital file for layered slumping experimentation.*
Five individual vessel pieces were designed to be assembled into two multilayered objects for firing.

Figure 5.22. *Excavated pieces from layered slumping experimentation (positioned in the layout they were printed).*
The two pieces in the bottom right were printed one inside the other which resulted in the breakages which can be seen here.

Figure 5.23. *Fired part from layered slumping experimentation (front view).*

Figure 5.24. *Fired part from layered slumping experimentation (top view).*

5.5.2 Lattices 1.0

The previous experiments have revealed the extent to which the firing process impacts the geometries that can be accurately produced. Parts with unsupported walls and overhangs have bent and deformed during the firing. So, whilst a range of geometries can be printed, the real challenge lies in creating geometries that can be fired without undesirable slumping or deformation. Consequently, geometries with self-supporting features were investigated. It was hypothesised that a lattice with truss-like struts may hold its shape in the kiln as these struts would slump into each other and become self-supporting. Furthermore, one of the primary advantages of BJT printing lies in the virtually limitless geometries that can be achieved, due to the lack of need for support structures. A key objective of this research was to harness these capabilities to create complex geometries from glass. While the vessel and tile typologies have potential and are highly compatible with extrusion-based methods of 3D printing, they do not fully exploit the capabilities of BJT.

Lattice geometries, on the other hand, are well-suited and provide the advantage of reducing the weight of a part while maintaining its strength or stiffness (Gibson et al., 2021). Lattices are broadly defined as three-dimensional structures composed of a repeated arrangement of cells (Pan et al., 2020). There are a variety of types, some using nodes and struts, others using surfaces. The arrangement of cells can also vary between uniform (periodic) or randomised. 3D printing has opened up opportunities for the application of lattices, and much attention has been given to the engineering of lattices with different functions such as heat transfer efficiency, energy absorption and acoustic insulation (Tao & Leu, 2016).

A series of lattices were designed in Grasshopper and Rhinoceros based on a truss system. These started as single-height uniform lattices and evolved into lattice forms with skins and lattices that conformed to an organic shape (see Figure 5.25-5.27). The struts of the largest lattices had a diameter of 6mm, and a 6mm radius was applied to all connecting joints, which provides the lattice with greater strength. Other smaller lattices were modelled to explore the limitations of scale. 4% HPS was combined by hand with the glass fines (w/w). This was increased from 3% of the previous set as it was anticipated that the lattice structures would need higher green strength to be successfully depowered. The print settings and production parameters remained unchanged from the previous experimentation with layered slumping.

Both sets of lattices were printed successfully with minimal swiping. It is hypothesised that this is due to the small amount of liquid activator needed in the initial layers, as there were no large flat sections. The uniform lattices were easily excavated without any breakages. However, the more organic lattices were more challenging to remove the powder from, resulting in some breakages, particularly on the corners and edges pieces. The middle section of the concave conformal lattice could also not be fully excavated as the lattice openings were too small (see Figure 5.27). This indicates that further experimentation with non-uniform lattices is needed to ensure the cell size is suitable for excavation. It also suggests that continuing to increase the green strength would be beneficial to ensure no breakages occur.

Parts were fired according to the schedule in Appendix 4.4. This is the same as the initial firing schedule seen in Figure 5.5, however, the peak temperature was raised from 760°C to 780°C. This change is due to using a different kiln, which showed a slight variation in the temperature readings. Adjusting a firing schedule when utilising a new kiln is standard practice in glasswork. The fired parts can be seen in Figures 5.28-5.31. During the firing, the pieces performed better than anticipated, despite worries that the struts might collapse and slump as the glass softened. Fortunately, the truss systems became self-supporting inside the kiln, and while there was some shrinkage and slumping, the lattices preserved their overall form. Some

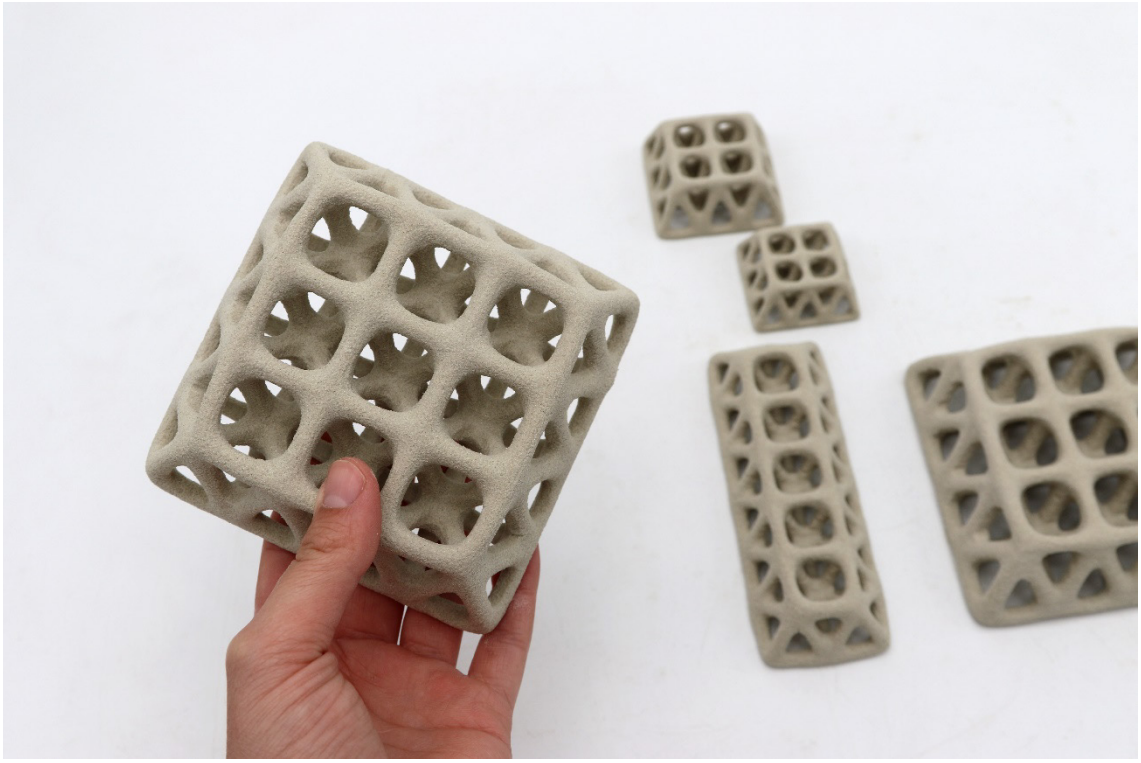

Figure 5.25. *Close-up of uniform single-height lattice green part.*

Figure 5.26. *Single-height uniform lattices of varying sizes and shapes (green parts).*

Figure 5.27. *Various lattice forms (green parts).* Including lattices shapes with skins and lattices which conformed to an organic shape.

Figure 5.28. *Fired uniform single-height lattice.*
The overall lattice form was maintained, with minimal slumping.

Figure 5.29. *Fired various single-height uniform lattices.*
The overall form was largely maintained in the kiln, across these varying scales.

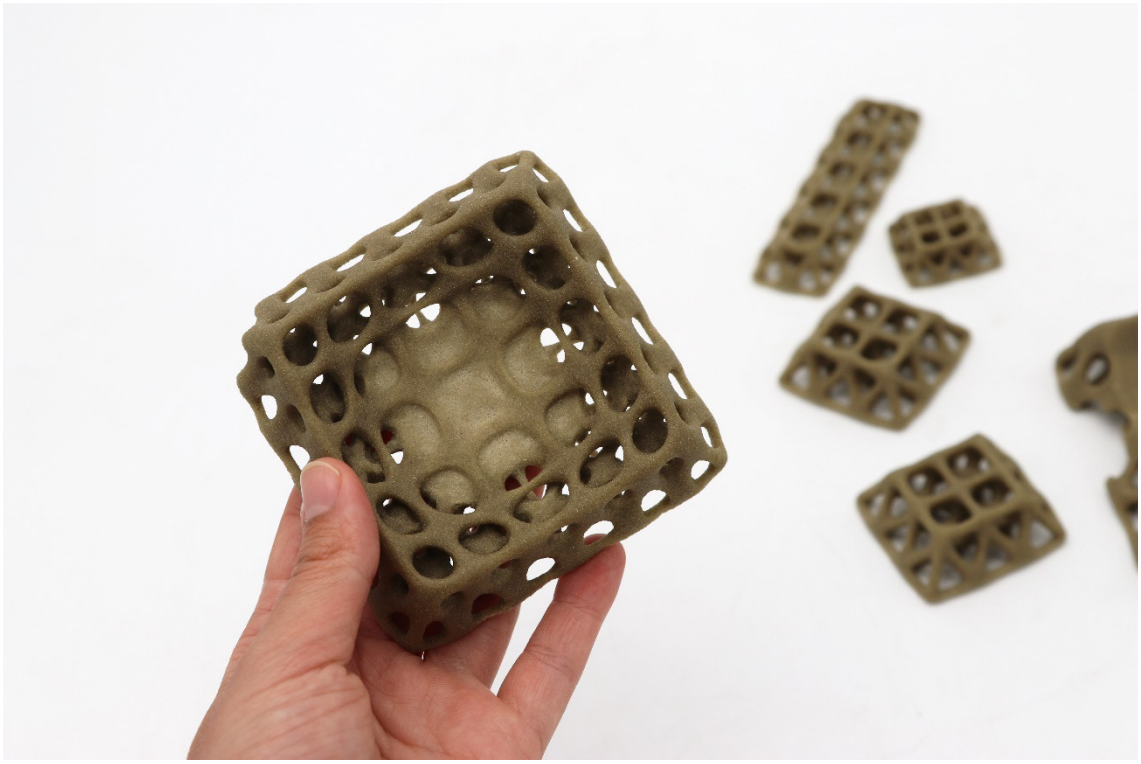

Figure 5.30. *Fired lattice shape conformed to an organic shape.*
The overall shape was maintained in the firing, however the organic lattices were more difficult to excavate causing some breakages as seen here.

Figure 5.31. *Fired rectangular lattice with reduced radius truss structure.*
Single uniform lattice, exploring the impact of scale.

of the glass in the organic pieces appeared to be less fused (less glassy in appearance) so optimisation of the firing schedule should still be conducted. This, however, is a positive step forward as the uniform lattice parts could be printed, excavated and fired without major distortions occurring. This represents a promising direction for the BJT of glass fines as producing lattices in recycled glass has not yet been achieved and remains difficult, if not impossible, in conventional glass manufacturing methods.

5.5.3 Lattices 2.0

The success of the initial exploration with lattices led to further investigation. The aim of this testing was to scale up the lattice geometries to the maximum size of the print bed and to investigate different variations of the truss-based lattice. Increasing the scale allows for more application opportunities to be envisioned. While the experimentation began with lattices, further pyramidal forms were also explored. These employed the same concept as the lattices, relying on the self-supporting nature of triangular forms. This set of tests continued to take the form of 'expansive' prototyping, in which a broader understanding of the aesthetic possibilities and behaviour of the glass when fired could be built.

A range of parametric pyramidal designs were modelled in Rhinoceros and Grasshopper. Each could be adjusted in terms cell number and cell size. Both struts and surfaces were utilised, and gradients were employed to reveal the points at which the lattices or pyramids were no longer self-supporting. All variations remained geometric rather than organic as the previous experimentation had revealed the difficulties of excavating non-uniform cell sizes. Each overall design was square and approximately the same size at 200mm x 200mm with a height of approximately 30mm. For every test the printing parameters, material formulation and firing schedule were kept constant; the only change was the geometry itself.

Twelve experiments were conducted, with some breakages occurring and reprints required (Experiments 8.01-8.12). This was largely due to design flaws, such as wall thickness being too thin or the lattice density being unsuitable. To overcome these issues the CAD models were adjusted. Prototyping of this nature is part of any design process, particularly when utilising 3D printing technology to understand the constraints of the process. See Appendix 3.1 and Appendix 3.2 for full detail. The six most significant experiments are discussed here. Experiment 8.01 and 8.02 adapted the uniform square lattices of the previous section, examining the effect of scale (see Figure 5.32 and Figure 5.33). Experiment 8.04 and 8.09 removed the top grid structure of the lattice, allowing for a more simplified lattice structure (see Figure 5.34 and Figure 5.35). Experiment 8.05 and 8.07 added surfaces to the lattices (see Figure 5.36 and Figure 5.37).

All parts were fired according to the schedule in Appendix 4.4. The results of the firing varied based on the design (see Figures 5.38-5.43). Experiment 8.01 and 8.09 largely held their shape as the lattices in the previous testing had done (see Figure 5.38 and Figure 5.41). This is likely due to both the uniformity and size of each lattice cell. Whereas Experiment 8.02 and 8.04 revealed the dimensional constraints of the truss structure (see Figure 5.39 and Figure 5.40). Meaning that the angle and height of the truss struts impacts how much it slumps in the kiln. It can be seen in this testing that lattice cells with a truss angle greater than approximately 55 degrees collapsed during firing. This needs to be accounted for in the design phase. In Experiment 8.05 and 8.07, the incorporation of surfaces resulted in greater slumping (see Figure 5.42 and Figure 5.43). The weight of the surface on top of the lattice structure, caused the lattice to collapse. Similarly, the half pyramid shapes slumped down onto themselves.

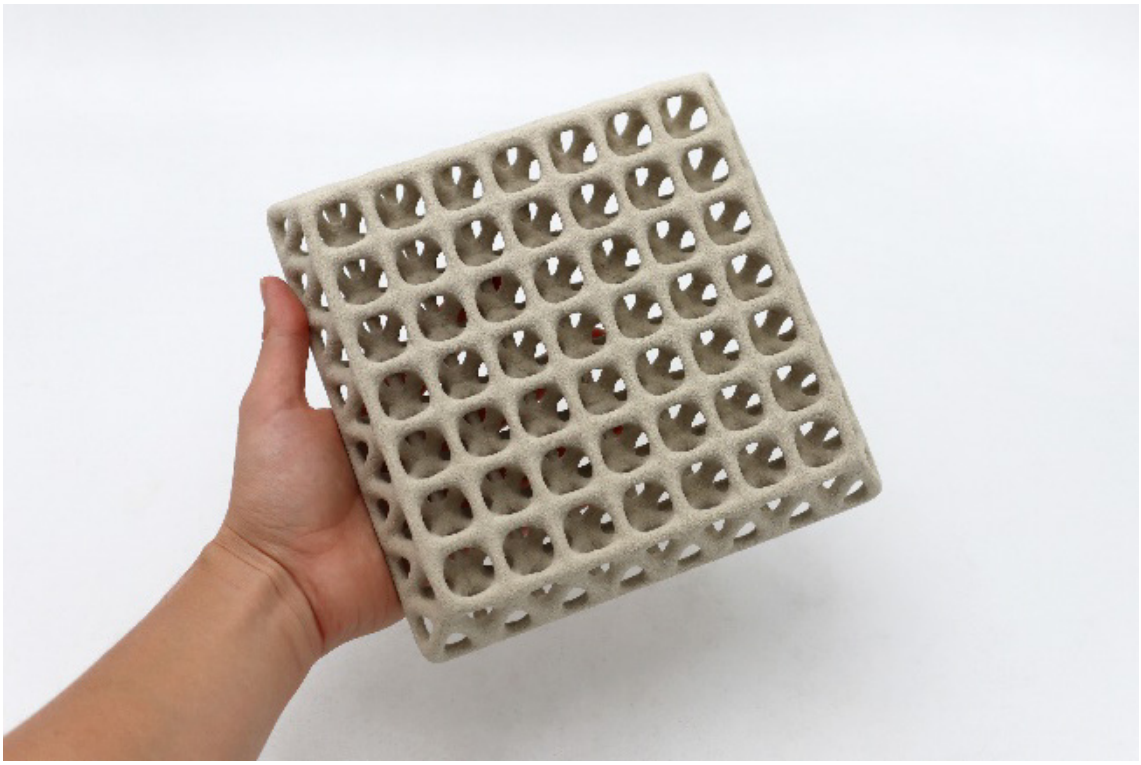

Figure 5.32. *Experiment 8.01 green part.*
Uniform, single-height lattice.

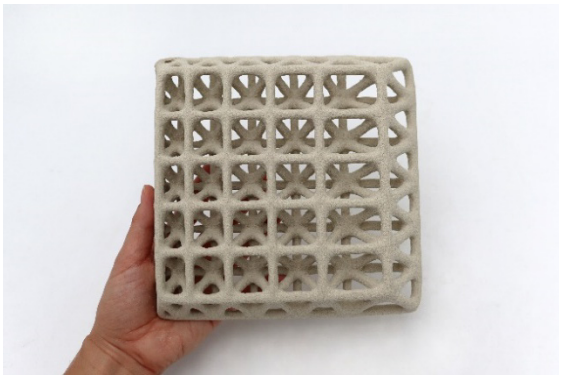

Figure 5.34. *Experiment 8.02 green part.*
Varying the cell size to understand the limits of the lattice scale.

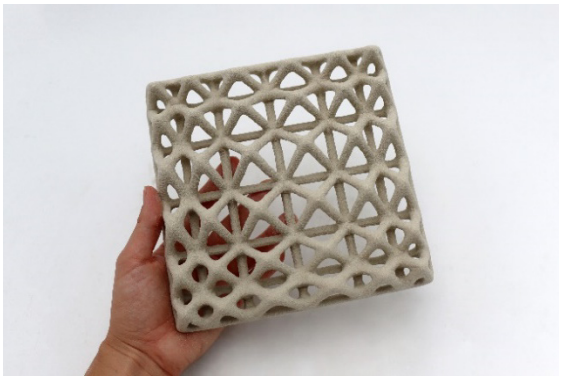

Figure 5.33. *Experiment 8.04 green part.*
Varying cell size and removing the top grid.

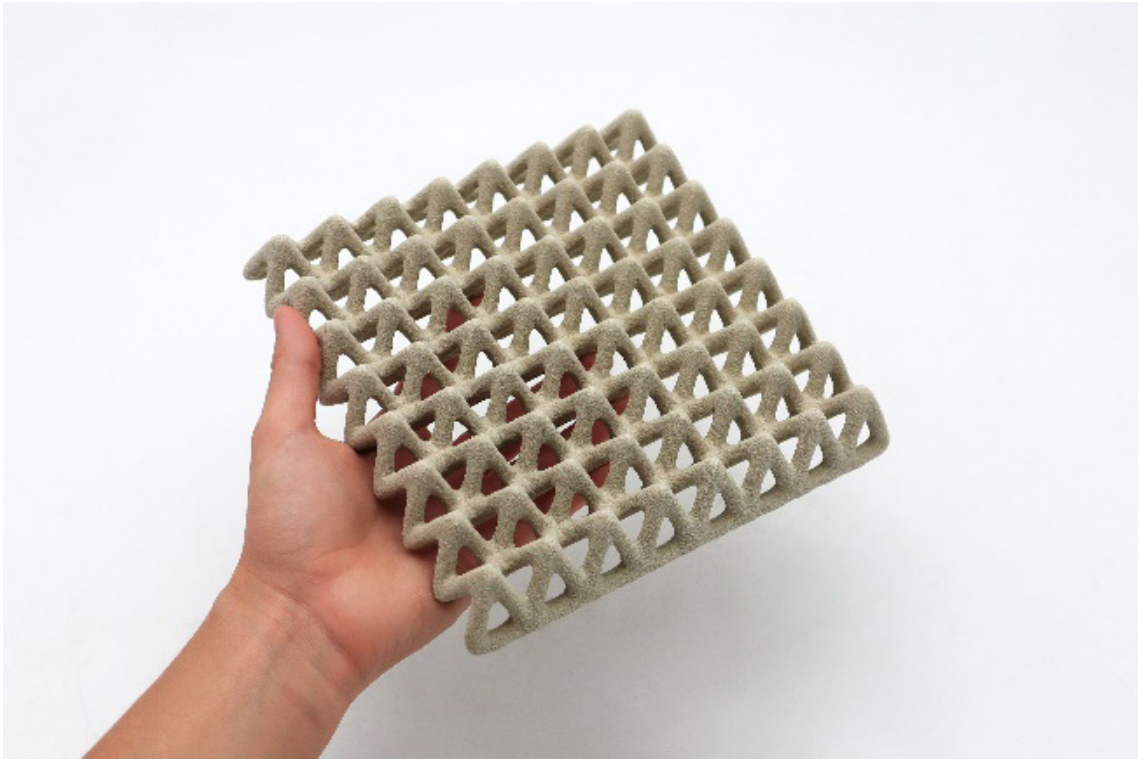

Figure 5.35. *Experiment 8.09 green part.*
Uniform cell size, removal of top and base square grid.

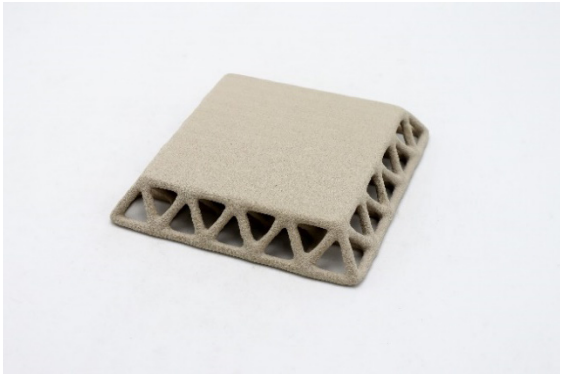

Figure 5.37. *Experiment 8.05 green part.*
Uniform, single height lattice with top surface.

Figure 5.36. *Experiment 8.07 green part.*
Incorporating surfaces into the lattice creates partially enclosed pyramids. The height gradually increases throughout the piece.

Figure 5.38. *Experiment 8.01 post firing.*
Overall form was maintained in the firing.

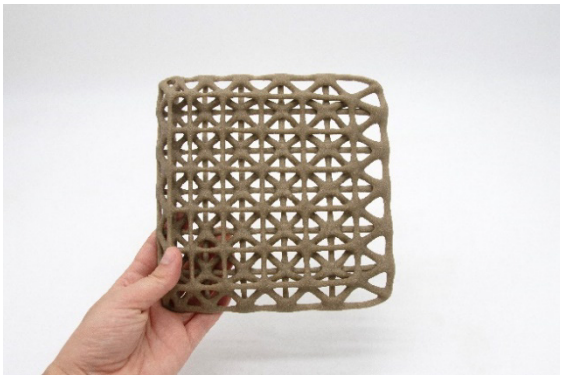

Figure 5.39. *Experiment 8.02 post firing.*

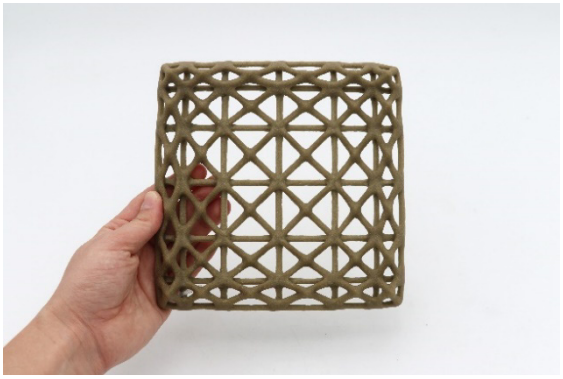

Figure 5.40. *Experiment 8.04 post firing.*

Figure 5.41. *Experiment 8.09 post firing.*

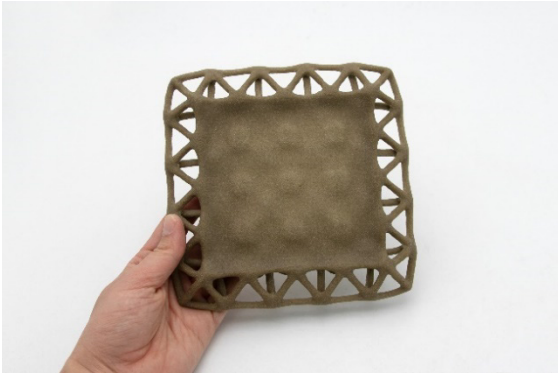

Figure 5.43. *Experiment 8.05 post firing.*

Figure 5.42. *Experiment 8.07 post firing.*

The shrinkage of the uniform single-height lattice was investigated by 3D scanning the parts before and after firing using an Einscan Pro 2X scanner. It was found that the shrinkage was consistent in the x and y axes at 8% whilst the z axes experienced shrinkage of approximately 29%. This increased shrinkage is likely due to gravity. However, based on the other experiments, it is clear that the z-axis shrinkage is also dependent on the geometry and if the lattice cells were larger, so too might be this shrinkage.

Overall, this lattice investigation demonstrated that complex geometries can be printed, excavated, and fired. However, there were varying degrees of predictability in the forms during the firing process. While Experiments 8.01 and 8.09 remained true to their initial design during firing, without any significant warping or slumping, the other four designs exhibited a range of results. Of note, is the impact of scale; a geometry that can fire accurately at one size may not do the same when scaled up.

More broadly, this experimentation revealed that it is not possible to determine overarching rules for all shapes. Even though these designs all fit within a similar typology, the addition of surfaces and changes in dimensions impacted the result. This indicates the need to determine an application and design specifically for it, tailoring the materials, production, and geometries accordingly. This could be seen as a barrier in some disciplines and result in this material and production method being labelled as unfeasible. However, for an RtD project, this allows for the real integration of design expertise in finding and developing a suitable application. The localisation and customisability that 3D printing provides also allows for a specialised application to be feasibly developed. Moreover, this approach aligns with thinking in materials design projects, in which the material and production method should drive the application.

5.6 Colour

As controlling and adjusting colour is an important part of any product design process, initial experimentation with colour was conducted. There are a wide variety of inorganic pigments that are used in glass and ceramics. These are mostly metallic oxides and salts, which can be found naturally or produced synthetically. They can be dispersed throughout the ceramic or glass material or applied on top as a glaze or enamel. Iron oxide was investigated as it is one of the most commonly used pigments due to its abundance, low cost and non-toxicity (Tanisan & Turan, 2011). There are various types of iron oxide that can produce a range of colours, from yellows to dark browns, oranges, and reds. This colour variation depends on the amount of iron present in the chemical compound, with more iron resulting in darker colours.

With this in mind, two types of powdered iron oxide were sourced from Walker Ceramics and Dulux. A series of geometries were printed using material formulations which contained between 0.2-0.4% iron oxide (see Figures 5.44-5.46). This produced a powder feedstock that was dark grey in colour. This pigment was uniformly mixed in a commercial mixer. A variety of small vessel shapes that curved inwards slightly to aid slumping were modelled, along with various lattice shapes previously printed in Section 5.5.4. Details on these Experiments can be found in Appendix 3.3.

After firing, a range of different shades were produced, from a dark chocolate brown, to a red clay colour (see Figures 5.47-5.49). The change from dark grey is due to the oxidation of the iron which happens during the firing process. The small concave vessels slumped inwards, retaining their general form but creating an ellipsis opening rather than a circle.

Figure 5.44. *Colour experimentation with various lattice and vessel forms.*
Construction grade iron oxide.

Figure 5.45. *Rectangular lattice colour experimentation.*
Construction grade iron oxide.

Figure 5.46. *Colour experimentation with single-height uniform lattice.*
Iron oxide sourced from Walker Ceramics.

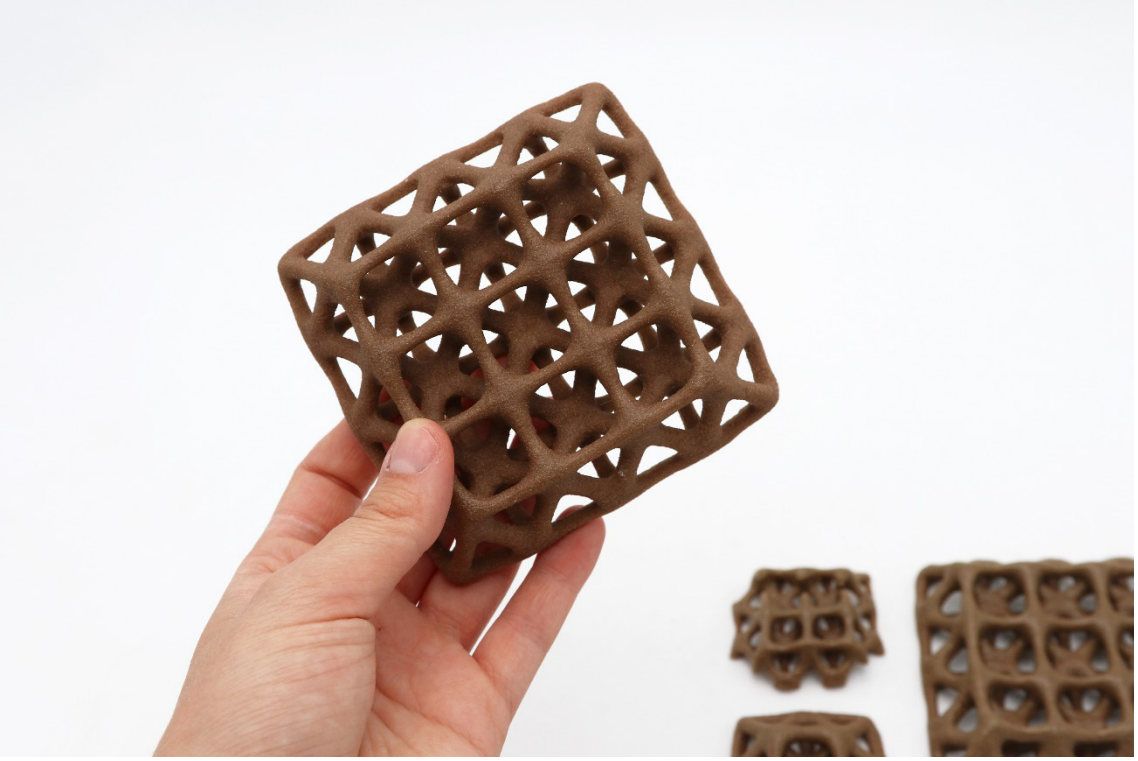

Figure 5.47. *Fired lattice sample with iron oxide colouring.*
The Walker Ceramics iron oxide at 0.2% concentration resulted in a brown colour.

Figure 5.48. *Fired organic lattice with iron oxide colouring.*
The Walker Ceramics iron oxide at 0.4% concentration resulted in a red clay colour.

Figure 5.49. *Fired vessel forms with iron oxide colouring.*
Construction grade iron oxide at 0.5% resulted in a dark chocolate brown colour.

The lattices with 0.2% iron oxide behaved similarly to those without colouring in previous tests. However, the parts with 0.4% iron oxide behaved unexpectedly. As shown in Figure 5.48, parts of the prints did not just slump in the kiln but crumbled apart. This phenomenon has not been observed in any previous firings. It is believed that this may be due to iron oxides also functioning as a flux, which means that they lower the softening temperature of glasses and disrupt the regular fusing of the 3D printed parts.

Whilst at lower concentrations, the addition of iron oxide has aesthetic potential, ultimately, there was concern for how this would impact the circularity of the glass fines material. As ceramic pigments are required to be heated to high temperatures, they will remain in the glass fines material (Gol et al., 2022). Any addition, like this impacts the material integrity. Furthermore, whilst there is research into synthesising iron oxides from waste resources, it is largely still a mined material or made from virgin resources (Tanisan & Turan, 2011). As a result, using a pigment like this produces an additional environmental impact—even if potentially small. As we develop materials during a climate crisis, this must be taken into consideration.

5.7 Porosity Investigation

As highlighted previously, achieving fully dense parts is difficult in BJT due to the nature of the powder-based process. As a result, many parts will retain a certain level of porosity even after firing or sintering. According to Du et al. (2020), density and porosity are the most assessed material properties in ceramic BJT. This is largely because they have a significant impact on the mechanical properties of a part and are highly sensitive to the characteristics of the powdered feedstock (including flowability and particle shape and size) and printing parameters (such as layer thickness) (Chen et al., 2022). As a result, two key groups seem to have emerged in the literature. The first sees porosity as a barrier to application and investigates ways to create fully dense parts. This work includes a variety of techniques, such as using slurry instead of powdered feedstock[13] (Diener et al., 2021) or dispersing nanoparticles in the liquid activator (Zhao et al., 2022).

The other group looks to harness the porosity of BJT parts by developing applications that require this characteristic. As a result, significant research has emerged in the biomedical field where BJT is used to make bone scaffolds or implants with complex shapes and different levels of porosity that promote cell adhesion and interlocking between host tissue and the scaffold (Butscher et al., 2012; Tarafder et al., 2013; Will et al., 2008)[14]. Furthermore, in industry BJT has been used extensively for the printing of casting moulds and cores due to the high complexity of geometry, which can be rapidly and cost-effectively produced (Upadhyay et al., 2017; Ziaee & Crane, 2019). The porosity of the printed moulds and cores facilitates gas transport and creates a suitable level of weakness for easy removal of the cast part (Upadhyay et al., 2017).

[13] In slurry based BJT systems fine ceramic powders are dispersed in a liquid which is deposited on the print bed via either a nozzle or doctor blade in a thin layer and dried, evaporating the liquid content (Du et al., 2020). The binder is then deposited onto the dried slurry layer in the required geometry. This method produces higher packing and green densities, resulting in improved final properties and reduced post-processing steps (Diener et al., 2021).

[14] Biomedical applications make up 56% of the papers on BJT of ceramics found by Du et al. (2020). Phosphate ceramic materials, in particular hydroxyapatite and tricalcium phosphate, are most commonly used due to their compositional similarity to human bone. These bio-ceramic materials are described as bioactive, meaning they are non-toxic and allow bonds to form with living tissues in the body (Lv et al., 2019; Thangavel & Elsen Selvam, 2022).

With this in mind, the density and porosity of the BJT glass fines materials was investigated. Whilst parts fired according to the initial firing schedule in Figure 5.5 appear fully dense and waterproof, this has not yet been verified. This investigation will allow for an appropriate application to be determined. To start with, a prototype as an experimental component was conducted to better understand the properties of the fired glass material. This was followed by a series of prototypes that explored the possibility of creating 3D printed glass parts with porosity. Finally, another prototype as an experimental component was conducted to evaluate the porous glass materials.

5.7.1 SEM Analysis

An SEM analysis was undertaken on the cross-section of a glass 3D printed sample. This was conducted early in the research while working with the CMC binder (see Section 4.6.1). The sample was fired according to the schedule in Figure 5.5. The SEM results confirmed the presence of porosity in the sample (see Figures 5.50-5.52). The images reveal that the 3D-printed glass parts contain evenly distributed closed spherical pores, ranging in size from approximately 5µm to 200µm. These SEM images differ significantly from those found in ceramic BJT literature, where the sintering process creates polycrystalline ceramics characterised by irregularly shaped pores. In those studies, the outline of each particle is clearly visible in the SEM images. In contrast, these glass samples have been heated to the point where the particles soften and coalesce, meaning that there are no longer individual glass particles present. These observations align with research by Cho et al. (2020), who also fired BJT glass samples. Specifically, Cho et al. (2020) found that angular powder particles flowed more quickly than spherical glass powders, and fewer pores were observed. This is relevant as the glass fines utilised in this study are irregular and angular in morphology.

Whilst pores are present in the sample, the closed, unconnected nature of them is preferable as this type of porosity is known to have less of an impact on mechanical properties than open, interconnected pores (Mostafaei et al., 2016; Özgün et al., 2013). However, it is important to note that this SEM analysis does not reveal what is happening on the surface of the sample.

Porous materials are typically associated with water absorption (e.g., sponges). However, closed internal pores do not facilitate this. In observational tests of all parts fired according to the schedule in Figure 5.5, they appeared to be waterproof, with droplets remaining on the surface of the objects rather than permeating through. As waterproofness is a key property of glass and glazed ceramics, understanding the impact of porosity on the water absorption of these parts is important for determining applications that may require watertightness.

5.7.2 Developing porous parts

The previous experiment sparked interest into how this property of porosity could be optimised to become a functional element of the material and what kind of application could emerge from that - as has been done in several applications of porous BJT parts discussed above. Given what is known about the firing process of glass and the ability to create both fully fused and tack-fused objects, there is an opportunity to increase levels of porosity by tailoring the firing schedule.

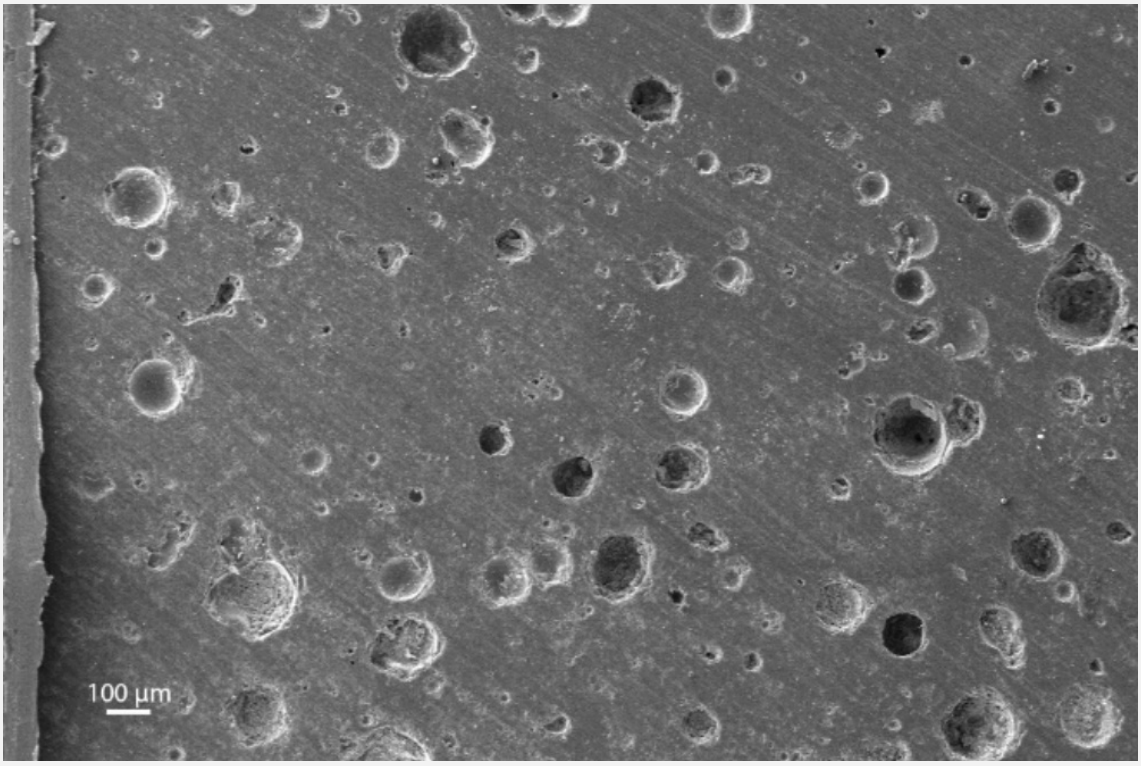

Figure 5.50. *SEM analysis of 3D printed glass fines sample.*
Magnification 43 X, Pixel size 2.595 um.

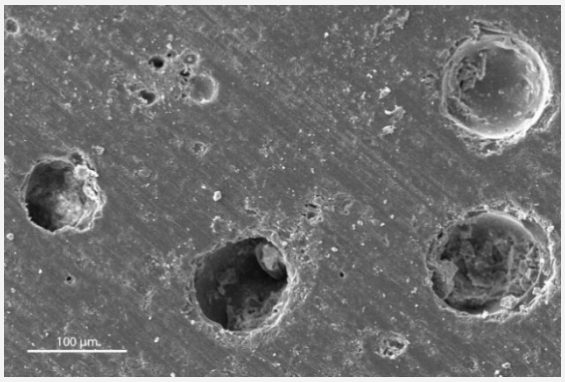

Figure 5.51. *SEM analysis of 3D printed glass fines sample.*
Magnification 200 X, Pixel size 556.9 nm.

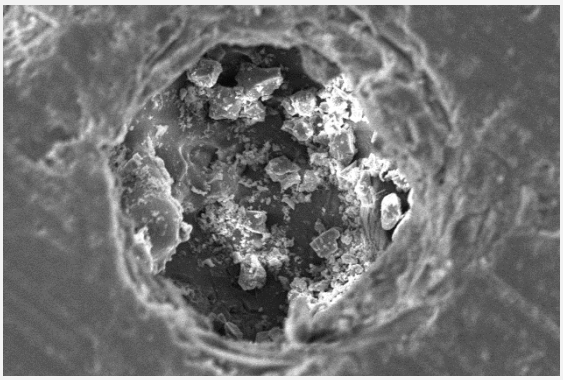

Figure 5.52. *SEM analysis of 3D printed glass fines sample.*
Magnification 501 X, Pixel size 223.1 nm.

This method eliminates the need for additional firing steps or the introduction of foaming agents, which are common in the production of porous glass. Instead, this approach can be characterised as a partial sintering process, sometimes used to produce porous ceramics[15] (Scarinci et al., 2005). This technique of incomplete firing has been used to produce ceramic parts with porosity ranging from 5%-75% (Roy, 2025).

Whilst there is significant research into the creation of porous glass and ceramic parts for a wide range of specialised applications, including filtration devices and thermal insulation, of interest to this research was the built environment. Most important inorganic building materials, including bricks and stone, contain porosity. This porosity responds to surrounding moisture, absorbing water, redistributing it in the fabric and eventually breathing it back into the air. This creates a "*delicate and dynamic relation between material and surroundings, which is apparent in good building and architectur*e" (Hall & Hoff, 2021). It is this relationship that has resulted in porous ceramic and clay materials being used to passively cool spaces for centuries. In particular, the process of evaporative cooling has been used where the porosity of fired clay allows water to permeate the surface, where it can evaporate and cool the ambient air. The porosity of these materials sits in the range of 7-24% (Hall & Hoff, 2021; Vallejo, 2018). Further discussion of this application area will be included in the following chapter.

This potential application area drove this set of experiments. The aim was to investigate whether porosity could be attained through a partial sintering method and, if so, whether a level could be achieved that would allow for its use as an evaporative cooling medium. This approach is very much an RtD strategy, whereby an eye for application drives the generation of knowledge.

To develop porous parts, a set of 14 experiments was conducted (see Figure 5.53). These can be viewed as a form of serial prototyping, in which the results of one experiment informed the next. Hollow cubes with a wall thickness of 10 mm were printed using the same material formulation and production parameters (see Figure 5.54). The only variable changed was the firing schedule, with the hold time and peak temperature adjusted incrementally to produce parts that appeared uniformly porous. All six other steps of the firing schedule remained unchanged (see Figure 4.7 for an overview of the production parameters). After firing, the water absorption of each part was preliminarily assessed by weighing the dry samples, submerging them in water, and then reweighing them. This provided an initial water-absorption percentage, indicating the level of porosity.

In the initial firing schedule (see Figure 5.5), the temperature increases steadily at the start, then rises sharply to the peak temperature and immediately decreases to the annealing point to mitigate slumping of the parts. However, in this experiment, the peak temperature was gradually reduced to produce parts that were tack-fused rather than fully fused. In doing so, a hold period at the peak temperature was introduced to allow uniform fusing. Without it, the top half of the shape appeared darker and more fused than the base (see Figure 5.55).

[15] Research into the partial sintering of glass to produce porous parts is limited. Porous glasses are typically produced by two methods: either by introducing fluids such as CO_2 or water vapour directly into molten glass, or by sintering glass powders mixed with a foaming agent such as calcium carbonate. When heated, calcium carbonate decomposes, releasing gaseous CO_2 that becomes trapped in the viscous glass, forming pores (Scarinci et al., 2005). Some of these techniques have been applied to glass fines and other waste glass streams (Flood et al., 2020). The level of porosity for glass foams formed with these techniques if is typically between 85-95% (Scarinci et al., 2005).

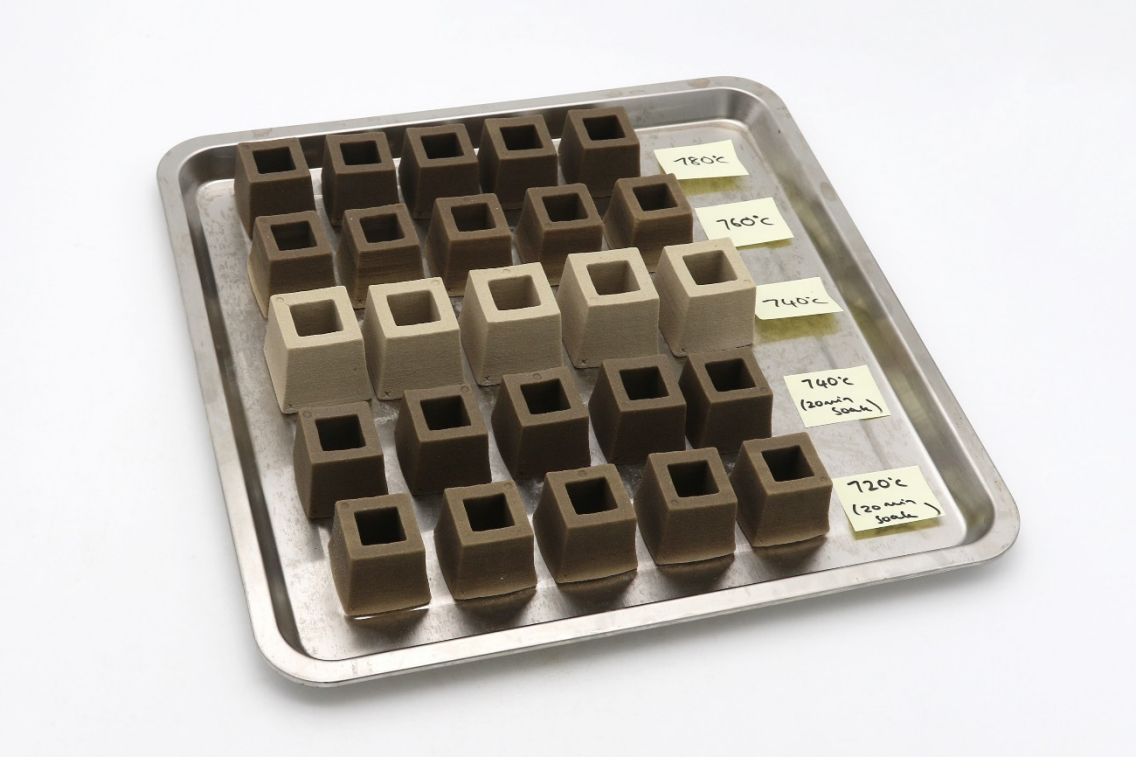

Figure 5.53. *Serial experimentation with firing schedule to develop porous parts.*
Fourteen experiments were conducted to develop a firing schedule by adjusting the peak temperature and hold time.

Figure 5.54. *Hollow cube geometries used for porosity development (green parts).*
Parts are photographed as they are positioned in print bed.

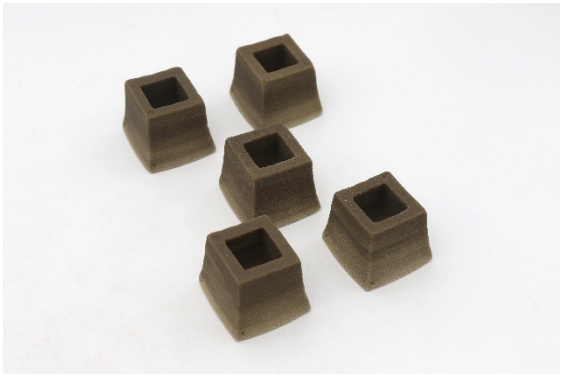

Figure 5.55. *Uneven fusing of parts due to insufficient hold time during firing.*
Parts produced by schedule with a 760 peak temperature and no hold time.

It was found that as the peak temperature decreased, the hold time needed to be increased. The schedule shown in Figure 5.56 was found to produce porous parts that appeared uniformly fused. In this schedule, a peak temperature of 680°C and a hold time of 120 minutes were used.

When placed in water, the initial water absorption was found to be 6% and bubbles formed on the surface of the part as it was submerged (see Figure 5.57). Furthermore, the hydraulic capacity of the part was observed. Vallejo (2018) describes this as the ability of a ceramic material to absorb and transport water through its pores. Different manufacturing methods can result in pores that are oriented in specific directions. This informs the way that the water flows through the material. Samples were observed to have omnidirectional hydraulic capacity, meaning that the material could absorb water in all directions. This is a result of the BJT printing process, which typically produces parts with a homogeneous internal structure. The unidirectional hydraulic capacity, defined as the upward transportation of water, was also examined to determine whether water could be moved from the base of the sample to the external surface. This can be seen in Figure 5.58. This is a characteristic that should be considered when designing ceramic evaporative cooling applications. The following section will validate and quantify the level of porosity and water absorption.

Although not the focus of this experimentation, slumping and shrinkage was also observed. As anticipated, parts that were fired at a higher temperature displayed more shrinkage due to the greater coalescence of the glass particles. All parts exhibited some slumping, largely maintaining their shape at the base but pulling inwards at the top (see Figure 5.55). During the design phase, it might be possible to counteract this by modelling a shape that flares outwards. While this option could be explored, as discussed in the previous section, different geometries respond uniquely in the kiln. Therefore, managing or fine-tuning shrinkage in the kiln should align with the specific application since universal rules cannot be established.

5.7.3 Quantifying porosity and water absorption

Throughout this experimentation, parts that appear both porous and waterproof have been produced, i.e. parts fired according to schedule in Appendix 4.4 appear waterproof, whilst parts fired according to schedule in Figure 5.56 have been observed to absorb water. However, neither property has been validated or quantified yet. As these properties lead to entirely different application opportunities, an experimental prototype was conducted to provide further insight into the material properties of parts fired at differing temperatures.

This experiment was designed in accordance with ASTM standard C20-00(2022b) and allows for the gathering of several data sets that provide insight into both the material properties and the printing process. These include volume, water absorption, apparent porosity and bulk density. Apparent porosity refers to the volume percentage of open pores in the bulk material and bulk density refers to density (mass per unit) of the bulk volume (total volume of the solid material, open pores, and closed pores) (Du et al., 2020). This ASTM standard is designed for ceramic refractory materials. It was found to be the most relevant as there are no testing standards for porous glass materials. However, some test specimen requirements needed to be modified to accommodate the BJT process (i.e., scaled down). This test is also similar to one conducted by Marchelli et al. (2011) in their glass 3D printing experimentation.

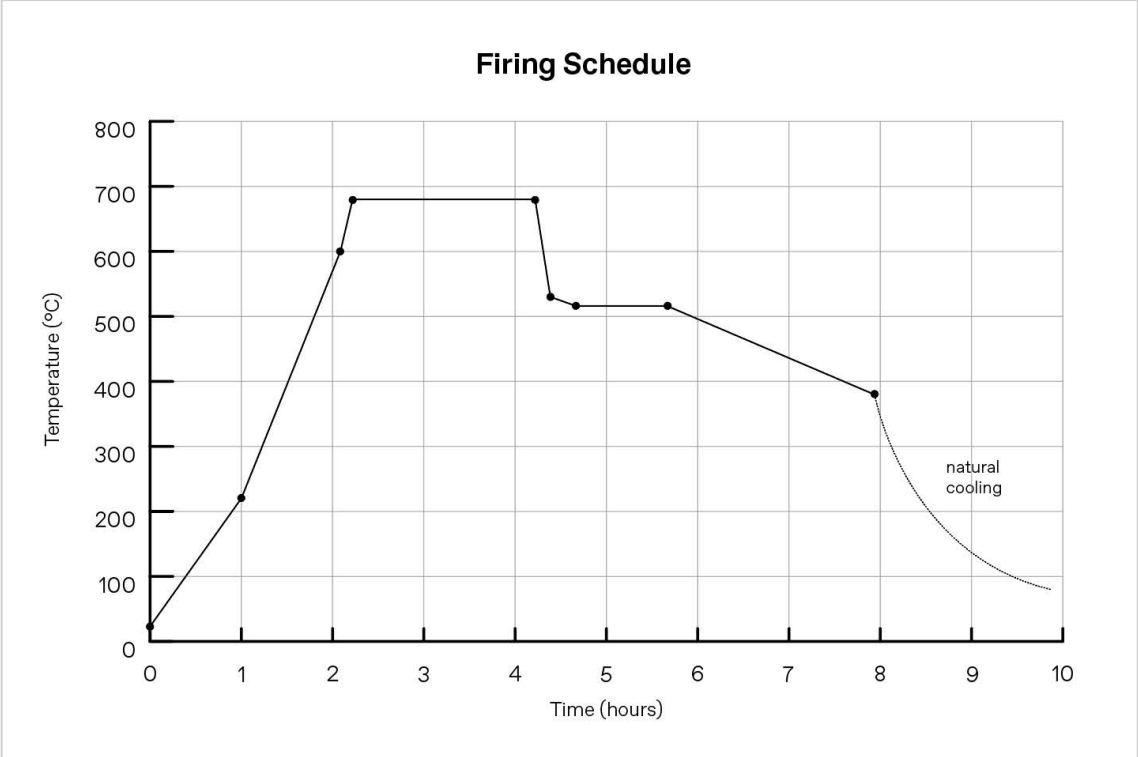

Figure 5.56. *Firing schedule for producing porous parts.*
A 680°C peak temperature and 120 minute hold time were adjusted from the initial schedule to create parts that were porous.

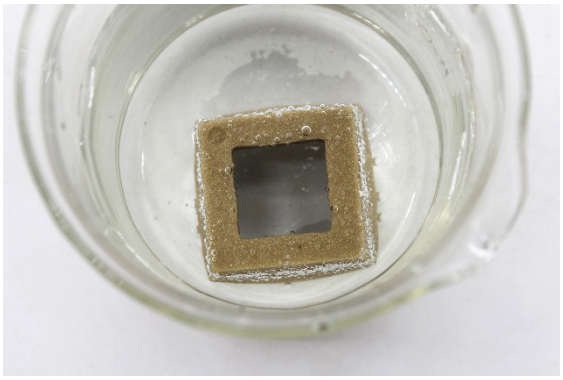

Figure 5.57. *Porous BFT glass fines sample submerged in water.*
Bubbles formed on the surface of the porous part when placed in water, indicating porosity.

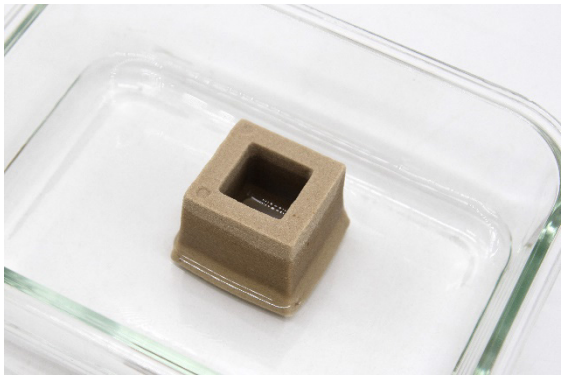

Figure 5.58. *Unidirectional hydraulic capacity of BFT glass fines samples.*
Water was transported from the base of the object to wet the entire sample.

Additive manufacturing standards like ISO/ASTM 52902:2023(E) also guided the quantity of samples printed, as these standards stipulate the need for 5 samples. This testing takes the form of a prototype as an experimental component that is akin to a scientific experiment. As such, the following section will be presented in line with the scientific method.

Aim:
To determine the apparent porosity and water absorption of two sets of BJT glass fines samples fired to different temperatures. The first set is fired according to the schedule in Appendix 4.4, which is hypothesised to be waterproof. The second set is fired according to the schedule in Figure 5.56 which is known to have porosity and water absorption properties.

Method:
To prepare the material, 4% (w/w) HPS was combined with glass fines in a commercial mixer for 10 minutes. Tap water was used as the liquid activator. Hollow cubes with a wall thickness of 10mm were modelled in CAD and loaded into the ZPrint software in the position and orientation shown in Figure 5.60. Each cube included an x and y label to capture orientation and a label of TL (top left), TR (top right), C (centre), BL (bottom left) or BR (bottom right) to capture position in the print bed. This was done as it is known that the strength and density of parts can differ across the print bed in BJT. Two sets of samples were printed using a 0.2mm layer height and 120% and 140% shell and core saturation with the ZPrint default powder setting ZP15E. Parts were left to dry in the print bed for 3 hours before removing the build platform and placing in a dehydrator at 70 degrees for 3 hours. Parts were then fully excavated and brushed off. The first set of parts were fired in a glass kiln according to the schedule in Appendix 4.4 and the second set of parts were fired according to the schedule in Figure 5.56. Each set of parts were fired on the same shelf using alumina kiln paper to prevent sticking.

Post firing, parts were heated to 110°C and the dry weight (D) was recorded to the nearest 0.1g. Parts were placed in water and boiled for 2 hours, keeping them entirely covered in water and ensuring no contact with the heated base of the pot (see Figure 5.59). After boiling, parts were left to cool in the water for 18 hours to ensure full water infiltration. The suspended weight (S) of each sample was then measured to the nearest 0.1g. This was done by suspending the sample in water using a loop of wire hung from one arm of the balance (see Figure 5.61). The balance was pre-calibrated with the wire submerged to the same depth as that used for weighing the samples. The saturated weight (W) was then determined by weighing the sample in air to the nearest 0.1g. Each sample was blotted using a damp linen cloth to remove drops of water from the surface. Care was taken to limit excessive blotting, which can extract water from the pores and lead to errors. Calculations were then conducted to determine the water absorption, apparent porosity, bulk density and apparent specific gravity.

Results:
The results of the experiment can be seen in Table 5.1 and Table 5.2. The samples are labelled according to their placement in the 3D print bed. The results show that in both sets, the placement affected the weight and volume of the parts, with those located on the left side of the print bed showing higher values for both.

In set 1, parts fired according to the proposed waterproof firing schedule (see Appendix 4.4) showed low apparent porosity, ranging from 0.8-0.9%, with a water absorption rate of 0.4% for all samples (expresses the relationship of the weight of the water absorbed to the weight of the dry sample). Bulk density ranged from 2.32-2.34 g/cm^3.

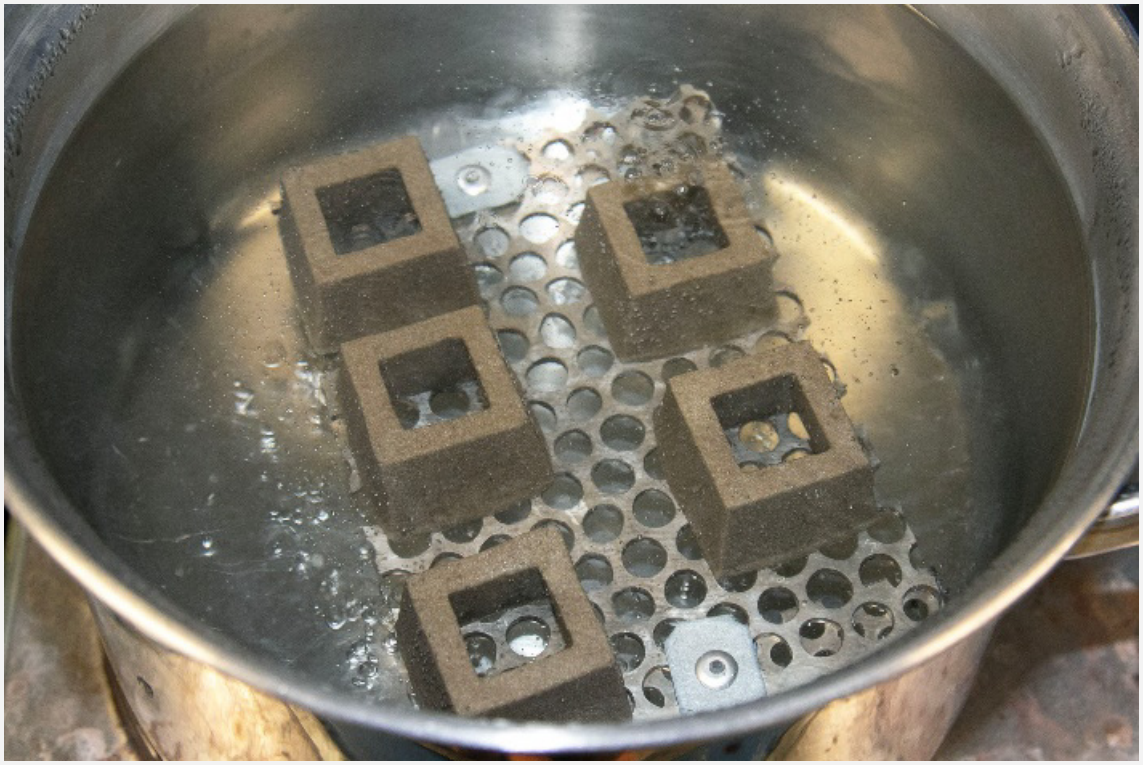

Figure 5.59. *Samples boiling in water to determine porosity.*
Parts fired according to schedule in Appendix 4.4.

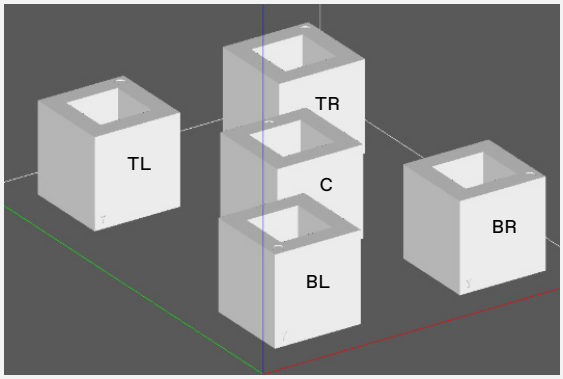

Figure 5.61. *CAD models for porosity testing loaded into the* ZPrint software in the correct position and orientation. A labelling system was incorporated into each model to capture their position in the print bed - TL (top left), TR (top right), C (centre), BL (bottom left) or BR (bottom right).

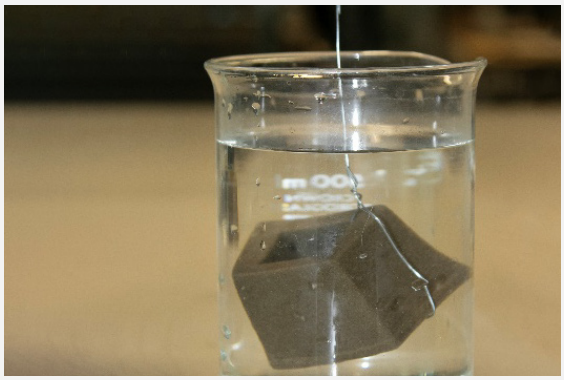

Figure 5.60. *Measuring the suspended weight of samples.*
The sample was suspended in water using a loop of wire hung from one arm of the balance.

Sample	Dry Weight (D) (g)	Suspended Weight (S) (g)	Saturated Weight (W) (g)	Exterior Volume (cm^3)	Water Absorption (%)	Apparent Porosity (%)	Bulk Density (g/cm^3)
TL	83.1	47.7	83.4	35.8	0.4	0.8	2.32
TR	77.1	44.4	77.4	33.0	0.4	0.9	2.34
C	79.6	45.8	79.9	34.1	0.4	0.9	2.33
BL	82.3	47.2	82.6	35.4	0.4	0.8	2.32
BR	77.8	44.7	78.1	33.4	0.4	0.9	2.33

Table 5.1. *Results of water absorption experiment for parts fired according to the schedule seen in Figure 5.5.*

Sample	Dry Weight (D) (g)	Suspended Weight (S) (g)	Saturated Weight (W) (g)	Exterior Volume (cm^3)	Water Absorption (%)	Apparent Porosity (%)	Bulk Density (g/cm^3)
TL	88.0	53.0	93.4	40.4	6.1	13.4	2.18
TR	80.9	48.7	86.7	38.0	7.2	15.3	2.13
C	84.5	50.9	90.3	39.4	6.9	14.7	2.15
BL	87.0	52.4	92.4	40.0	6.2	13.5	2.18
BR	82.5	49.7	88.6	38.9	7.4	15.7	2.12

Table 5.2. *Results of water absorption experiment for parts fired according to the schedule seen in Figure 5.56.*

In set 2, parts fired according to the proposed porous firing schedule (see Figure 5.56) exhibited higher apparent porosity, ranging between 13.4-15.7% and increased water absorption of 6.1-7.4%. The bulk density of the parts was lower than that of set 1, ranging from 2.12- 2.18 g/cm^3.

Discussion:

While printed using the same parameters and CAD models with identical volume, both test sets showed variation in the weight and volume of the five parts based on their placement in the print bed. The results show that the parts closest to the feed reservoir, the side the powder is spread over first, had a larger volume and weight than those printed on the right. The piece printed in the centre of the bed had a weight and volume between these two values. While the connection between higher volume and increased weight is clear, understanding the differences among the parts is of interest as it highlights the variations in powder packing density across the print bed. This has been reported in literature particularly in relation to the Z-axis where the repetition of the spreading process and gravitational force of each layer, result in an increase in the density of powder and therefore green density of parts in the bottom layers of the print bed, slowly decreasing in density as you reach the upper layers (Mostafaei et al., 2016).

It has also been shown that there is a variation in powder packing density across the XY dimension as well, where parts decrease in green density along the X-axis. Paudel & To (2025) found that parts closest to the feed reservoir and first to be spread over, obtained 5-8% greater green density than those on the side furthest from the roller. Dorula et al. (2024) suggest that the higher amount of fine powder at the start of the rolling process may contribute to this effect. The fine powder fills more voids as it spreads initially, leaving the coarse powder to accumulate on the far side of the print bed. Additionally, negligible change was seen in the Y axis. Their results are in line with the findings of this experiment. Research has shown that different spreading mechanisms, such as double spreading, can be employed to reduce this phenomenon (Dorula et al., 2024). While at this scale, the changes in volume are unlikely to have a significant impact, utilising these methods may become essential for ensuring uniformity of parts, since BJT technologies have been commercially scaled up to 4m^2.

With this in mind, it is hypothesised that the higher packing density of the left-hand side of the print bed resulted in parts of greater volume because there were more particles (potentially fine particles) in which the binder could seep out and bond to. This, along with the higher green density, resulted in the increased weight. Furthermore, the parts on the left exhibited slightly lower porosity, also likely the result of the increased powder packing.

Regarding apparent porosity and water absorption, the results of the first set, which were expected to be waterproof, showed that the apparent porosity (the volume percentage of open pores) of the components ranged from 0.8% to 0.9% when fired according to the schedule in Appendix 4.4. This resulted in a water absorption of 0.4% across all samples. Although not zero, this is considered to be an acceptable level of waterproofness for ceramic applications such as tiles. According to the Australian Standard (13006) for Ceramic Tiles, both dry-pressed and extruded tiles with water absorption below 0.5% are classified in the category with the lowest water absorption. As such, this material and production process could be used in ceramic tile applications requiring waterproofness. It verifies the ability to achieve waterproof BJT glass fines objects despite the inherent porosity of the parts. This opens application opportunities for the use of glass fines in this space.

The average bulk density of the parts was found to be 2.33 g/cm^3 . When compared to the theoretical bulk density of soda lime silica at 2.5 g/cm^3 the densification achieved is 93.2%. As discussed above, there is significant literature devoted to increasing the density of BJT parts, using a range of methods such as granulation, mixing of different size powder particles or using a slurry feedstock (Du et al., 2020). Whilst achieving fully dense parts is often emphasised in literature, this may not be necessary depending on the application- i.e. non-load bearing parts.

The apparent porosity of the parts fired according to the schedule in Figure 5.56 was found to be between 13.4-15.7%. This resulted in a water absorption of 6.1-7.4% and an average bulk density of 2.15g/cm^3 was found. When compared to the theoretical density of soda lime silica, the densification achieved is 86%. Porosity of between 5-75% has been achieved using this partial sintering approach of ceramic materials (Roy, 2025). While this result is situated at the lower end of the spectrum, it remains comparable to the levels of porosity observed in unglazed ceramics, such as terracotta, which range from 7% to 24% (Hall & Hoff, 2021; Vallejo, 2018). These ceramic materials are commonly used for evaporative cooling applications. Furthermore, it aligns with research from Vallejo (2018) who developed ceramic evaporative cooling elements with porosity levels in the range of 7.5-16.1%. This provides a potential application avenue for porous BJT glass fines products.

There is an opportunity to further optimise and tailor the level of porosity. This can be achieved by incorporating a foaming agent like calcium carbonate This method is frequently utilised to produce glass foams; however, it may affect both circularity and geometric precision. Additional burn-out techniques could be explored, where materials like sawdust are introduced that decompose in the kiln, creating voids (Bechthold et al., 2015). Additional analysis of pore characteristics, including shape, size, and morphology (the number of open or closed pores), could also be pursued, as these factors significantly influence the material's final properties (Roy, 2025). Some research also points to the changes in density that can occur with different geometries (Stevens et al., 2018). This could be further investigated.

As highlighted by (Roy, 2025) There is often a balance or trade-off between porosity and other mechanical properties. Glass and ceramics are inherently brittle materials with low fracture toughness, and pores can serve as defects that affect properties like flexural and compressive strength. It is crucial to highlight that this experiment has not examined how the porosity of the components influences these mechanical properties. As such, for this research non-structural applications should be envisioned.

Conclusion:
The samples fired to the schedule in Appendix 4.4 resulted in parts that can be considered waterproof. Although these parts contain some porosity and lack complete density, this does not compromise their waterproof qualities. It is likely that most pores are closed and internal, which affects material strength less than open pores would. This broadens the application possibilities where waterproof characteristics are essential. On the other hand, the samples fired to the schedule in Figure 5.56 attained an average porosity of 14.5%. This opens application opportunities for the BJT glass fines material to be used in evaporative cooling applications which require this level of porosity. This porosity further resulted in an average water absorption of 6.8%.

5.8 Reflection and conclusion

This chapter has presented the second phase of experimentation, focusing on the kiln firing process, geometric explorations and porosity. Figure 5.62 provides a diagrammatic representation of this experimentation, following the same visual format as the Research Diagram presented in the Methodology (see Section 3.5). The chapter began by introducing the final step in the production process, firing, which is essential for the creation of fused, solid components. Background information regarding the relationship between heat and glass was provided before establishing the importance of this step in terms of circularity. During the firing process, the binder burns away, leaving only soda lime silica glass, which can be recycled repeatedly. This is important as creating composite materials or using additives that leave residues can be a barrier to circularity. This led to the first experiment seen in the Figure 5.62, a TGA that verified the circularity of the BJT glass fines material. It showed that the sample remained stable when heated to 650°C, thereby demonstrating that the binder and other contaminants had decomposed during the initial firing process.

From here, an exploration into geometries was presented. As glass begins to flow when heated, this stage of experimentation revealed the difficulties of shrinkage and slumping of the glass material in the kiln. Several typologies were investigated to understand which geometries could be predictably fired. This included experimentation with vessels, tiles, and an explorative layered slumping technique. Although results varied, it was evident that any unsupported walls were prone to significant slumping in the kiln. As a result, a series of lattices featuring a pyramidal truss structure were tested, leveraging the self-supporting design of the struts. Uniform, single-height lattices were successfully printed, excavated, and predictably fired with minimal slumping. These signify a breakthrough in recycled glass 3D printing, as fired geometries of this complexity have not yet been presented. It also opens compelling application opportunities as these forms would be impossible to achieve via traditional glass manufacturing methods.

However, further exploration of lattices revealed that the shrinkage and slumping were dependent not only on the geometry but also on scale. The same lattice printed with a different cell size would behave differently in the kiln. This made it clear that creating universal design rules for the material and production method would be extremely difficult. Instead, an application must be designed closely with the process to tailor the geometry specifically to that function. Although this could be positioned as a limitation, within the context of RtD, it presents an opportunity to leverage design expertise to identify and develop viable application pathways. As a result, materials and production processes that might be considered unfeasible within conventional material science or engineering disciplines can find appropriate and meaningful uses. This approach is particularly well-suited to 3D printing technologies, which enable rapid prototyping, flexibility, and customisation opportunities. It also aligns with approaches in the field of materials design, where the traditional model of selecting a material to suit a predetermined application is being replaced by a more integrated model in which the material and its production process actively inform and shape the final application.

With this in mind, further exploration of the material properties was undertaken to make an informed decision around application. Of particular interest was porosity, as parts produced by BJT often retain some level due to the powder-based production method. Porosity and density are widely studied in BJT literature as these characteristics are closely linked to mechanical performance and affect water absorption. An SEM analysis revealed the presence of closed, unconnected pores in the 3D printed glass fines samples. This sparked interest in whether porosity could be optimised to serve as a functional element of the material and the potential applications that could emerge from it. This line of inquiry was informed by literature, which revealed two prevailing approaches in BJT research: one aimed at minimising porosity to enhance structural performance,

and another focused on leveraging porosity for specific functional applications such as filtration systems or bone scaffolds. Coupled with existing knowledge of glass firing, this insight led to the hypothesis that reducing the peak temperature in the firing schedule could increase porosity levels. A total of fourteen tests were carried out to explore this possibility. The results showed that it was feasible to create both waterproof components and samples with approximately 15% porosity capable of absorbing water. This was verified using an experimental prototype based on ASTM standards for ceramic materials.

During this porosity investigation, an application avenue began to crystallise. Although conventional applications for ceramic and glass, such as vessels or basins, remain viable options, the unique properties of the porous glass material offers compelling opportunities, especially within the built environment. Porous ceramics have been used to cool spaces via evaporative cooling for centuries. The porosity levels attained in this study are comparable to those of unglazed ceramics used for this process, in the range of 7-24% (Hall & Hoff, 2021; Vallejo, 2018). This application also provides an opportunity to utilise the 3D printing capabilities of complex geometries and customisation. The following chapter will discuss the development of this application in detail.

While the lattice geometries proved successful in this chapter and have potential for future development, the next chapter will investigate additional geometric typologies. The aim is to continue expanding knowledge around the range of achievable forms and to design these forms with the specific application in mind, rather than attempting to fit the lattice designs to the application. As a result, the lattices in this research serve as an example of the level of geometric complexity that can be achieved using this technology and material. There is significant scope to develop these and apply them in differing application contexts. It is also important to highlight that the emphasis on geometric complexity is tied to the role 3D printing can play in enabling the CE. By producing forms that cannot be achieved via traditional manufacturing methods, different aesthetics and functionalities can be developed, thereby opening new and compelling application opportunities. This can add value to waste streams and promote their upcycling.

This chapter also allowed for further reflection on circularity. The research has focused on material circularity and integrity, meaning the material retains its original properties even after recycling, enabling repeated use (Sauerwein, 2020). While this is an indispensable part of circularity—as it is only by maintaining the properties and value of our materials that they can have longevity in circular loops—it is not the whole picture. It is important to highlight that the energy and associated emissions of the production process have not yet been quantified. This encompasses aspects controlled by this research, including printing and kiln firing, as well as impacts from the processing of glass fines, modification of organic binders, transportation, and even energy associated with CAD modelling. An in-depth analysis of these impacts is beyond the scope of this research, especially at this stage of development, when accurate comparisons with other materials would be challenging. These factors have, however, consistently influenced the development of the process. Toxic materials have been avoided, glass fines have been sourced locally, and firing temperatures have been kept as low as possible, at nearly half those used in traditional glass manufacturing and recycling. Greater quantitative analysis of the process and integration of these findings throughout material, production, and application development would benefit from interdisciplinary collaboration. Such analysis demands substantial expertise, time, and familiarity with specialised tools, highlighting a valuable direction for future materials design projects.

Overall, this chapter facilitated several key developments. Firstly, the circularity of the glass fines material was established, and an understanding of the behaviour of the geometries in the kiln was developed, including the potential for self-supporting, pyramidal, and truss forms. Additionally, two firing schedules were created to produce either waterproof or porous parts, leading to the formation of an application direction.

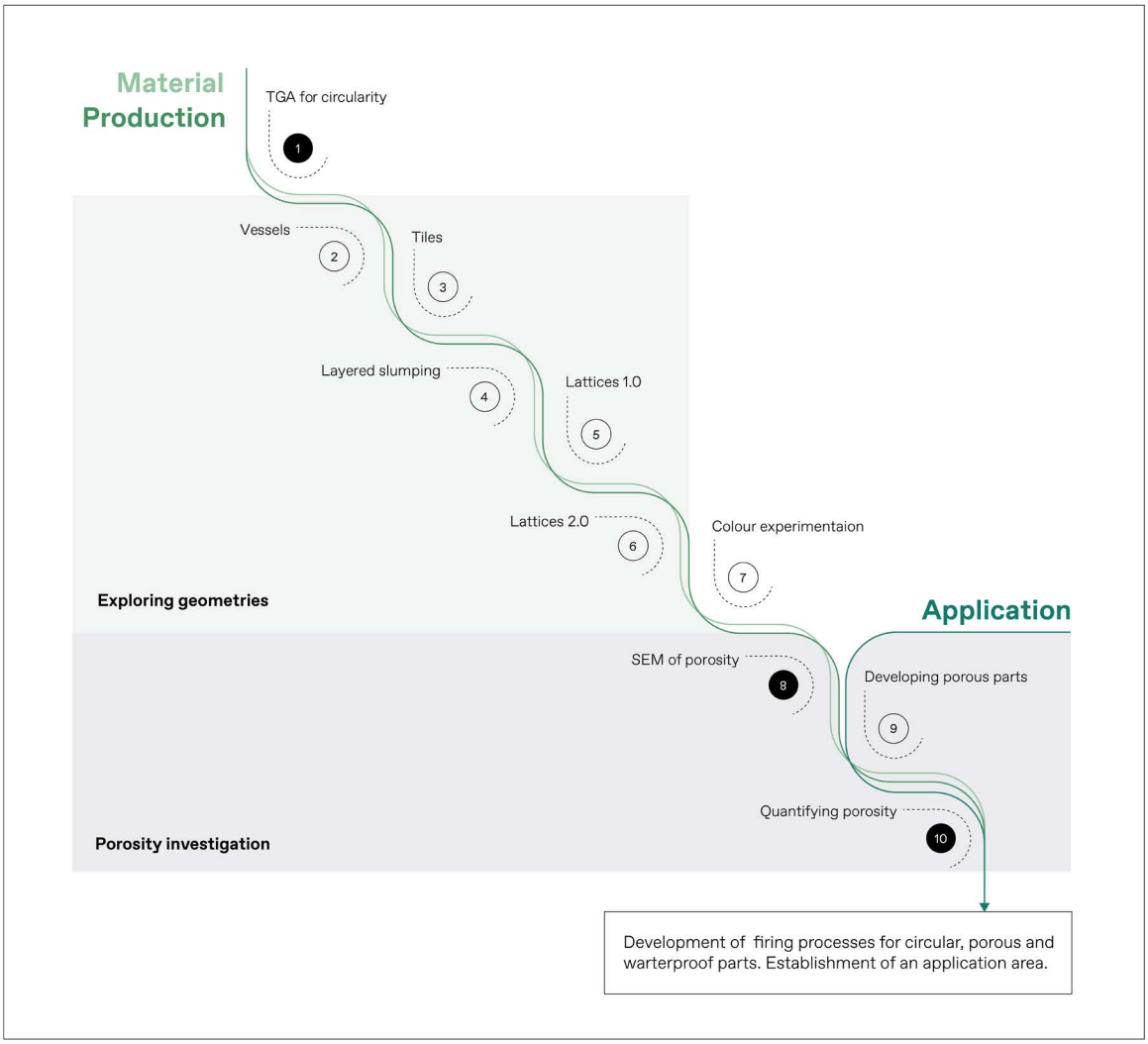

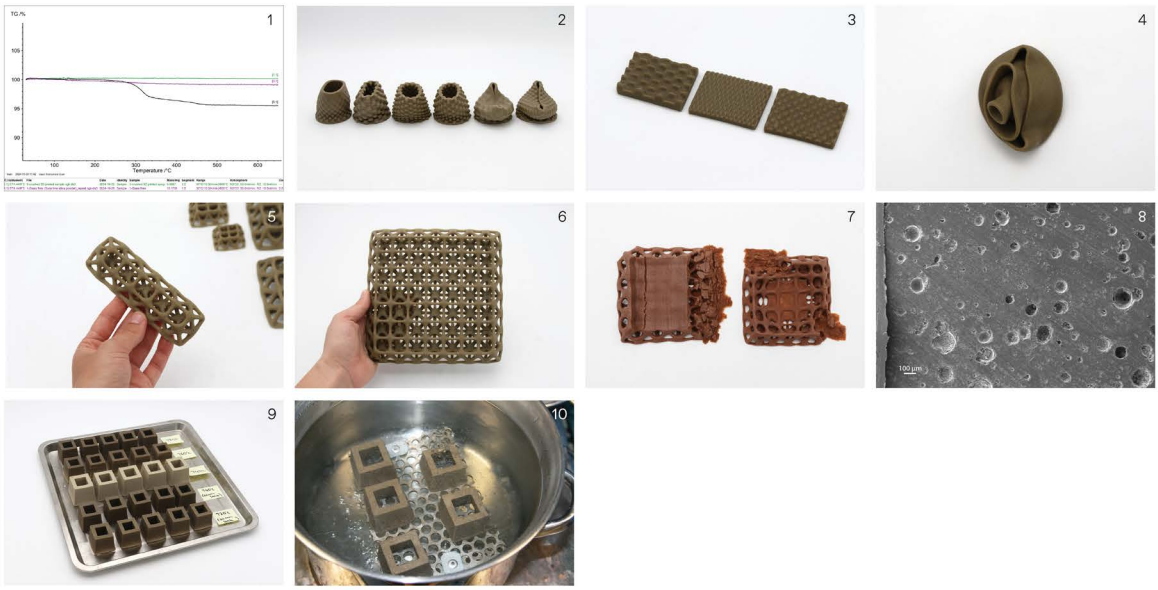

Figure Error! No text of specified style in document.**.2.** Diagrammatic representation of experimentation presented in Chapter 5.
This chapter began with a focus on the material and production threads of the research questions before incorporating the application thread later in the experimentation. These questions were addressed through ten sets of experiments, symbolised by the cascading circles. The experiments in the diagram are numbered to correspond with their respective images.

6

Application

6 Application

6.1 Introduction

Through the experimentation in the previous two chapters, it has become clear that there are numerous application opportunities for binder-jet 3D-printed glass fines. These could include conventional ceramic products such as crockery, tiling, and basins, as well as lighting, decorative homewares, or even insulation media. Whilst many of these avenues could be examined, this research has opted to focus on developing and exploring a single application in detail. This approach can support industrial translation and communication of the research, while also enabling substantial knowledge creation by understanding the real-world constraints involved with designing for a new material and production system.

Based on the findings in Chapter 5, the built environment was selected as the potential application area to be explored, with a specific focus on evaporative cooling components. This application was chosen because of the way it uniquely harnesses the capabilities of both the material and production method. In particular, the inherent porosity of parts produced via BJT lends itself to this application. The previous chapter showed how this level of porosity could be tailored by optimising the firing schedule to produce parts suitable for this application. Furthermore, the complex geometries and customisation offered by 3D printing can contribute to the functionality of evaporative cooling systems. The reasoning behind this choice and the way it cohesively combines the three core elements of this research (material, production and application) will be further discussed throughout the chapter. Firstly, contextual information on the built environment and evaporative cooling will be discussed. This will include a series of design precedents and the setting out of a design brief. Following this, the design development of an evaporative cooling system using the BJT glass fines material and production method will be described. The final design and prototype will then be presented.

6.1.1 Cooling the built environment

The built environment sector is responsible for 37% of the world's energy-related emissions (United Nations Environment Programme, 2022). These are broadly split into two categories: embodied emissions and operational emissions. Embodied emissions are those associated with the construction of the building. These are produced during the extraction, manufacturing, transport and on-site construction of the building materials (United Nations Environment Programme, 2023). Operational emissions are those generated through the function and maintenance of the building, including heating, cooling, lighting and electrical appliances (United Nations Environment Programme, 2023). The material and production elements of this dissertation aim to address the embodied emissions by introducing a circular material made from a waste resource. The application component of this research looks to the operational emissions.

The cooling of spaces is a large portion of these operational emissions. The energy consumption for space cooling has more than tripled since 1990 (International Energy Agency, 2018). As extreme heat events and record-high temperatures persist, this demand is expected to keep rising (Santamouris, 2016a). This has not only adverse environmental impacts but also social ones, putting many people at risk of heat stress. Furthermore, vulnerable groups without access to indoor cooling are more likely to be impacted (Santamouris & Kolokotsa, 2015).

The urban heat island effect further exacerbates the need for cooling. This is the well-documented phenomenon in which cities experience higher ambient temperatures compared to the surrounding rural or suburban areas (Feng et al., 2023; Santamouris, 2015). This effect has been documented in more than 400 cities worldwide, where temperature increases average around 5°C but can reach up to 10°C (Santamouris, 2020). The urban heat island effect is attributed to a number of complex factors, including: the heat released from human activities such as cars and air conditioning; the overall form of cities with tall buildings and canyons, which can limit ventilation, reflect and trap heat; and the thermal properties of the materials that are used (Prasad et al., 2022). This urban overheating drastically increases demand for cooling in cities and the associated energy, creating a vicious cycle that further worsens the situation (Santamouris et al., 2015).

The specific impact that materials have on urban ambient air temperature is well studied (Doulos et al., 2004; Santamouris, 2015). The widespread use of materials such as concrete and asphalt (usually dark in colour) significantly impact the thermal balance of cities as they absorb and re-radiate solar energy (Feng et al., 2023). As a result, there has been a focus on developing and implementing "cool materials" and coatings that can reflect solar radiation and maintain lower surface temperatures (Santamouris et al., 2011). These materials are typically highly reflective and possess a high emissivity factor, which indicates the capacity of the surface to emit absorbed heat. They are positioned as a cost-effective and passive method for reducing both surface and air temperatures (Santamouris et al., 2011).

Alongside "cool materials," a range of other mitigation strategies have attracted the attention of researchers from across disciplines, including energy experts, material designers, climatologists, and urban designers (Santamouris, 2015). The objective of these strategies is to minimise the intensity of heat sources and maximize the potential of heat sinks within the urban environment (Santamouris, 2016b). Key mitigation strategies include the integration of greenery or "green infrastructure", solar control strategies such as shading and the use of heat sinks such as the ground and bodies of water (Akbari et al., 2015; Haddad et al., 2018). Combining and tailoring these mitigation strategies to specific areas has proven to have a significant and holistic impact on urban overheating (Santamouris et al., 2020). Of specific interest to this research is the integration of new materials in the urban landscape and the cooling potential of water.

6.1.2 Evaporative cooling

Water has always been a key strategy for cooling cities. Two of the key reasons for this are its high specific heat capacity and evaporative action. High specific heat capacity means that water absorbs a significant amount of heat without experiencing a large increase in temperature itself (Domínguez & Flor, 2016). This property allows water to act as a buffer against temperature changes, making it effective for absorbing heat from its surroundings. As a result, bodies of water serve as heat sinks in urban environments. Furthermore, the evaporation process of water requires a significant amount of energy (known as its latent heat). As the water evaporates, this energy comes from the surrounding air and water, resulting in the cooling of both. According to Domínguez & Flor (2016) this cooling effect is substantial, with 1kg of water decreasing the temperature of more than 2000m^3 of air by 1°C and increasing the relative humidity by 5%. The rise in humidity demonstrates that the cooling power of water naturally increases in hot, dry conditions, where high evaporation rates occur. It also indicates that the cooling potential is intrinsically responsive to extreme weather events, such as heat waves (Feng et al., 2023).

Evaporative cooling systems have been used in hot, dry climates for centuries (Ford, 2001). For example, Malqaf towers, which date back to Ancient Egypt, capture and funnel wind into spaces to cool them. These towers can be combined with wetted matting suspended in their interior to enhance the cooling effect (Fathy et al., 1986). Salsabils are another example found in hot climates across the Middle East. These are carved marble fountains that are installed on an incline to allow water to trickle down and evaporate, cooling the surrounding air (Fathy et al., 1986; Ford, 2001).

With growing concerns over rising temperatures, recent years have seen an increased focus on evaporative cooling techniques and their potential applications in urban environments. Researchers have explored the cooling impacts of water bodies and water-based infrastructure, sometimes termed 'blue' infrastructure. The cooling effect of natural water bodies such as lakes and rivers on urban areas in close proximity has been well documented (Xu et al., 2010; Zheng et al., 2021). Smaller-scale, water-based systems such as pools, ponds and fountains and systems such as evaporative wind towers, sprinklers and water curtains have been integrated into urban environments to decrease ambient temperatures (Domínguez & Flor, 2016). These man-made water systems are attracting attention due to their scalability, versatility and controllability (Feng et al., 2023). Studies further suggest that water-based technologies have the highest local impact when compared to equal coverage of other heat mitigation strategies such as shading and greenery (Haddad et al., 2018; Santamouris et al., 2017). Other techniques, such as permeable and water-retentive pavements, have been investigated (Wang et al., 2022).

Evaporation has also been used in the design of air conditioning units, where both direct and indirect systems have been developed (Watt, 2012). Direct evaporative cooling is when water evaporates into the air to be cooled and simultaneously humidifies the air. Indirect evaporative cooling was developed approximately seventy years ago and was specifically designed to prevent this form of humidification (Watt, 2012). This is achieved by isolating the evaporation process from the air that needs to be cooled using a surface or plate. Typically, these are active systems driven by electricity rather than the passive systems (requiring no energy) described above. Despite the prevailing commercial dominance of vapour compression coolers, evaporative systems are receiving attention as they generally consume less energy (Amer et al., 2015).

6.1.3 Evaporative ceramics

There is a long history of using ceramics in direct evaporative cooling systems due to the porosity of fired clay. This porous structure allows water to permeate the surface, where it creates a thin water film that can evaporate and cool the ambient air. Generally, a higher level of porosity results in higher cooling (Ibrahim et al., 2003). The use of porous ceramic materials to cool both spaces and liquids is said to date back to Ancient Egypt. Frescoes from 2500 BC show water-filled ceramic jars being fanned to cool rooms. The unglazed ceramic jars were porous enough to allow for the surface to remain wet and facilitate the evaporative process (Watt, 2012). For example, "maziara" jars are a traditional water-cooling system used in Egypt. These are large water pots made from porous unglazed ceramic, which are mounted in specifically designed window openings. As air passes over them into the room, it cools both the air and water through evaporation (Cain et al., 1976; Fardeheb, 2009).

In recent years, attention has been given to these ancient cooling techniques as low-energy or passive alternatives to air conditioning systems. In particular, porous ceramics have been integrated into contemporary architecture in the form of towers, walls, screens and roofs, facilitated by significant advances in ceramic engineering (Bechthold et al., 2015; Vallejo, 2018). Two of the most influential ceramic evaporative cooling systems at the architectural scale include the Spanish Pavilion in Expo Zaragoza 2008 and The Bioskin façade on the Sony Research and Development office built in 2011. The Spanish Pavilion was made up of a network of columns, designed to evoke a forest (see Figure 6.1). These columns were clad in custom ceramic elements with a porosity of 10%. A misting system on the inside of the columns kept the ceramic surfaces wet and allowed for evaporation to occur. The cooled air was then pushed downwards using fans and delivered at ground level through slits in the ceramic tiles.[16] The fans were powered by solar panels installed on the roof, and water came from rainwater tanks in the basement (Martín Gómez, 2012). Studies of the design revealed that the ceramic surface temperature ranged from 25.2-32.5°C, while the ambient outdoor temperature was 34.9°C and the relative humidity was 33.6% (Martín Gómez, 2012).

Similarly, rainwater was used to fill the system of porous terracotta pipes which make up the Bioskin Façade (see Figure 6.2). This system was inspired by the traditional Japanese Sudare screens, made of horizontal bamboo or wooden slats (Bechthold et al., 2015). The porous pipes feature a titanium oxide photocatalytic coating to eliminate any mould or moss growth, while a stainless-steel irrigation system directs water through the network of horizontal ceramic pipes. A numerical simulation using measured data suggested that on the hottest summer day, the pipe surface temperature could be 10°C lower, while airflow analysis showed that the surrounding walkways could see a reduction of 2°C (Yamanashi et al., 2011).

Interestingly, the designers of BioSKin have rejected suggestions to commercialise the design, reflecting that mass production is an 'old-fashioned way of producing goods' and is not in line with environmental concerns (Yamanashi, 2015, p. 47). Instead, they believe in mass customisation, where high-quality architecture is crafted according to the unique conditions of each project and site. This perspective is consistent with the premise of this research, wherein materials, production methods, and applications must be interwoven and carefully tailored to one another. It also corresponds with the capabilities of 3D printing, which enables customised, small-batch production as opposed to the mass production of identical designs. Both of these real-world examples act as strong precedents for the use of evaporative cooling ceramics in buildings..

There are also a range of smaller-scale examples or prototypes of evaporative cooling systems using ceramics. These are from designers, architects and researchers globally. For example, Studio Ant in India designed an outdoor cooling system using cylindrical terracotta cones that was inspired by a beehive structure (see Figure 6.3). The system was placed in front of a generator at a factory that was radiating heat, causing discomfort to workers. Recycled water was used to keep the cylinders wet, allowing for the hot air from the generator to pass through and be cooled. It was found that the temperature around the installation dropped to approximately 36°C whilst the outside temperature remained as high as 42°C (Ant Studio, n.d.). Whilst the system only requires a small amount of electricity for the water pump, the designers also propose a zero-energy prototype in which water could be manually poured over the terracotta twice a day. A major strength of this system lies in its scalability and adaptability to various contexts. They have proposed several additional iterations of ceramic cooling systems.

[16] It is important to note that the use of fans and misting system means that this system is not entirely passive.

Figure 6.1. *Spanish Pavilion EXPO 2008, Zaragoza, Spain, Francisco Mangado.*
Pillars clad with custom, porous ceramic elements with an integrated misting system enabled evaporation.

Figure 6.2. *Bio Skin, Sony Research and Development Office, Tokyo, Nikken Sekkei, 2011*
The Bioskin Façade features a stainless-steel irrigation system that channels water through a network of horizontal, porous ceramic pipes.

TerraCool is a Masters project from the Bartlett School of Architecture by Lachlan Fahy and Dilara Temel (see Figure 6.4). This project sits at a prototype scale and aims to advance ceramic evaporative cooling through optimised surface geometry and modular manufacturing. Existing research on the performance of ceramic evaporative cooling has confirmed the importance of the surface area to volume ratio. Whilst responses to this often manifest in simple surface area increases such as grooves, waves or folds, TerraCool utilises triply periodic minimal surface geometries to maximise the surface area of contact between wet ceramic and warm air (Temel et al., 2024). They paired a parametric script with a modular mould system to ensure that TerraCool could be mass-customised for various spaces and purposes. The individual bricks are stacked in a staggered formation (like traditional bricklaying), which allows for a more secure structure as well as for water (which is fed from the top) to flow both vertically and horizontally. Machined aluminium caps are screwed onto the tops and bottoms of each brick and threaded rods and O rings are used to secure and seal the elements together. The focus on surface area optimisation as the design driver is a defining characteristic of this project.

Within the research space, significant work has been conducted by He & Hoyano (2010, 2011). They have developed a passive evaporative cooling wall using porous pipe-shaped ceramics with high water soaking-up ability. This means that the ceramics can absorb water from a water tank base without the need for pumps or irrigation. They achieved this through the creation of a specialised ceramic material and found that the pipes could absorb water up to 1.3m whilst traditional ceramics can only soak up around 30-40cm high. The maximum absorbed water content in weight was found to be 30%, which allowed for the surrounding air to be cooled by 2°C. The design consisted of four rows of ceramic pipes that enabled airflow between them and facilitated easy replacement if one was damaged. Harnessing the capillary action of the ceramic material for passive cooling is a key advantage of this system.

Of particular relevance to this dissertation are examples of ceramic evaporative cooling systems produced via 3D printing. The examples of this all remain at the prototype scale. A recent Masters project by Rameshwari Jonnalagedda called TerraMound explored the potential of 3D printing to create complex geometries in ceramic which can promote high evaporation (see Figure 6.5). These geometries were inspired by natural formations such as termite mounds and, similarly to the TerraCool project, utilised minimal surface geometries. An extrusion-based 3D printing system was used to produce these forms. Although at this stage the work culminated in the prototyping of a desktop fan, the potential for the built environment is clear. Also using an extrusion-based 3D printing system, (2022) presented an interlocking modular evaporative ceramic system (see Figure 6.6). They presented a workflow for using a 6-axis robotic arm and printing onto CNC machined surfaces, with a focus on part customisation. They proposed various infill patterns where the density could be adjusted to create more or less surface area. This means that the aesthetic and functionality of each module could be customised, reflecting a key benefit of employing 3D printing technologies.

Furthermore, one of the most well-known examples of 3D printed evaporative ceramics is The Cool Brick by Emerging Objects (see Figure 6.7). This is the only 3D-printed ceramic brick produced via BJT. The porosity created by the BJT system allows the bricks to absorb water like a sponge. A 3D printed lattice structure facilitates air flow through the wall, enhancing the evaporation of water. This results in two levels of porosity: macro porosity within the bricks and micro porosity in the material itself. The bricks are also designed to be modular and interlocking, and their shape creates shaded surfaces on the wall. This keeps a large percentage of the surface of the wall cool and improves the evaporative performance. The self-shading feature of the design is unique and not discussed widely in other examples.

Figure 6.3. *Deki Cooling Installation, Ant Studio (2017).*
A terracotta cooling installation installed in Uttar Pradesh, India.

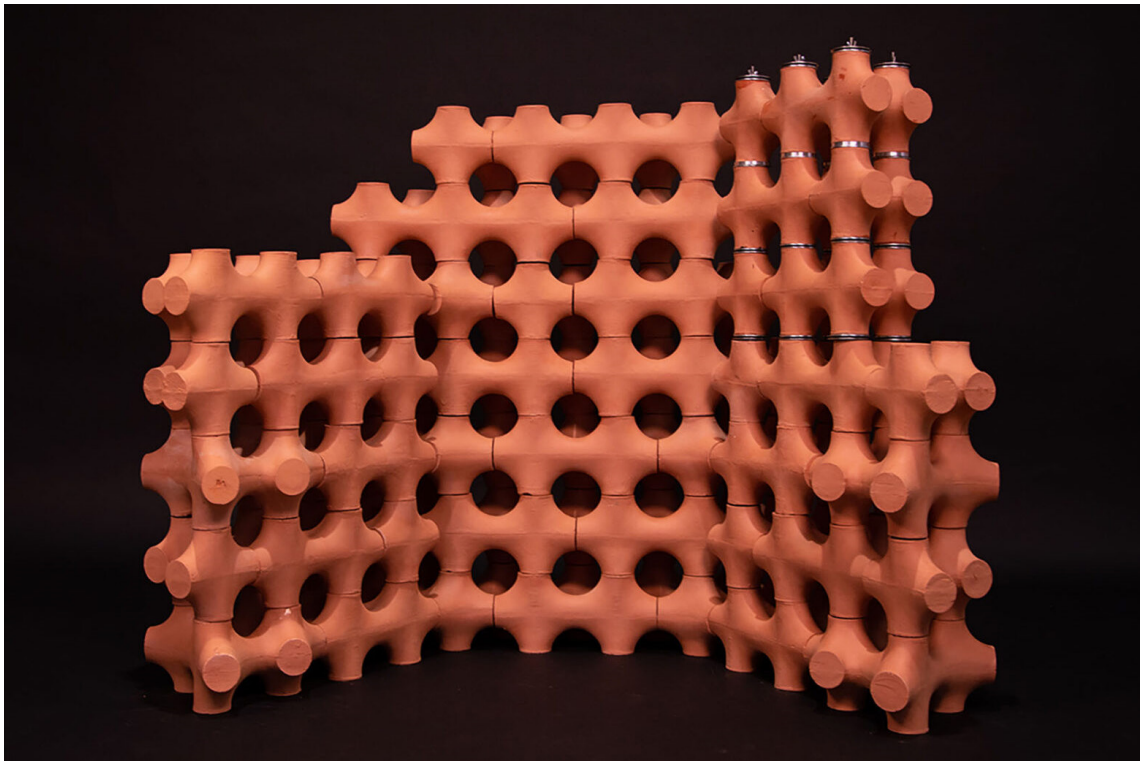

Figure 6.4. *TerraCool, Dilara Temel and Lachlan Fahy (2022)*
TerraCool focuses on optimising surface geometry through the slip casting of triply periodic minimal surfaces.

Figure 6.5. *TerraMound Rameshwari Jonnalagedda (2023).*
TerraMound uses extrusion based ceramic 3D printing to explore triply periodic minimal surfaces inspired by termite mounds.

Figure 6.6. *3D printed ceramic evaporative cooling facade modules by Gan et al. (2022).*
Infill density and patterning was explored for aesthetic and functional opportunities.

Figure 6.7. *Cool Brick, Emerging Objects (2015).*
Binder jet 3D printed ceramic brick with lattice geometries to enhance evaporation.

Overall, these precedents demonstrate the validity and potential of ceramic evaporative cooling systems in the built environment. They also provide valuable insight into the design criteria of these systems and potential areas for improvement. This will be discussed further in the next section. It is important to note that the use of porous glass has not yet been seen in evaporative cooling systems.

6.1.4 Design Criteria

Based on the precedents discussed in the previous section and additional literature, criteria for designing a direct ceramic evaporative cooling system have been developed. This will be used to underpin the design development in this research. Evaporative cooling systems can be understood as a synergistic combination of an airstream, an evaporation media, and a water supply method (Vallejo, 2018). For this research, the evaporation media is the BJT glass fines material. In addition to these elements, the system's scale, location, integration into architecture and water supply method must be considered (Vallejo, 2018). The main requirements of an evaporative cooling system using the BJT glass fines material will be described below.

Porosity

The interconnected porosity of the material is key to the evaporative potential of ceramic materials. Typically, unglazed terracotta is used as the evaporation media in these systems. Terracotta generally has porosities in the range of 7-24% and is fired at approximately 900-1000°C (Hall & Hoff, 2021). This level of porosity can be tailored depending on the blend mixture, as seen in the work of He & Hoyano (2011). In the experimentation in Section 5.7.3, the BJT glass fines material was found to have an average apparent porosity of 14.5% when fired to the schedule seen in Figure 5.56. This fits within the range mentioned above and is further confirmed by the 10% porosity of the ceramic cladding on the Spanish Pavilion, as well as evaporative ceramic components produced by Vallejo (2018) with approximately 15% porosity. Furthermore, in work by Ibrahim et al. (2003), the cooling effect of evaporative ceramics with porosities ranging from 12.4%-18.3% was measured, with higher porosities resulting in greater cooling.

Water supply

As explained above, one of the three key elements of evaporative cooling systems is the water supply which is required to keep the porous surface wet. There are several techniques which can be used to do this, including spraying or misting systems as seen in the Spanish Pavillion at Expo Zaragoza, irrigation systems as seen in the BioSkin facade, or filling the ceramic vessels with water as seen in the TerraCool project or by hydraulic absorption with a water tank at the base, as seen in He & Hoyano's (2010, 2011) work. These methods can also be combined. A suitable water supply method should ensure uniform distribution of water over the ceramic. This will be influenced by the geometry, system assembly and scale as well as the ceramic hydraulic capacity, meaning its ability to absorb and transport water through its pores (Vallejo, 2018). Different manufacturing methods can produce pores that are oriented in different directions, which influence how water flows through the material (Vallejo, 2018). In terms of the BJT glass fines material, observations of the hydraulic capacity indicated that the material could absorb water in all directions (see Section 5.7.2). This will inform the water supply method. To avoid excess water use, all systems should utilise collected rainwater, and water should be recirculated. This may require maintenance to avoid the known issue of Legionnaires growth.

Geometries – modularity, surface area and customisation

As seen in the precedents explained above, most evaporative ceramic systems are made up of individual modules that are assembled into a larger whole. Several approaches to this assembly can be seen, including the stacking of modules and mounting onto a steel substructure. The modularity allows for individual pieces to be replaced if damage occurs. This approach will be adopted in this research, with each module constrained in size by the print bed of the Z-Corp 310. As highlighted by the TerraCool project, and also evident in most ceramic evaporative cooling systems, there is a need to maximise the surface area of the ceramic geometries. This increases the evaporative potential by increasing the amount of wet surface exposed to the air. This is a great opportunity to harness the almost unlimited geometric complexities that can be produced via BJT printing. The capability of 3D printing to produce custom parts without moulds allows each evaporative ceramic module to be distinct. This allows for aesthetic and functional customisation across the evaporative system as seen in the work by Gan et al. (2022), and also allows for parts to be easily replaced if damaged.

Site Specific

The effectiveness of direct evaporative cooling systems is dependent on the climatic conditions, in particular humidity and temperature. As described above, evaporative cooling occurs when water evaporates, absorbing heat from the surrounding air and reducing the temperature while simultaneously increasing the humidity. This means that humidity becomes a limitation; as humidity increases, the air's capacity to hold more moisture decreases, reducing the effectiveness of evaporative cooling. As a result, evaporative systems are typically most effective in hot and dry climates; in climates with relative humidities of more than 50-60%, the cooling capacity decreases (Baca et al., 2011). Other climatic conditions, including wind speed, turbulence and solar radiation, can also impact the evaporative capacity (Santamouris et al., 2017). It is, therefore, important to locate these systems intentionally for them to be effective. In the context of this research, water-based cooling strategies have been identified as having a potential impact in the western suburbs of Sydney, where the climate is both hotter and drier than eastern parts of the city (Prasad et al., 2017)[17].

Whilst ceramic evaporative cooling systems have been installed in a range of spaces, including interiors and on office buildings, this research will look to outdoor public spaces. As temperatures continue to rise, the impact on populations who do not have access to indoor cooling will be exacerbated. Creating passive cooling solutions for outdoor public spaces ensures access to all communities. Areas investigated in this research include outdoor public seating or congregational spaces such as bus stops and railway stations, open spaces around buildings (particularly public buildings or areas with many workers, e.g. museums, business precincts) and parks (playgrounds, picnic areas etc,). Furthermore, placing these cooling systems at street level can be more efficient as the cool media is closer to people (Domínguez & Flor, 2016). With this in mind, the evaporative cooling system will be designed for scalability and versatility, allowing for it to be applied in different contexts.

[17] Temperatures in Western Sydney during heat waves can be up to 6-10°C higher than in eastern zones of the city. As a result the associated energy consumption due to greater cooling can be up to 100% higher (Prasad et al., 2017)

Airflow

As explained above, the third key element of evaporative cooling systems is airflow. Evaporative cooling systems are often paired with ventilation strategies to enhance their efficiency. Precedents have demonstrated this can be done using fans, as in the case of the Spanish Pavillion, or passively via wind driven down draughts or simple cross ventilation (Vallejo, 2018). Whilst airflow isn't required for evaporation, it accelerates the process by replacing saturated air with drier air near the evaporative surface. This increases evaporation. Vallejo (2018) also emphasises that the geometric forms should minimise their resistance to airflow, utilising more aerodynamic forms to aid evaporation.

The Prototype

The above criteria will be integrated into an evaporative cooling system made from the porous BJT glass fines material. A modular, adaptable design will be developed using individual components that will be assembled into a larger whole. The assembly system will evolve with the design development but must be able to be disassembled and reused or recycled. This is in line with the principles of circularity discussed in Chapter 2. As such, glues or grouts will not be used; instead, a mounting system that does not impact the material integrity of the glass fines material or any other components will be utilised. The overall system will be designed and presented in several contexts. A 1:1 prototype will be built of approximately $1m^2$. This can be seen as a prototype, a research archetype, which is used to demonstrate and present the research (Wensveen & Matthews, 2014). This could also be described as a demonstrator that allows for the interfacing of the research with real-world constraints (Thomsen & Tamke, 2009). See Chapter 3 for further details on this type of prototyping.

6.2 Design Development

The design, prototyping, and production of a demonstrator evaporative cooling screen using porous BJT glass fines will examine outcomes that have not been previously investigated in research. This is a clear embodiment of the RtD approach, where the design process generates knowledge. The key areas of investigation include:

1. Connections- investigating how to connect the parts to each other and to a substructure.
2. Tolerances- predicting and dealing with tolerances, particularly as a result of the firing process. Developing strategies to account for tolerances.
3. Serial Production- as there has always been variation in the fired parts and only certain geometries can be predictably fired, investigating and developing consistency in the results through serial production.

Given the constraints of the print bed size, it was necessary for all designs to be made up of modular components that would connect together in some way to make the larger evaporative cooling system. For each design, the water supply method, assembly, and potential for airflow were considered. Harnessing the benefits of a 3D printing production method was also a key consideration, particularly regarding how parametricity could be incorporated and how complex geometries could be utilised to facilitate greater surface area.

This section is divided into three sections: early designs, controlling the form, and ridges. The first section begins with an expansive approach to the geometry development based on a vessel water supply system. Following these results, the next section shifts to a flatter tile typology featuring an irrigated water supply

system. The final section refines the geometry and the fixing system into one that can be predictably fired and assembled into a demonstrator.

6.2.1 Early Designs

Early designs were based on a water vessel supply system, like that shown in the TerraCool project. In this system, water is supplied from the top and flows down to fill each of the vessels in the system. This means that the individual components need to be hollow and have openings that connect to each other to allow water to flow through. Four distinct modular designs were developed, each based on a standard geometric shape: pyramid (Prototype 10.1), cube (Prototype 10.2), cylinder (Prototype 10.3) and arc (Prototype 10.4) (see Figure 6.8). Each design can be arranged in multiple ways, allowing for customisation of the system (see Figure 6.9). Although only one design incorporated high surface area geometries (Prototype 10.3), it was envisioned that the surface textures printed in Sections 5.5.1-5.5.2 could be applied to the other designs should they be taken further. Additionally, while not modelled, each design has potential for parametricity. For instance, by modifying dimensions such as height or width, the size of the openings, the angles of the arcs, or the surface textures.

These designs were a significant venture from the forms printed in the previous chapters, with a dramatic increase in height and a move to hollow vessel typologies. Each prototype was printed using the parameters and method found in Appendix 4.2. Details on each can be found in Appendix 4.6. For Prototype 10.2 and 10.4, the base was printed as a separate part, as it was hypothesised that removing the powder from the internal cavity would be too difficult. Both parts were printed at a slight angle to mitigate swiping, which often occurs on large flat planes. Whilst most parts were excavated with ease, the excavation of prototype 10.3 was extremely time-consuming, taking over 4 hours. The intricacy of the design made it difficult to remove powder from both the inside and outside of the part, and each cell had to be excavated by hand using tools and brushes. Furthermore, the base pieces of Prototype 10.2 experienced some breakages at the corners. The two base pieces were also discovered to be slightly out of tolerance, so they were excluded from the firing process. The final excavated parts ready for firing can be seen in Figure 6.8.

All prototypes were fired according to the schedule shown in Appendix 4.3. The porosity testing in Section 5.7 resulted in a drop in peak temperature of 90-100°C during firing. It was hypothesised that this would lead to a reduction in the slumping of the parts and enable these kinds of shapes to be fired successfully. However, the firing revealed that this was not the case. Prototypes 10.1-10.3 slumped significantly, collapsing in on themselves and causing breakages in the case of 10.2 (see Figures 6.10- 6.13). While this may not have been surprising for Prototype 10.3, which features an unsupported middle section, it was hypothesised that the other two prototypes could more effectively slump into themselves owing to the tapered angles utilised in the design, thereby achieving self-supporting structures akin to the lattices discussed in Chapter 5. However, this assumption may have been overly optimistic. Given that glass begins to soften and slump under its own weight at approximately 550°C, and the prototypes were subjected to a soaking period at 690°C for 100 minutes, the firing outcomes were likely predictable. The concertina effect observed in the firing of Prototype 10.3 was unexpected and holds potential for further aesthetic investigation (see Figure 6.13).

Figure 6.8. *Early designs for evaporative cooling modules pre firing.*
Top to bottom: Prototype 10.1. (pyramidal), Prototype 10.2 (cube), Prototype 10.3 (cylindrical), Prototype 10.4 (arc).

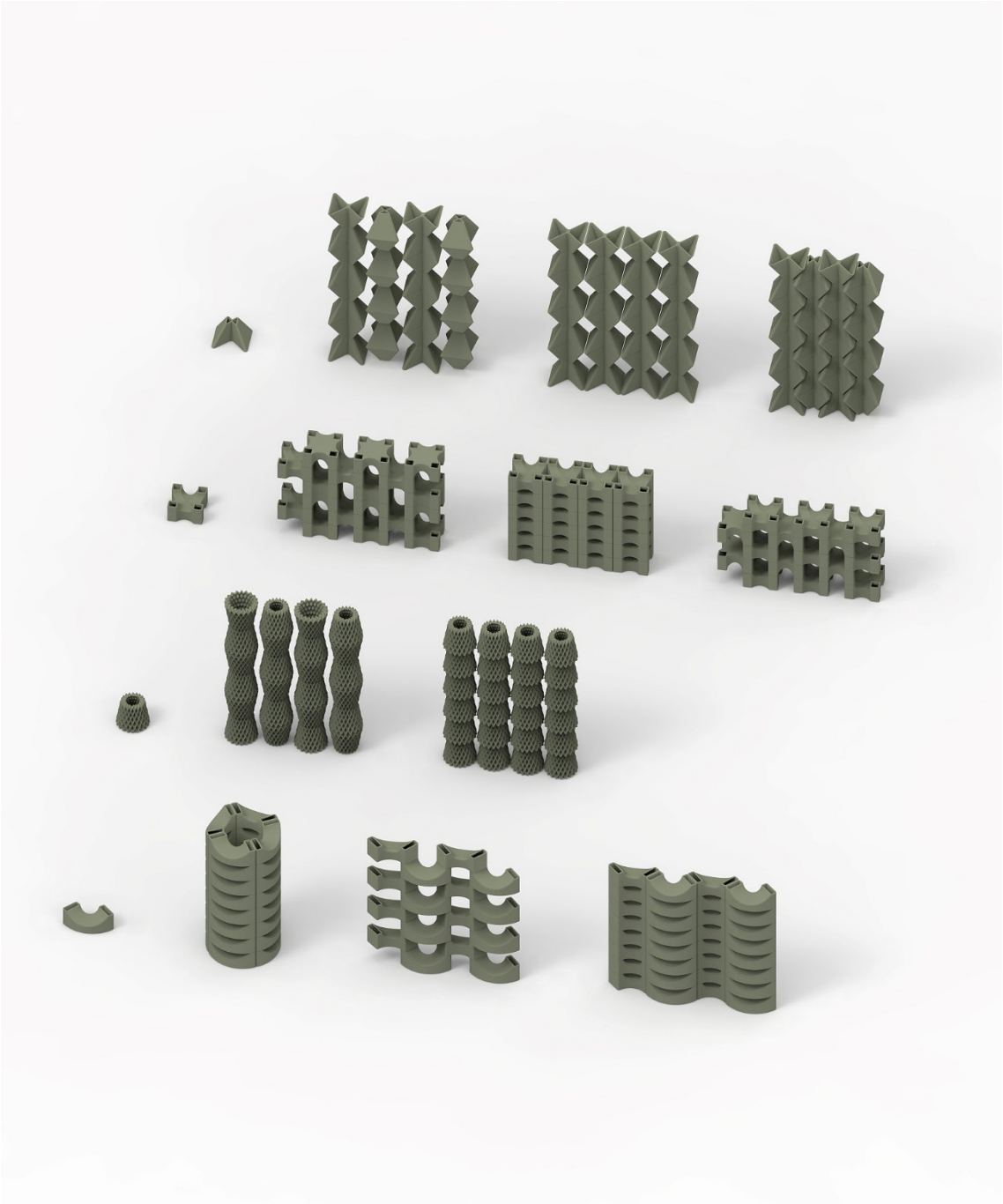

Figure 6.9. *Assembly variations for early concept designs.*
Top to bottom: Prototype 10.1. (pyramidal), Prototype 10.2 (cube), Prototype 10.3 (cylindrical), Prototype 10.4 (arc).

Figure 6.10. *Prototype 10.1 post firing.*
Geometry based on a pyramidal typology experienced significant slumping during the firing process.

Figure 6.11. *Prototype 10.2 post firing.*
Geometry based on a cube typology. Part experienced significant slumping which caused the middle, unsupported section to pull apart and break.

Figure 6.12. *Prototype 10.3 post firing (bottom view).*
Inside of the part also has high surface area to aid evaporation.

Figure 6.13. *Prototype 10.3 post firing (side view).*
Geometry based on cylindrical typology with high surface area. The part slumped significantly in the kiln, causing the surface design to fold together like a concertina.

6.2.1.1 Firing with Talc

As a result, a different approach was taken for the firing of Prototype 10.4. The same firing schedule was used; however, the prototype was filled with talc before placing in the kiln. Talc is an inert powder, widely used in ceramics. This approach is outlined by Ørvik & Stewart (2022) in relation to the firing of Pate de Verre pieces. Filling the glass piece with talc serves as a support material to reduce slumping. Additionally, the talc moves freely, enabling simultaneous shrinkage of the part instead of cracking. Arlotti & Knor (2015) also presented this method in a patent, utilising different inert powders like alumina and zirconia. During the filling process, the part was lightly agitated to allow for the talc to settle, removing as much air as possible. Due to the unconventional shape of Prototype 10.4, the process was time-consuming, and care had to be taken to avoid breakages. In Ørvik & Stewart's (2022) process, they also place the parts in terracotta containers and fill the outside with silica sand. This step was not included in this test as it was hypothesised that the shape of the design did not require this extra support. Furthermore, the firing schedule would need to be updated to include a longer soak to allow for the proper fusing of the part, as the silica sand and terracotta act as insulators. This means that several trial-and-error steps may be needed to find the right schedule.

The results of the firing of Prototype 10.4 can be seen in Figure 6.14-6.15. As hoped, the talc acted as a support structure, mitigating the slumping of the piece and allowing for the overall shape to be maintained. The part was able to shrink, pushing the excess talc out of the openings at the top. The part lifted off the base when fired (see Figure 6.15), perhaps indicating that too much talc was used, or there was not enough room for it to escape as the part shrunk. A small crack which was incurred in the excavation process was exacerbated during the firing and some small cracks could be seen on the inside of the piece, perhaps also a result of too much talc. The edges of the top openings experienced some warping; while the corners largely maintained their shape, the edges bowed and slumped at the centre. A residue of talc remained on the part after firing, and it appeared less fused compared to prototypes 10.1-10.3, indicating a potential need to adjust the firing schedule by extending the soak time. Despite these issues, the overall method produced a very promising result. With refinement, this could provide a way of controlling the slumping of the 3D printed samples, improving the precision and predictability of the firing results.

Despite the potential of this method, a different avenue was pursued in this research. Given the intended scale of application, incorporating an additional production step was not desirable. Furthermore, the lattices in the previous chapter demonstrated that developing geometries capable of being predictably fired without this method is feasible. As a result, this chapter aims to explore other geometries (suited to the intended application) that could be reliably fired by allowing the material to guide decisions about the form rather than attempting to control it by introducing new production steps. This chapter will investigate the balance between material behaviour and the creation of predictable forms.

The major finding from this first set of designs was that a vessel water supply system was not suited to the glass material. This is because the hollow parts required for this type of water supply system are more likely to experience slumping due to their unsupported edges. Unless a method like the talc process is utilised to provide support structure, a different water supply method is considered more suitable for this material and production method. As a result, other water supply systems are investigated in the following sections.

Figure 6.14. *Prototype 10.4 post firing removal of talc.*
Part was filled with talc before firing. The talc acts as a support material to mitigate slumping.

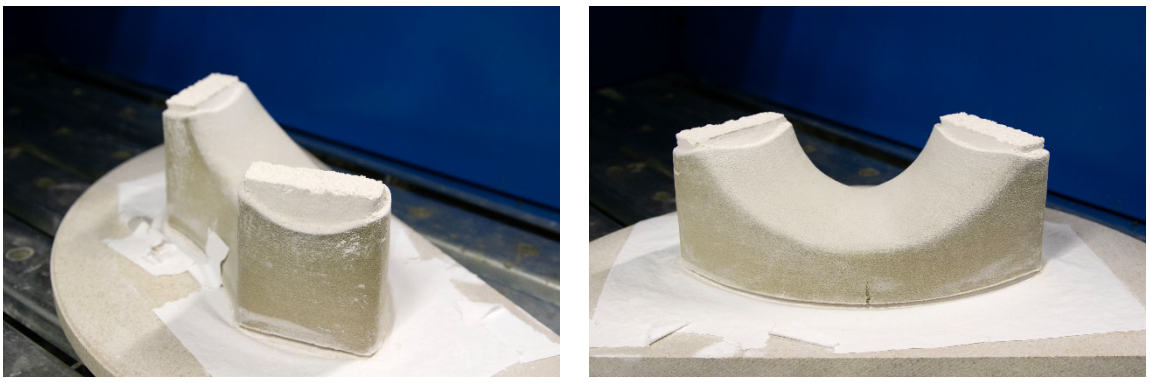

Figure 6.15. *Prototype 10.4 post firing with talc.*
Part was able to shrink, pushing excess talc out of the top openings. The top edges bowed at the centre.

6.2.2 Controlling the form

Based on the previous prototyping, a series of new designs were developed. These designs utilise irrigation or misting systems for the water supply. This means that water is dripped or sprayed onto the porous glass components, and the water evaporates off the surface. In this way, the glass parts are not required to hold water like a vessel; instead, the components act purely as the evaporative medium. Considering this, the design shifted from a brick-like typology to a more tile-like one, where parts are flatter and can be assembled into an open screen that is wetted from the back. By reducing the height of the parts, the impact of gravity in the firing process is lessened, resulting in less slumping. This is a key strategy for starting to control the form and being able to make parts that are more predictable in the firing process.

Other control strategies were also incorporated into this group of designs, including revisiting pyramidal forms. It was reported in the previous chapter, with the success of the lattice forms, that the pyramid typology allows for the material to slump in on itself and become self-supporting. The aim was to investigate this on a larger scale. The other strategy was the incorporation of ribs. These are commonly used in injection moulding to provide strength and avoid sink marks or warping. It was hypothesised that ribs could provide internal support structures to mitigate slumping.

Eight designs featuring pyramidal shapes of varying scales, ribs, and a reduced height were developed (Prototypes 11.01-11.08). Four key designs will be discussed in this section (Prototype 11.02, 11.03, 11.06 and 11.07) (see Figure 6.16). Refer to Appendix 4.7 for details of all prototypes. Each prototype was designed to be assembled into a screen by mounting onto an aluminium frame. The screen designs all have open sections to allow for airflow and encourage evaporation. As with the previous designs, the components continued to be modular and adaptable, allowing for assembly into a range of different overall designs (see Figure 6.17). In contrast to the previous set, where four distinct forms were developed, this set of prototypes was created through an iterative process in which the insights gained from one prototype informed the design of the subsequent.

Prototype 11.02 incorporated high surface area through complex, open structures. The design consisted of four irregular, curved pyramidal shapes with a slight overhang at the peak. An internal rib at the centre of the peak was included to maintain the structure and prevent slumping. Prototype 11.03 was a simplified curved pyramid form supported by internal ribbing. This was designed to create negative space between each component rather than within the components themselves. This concept was carried through to Prototype 11.06, which was based on a trapezoidal prism shape with surface ridges for higher surface area. Internal ribbing in the form of a series of slats was also tested. Prototype 11.07 was based on the ridged surface texture, developing it into the overall form. Opportunities for parametricity were digitally explored for prototypes 11.03 and 11.06 (see Appendix 4.1). This primarily focused on adjusting the placement of the 'peak' in the designs but could also be expanded to include modifications to the overall shape, height, and surface treatments.

Each prototype was printed using the parameters and method found in Appendix 4.2. Largely, the prototypes were excavated with ease and minimal breakages. However, one notable exception was Prototype 11.06, in which the small gaps between the ribs required considerable time and force to remove the powder, which caused a crack in the side of the piece. Fortunately, the crack was repaired using a slurry mixture of the glass fines and binder to glue the piece back together before firing. The final printed pieces that are ready for firing can be seen in Figure 6.16.

Figure 6.16 *Controlling the form prototypes pre firing.*
Top to bottom: Prototype 11.02, Prototype 11.03, Prototype 11.06 and Prototype 11.07.

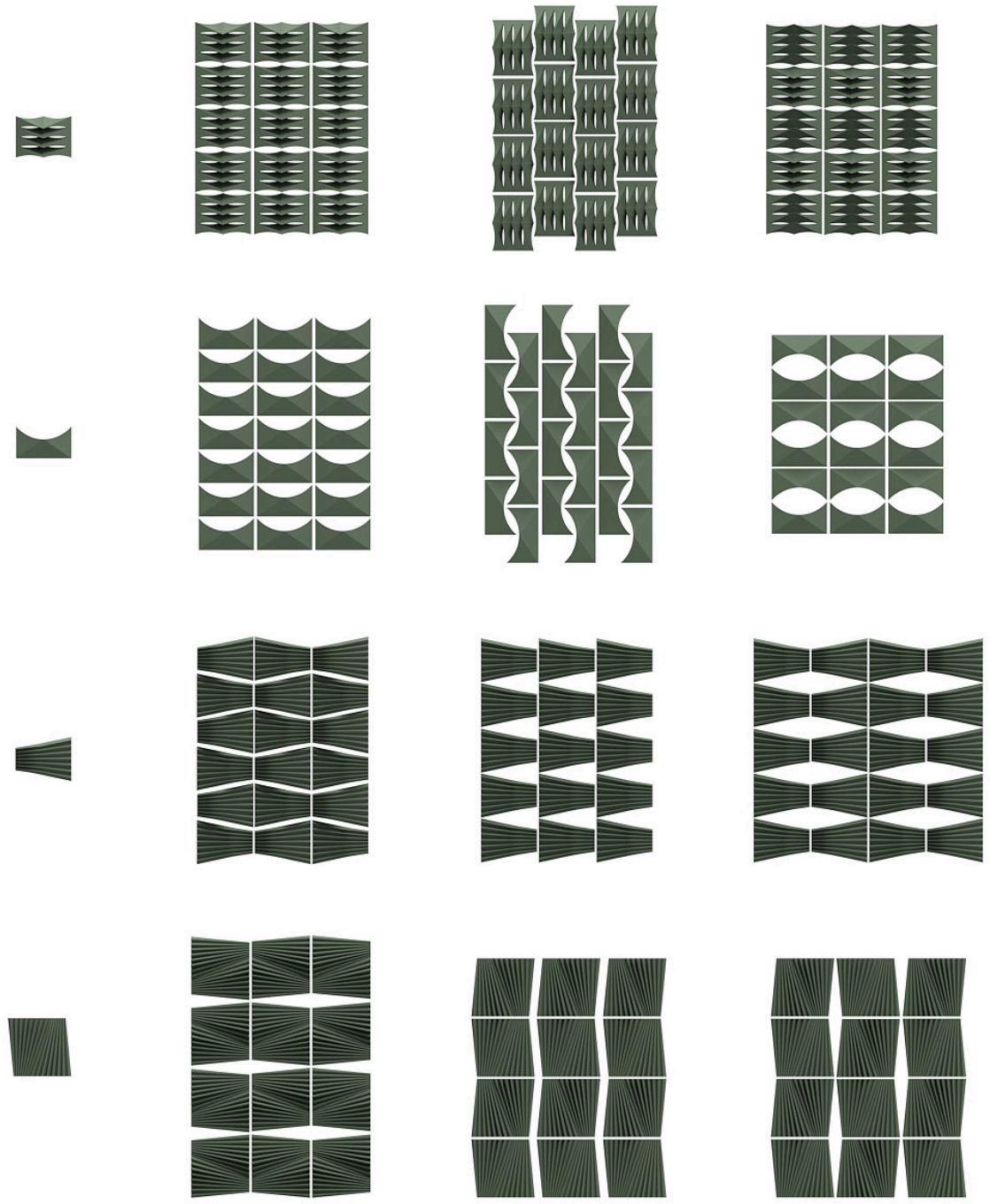

Figure 6.17. *Assembly variations for controlling the form prototypes.*
Top to bottom: Prototype 11.02, Prototype 11.03, Prototype 11.06 and Prototype 11.07.

All prototypes were fired according to the firing schedule in Appendix 4.3. There was varying level of success across the different designs. Prototype 11.02 held its overall shape during firing and the central rib allowed for the peak to stay upright (see Figure 6.18). However, the sides slumped slightly, becoming curved. This could be improved with further ribbing and adjustments to the scale of the pyramidal form. However, it was noted that the complexity of the design made it less suitable for large-scale applications. Similarly to the lattice forms in the previous chapter, when multiple components are assembled over a large scale, the intricate features get lost, reading more like a mesh and becoming visually overbearing.

For this reason, the overall form was simplified for Prototype 11.03, which, as stated above, was designed to create negative space between each component rather than incorporating openings in the components themselves. This also has potential benefits in terms of designing a water supply system that can be mounted on the back and remain hidden. Despite the pyramidal shape and the internal ribbing placed in line with the edge of the pyramid, Prototype 11.03 experienced slumping (see Figure 6.19). The ribs were effective in holding up the edges of the shape, but sagging occurred on the unsupported surfaces between the ribs. The design was adjusted for Prototype 11.06 to a tapered trapezoidal prism shape that came to a peak at an edge rather than a point. This design also incorporated a series of internal slats to mitigate slumping. However, during firing, the slat-type ribs largely collapsed. This is likely because the ribs themselves became unsupported walls with no cross-bracing (see Figure 6.20). As a result, it can be seen that the ribs are likely to be more successful when placed along the edges of a form and should include some form of cross-bracing to work more effectively. Despite this, the ridged surface textures in Prototype 11.06 were effective. This reflects a promising avenue for taking advantage of the pyramidal structure in a different way.

Prototype 11.07 developed this ridge typology further. In this prototype, the whole component is designed around a zig-zagged cross-section, where the peaks can slump into each other and become self-supporting (see Figure 6.21 and Figure 6.22). The design incorporates a tapering effect where the ridges become wider as the height of the piece increases. During the firing process, this prototype largely retained its shape. As hoped, the pyramidal peaks became self-supporting and did not collapse or warp. However, some cracking down the centre was observed. As the material shrank, the change in the direction of the tapering elements appears to have caused them to pull apart. Ways of mitigating or designing for this should be investigated.

Despite the mixed results in this set of prototypes, some key findings emerged. Firstly, the small successes of the central ribs used in Prototype 11.02 and Prototype 11.03 suggest that with further investigation, they could be a useful tool to mitigate slumping in some areas. To achieve more predictable results, it's important to determine the amount of cross-bracing required and to examine at what height the material can maintain stability. There is also the potential to use ribs to support the edges of a shape while allowing the material to sag in other areas. This technique could be further developed to create a compelling aesthetic. Secondly, it is clear that the scale of the forms and features is a key variable in slumping. While the pyramidal structure has been shown to be effective in Prototype 11.02, slumping occurs when the form is scaled up (as observed in Prototype 11.03). This aligns with the results in Section 5.5.5 regarding the change in scale of the lattices. Additional ribbing is unlikely to mitigate this. As a result, there is a limit to the height and angle at which the pyramidal structure can be predictably fired. In line with this, the ridges used on the surface of Prototype 11.06 reflect a way of taking advantage of the pyramidal structure at a different scale and form. As a result, Prototype 11.07 was designed with an entirely ridged cross-section. The minimal slumping that occurred in this prototype represents a promising avenue for creating a form that can be more predictably fired. This ridge forms will be explored further in the next section.

Figure 6.18. *Prototype 11.02 post firing.*
The part largely held its shape, although some slumping can be seen in the way the edges have curved.

Figure 6.19. *Prototype 11.03 post firing.*
Internal ribs along the edges allowed for the overall shape to be maintained but unsupported walls experienced some sagging.

Figure 6.20. *Prototype 11.06 post firing.*
Internal slat rib design collapsed during firing. However, the surface ridges were successful.

Figure 6.21. *Prototype 11.07 post firing (side view).*
The design was based on a zig-zagged cross-section which successfully resulted in the peaks slumping into each other and becoming self-supporting.

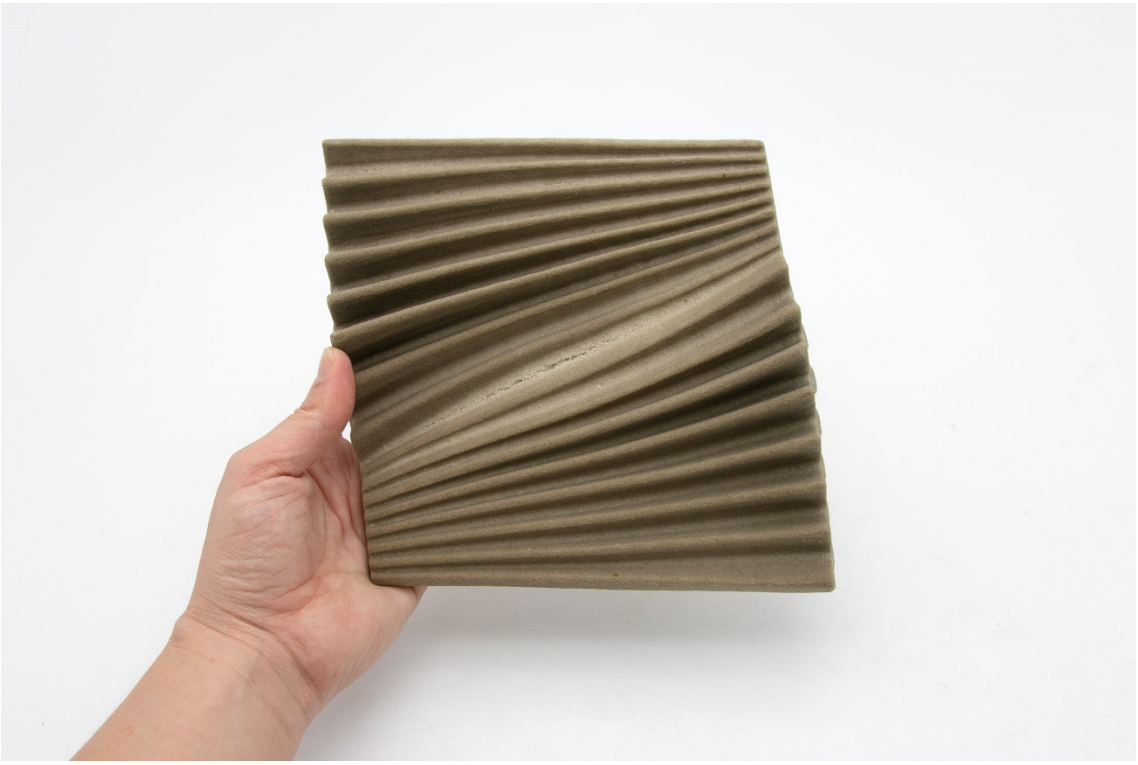

Figure 6.22. *Prototype 11.07 post firing.*
As the material shrunk, the change in the direction of the tapering ridges caused them to pull away from each other and cause cracking.

6.2.3 Ridges

Building on the findings of the previous section, the ridge typology was developed further. The aim was to advance the concept of the zig-zagged cross-section, where the ridges slumped into one another, by transitioning away from modular, adaptable components to a design in which the ridges flowed seamlessly across multiple tiles. In this way, the pieces resemble a jigsaw puzzle that fits together, where each is uniquely customised to integrate into a larger overall design. This type of design is made possible by the customisation capabilities of 3D printing. The continuity or flow also evokes the movement of water, central to evaporative cooling systems. Furthermore, the ridges provide high surface area to allow for maximum evaporation whilst allowing for airflow across the components, both key requirements of evaporative systems.

Early screen designs based on the ridge typology can be seen in Figure 6.23. All designs incorporated a variation in the height and width of the ridges across the tiles. Both organic, curved forms and more geometric forms were explored in the screen design. Significant attention was given to dividing the screen into individual tiles and to understanding the role of negative space within the design. Segmenting organic patterns into tiles influenced the overall aesthetic, revealing that a cohesive design could not simply be created and then subdivided. Rather, the shape of each tile needed to be carefully designed to integrate seamlessly into the larger composition. The prototyping in this phase can be divided into sections, each focusing on different elements. Firstly, the emphasis was on understanding the geometric limitations of the ridges regarding the width and height that would allow for slumping to be predicted. Then, ensuring a seamless connection between tiles was explored. This was followed by the prototyping of the fixing system and the assembly of the overall screen. Additionally, some experimentation with increasing airflow was conducted. Throughout this prototyping, further knowledge was also generated about the printing process.

The findings of each prototype were fed into the overall screen design, which changed and developed iteratively over the course of the experimentation. As the aim of this design is to create individual modules that can be aligned seamlessly, many of the prototypes are made of multiple modules. All prototypes in this section were printed and fired using the parameters and method found in Appendix 4.2. During this phase of experimentation, fourteen prototypes were developed (Prototypes 12.01-12.14); however, this section will focus on the ten key prototypes that predominantly influenced the design process (Prototypes 12.01, 12.04, 12.05, 12.07, 12.09-12.14) Further details on all prototypes can be found in Appendix 4.8 and Appendix 4.9.

6.2.3.1 Predicting slumping – height and width of the ridges

Prototypes 12.01, 12.04 and 12.07 allowed for the geometric parameters of the ridges to be established. While previous testing has revealed that this typology and pyramidal design, in general, have potential due to their self-supporting nature, it has also been found that the scale of these geometries affects their success. As a result, significant testing is needed to understand the relationship between the parameters of this geometry and its slumping in the kiln.

Prototype 12.01 consisted of three adjacent components with eight narrow ridges. Each component varied in height across the x-axis (by approximately 20mm), lower at the sides and higher in the middle, creating a curved effect. These ridges also varied in height across the three components.

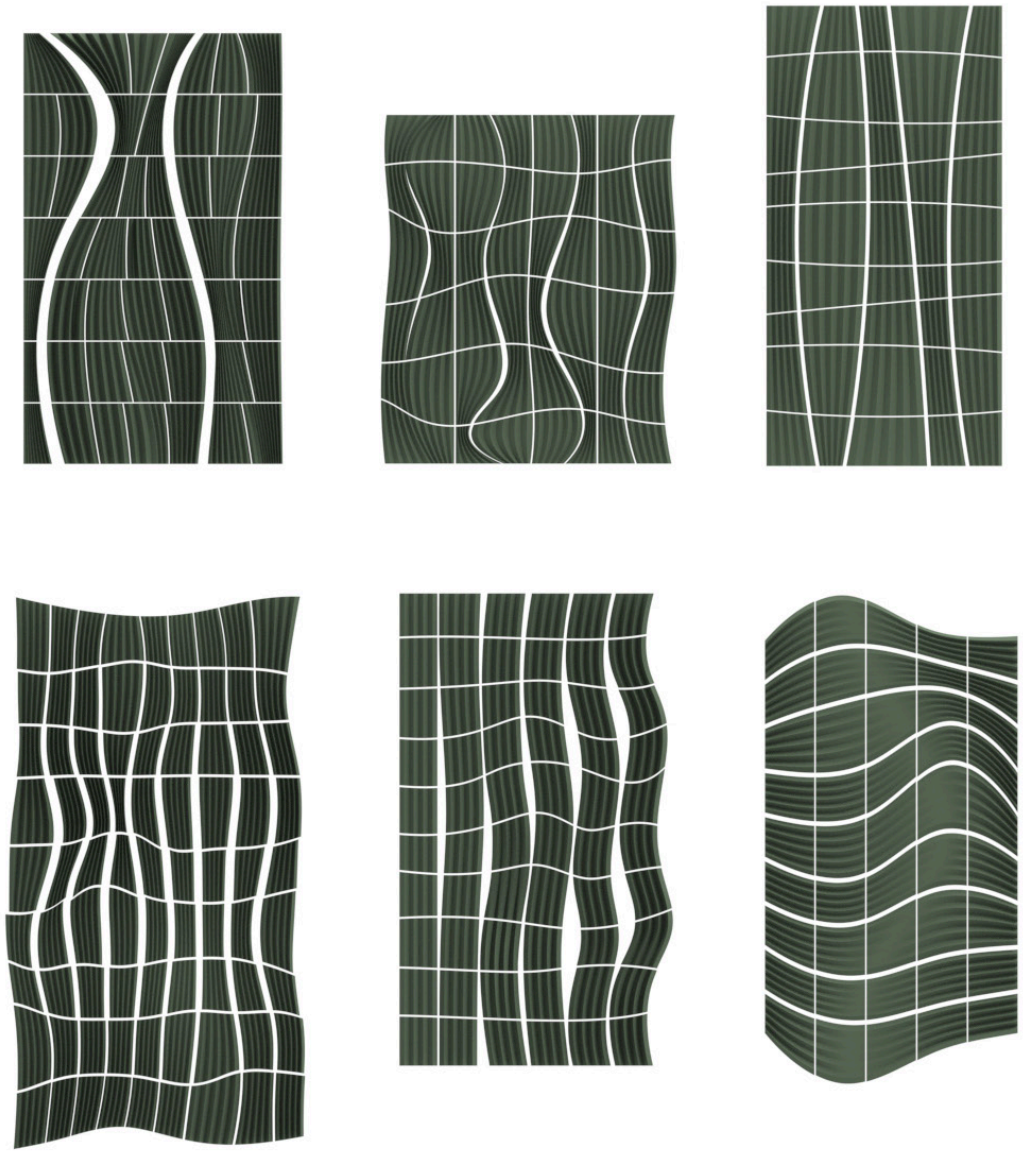

Figure 6.23. *Initial evaporative screen designs based on the ridge design typology.*
Several iterations were developed, with particular attention given to the segmentation of the screen into individual tiles and how negative space could be harnessed in the design

They were smaller in the top and bottom components and higher in the middle component, creating a doubly curved effect (see Figure 6.24). The height variation was significant, ranging from just 11mm in height in the top component to almost 75mm at the centre of the middle component. During the firing process, the top and bottom pieces experienced some slumping but managed to largely hold their shape, particularly where the ridges were less high. On the other hand, the middle piece exhibited significant warping, with the ridges slumping irregularly to resemble an open book. The combination of the narrowness of the ridges and their height resulted in a shape that was no longer self-supporting when fired; the weight of the material, coupled with the force of gravity, caused the piece to slump.

It is evident that it is not solely the height of the ridges that affects the slumping, but also the width and consequently, the angle of the pyramidal structure. As a result, for Prototype 12.04, both the number of ridges and height were reduced whilst the overall dimensions of each component were kept roughly the same as the middle and bottom pieces in Prototype 12.01. This drastically decreased the base angles of each ridge, encouraging the sides to slump into each other rather than fold over themselves. Three adjacent components were designed with a maximum height of approximately 65mm and four ridges. The height was gradually decreased across the three tiles to approximately 20mm. During firing, the overall shape of the tiles largely remained the same, allowing the ridges to line up and flow across the pieces. However, the height of the ridges significantly impacted the slumping of the piece. Only slight slumping occurred on the piece with the lowest ridges, while significant slumping was observed on the piece with the highest ridges. Additionally, the slumping gradually increased on the middle piece as the height of the ridges rose. Between approximately 25 mm and 55 mm, the ridges appeared most effective in maintaining their shape.

This reduction in height informed Prototype 12.07. Additionally, it became clear that the tiles were more visually appealing with five ridges rather than four. Five ridges also have the added benefit of greater surface area, which is important for evaporative cooling systems. In this design, the ridges were also rotated to flow horizontally, aligning with the ongoing evolution of the overall screen design. Three adjacent tiles were designed with five ridges that gradually increased in height and width. The height ranged approximately from 20mm to 40mm. The reduction in height from Prototype 12.04 was to accommodate the addition of a fifth ridge while maintaining a similar angle of the ridge walls. A wavy surface texture was also added to the forms to provide even greater surface area. During firing, minimal slumping occurred, with all three components largely maintaining their shape. There was minor bowing on the outer edges, but this remained at an acceptable level and did not affect the overall footprint of the shape. Furthermore, while the surface texture was successfully printed and fired, the aesthetic did not cohesively work with the horizontal ridges. Instead, it somewhat detracted from the crisp flow of lines. Given that BJT printing already produced a somewhat textured surface, it was decided that the original surface should be utilised.

These geometric parameters were further validated in Prototype 12.09 (which will be further discussed in the next section). Three adjacent tiles with five ridges were designed and printed (see Figure 6.27). A maximum height of approximately 40mm was used, which faded out to nothing in the middle tile. The idea was that the water from the evaporative cooling system would run along the ridges and then drip to the next layer of tiles below. This concept can be seen in the designs in Figure 6.33. As the ridges faded to nothing on the middle piece, 10mm stilts were also added to the base of each ridge to provide additional thickness to the tiles. In the firing process, minimal slumping occurred with the ridges maintaining their shape (see Figure 6.28). The addition of the 10mm stilts did not impact the slumping.

Figure 6.24. *Prototypes 12.01, 12.04 and 12.07; pre-firing (left), post-firing (right).*
Top to bottom: Prototype 12.01. Prototype 12.04, Prototype 12.07. Exploring the geometric parameters of the ridge design typology.

Although this prototype was successful, it was decided that the design would not include ridges that faded out to nothing, as they were less visually appealing than expected and not functionally required.

Overall, these prototypes validated the ridge design concept by determining the geometric parameters for producing components with predictable slumping. Five ridges with a maximum height of approximately 40mm and an overall width of approximately 200mm were found to slump and shrink in a way that retained a degree of geometric accuracy and could, therefore, be used for serial production. These prototypes also demonstrated that the tiles could be aligned to form a continuous ridge pattern that flowed across multiple components.

6.2.3.2 Connecting the tiles – chamfer

Prototypes 12.04, 12.07, and 12.09 indicated that the adjoining edges between tiles required further refinement. During the firing process, these edges tended to pull inwards, resulting in a noticeable gap at the peak of the ridges, despite the bottom edges of the tiles meeting. To address this issue, it was hypothesised that components could be printed with chamfered edges designed to counteract this shrinkage. This hypothesis was initially tested on the middle piece of Prototype 12.04. The angle of shrinkage of the original middle tile was measured to be approximately 5 degrees; therefore, the CAD file was modified to incorporate a 10-degree tapered angle. The tile was reprinted with the modified geometry, resulting in Prototype 12.05. In this prototype, the chamfering of the adjoining edges successfully compensated for the shrinkage, leading to the edges of the tile shrinking inwards and forming an almost perpendicular edge (see Figure 6.*25* and Figure 6.*26*).

As such, this approach was applied to Prototypes 12.07 and 12.09. In Prototype 12.07, a 10-degree chamfer was applied to each adjoining edge. However, upon firing, the chamfered edge was found to be too angled, with the edges of the piece pulling inwards less than in the previous prototype. This was particularly apparent on the tile with the lowest ridges, but less apparent when the ridges were higher. It was, therefore, hypothesised that the angle of the chamfer is contingent upon the height of the ridge. As a result, Prototype 12.09 looked at adjusting the angle of the chamfered edges based on ridge height. The chamfer angle was lowered to 8 degrees for ridges measuring 40mm in height, while a 4-degree chamfer was applied to ridges approximately 15mm high (see Figure 6.27). The change in the chamfer angle had varied results; 4 of the 6 edges successfully shrank to an almost perpendicular angle, whilst 2 of the edges continued to shrink inwards on an angle (see Figure 6.28). The reason for this is unclear, as there did not appear to be any correlation between the height of the ridges and the way they shrank.

Despite this variation, adding a chamfer overcame the visual impact of the peak of the ridges pulling inward and created a more seamless connection between the tiles. Further investigation would undoubtedly refine this method; however, for the scale of this demonstrator, these preliminary studies provide a suitable solution. Whilst these prototypes were being conducted, the overall screen design continued to be developed (see Figure 6.29). These iterations were informed by a greater understanding of the geometric limitations of the design and the production system.

Figure 6.25. *Prototype 12.05 pre firing with tapered edges to offset for shrinkage.*
A 10-degree chamfer was added to the edge of the component.

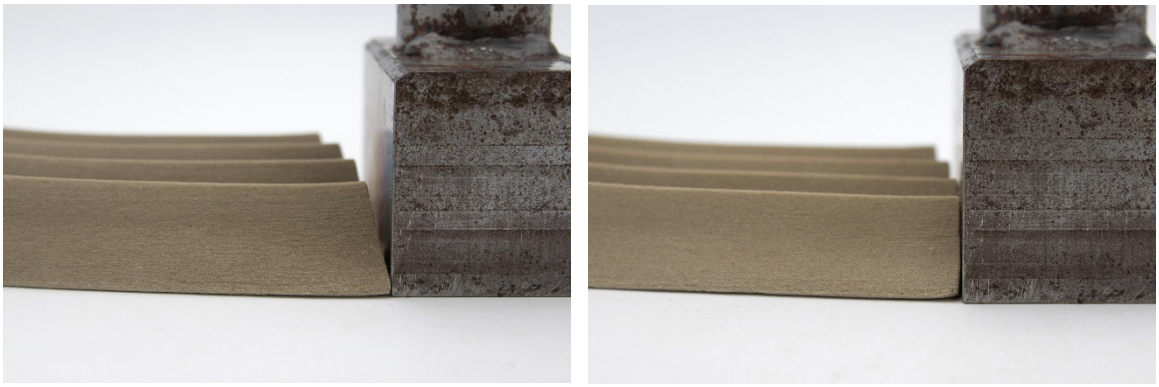

Figure 6.26. *Comparison of fired results of original component from Prototype 12.04 and redesign of Prototype 12.05 with tapered edges.*
The 10-degree chamfer resulted in an almost perpendicular edge after firing.

Figure 6.27. *Prototype 12.09 pre firing.*
Prototype 12.09 added a chamfered edge based on the height of the ridges.

Figure 6.28. *Prototype 12.09 post firing.*
The varied chamfered edge had mixed results. The three components aligned well and maintained their shape in the firing process.

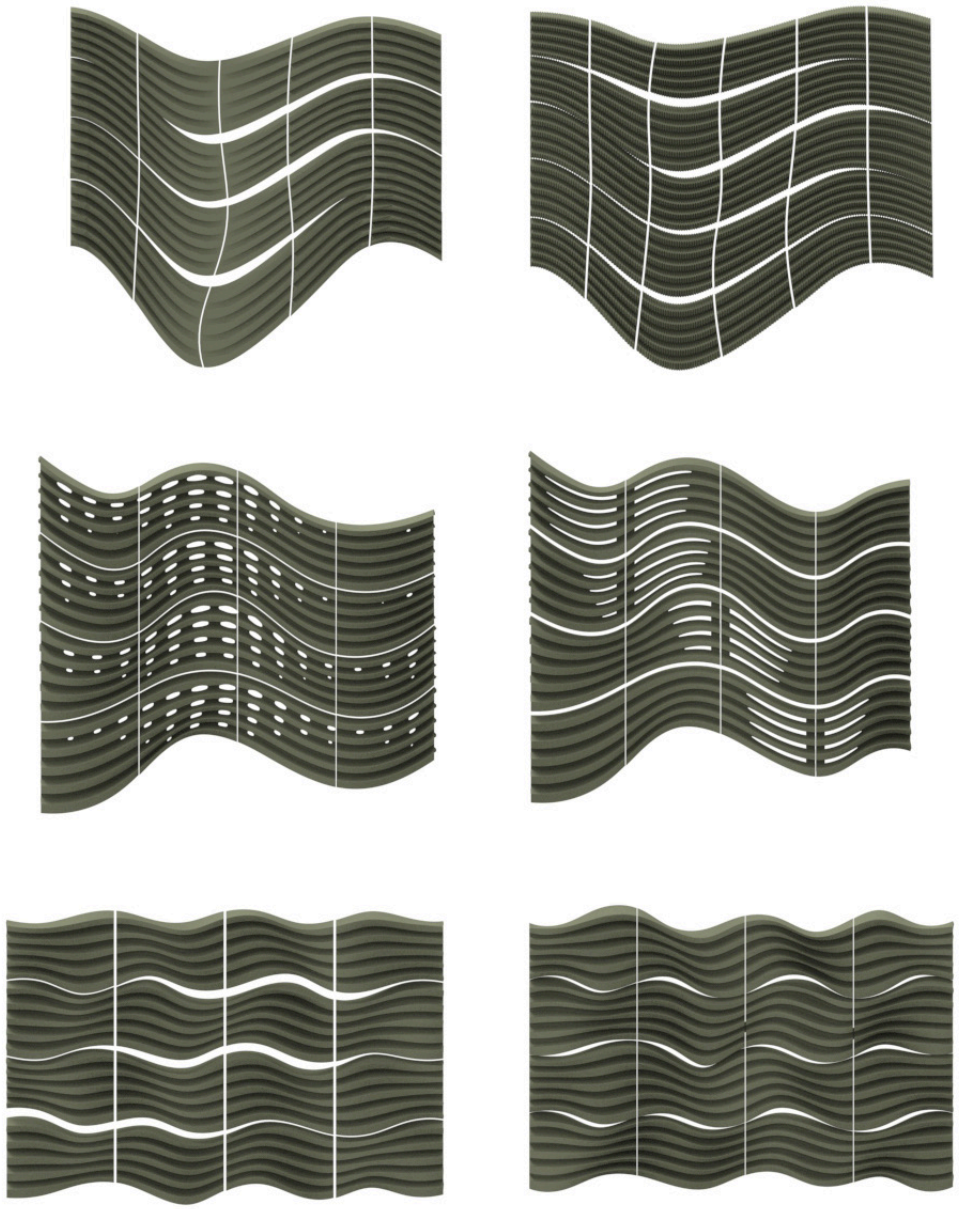

Figure 6.29. *Digital rendering showing the iterative design evolution of the evaporative cooling screen.* Continuing to refine the design based on the ridged design typology.

6.2.3.3 Airflow

As explained previously, airflow is a key component of an evaporative cooling system. While most prototypes in this section have accounted for airflow around each tile, two prototypes were developed to allow for airflow through each tile. Prototypes 12.12 and 12.13 modified the ridge design to include openings at the valley of each ridge (see Figure 6.30 and Figure 6.31). This meant that a gap of up to 8 mm was created between each ridge to allow for the addition of air vents. Corresponding overall screen designs were developed and digitally rendered in CAD (see the middle two designs in Figure 6.29).

Prototype 12.12 incorporated air vents that gradually widened or narrowed to create a fading in or out effect. This design aligned with the organic, wave-like aesthetic of the overall screen. Two adjacent tiles were printed and excavated successfully (see Figure 6.30). However, the incorporation of the vents reduced the number of contact points in the valleys between the ridges, significantly increasing the fragility of the tiles. While the overall shape was maintained during firing, some shrinkage, especially along the adjacent edges, occurred due to the vents, resulting in a concave shrinkage that affected alignment (see Figure 6.32). The curvature of the outside edges on both parts was also slightly warped. While this design is promising, significantly more prototyping is needed to refine this concept.

As a result, a more uniform and potentially predictable approach was tested. Prototype 12.13 incorporated evenly spaced slot-shaped vents. Overall screen designs were proposed in line with this, with one experimenting with a gradual decrease in size of the slots (see Figure 6.29). This design involved leaving a 6mm flat section between each of the ridges. The part was printed and excavated with no issues (see Figure 6.31). During the firing process, minimal slumping occurred. The ridges all maintained their shape, even the narrow, tall ones (see Figure 6.32). However, the aesthetic of the slotted vents is incongruous with the overall design. The organic, flowing shapes contrast sharply with the uniformity of the slots. This discrepancy becomes more apparent on a larger scale, as shown in the renderings, making the overall aesthetic seem disjointed.

While several other versions of the air vents could be considered, it was decided that the airflow would continue to circulate around each tile rather than through them. Given that each tile is approximately 200mm in length and that the ridges remain aerodynamic when the wind blows across them, including air vents is not necessarily required. This aspect could be explored and refined in the future based on the specific requirements of a site. Negative space should be intentionally incorporated into the overall screen design to allow for airflow and a cohesive subdivision of the tiles.

6.2.4 Fixing system and assembly

During this design stage, a fixing system was also being considered. The decision was made that the tiles would be mounted on an aluminium frame, which could function as either a free-standing screen or be wall-mounted. This approach aligns with how ceramic façade panels or tiles are often mounted onto buildings. After exploring several ways to divide the screen into individual tiles, it was concluded that maintaining some uniformity was essential. This would facilitate the use of a more standard mounting system instead of a fully custom solution. As a result, the screen was divided into uniform vertical strips, with each tile having the same length and straight, seamlessly fitting edges. Curvature was applied along the horizontal axis.

Figure 6.30. *Prototype 12.12 pre-firing.*
Prototype 12.12 incoporates an organic air vent design which fades out gradually.

Figure 6.31. *Prototype 12.13 pre-firing; left (front view), right (bottom view).*
Prototype 12.13 incorporates a uniform slot air vent design.

Figure 6.32. *Prototype 12.13 post firing.*
Prototype 12.13 with uniform slot shaped air vents held its shape during the firing process.

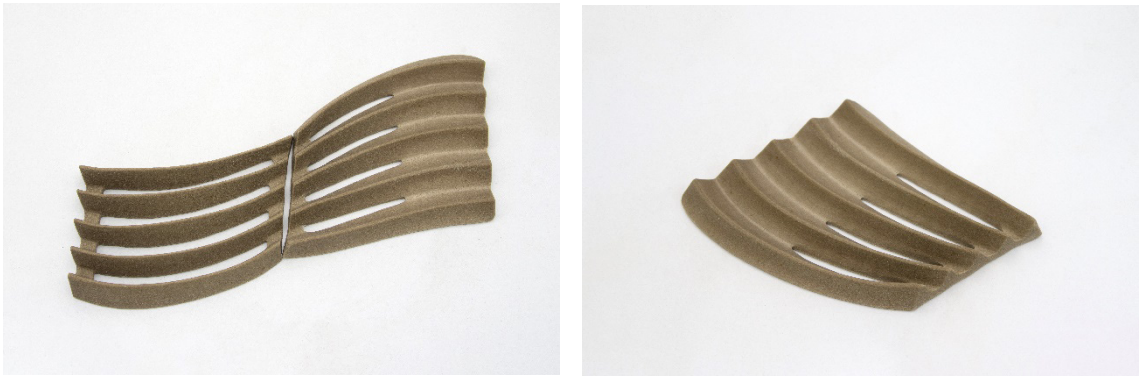

Figure 6.33. *Prototype 12.12 post firing.*
Prototype 12.12 was made up of two components with an organic air vent design which gradually fades out. These air vents caused some warpage during the firing process.

To mount the tiles to the frame, a series of prototypes were developed based on using an L-shaped bolt as the primary fixing component. The idea was that this could be easily hooked into the tile and bolted onto an aluminium extrusion. The L-shaped bolt could also be angled slightly to fit comfortably in the ridges, accounting for the unique shape of each tile and the potential tolerances required when using recycled materials and firing glass. Four prototypes were iteratively developed to determine the best method for securely attaching the bolt to the tile. These focused on how the fixing design would be integrated into the 3D printed part. Additionally, two more prototypes examined how this system would connect to the aluminium frame.

The first prototype to test this was Prototype 12.09 (also discussed in the previous sections). In this prototype, the ends of each of the tiles were capped, and a hole was placed in the centre of two of the ridges. The 10mm stilts that had been added to the ridges allowed for extra space for this fixing point (see Figure 6.34a). While this design was printed and excavated without issues, during the firing process, the holes partially collapsed and became elliptical. This hindered their use on some of the tiles. The visibility of the fixings was also undesirable in this prototype. As a result, Prototype 12.10 and Prototype 12.11 moved away from the holes, to use a tab or ledge that the L-shaped bolt could be hooked onto (see Figure 6.34b-c). Both prototypes incorporated two ledge pieces at either end to allow for four fixing points. Prototype 12.10 also removed the capped ends, as these had initially only been added to allow for the hole fixing. Through these two prototypes, it was found that the ledge system was feasible as the ridges held their shape during firing, leaving space for the bolt to be inserted. It also appeared that the capped ends provided some stability during firing and that the ledges should be at least 12mm in width, as those in Prototype 12.11 were too shallow.

These findings were integrated into the final design, seen in Prototype 12.14 (see Figure 6.34d). The dimensions were adjusted, and a ledge was added to every ridge, rather than just at two points. This provides more flexibility and space to make adjustments if needed during the mounting process. Furthermore, this design utilises undercuts to secure the bolt, which could not be manufactured using conventional methods such as compression moulding. While this is a seemingly simple geometry, it is a form that could not be produced without 3D printing.

Alongside these prototypes, a system was developed for mounting the tiles with the L-shape bolts to the aluminium frame. Two prototypes were constructed to test the entire assembly system, exploring what additional components were necessary to ensure secure fastening to an aluminium structure. The first design utilised standard U channels and L-shaped brackets (see Figure 6.35 and Figure 6.36). Four L-shaped bolts were used to attach the tile to the bracket and the bracket to the aluminium channel. Rubber spacers provided padding between the glass material and the bracket. They, along with several washers, were also necessary to securely hold the parts together as the dimensional tolerances were still being adjusted.

As can be seen in Figure 6.36, there were some issues with this assembly system. Firstly, the tolerances mentioned above were an issue that affected the stability of the tile. This was exacerbated by the way the L-shaped bolt became angled when tightened, pulling out of the ledge in the tile. The aluminium channel was also not as strong as anticipated, with even just the single frame allowing for movement. This is a concern, as the glass material (like all glass and ceramics) is brittle and shear force or wobbling of the frame could cause breakages.

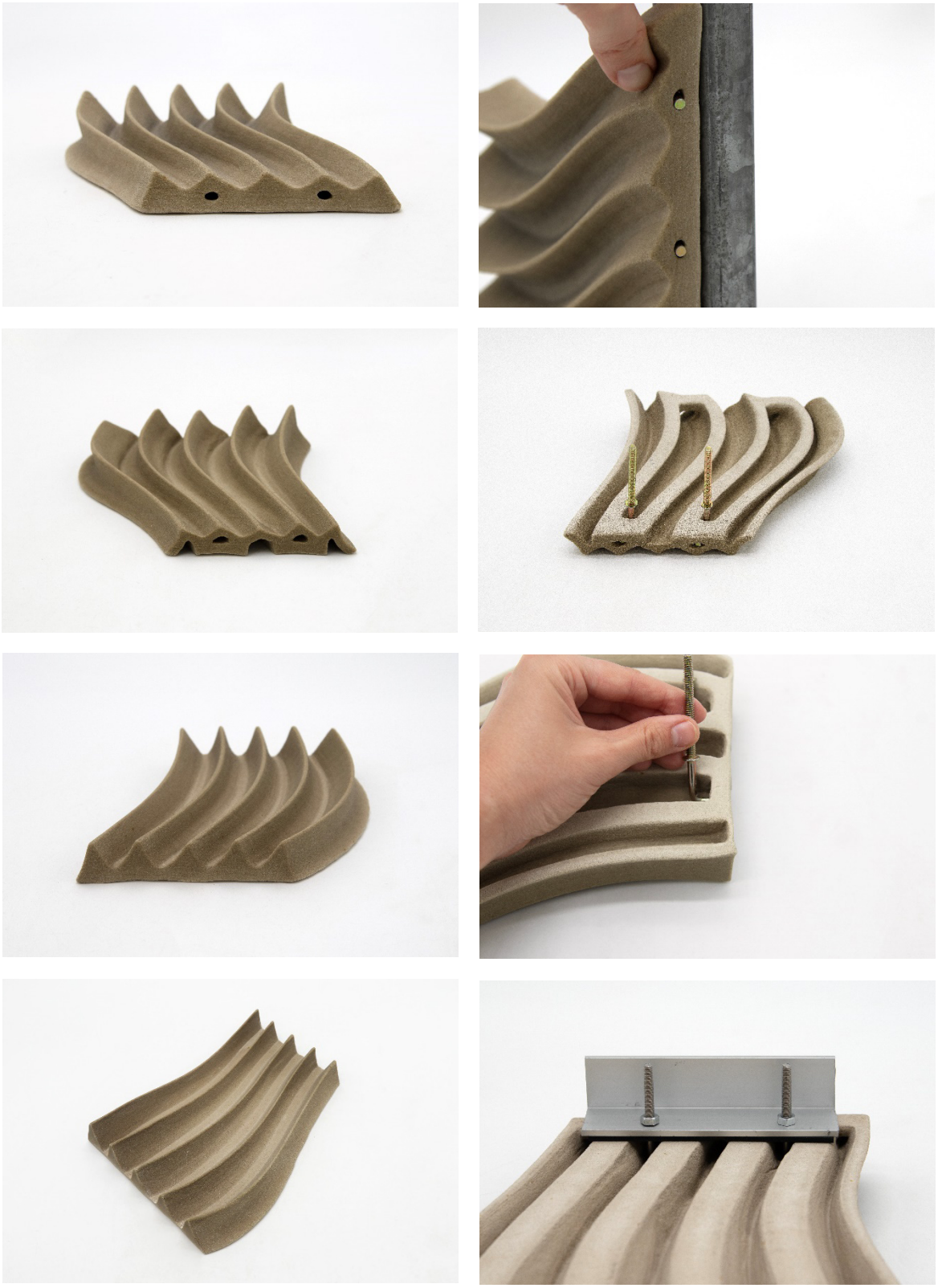

Figure 6.34. *Prototyping of fixing system using L-shaped bolts.*
Top row to bottom row; (a) Prototype 12.09, (b) Prototype 12.10, (c) Prototype 12.11, (d) Prototype 12.14.

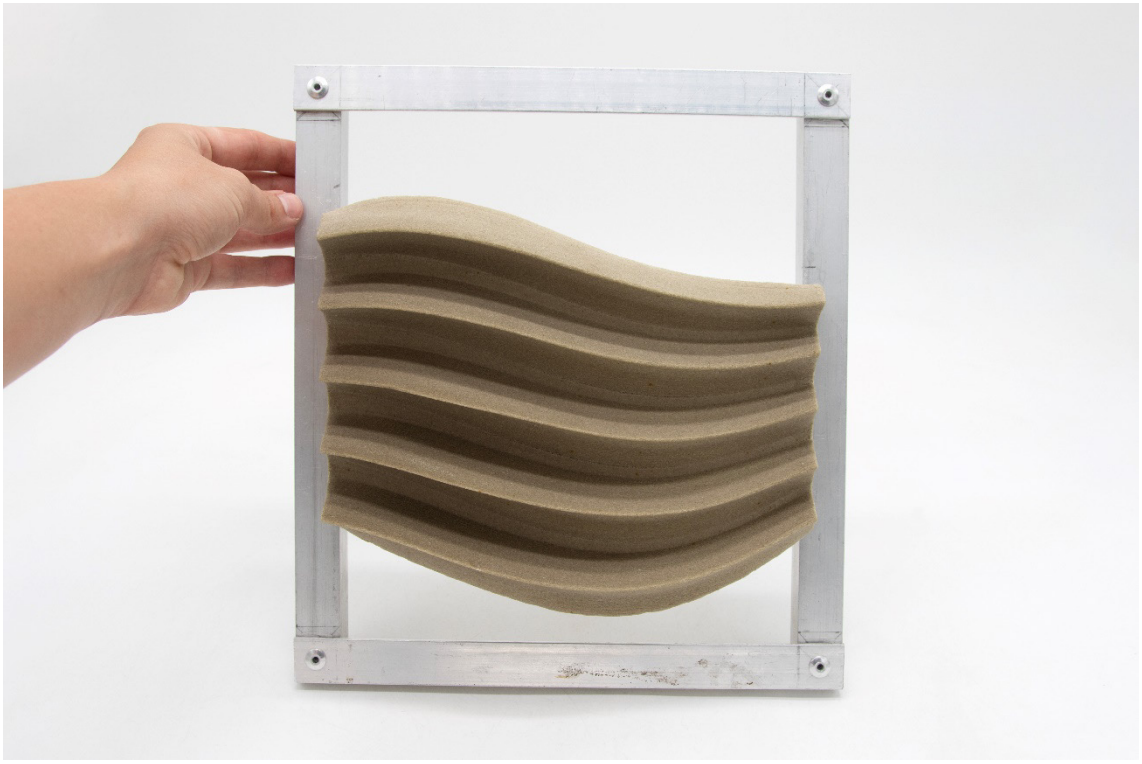

Figure 6.35. *Assembly system Prototype 13.1 (front view).*
Tile fixed to aluminium U channel, using brackets and L-shaped bolts.

Figure 6.36. *Assembly system Prototype 13.1 (back view and closeup).*
Prototype 13.1 revealed issues with assembly system design. Rubber spacers and washers were needed to overcome issues with dimensional tolerances. The L-shaped bolts became angled when tightened, pulling out of the ledge in the tile.

Given the size of the tiles, it was undesirable to use a bigger channel as this may have become visually overbearing. This method of assembly also meant that a closed square channel could not be used, as there would be no way to access the bolt to tighten the bracket to the channel. Furthermore, to attach the bracket to the channel, holes had to be drilled into the side. Since each tile is unique, this likely means that holes must be measured and drilled specifically for each tile, making the process time-consuming.

As a result, the assembly system was redesigned with two key new elements. A T-slot aluminium extrusion system and a custom 3D printed bracket. T-slot aluminium extrusions are flexible framing systems that have slots running down their faces. This slot enables pieces to be assembled in various configurations, and secure anchor points to be adjusted using T-nuts that slide into the slots. This system eliminates the need for drilling to secure the bracket to the aluminium frame. Instead, T-nuts can be utilised and adjusted for each individual tile. T-slot channels of the same dimensions used in the previous prototype are also significantly stronger, allowing for the assembly of a sturdy frame with flexural stiffness. The custom 3D printed bracket was designed to specifically meet the dimensions of the tiles and extrusions and to provide support for the L-shape bolt so that when tightened it could not become angled and pull out of the opening in the tile. A slot was used instead of a hole so that the bracket could be adjusted easily. The prototype of this system can be seen in Figure 6.37 and Figure 6.38. These changes led to a secure and adjustable assembly system. Multiple tiles were mounted successfully using this system, allowing for the anchor points to be easily moved to account for the differing placement of the ridges. Whilst these brackets were adequate, increasing the material thickness and adding further ribbing could increase their strength.

At the core of this assembly design is a strategy of designing for unpredictability and adjustability. Although tolerances are always incorporated into the design of an assembly, whether it be in product design or engineering, working with the BJT glass fines materials revealed that this must be at the heart of the approach to designing this system. The heterogeny of the recycled glass fines combined with the unpredictability of glass in the firing process means that any assembly system must allow for tolerances that are much greater than what would be expected in mass manufacturing. Given the need to move towards circular and regenerative manufacturing systems, this approach is likely to become increasingly relevant as we must learn to work with irregular recycled materials and biobased resources.

Throughout this prototyping process, the overall design continued to evolve to incorporate and account for the mounting system. Various scales and forms of the overall screen were digitally modelled to ensure cohesion of the design and allow for it to be envisioned in a range of contexts (see Figure 6.39). The parametric nature of the digital model enabled this adaptation.

6.2.5 Printing - drying and swiping

Throughout this design development phase, additional knowledge was generated about the printing process and parameters. Firstly, it was found that each module should be printed separately. Whilst almost three tiles could fit in the print bed at once, it is far more difficult to excavate the parts when they are printed together. This was discovered during the printing of Prototype 12.01. In this process, two of the three pieces were printed in the same bed while the third was printed separately. Although all pieces printed without issues, it was noted that the components printed together took significantly longer to dry and were challenging to separate without breaking. This insight led to a refinement of the drying process.

Figure 6.37. *Assembly system Prototype 13.2 (back view close-up).*
T-slot aluminium extrusions and custom 3D printed brackets were used to attach tile to the frame.

Figure 6.38. *Assembly system Prototype 13.2 (front and back view).*
The T-slot extrusion provided greater rigidity to the frame and adjustability of the anchor points allowing for more efficient and flexible assembly. The 3D-printed brackets allowed for secure fixing with some adjustability.

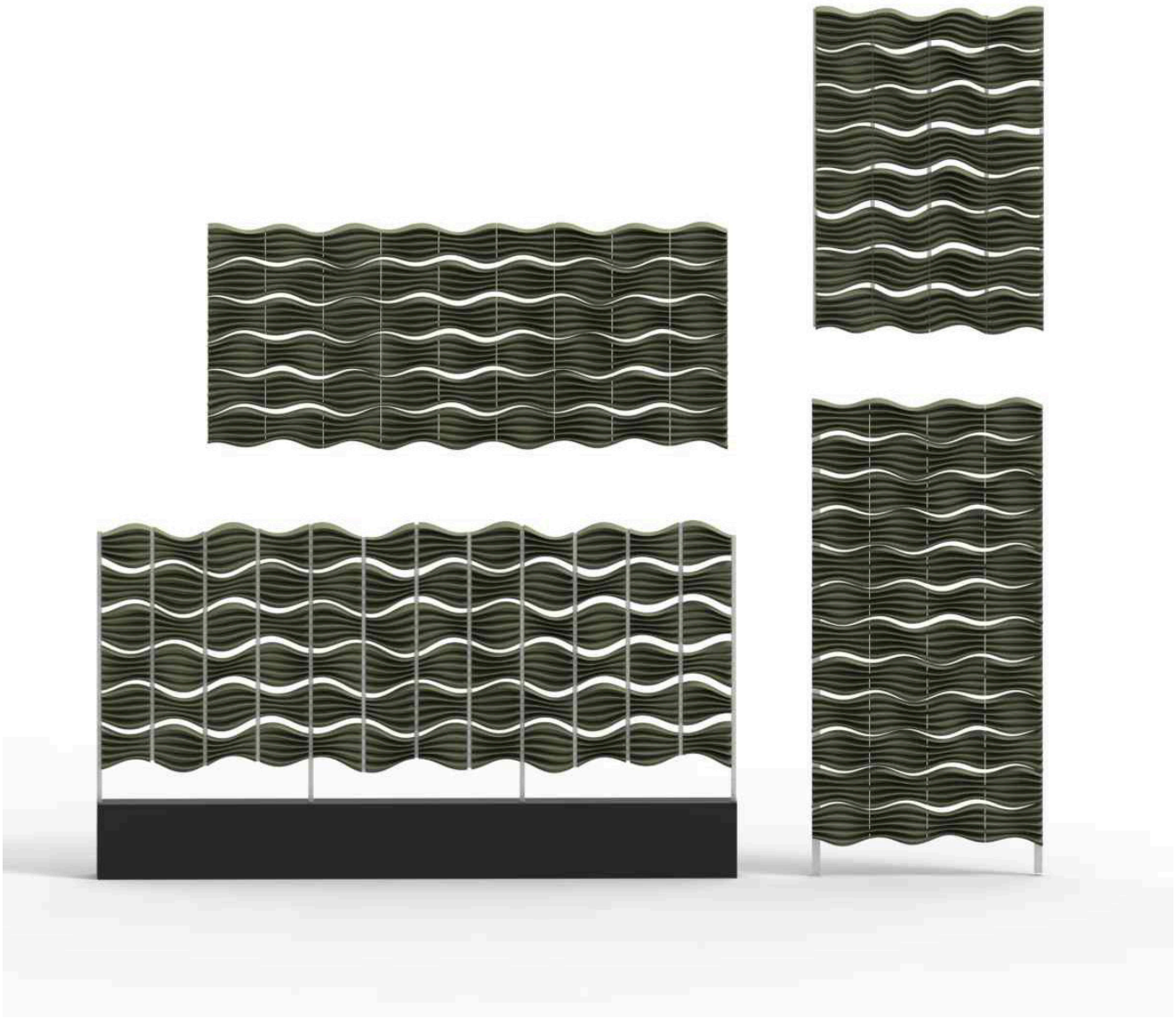

Figure 6.39. *Design evolution with incorporation of mounting system.*
The development of the mounting system has also allowed for a refinement of the design and exploration of potential variations.

Given that the parts were about 50mm tall, the entire bed could be removed from the printer and placed in the dehydrator without causing breakages. As a result, the parts could be dried significantly quicker. It was found that components should be left in the print bed for a minimum of 2 hours after printing, and then the whole bed would be carefully removed and placed in the dehydrator at approximately 80°C for a minimum of five hours. Occasionally, parts were put in the dehydrator at a lower temperature and left overnight.

During this design development phase, swiping again emerged as an issue. This is due to the types of geometries that were being printed. The ridge designs are made up of a series of lines, which, when the roller spreads a new layer of powder over them, tend to shift. This was particularly evident on parts that were printed with the ridge running along the y-axis, meaning that the roller came into contact with the entire line. This issue was eventually overcome by heating the powdered feedstock before printing. The glass fines and binder mixture was heated in a dehydrator for a minimum of 3 hours at 90°C and immediately used. This process almost completely eliminated swiping, which occurred on the first layer only occasionally, with no noticeable impact on excavated parts. It has been reported that the temperature of a powder bed can affect the impact behaviour of droplets, affecting both how they impact the surface (rebounding, spreading, splashing) and how they infiltrate the powder (Cheny et al., 2024; Liu et al., 2018c). However, it is unclear exactly how and why this reduced the swiping, and no literature was found examining the link between layer shifting and powder bed temperature. It could also potentially be the result of removing excess moisture from the feedstock, as this has been reported to reduce powder flowability (Hirschberg et al., 2019). There is scope to study this further.

Despite the lack of clarity here, the powder preheating process and changes to the drying method improved the production process significantly, allowing for multiple parts to be produced accurately and efficiently.

6.3 Final Prototype

The design development outlined in the previous section led to the construction of a final demonstrator. This is a prototype as a research archetype, which is used to present the research outcomes. The production of this prototype itself also leads to the generation of new knowledge. The final prototype can be seen in Figures 6.40-6.43. It is approximately 1m^2 in size and is made up of 16 individual tiles. It should be viewed as an excerpt of a larger evaporative screen. An organic, ridged design has been developed that evokes the flow of moving water. Each tile is unique and fits seamlessly into the larger overall design, like pieces in a jigsaw puzzle. This harnesses the customisation capabilities of 3D printing technologies. Space is left between each tile to allow for air flow, aiding evaporation.

As has been described in the previous chapters, each tile was 3D printed using the glass fines material and a binder jet 3D printing system. Once printed, the tiles were fired in a kiln to produce parts with porosity of approximately 15%. This allows for the tiles to absorb water, at a similar capacity to unglazed terracotta products, which are widely used in evaporative cooling. They are also fired to a peak temperature of 680°C, representing a significant decrease compared to the temperatures used in conventional glass manufacturing and recycling. This signals the potential for energy reduction. During the firing process, the organic HPS binder burns away leaving an entirely soda lime silica glass object, which remains circular.

Figure 6.40. *Final prototype (front view).*

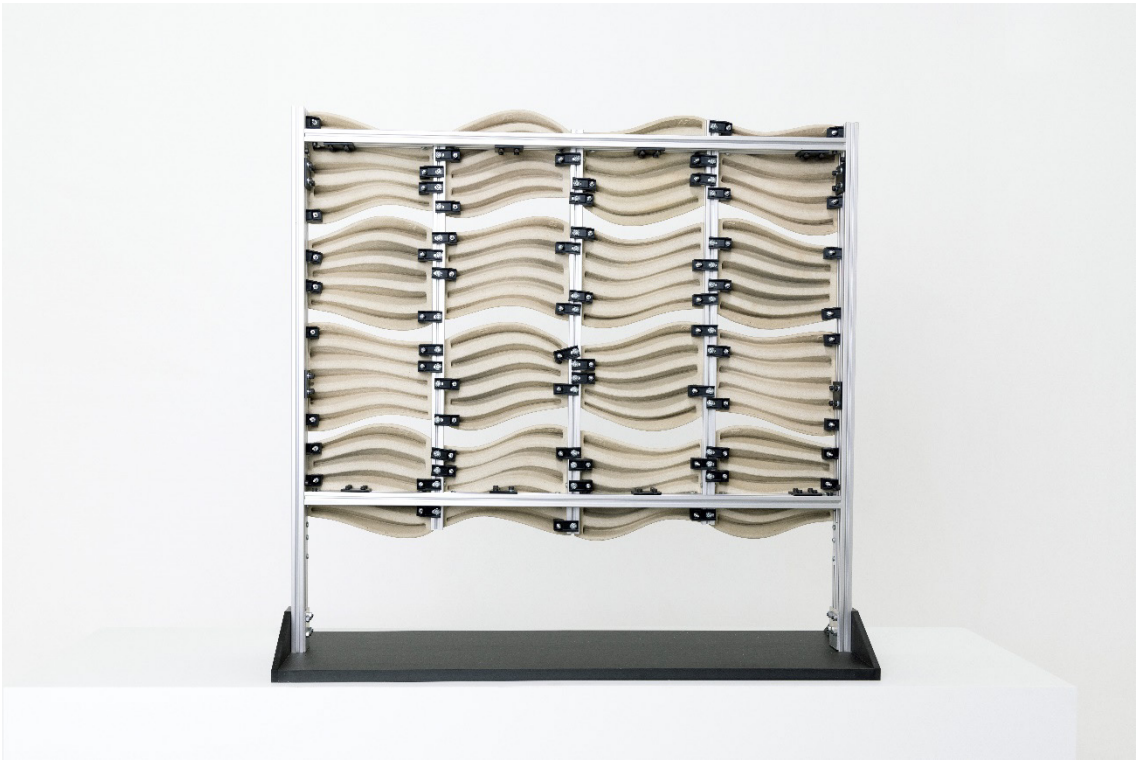

Figure 6.41. *Final prototype (back view).*

Figure 6.42. *Final prototype with figure.*

Figure 6.43. *Close-up of assembly system on final prototype (back view).*

The ridged design utilises self-supporting triangular structures that provide a level of predictability in the firing process. This form also increases the surface area of the components, which is a requirement of evaporative cooling systems. Each tile has a label in the CAD model, enabling easy identification and demonstrating the accuracy and fidelity of the printing system.

The tiles are mounted onto an aluminium frame made from T-slot extrusions using custom 3D printed brackets and L-shaped bolts (see Figure 6.43). A fixing system has been integrated into each tile, allowing for the bolts to hook into them. This could not be achieved using conventional glass manufacturing or moulding processes. The assembly system has been designed to ensure both stability and adjustability. As the tiles are made from a recycled material, designing for greater tolerances is required. The system also has disassembly at its core, utilising components that can be easily taken apart instead of relying on glues or adhesives. This further enables the circularity of the material. An irrigation system runs through the aluminium channels to keep the tiles wet and allow for the evaporative cooling action (see Figure 6.44). To mitigate excessive water use, rainwater should be utilised in conjunction with a water pump. The modular and 3D printed nature of this design also facilitates maintenance and repair, as individual tiles can be removed and reprinted if necessary.

As this prototype will be used for demonstration purposes, it includes a dual mounting system with two frames that can be attached and taken apart. The front frame allows for mounting on a wall whilst the back frame is attached to a black base that allows for a standalone table height demonstrator to be exhibited.

The overall design has adaptability and customisability at the heart. By employing parametric design tools in conjunction with 3D printing, the system can be scaled and adjusted for specific spaces. This ties to the site-specific requirement of evaporative cooling, allowing for a site analysis to be conducted and the system designed and located accordingly. The flexibility of the T-slot assembly system also aids this adaptability. Digital renderings and drawings seen in Figures 6.45-6.48 demonstrate this adjustability and show specific sites in which this evaporative cooling screen has been envisaged. As was discussed earlier in the chapter, outdoor public spaces such as public seating areas, bus stops and the entrances to public buildings are the focus.

Through the production of the final prototype, findings continued to be generated. The most significant was that some tiles shrank more than others. This was related to the geometry of the tiles; those that were more bulbous tended to shrink more in the x-axis. This was only visible when multiple tiles were manufactured together, but could be easily accounted for in CAD models going forward. Further prototyping of these tolerances and developing a digital tool to predict this shrinkage could be considered in the future.

6.4 Reflection and conclusion

This chapter details the development of an application that demonstrates the capabilities of the glass fines material and BJT production process. The investigation into porosity conducted in the previous chapter identified evaporative cooling systems as a potential avenue that could fully leverage the material properties and capabilities of 3D printing. This chapter began by emphasising the need for more passive cooling solutions in the built environment, particularly focusing on evaporative technologies and various precedents using ceramic materials. This culminated in a design brief aimed at guiding the creation of an evaporative cooling system utilising glass fines material. The majority of the chapter then discussed the design development phase.

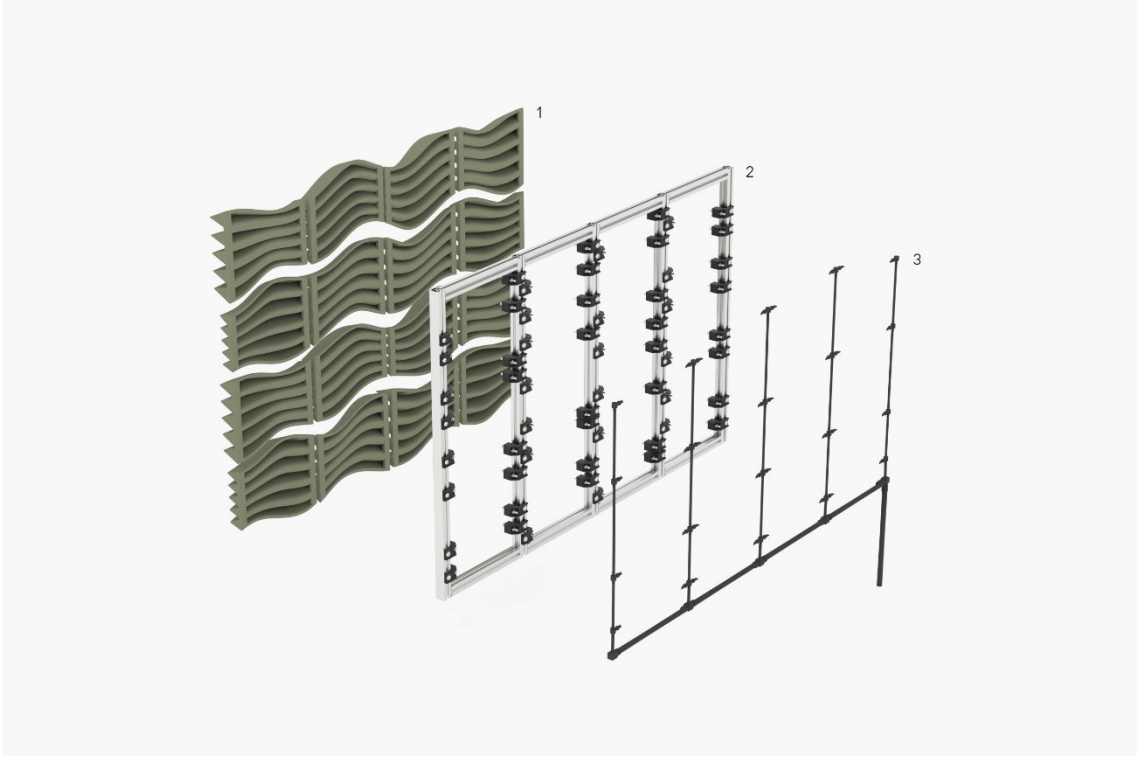

Figure 6.44. *Exploded view of evaporative screen design.*
The overall design is made up of three layers: 1. 3D printed glass fines tiles, 2. Aluminium frame with custom brackets and fixings, 3. Irrigation system for water supply.

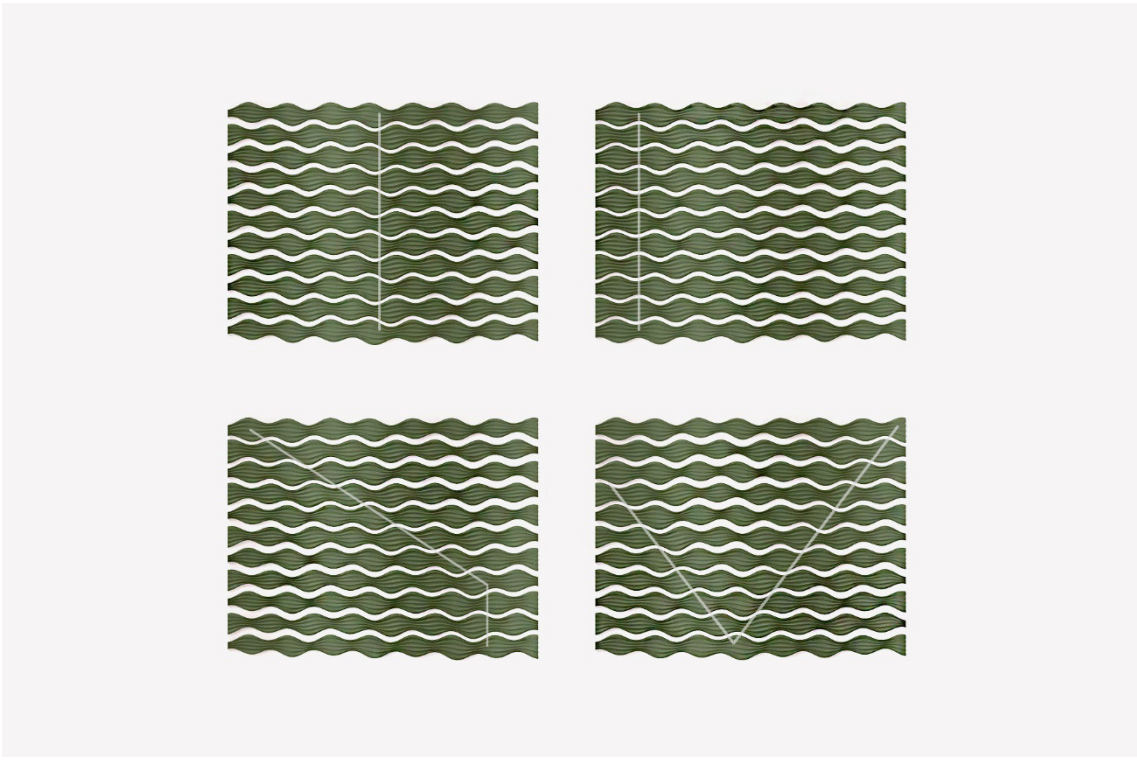

Figure 6.45. *Customisation of screen design based on parametric design of tiles.*
The size and curvature of the tiles can be adjusted to vary across the screen.

Figure 6.46. *In-situ digital rendering of evaporative screen installed at the entrance of a public building.*

Figure 6.47. *In-situ digital rendering of evaporative screen installed as part of a bus stop.*

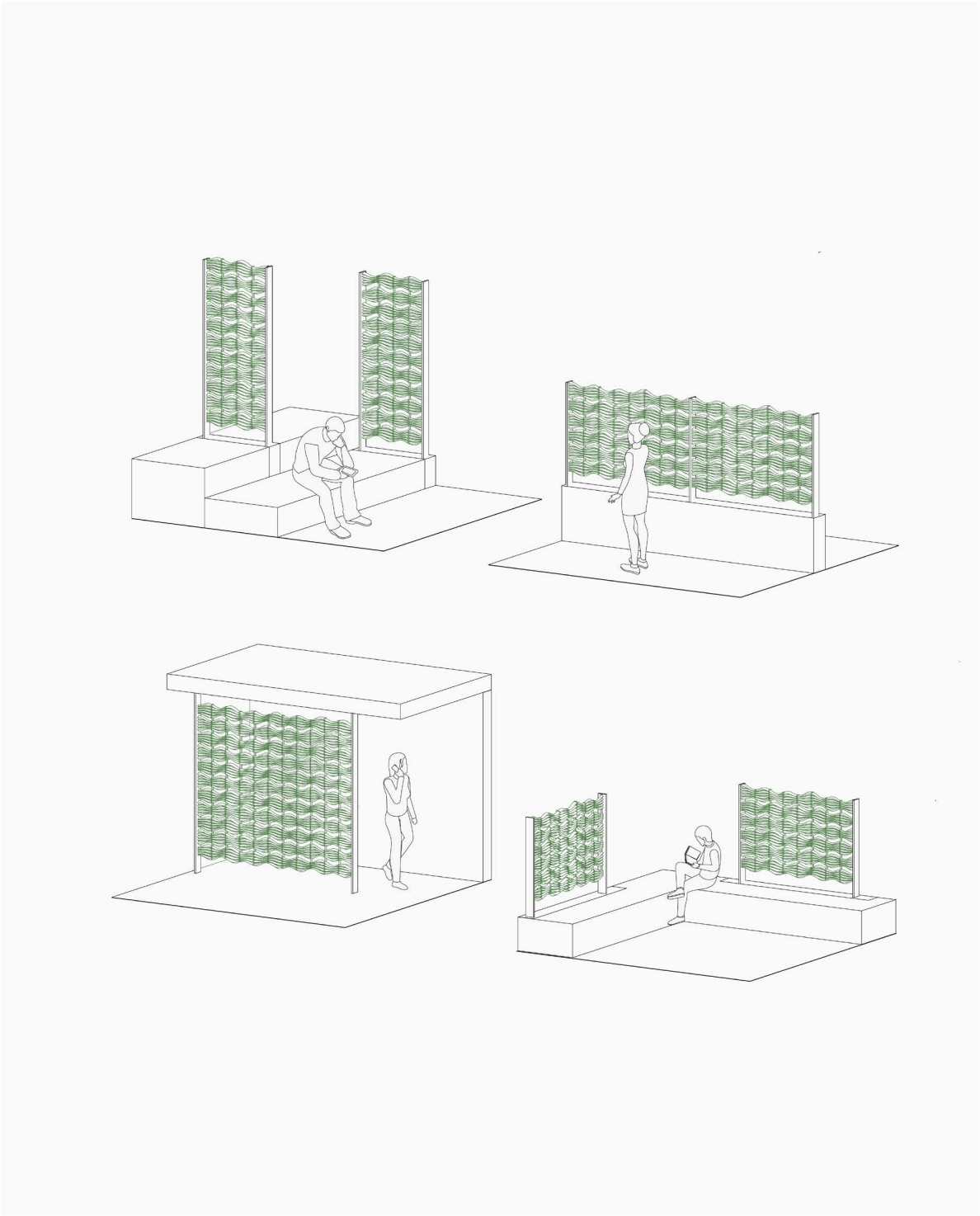

Figure 6.48. *Drawings depicting various customisation and installation options of the evaporative screen design.* The parametricity of the design in combination with 3D printing enables this level of adaptability.

Figure 6.49 provides a diagrammatic representation of this development. As in the preceding chapters, this figure is based on the research diagram presented in the Methodology, using cascading circles to illustrate the sequence of experiments where insights flow from one prototype to the next. It can also be seen here that the three threads of the research—the material, production, and application— each corresponding to a sub-research question, came together to drive this final phase of the research.

As can be seen in Figure 6.49, several design experiments were conducted to develop the final demonstrator. All designs were made up of modular components that could be assembled into larger evaporative screens. Each design considered water supply, assembly, and airflow potential. Leveraging 3D printing advantages was crucial, especially in integrating parametricity and utilising complex geometries to enhance surface area. The initial designs were expansive and potentially ambitious in form, based on a water vessel supply system and including a new firing method that employed inert talc as a support medium during the firing process. Although this technique appeared promising, the subsequent experiments focused on exploring forms that could be fired predictably without needing an additional, potentially time-consuming production step. As a result, a series of designs that revisited pyramidal forms and utilised ribs were developed. This experimentation again demonstrated the potential of the pyramidal structure during the firing process, as the forms became self-supporting and maintained their shape. Consequently, a ridged design typology with a zigzagged cross-section emerged, as it could be predictably fired while allowing for a high surface area.

From here, several experiments were conducted to further develop the ridged typology. This involved the decision to create ridges that seamlessly flow across multiple tiles, resembling a jigsaw puzzle in which each piece is entirely distinct. This feature is enabled by the customisation capabilities of 3D printing. Additionally, it evokes the movement of water, which is fundamental to evaporative cooling systems and can facilitate airflow across the components. Prototyping was conducted to understand the geometric limitations of this typology; specifically, determining the maximum height of the ridges before they start to slump and distort. This was followed by prototyping that concentrated on creating a seamless connection between the tiles by compensating for the shrinkage in the CAD-modelled file. Additionally, tests were conducted to enhance airflow, prior to concentrating on the fixing and assembly system. Various assembly techniques were examined to enable secure and efficient attachment of components to an aluminium frame that would have an irrigation system mounted on the back. A level of adjustability was also built into this assembly system, as this is essential when working with circular materials that exhibit heterogeneity and unpredictability. This experimentation resulted in the production of a final demonstrator or prototype as a research archetype: oa $1m^2$ section of an evaporative cooling system made from BJT glass fines tiles with a porosity of approximately 15%.

The production of this demonstrator offers several advantages. Firstly, it serves as a communication device, enabling the presentation of both the outcomes and the potential of the developed material and production system. As discussed in Chapter 2, such demonstrations can facilitate greater industry translation. Moreover, creating demonstrators or prototypes as research archetypes is a defining feature of many RtD projects, as they are required to engage both the academic and design communities. In this particular project, positioned at the intersection of design, architecture, materials science and engineering, the demonstrator can act as a translator between disciplines (Moultrie, 2015). Furthermore, in the context of RtD projects, the production of demonstrators, along with the broader effort to design applications beyond exhibitable artefacts, enables designers working with materials to propose ambitious and potentially more impactful applications. In contrast, industry's pragmatic and risk-averse tendencies might lead to conservative uses, such as recycled glass crockery—a valid but limited application that may not fully exploit the material's potential. Pursuing the research to this stage can allow for a broader range of possibilities to be envisioned.

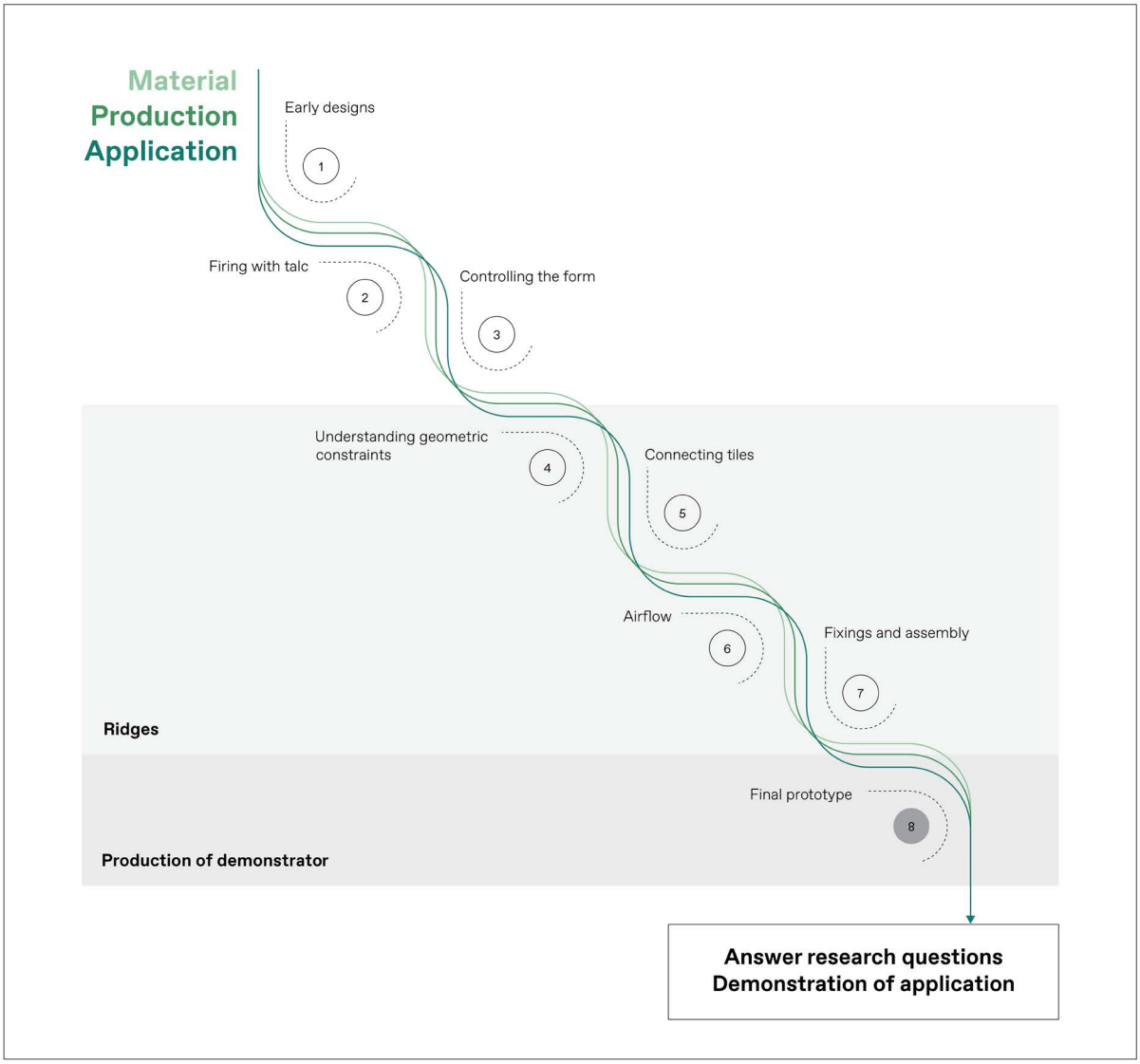

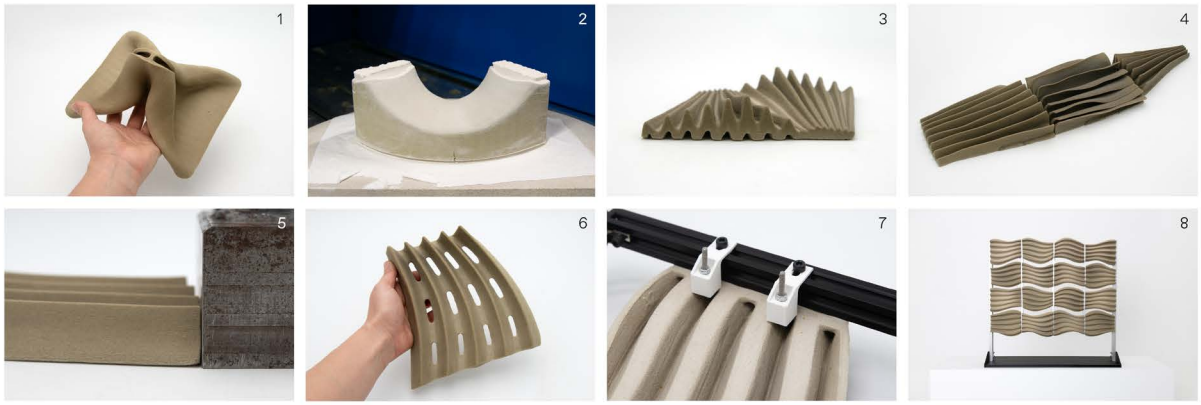

Figure 6.49. *Diagrammatic representation of Chapter 6 experimentation and design development.*
All three threads of the research, material, production and application, drove this stage of experimentation and design development. Eight sets of experiments were conducted to address these research questions and produce a demonstrator of the application.

Developing a demonstrator drives research to engage with real-world constraints, and this process contributes to the creation of additional knowledge (Thomsen & Tamke, 2009). In this research, engaging in serial production has led to the generation of further knowledge regarding the printing process and tolerances, aspects that may have gone unnoticed if only singular tests had been conducted. The production of a demonstrator holds particular significance for this study, as the mixed results during the firing process rendered it imperative for industrial practical application to demonstrate a level of predictability and reliability in forms. Serial production facilitates this demonstration. Moving forward, there is an opportunity to utilise the demonstrator for further experiments, such as investigating the specific cooling capacity, airflow, and placement of the screen. Additionally, it can be exhibited for broader dissemination of the research.

While this demonstrator presents a potential application avenue for glass fines, it remains in the concept phase. Further optimisation of material properties and in situ testing of the evaporative capacity is required for commercialisation. A site analysis strategy should accompany this, ensuring factors like wind, turbulence, and solar radiation are considered to optimise both the location and size of the evaporative screen. Although further development is required, the accessibility of BJT technologies and kilns, alongside the abundance of low-cost glass fines, give potential for this design to be further developed in an economically feasible way. The proposed design can also be considered an 'upcycling' of the glass fines, creating a product that adds significant value to the waste stream which can justify the processing costs as outlined by (Flood et al., 2020). This directly contrasts with the widespread practice of downcycling glass fines as aggregate in road construction and bases.

The design development presented in this chapter focused on creating forms that can be predictably and reliably fired without support structures. However, the firing method using talc, presented in Section 6.2.1.1, has potential for further exploration. This technique could allow for the successful firing of forms in a broader range of geometries, thereby removing the current limitations on design freedom. Further refinement of the method is required, including investigation into the feasibility of fully submerging pieces in a vessel of talc and identifying the necessary adjustments to the firing schedule to ensure even fusing. It is also critical to address the prevention of crack formation during the process.

Additional reflections on circularity have emerged. While the previous chapter confirmed the circularity of the material, the design development presented here further emphasises that this is just one part of the circularity picture. Without the integration of design for circularity at both the product and system levels, the recyclable material risks being compromised or ultimately ending up in a landfill. R strategies as outlined in Chapter 2 (see Section 2.2.1), including refuse, repair and recycling, were embedded in the design of the overall evaporative screen. For instance, glues, adhesives and pigments that could undermine circularity were refused and parts were assembled in a way that individual pieces could be repaired via on demand 3D printing without the need to disassemble the whole screen. Furthermore, recycling considerations were embedded in the selection of stainless steel and aluminium hardware, as well as the glass fines material itself. The key circular design strategy of designing for disassembly was also central to the overall system design, facilitating the separation and reuse or recycling of all materials.

It is important to note that crushing and recycling of the 3D printed tiles is not the ideal end-of-life strategy, as this ranks relatively low on the R-Strategies list. Instead, reusing or repurposing would be more beneficial. As a result, opportunities to enhance the design to promote such repurposing and to facilitate multiple uses or lifecycles could be investigated. Furthermore, construction sites are frequently characterised by a lack of recycling and significant waste generation. As this is likely the context in which decisions around the end of life of the evaporative system are made, it is important to have alternate systems in place to ensure that the screens

can be properly disassembled and managed. Adding labels to the glass fines tiles within the CAD models to identify the material may also enhance the recyclability of the material and prevent it from ending up in a landfill. Additionally, conducting a lifecycle assessment on the tiles and larger evaporative system would provide more information around the overall environmental impact. However, it is crucial to acknowledge that the absence of precedents makes this analysis challenging to complete.

Overall, this chapter presented the design and development of an evaporative cooling system using the BJT glass fines material. The experimentation, analysis and production of a demonstrator culminated in the answering of the three sub-research questions and the demonstration of a potential application avenue.

7

Discussion and Conclusions

7 Discussion and Conclusions

7.1 Introduction

This chapter concludes the research by presenting a final discussion of the findings. The research has investigated a method of binder jet 3D printing with recycled glass fines for circular product applications. To achieve this, a RtD methodology has been employed, allowing for the exploration and connection of the three key areas of material, production, and application. This chapter begins by summarising the research and discussing how the research questions have been addressed. Based on these findings, the contribution and significance of the research are then presented, along with an analysis of limitations. Finally, future research directions are presented.

7.2 Overview of the Research

This dissertation began by outlining the devastating impacts of linear models of production and consumption, the waste, the emissions, and the endless demand. It was argued that industrial designers have not only the opportunity but the responsibility to shape new ways of building products and services. The CE has been positioned as an avenue to achieve this by creating cyclical loops of materials and products, wherein their value can be maintained and waste and emissions are reduced. The emerging field of materials design has opened new ways for designers to engage with the CE, encouraging hands-on material development, which gives designers greater control and opportunity to embed circularity into the material and production chain. This has further been enabled by the democratisation of self-fabrication tools such as 3D printing. The CE provides the conceptual framework for a holistic approach to this research by investigating the cohesive design of a circular material, production process and product application.

Within this context, the material loop of glass fines was identified as holding significant potential for circular applications, due to the ability of glass to be recycled almost infinitely without impacting material quality. Difficulties in the collection and sorting process of glass have led not only to low global recycling rates but also to the production of a byproduct known as glass fines. These mixed small particles of glass are unable to serve as feedstock for traditional glass recycling, and as a result, large quantities end up in landfill or are stockpiled. This represents a significant waste stream; in 2018, 15% of all glass packaging consumed in Australia became glass fines, equating to approximately 190,000 tonnes. In recent years, there has been a push to find applications for glass fines. Most of these have been in the building and construction industries, where glass fines are used as a replacement for aggregate in roads and pavements or as an embedment material for pipes. While this is a straightforward solution to stockpiling, these applications essentially bury what is a valuable material. As a result, applications of this nature have been characterised as ‘terminal’. While they utilise a waste stream once, any subsequent recovery is difficult, if not impossible. To build truly circular systems, applications in which resources can be repeatedly recovered and recycled is needed.

Research into the current applications of glass fines also revealed the need for higher-value application avenues to enhance the economic viability of the waste stream. This dissertation argues that 3D printing can enable this, as it has several advantages such as complex geometries, customisation and localisation that can be harnessed. The scalability of the technology also allows for greater application potential in industry to be envisioned—something which is often missing in more craft-based design projects. As a result, the state of the art of glass 3D

printing was analysed to determine the opportunities and limitations of various printing technologies in relation to the glass fines material. This revealed that recycled glass 3D printing was extremely limited and largely focused on the inclusion of waste glass in composite materials. It also allowed for BJT to be identified as a technology with significant potential for the use of glass fines. This is due to its powder-based nature, meaning that minimal additional material processing is required and it has almost unlimited geometric capabilities. The opaque parts produced by BJT were also seen as an opportunity to develop novel material aesthetics and functionalities that could expand the traditional perception of glass materials and their application. The scalability of BJT technologies was a further factor as it is the 3DP technology with one of the largest build volumes available, up to $4m^2$ (Gibson et al., 2021). Furthermore, the work of Marchelli et al. (2011) established a solid foundation for BJT printing both virgin and recycled glass powders, which could be further developed.

The review of literature culminated in the formulation of one overarching research question with three sub-questions:
How can recycled glass fines be transformed into a product application using a binder jet 3D printing system that can remain in a closed circular loop?

a. What are the requirements of a material formulation that remains circular?
b. What are the manufacturing process steps and parameters?
c. What product application can be developed that demonstrates the opportunities of the material and production system?

These sub-questions relate to the key areas of material, production and application, which are addressed concurrently. They can be seen as the threads that make up the overarching research question. They are intertwined, and one cannot be addressed without the other. A material formulation cannot be developed without understanding the method of production, and the capabilities of the material and production system will inform the application. As a result, all three must come together cohesively. This is a more holistic and tailored approach that allows for the emergent affordances of the material or production to guide the application, ensuring they are well-matched. This avoids issues we have observed with materials like plastic, where their short-term use is incongruent with their long-lasting nature.

The research questions were presented in Chapter 3 alongside the RtD methodology. This methodology involves using design practices and methods as a way of generating new knowledge. While RtD is now a well-established approach, there is no singular method for conducting it. Similar to design practice more broadly, the processes and methods employed by design researchers can vary greatly. Consequently, it is important to clearly identify the way RtD is employed in this research, particularly in relation to a materials-based project. Firstly, prototyping is the primary data collection method, with three types of prototypes employed (Wensveen & Matthews, 2014). The first is prototyping as a vehicle for inquiry. This refers to when the process of making the artefact is the main contribution to the research rather than the artefact itself. The second type is prototyping as an experimental component. This is most akin to traditional scientific experiments, where a prototype is constructed and then tested to examine a specific hypothesis. Finally, prototypes as research archetypes are employed to illustrate and showcase the research and the chosen application.

The prototyping is conducted in a serial manner whereby the knowledge generated from one prototype informs the next. This builds a chain of knowledge in pursuit of the research questions. To ensure that knowledge was captured, all prototypes were rigorously documented in reflective experimental logs, which allowed for the capturing, analysis and emergence of knowledge.

Chapter 4 discussed the preliminary experimentation conducted in this research. Prior work on the paste extrusion of glass fines was first presented to provide context and clarify the starting point of the research. Based on this, the multi-step production process was introduced: material preparation, printing, drying, and firing. This chapter covered the first three steps of this process. Manual testing of the binder jet principle was conducted to ensure that the initial material formulation (determined by the paste extrusion work) and the process had potential. Then, two stages of experimentation were introduced: finding the printing parameters and finding the binder formulation. These were the initial factors required to establish a process for the BJT of glass fines. In the first stage, printing parameters such as layer height, saturation, and drying time were incrementally adjusted to develop a set of stable parameters that would allow for the accurate printing and excavation of parts (see Figure 4.7 for an overview of the production parameters). This stage revealed the importance of green strength in ensuring that parts could be excavated from the print bed without breaking. As a result, the second stage focused on optimising the binder formulation. Several organic binders were iteratively tested to assess their adhesive ability in the BJT process. A cold swelling hydroxypropyl starch (HPS) was found to provide suitable green strength for the printing and excavation of parts. This chapter facilitated an understanding of the variables and the interrelations between the material and the production system.

Chapter 5 introduced the final step in the production process, firing. This step is crucial for fusing the glass particles into usable objects. It is also crucial for ensuring the circularity of the material, as during firing, the binder burns away, leaving only glass that can be recycled repeatedly. This is important, as creating composite materials or using additives that leave residues can hinder circularity and compromise the material integrity. To validate that the HPS binder would, in fact, burn out during the firing process, a TGA was performed. This widely used thermal analysis technique monitors a sample's mass as it is heated, allowing the compounds in the sample to be characterised based on physical or chemical changes. The TGA confirmed the circularity of the BJT glass fines material, with the sample remaining stable when heated to 650°C, demonstrating that the binder and other contaminants decomposed during the initial firing process. With these results, the first sub-research question could be addressed.

Chapter 5 also delved into exploring different forms and geometries that could be achieved via this production process. As glass begins to flow upon heating, this testing phase revealed the challenges associated with the shrinkage and slumping of the glass material in the kiln. Several typologies were investigated to understand the kinds of geometries that could be the most predictably fired (see Figure 7.1). It was found that pyramidal truss shapes had significant potential due to their self-supporting nature. This allowed for several lattice forms to be printed, excavated and fired predictably with minimal slumping. These lattices represent a breakthrough in recycled glass 3D printing, as fired geometries with this level of complexity have not yet been presented. This development also opens compelling application opportunities, as these forms would be impossible to achieve using conventional glass manufacturing methods. However, it is important to note that this iterative testing also made it clear that the slumping and shrinkage were scale-dependent and that it would not be possible to create universal design rules. Instead, an application must be designed closely with the process to tailor the geometry specifically to that function. Whilst this could be seen as a barrier, this is exactly the type of research that the RtD methodology is best suited for. It also aligns with the customisation capabilities of 3D printing and the need for more localised manufacturing in the CE.

Chapter 5 concluded with an investigation into the porosity of the fired material. Through iterative testing and an experimental prototype, it was revealed that it is possible to create both porous and waterproof parts via the BJT of glass fines by altering the firing schedule. This allowed for the second sub-research question to be answered and opened an opportunity for porous applications to be uncovered.

Figure 7.1. *Various samples presented in Chapter 5.*

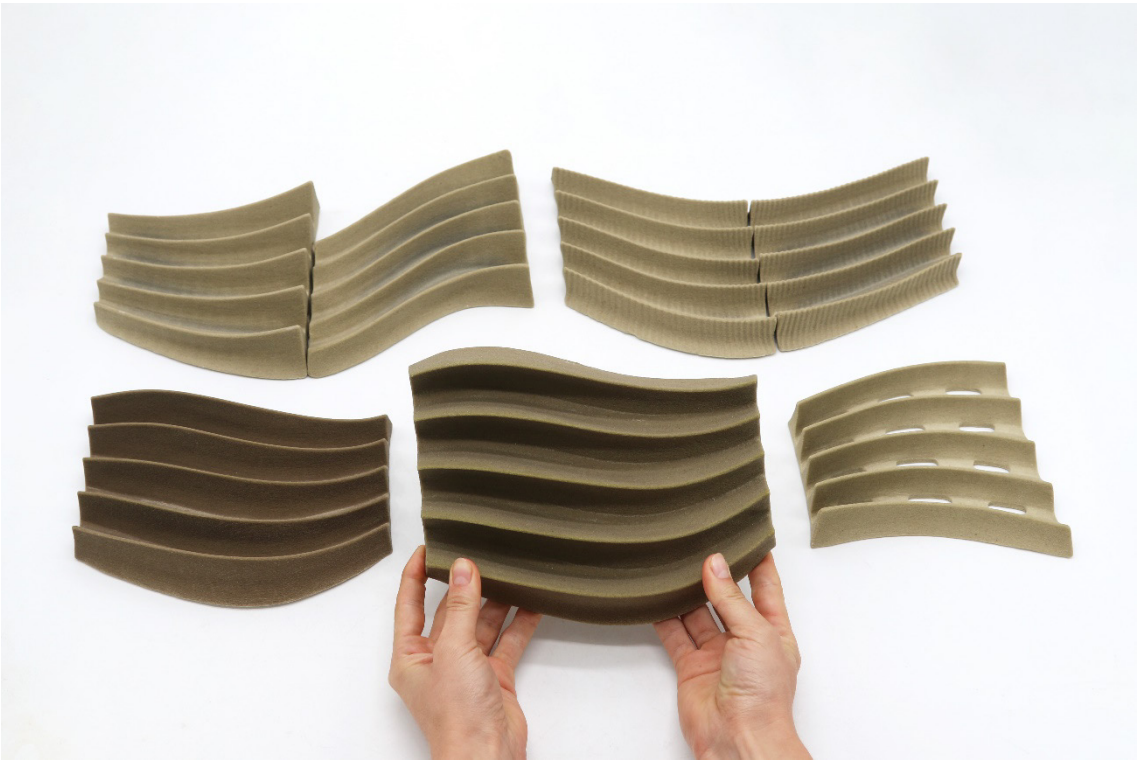

Figure 7.2. *Various prototypes presented in Chapter 6.*

Chapter 6 outlined the development of an application that demonstrates the capabilities of the glass fines material and binder jetting process. The porosity of the parts achieved in the previous chapter generated interest in the potential application of the material for the evaporative cooling of spaces. Porous ceramic materials have been used to do this for centuries, as their porous structure allows water to permeate the surface, creating a thin film of water that can evaporate and cool the ambient air. The level of porosity attained in this investigation is comparable to that of unglazed terracotta, which is typically used in this process, ranging from 7% to 24% (Hall & Hoff, 2021; Vallejo, 2018). Furthermore, the complex geometries and customisation offered by 3D printing can enhance the functionality of evaporative cooling systems by providing greater surface area for water to evaporate and allowing for site-specific adaptability of the design. Moreover, as temperatures continue to rise, there is a real need to develop more passive cooling systems for the built environment. This choice of application addresses the operational emissions generated by the built environment sector, while the material and production methods address the embodied emissions.

With the framing of this application, Chapter 6 discussed the design development of an evaporative cooling screen made from the porous glass fines material via a BJT process. Designs were based on individual modules that would be assembled into a larger whole. Several geometries were explored, considering different water supply and assembly systems. While these were initially more expansive, the success of the pyramidal structure was once again evident. As a result, ridged geometries were developed in which the pyramidal structure became self-supporting and maintained its shape (see Figure 7.2). This allowed for predictable results during the firing process and high surface area. Various assembly techniques were examined to enable secure and efficient attachment of components to an aluminium frame structure. A degree of adjustability was also integrated into this assembly system, as this is essential when working with circular materials that exhibit heterogeneity and unpredictability. This prototyping culminated in the creation of a final demonstrator that presents a potential application avenue for the BJT of glass fines, addressing research sub-question three.

7.3 Discussing the Research Questions

As stated above, this research was guided by one overarching research question and three sub-questions, relating to the interconnected areas of material, production, and application. This section will elaborate on how each of the sub-research questions has been addressed, providing further analysis and discussion of the findings that emerged in relation to each. The following section, which outlines the contribution to knowledge, will discuss how these findings collectively address the overarching research question.

7.3.1 What are the requirements of a material formulation that remains circular?

For this research, creating a material formulation that remains circular means creating one that can be recycled repeatedly in a closed loop without impacting the material integrity. As discussed in Chapter 2, this means that the material retains its original properties even after recycling (Sauerwein, 2020). It is not sufficient to find an application where the glass fines are turned into a new product but have no avenue for recycling or recovery at the end of life. In this research, this meant that while a binder was required for the printing process, it must not compromise the circularity of the material. Additionally, the emphasis was on keeping glass as glass, as its ability to be recycled repeatedly without affecting material quality makes it already inherently suited to circularity. Consequently, a range of organic binders that were hypothesised to burn away in the kiln, leaving only glass, were tested. These include a range of cellulose derivatives such as

CMC and maltodextrin, which is commonly used in the BJT of ceramics. During this experimentation, other key requirements of the material formulation became apparent, in particular, the need for the binder to provide adequate green strength so that parts could be excavated without breakages.

The research found that a pregelatinized hydroxypropyl starch (HPS) binder provided suitable green strength and did not impact the circularity of the glass fines. As discussed in Chapter 4, this is a modified starch that is water-soluble at room temperature. By combining just 4% w/w with the glass fines and using tap water as the liquid activator, complex geometries could be printed and excavated. The TGA analysis discussed in Chapter 5 confirmed that this binder burns out during the firing process, with decomposition starting at 210°C and reaching a maximum at 317°C. Approximately 1% of other organic matter or contaminants present in the glass fines also burn out until approximately 480°C. The TGA confirmed that the fired 3D printed glass fines material remained stable when heated to 650°C, demonstrating that the binder and other contaminants decomposed during the initial firing process. As a result, this material formulation and production process can facilitate the creation of circular products made from glass fines, which can be recycled repeatedly. This applies to both waterproof and porous parts that can be created by adjusting the firing schedule. Engaging with materials science and engineering methods to validate material properties can ensure that claims of circularity and sustainability are legitimate.

The choice of glass fines as a material was partly due to the localisation of this waste source. Although it exists globally, glass fines are abundant in Australia and can be sourced in various locations around the country. For this research, they came from a facility on the Central Coast of New South Wales, just an hour from where this research is based. This illustrates how localised materials can be sourced for production and application in local areas, something which 3D printing can enable. It also aligns with emerging practices in the field of materials design, which is rejecting the widescale relocation of resources that has defined the last 200 years of globalisation, instead seeking to establish deeper relationships with local resources and rhythms of resource availability (Thomsen et al., 2024). This is particularly significant given that this research began at the tail end of the COVID-19 pandemic, a period marked by significant disruptions to global supply chains, emphasising the importance of localised production systems. While this research has demonstrated a method for transforming glass fines into higher-value applications, it is crucial to emphasise that the primary objective should still be the minimisation of this waste resource. There are various upstream initiatives that could prevent the generation of such substantial quantities in Australia, including the implementation of a dedicated glass recycling bin.

Furthermore, while the material formulation may be circular, systems to ensure that parts can be collected and recycled also need to be in place. As the resulting fired material is just soda lime silica glass, parts could potentially be placed back into traditional recycling streams in Australia. However, since the application is situated in public spaces, it is necessary to ensure that parts do not end up in non-municipal construction waste streams destined for landfill.

7.3.2 What are the production steps and parameters?

The production steps and parameters were developed throughout this research and specifically tailored to a chosen application. As discussed in Chapter 2, BJT was chosen for its accuracy, geometric capabilities and scalability. The powder-based nature of the system also meant that further processing of the glass fines into

a printing material was minimal. Through experimentation and prototyping, the following production steps and parameters were developed:

1. Material Preparation: 4% pregelatinised HPS is combined with glass fines (particle size 75–150 um) (w/w%) in a commercial mixer for a minimum of 15 minutes. The feedstock is then placed in an oven for a minimum of 2 hours at 90°C to preheat the powder and remove any moisture. Tap water is used as the liquid activator.
2. Printing: Heated powder is placed in the feed reservoir of the BJT printer (ZCorp 310). The chosen CAD file is loaded into the ZPrint software. The printing parameters of 0.2mm layer height, core saturation of 110% and shell saturation of 130% when using proprietary powder setting ZP15E are set. The print is then undertaken (see Figure 7.3).
3. Drying: Parts are left in the print bed for a minimum of 2 hours. The whole print bed is then removed and placed in a dehydrator at 75°C until fully dry. The required time in the bed and dehydrator varies depending on the geometry and scale of the print. Larger prints take longer to dry, and it can be more difficult to remove the whole print bed from the printer—as such, larger parts may need to be left for longer to cure in the bed before placing in the dehydrator. Once dry, the parts are fully excavated, and the loose powder is brushed off and reused (see Figure 7.4).
4. Firing: Green parts are placed in a glass kiln on Thinfire shelf paper, which stops parts sticking to the kiln shelves. Two firing schedules have been developed; one for the production of waterproof parts, another for the production of parts with porosity of approximately 14.5%. These schedules can be found in Appendix 4.4 and Appendix 4.5.

Many of these variables can be adjusted slightly as required. For example, more binder or higher saturation settings could be used to provide greater green strength if printing intricate shapes. However, it is important to note that many of these variables are interrelated; increasing the saturation will inevitably lead to longer drying times or may result in the binder bleeding out, causing inaccuracies. These parameters have been developed to find a balance that allows the parts to be printed accurately with adequate green strength. Chapter 4 discusses this development in detail. Excess powder from the excavation can be reused. However, it was observed that its quality began to decline with repeated use. Further work is needed to quantify the limits of reuse and how to rehabilitate the material.

It is important to note that this is one method for the BJT of glass fines. This is not the only method that could be developed, nor is it the most optimised. The extensive field of literature focused on optimising specific parameters in BJT could be drawn upon to enhance this process in various areas. For example, if highly dense parts are the aim, powder preparation methods such as granulation could be employed. Further quantitative analysis of specific parameters, such as saturation or roller speed, could also be conducted. While this type of testing would enable the fine-tuning of the process and material properties, this is not the focus of this project. As an RtD project conducted by an industrial designer, the emphasis was on creating a method that is repeatable and reliable, so that an application could be developed and presented. This allows for the potential of the material and process to be persuasively presented, allowing for the fine-tuning to occur later. While this order may seem counterintuitive, it embodies a design-oriented approach in which the pursuit of application drives the research. This perspective facilitates the envisioning of new possibilities and futures instead of confining research to a theoretical realm.

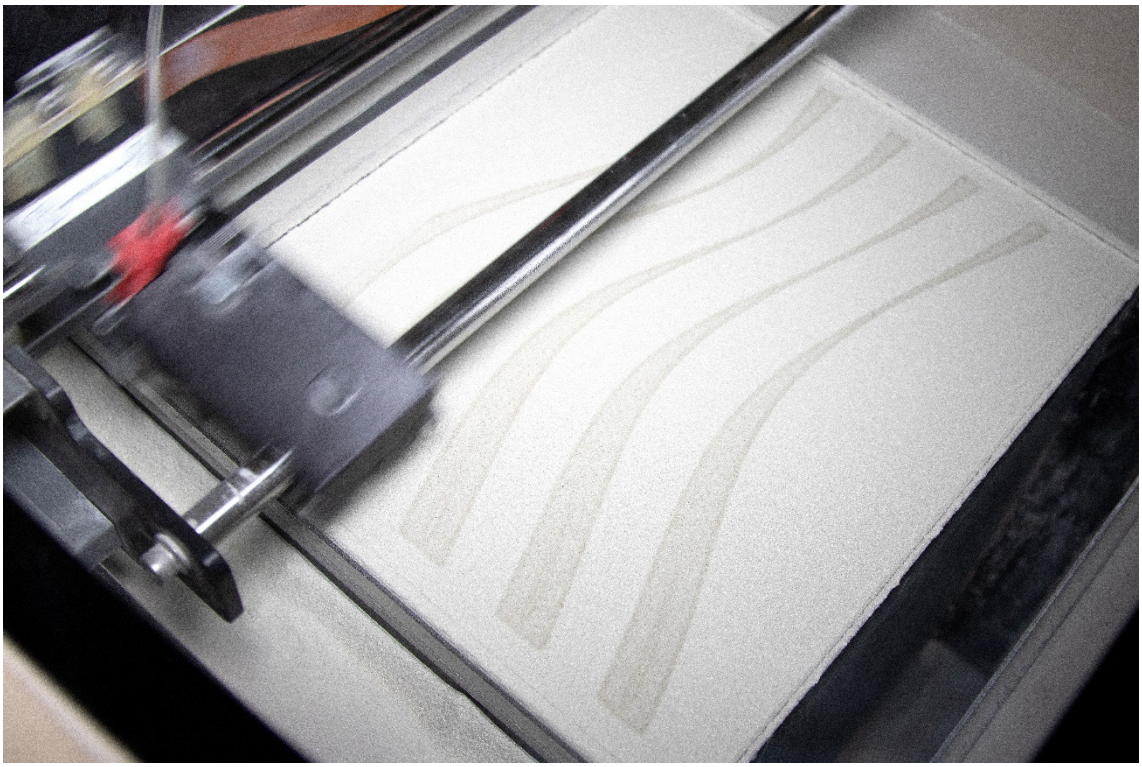

Figure 7.3. *3D printing of evaporative tile in progress.*

Figure 7.4. *Excavation of evaporative cooling tile in progress.*

One of the most important findings was that the geometric constraints were not dictated by the printing process but by the firing process. It was found that complex parts could be printed and excavated true to the CAD model; however, as glass begins to flow when heated, the firing caused slumping and shrinkage, inhibiting the geometric accuracy. Experimentation with a range of forms at differing scales, using both firing schedules, revealed the difficulty in establishing overarching rules for designing with the glass material. A firing process in which an inert powder was used as support material was tested with some success; however, the additional production steps involved were undesirable. The success of certain geometries also made it clear that while not all forms could be produced, there are typologies that allow for a level of predictability. Consequently, the aim was to work with the material, allowing it to dictate the possible forms instead of imposing geometries that were incompatible with the material and production methods by introducing extra production steps.

This approach means that an application must be designed closely with the process to tailor the geometry specifically to that function and aesthetic. Even so, a degree of unpredictability still occurs in this process. The idea was to develop the method and employ strategies such as pyramidal shapes, fins and ribs to reach a point where the firing process is as predictable as baking a loaf of bread. Granted, there would be some deviations, and each will be slightly different, but the overall result is predictable and controllable. While this differs from the extreme predictability and uniformity of mass manufacturing, this may be a way of working that needs to be more widely embraced as we transition towards circular and regenerative systems of manufacture, where irregular recycled materials and biobased materials are the norm. These are materials that, no matter what, will defy the predictability and perfection of injection moulded plastics or aluminium extrusions; learning to embrace this and design for unpredictability will be key.

7.3.3 What product application can be developed that demonstrates the opportunities of the material and production system?

An evaporative cooling system was developed as an application that demonstrates the capabilities of the material and production system. As described previously, porous ceramic materials have been used to cool spaces for centuries via evaporative cooling, as the porous structure allows water to permeate the surface, creating a thin water film that can evaporate. The process of evaporation simultaneously reduces air temperature and increases humidity. While the porosity of parts produced via BJT is often seen as a barrier to application, this research sought to harness this characteristic by developing this application avenue. Experimentation with the firing schedule confirmed the ability to produce parts with a level of porosity suitable for this application, approximately 14.5% (see Figure 7.5). Furthermore, the ability of 3D printing to produce complex geometries and customised parts provided the opportunity to increase surface area and create site-specific designs, which could aid the evaporative function. Although porous ceramics have a long history as evaporative cooling mediums, the use of porous glass parts has not been explored.

Through experimentation, a modular screen was developed based on an organic ridged design that evokes the flow of moving water (see Figure 7.6). The screen is designed to cool outdoor public spaces such as seating areas, bus stops, and entrances to buildings. Each tile is unique and fits seamlessly into the overall design, like pieces in a jigsaw puzzle. This harnesses the customisation capabilities of 3D printing technologies, allowing each piece to be slightly different. Negative space is incorporated into the screen, leaving gaps between each tile to facilitate airflow and aid evaporation. The ridged design utilises self-supporting triangular structures to provide predictability in the firing process. This form also increases the

surface area, enhancing the evaporative potential. Chapter 6 provides a detailed overview of the development of this design.

An assembly system was designed to allow for the secure and adjustable fixing of the tiles to an aluminium frame. This follows the way ceramic façade panels or tiles are often mounted onto buildings. Each tile is printed with a ledge on the back which L-shaped bolts can be hooked into. A custom 3D printed bracket secures this bolt to a T-slot aluminium frame. This assembly system incorporated a strategy of designing for unpredictability and adjustability. While tolerances are always integrated into the design of an assembly, whether it be in product design or engineering, working with the BJT glass fines materials revealed that there was a level of unpredictability that needed to be accounted for. As discussed previously, the heterogeneity of the recycled glass fines, combined with the behaviour of glass in the firing process, means that any assembly system must allow for tolerances that are much greater than what would be expected in mass manufacturing. As a result, T-slot extrusions were used to allow for easily adjustable anchoring points, slots were used instead of perfectly aligned holes, and the 3D printed tiles all had five possible anchor points on either side, allowing for the most suitable one to be used during installation. These design features ensure that varying tolerances do not hinder assembly.

The assembly system is also designed for disassembly, using components that can be easily taken apart instead of glues or adhesives, ensuring circularity can be achieved. It is envisioned that at the end of life, the tiles can be repurposed or recycled, while the aluminium frame and components can be reused and installed elsewhere. An irrigation system runs through the aluminium channels to keep the tiles wet and facilitate the evaporative cooling action. To mitigate excessive water use, rainwater is utilised and recirculated. The modular and 3D printed nature of this design allows for maintenance and repair, enabling individual tiles to be removed and reprinted if necessary.

A final prototype of approximately 1m2 in size was developed. This prototype consists of 16 individual tiles and should be viewed as an excerpt of a larger evaporative screen. Since the prototype will be used for demonstration purposes, it features a dual mounting system with two detachable frames. The front frame allows for wall mounting, while the back frame is attached to a base and can serve as a standalone table-height demonstrator. As is the case in most RtD projects, findings continued to be generated during the production of the demonstrator, which could inform the next iteration. In particular, it was observed that tiles that were more bulbous tended to shrink more in the x-axis. This could only be observed when multiple tiles were manufactured together. Further prototyping and adjustment of CAD models to account for this should be considered going forward.

The overall design has customisability at its core. By employing parametric design tools alongside 3D printing, the system can be scaled and adjusted for specific spaces. Consequently, a range of vertical and horizontal installations, both large and small, can be envisioned. This ties to the site-specific requirement of evaporative cooling, allowing for a site analysis to be conducted and the system designed and located accordingly. This also connects to emerging thinking surrounding the customisation of materials and production processes more generally. As highlighted in the previous section, the constraints of the material and production system require careful tailoring of the application and form. This aligns with a growing shift from designing for universality to designing for customisability, where specific materials are produced in specific ways for specific applications. This approach differs from what happened with the widespread adoption of plastics in the 20th century.

Figure 7.5. *Evaporative cooling tile absorbing water.*

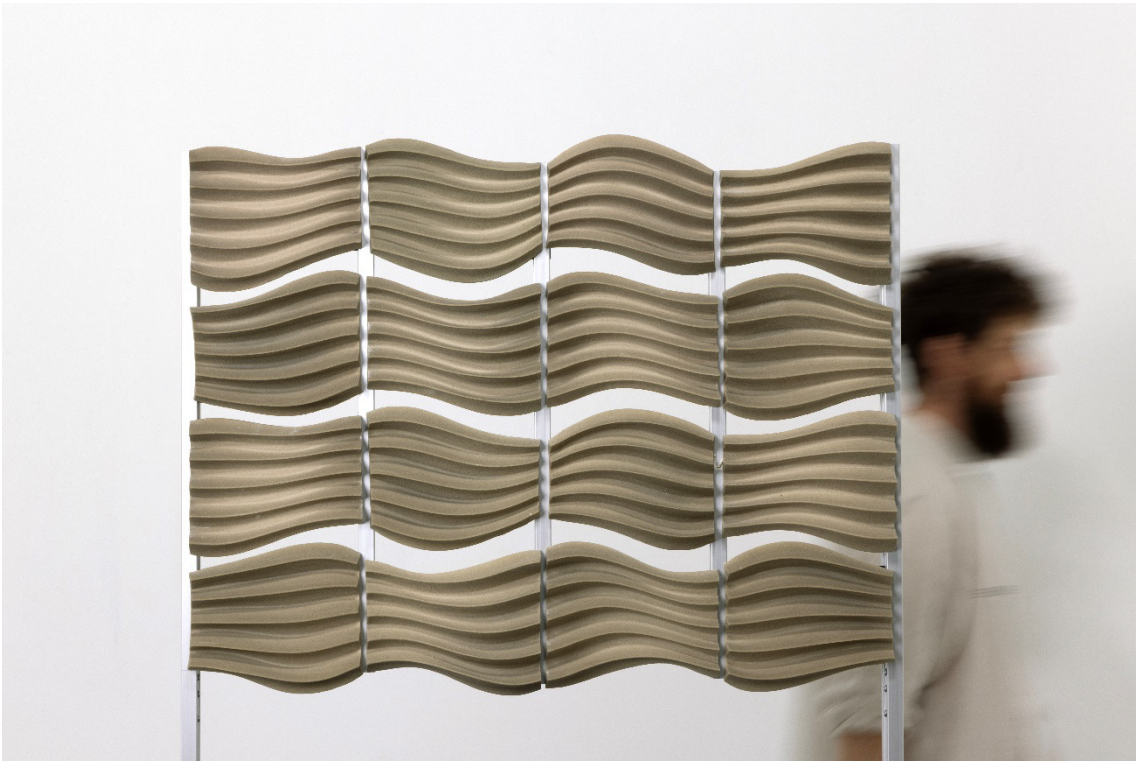

Figure 7.6. *Final prototype with figure in background.*

This “miracle material” became ubiquitous across various applications, despite the mismatch between its properties of longevity and the single-use nature of certain items. It fostered a one-size-fits-all approach, rather than a critical, tailored development where the advantages of plastic materials could be more sparingly matched with applications in which they were genuinely required. In this same vein, the designers and architects of the BioSkin evaporative cooling system discussed in Chapter 6 have refused commercialisation of their design as they believe that the “mass production” method does not align with the environmental concerns of the 21st century. Instead, they argue that high-quality outcomes, which respond to the conditions of each project and site, are the way forward. They highlight the role that 3DP can play in this, allowing for widespread customisation of designs in localised areas.

It is important to note that this is one possible application. It was chosen for its ability to harness the material qualities and production capabilities. However, numerous other avenues could be explored. The ability to produce parts that are waterproof or porous opens an array of potential areas, from homewares and lighting to tiling systems. As has been made clear, these applications would need to be designed and developed closely with the production process to ensure that geometries and forms with a degree of predictability can be created.

7.4 Contribution to Knowledge

The three sub-questions relating to the material, production, and application discussed in the previous section allow for the overarching research question to be addressed and the contributions of the research to be evaluated. This research was underpinned by the question, ‘How can recycled glass fines be transformed into a product application using a binder jet 3D printing system that can remain in a closed circular loop?’ In addressing this question, theoretical, methodological, empirical and practical contributions have been made. In assessing these contributions, the evaluation criteria for RtD projects discussed by Zimmerman et al. (2007) in Chapter 2 have also been considered.

7.4.1 Theoretical Contributions

The theoretical contribution of this research lies in the way it has consciously, thoroughly and fluidly drawn together the fields of design, circularity, materials, and 3D printing. Although each of these domains has been examined extensively in isolation, and there is growing literature that addresses the intersection of two or three of these areas—for example, it is widely acknowledged in both literature and design examples that 3D printing can act as an enabler of the circular economy or that 3D printing can enhance material engagement from designers—there remains limited work that critically examines all four areas together.

This research has highlighted not only why these domains align but how they can be effectively and holistically integrated. By layering the opportunities of 3D printing with circular strategies and material design practices, each of the domains informs and strengthens one another. This has allowed for the development of a cohesive material, production process and application that is underpinned by circularity. This is significant, as although the role of designers in producing circular products has been well established, an understanding of the role they can play in material and production processes for circularity is still evolving. Much of the literature sits in science and engineering disciplines or exists within craft-based design projects where circularity has not necessarily been subjected to critical analysis. This research

addresses that gap, highlighting how the convergence of these domains and the integration of methods from both science and design enables designers to meaningfully embed circularity at every level. This expands the scope of conventional product design, asking for designers who can fluidly work across domains to incorporate circularity not only at the product stage but also during material and production process development. As a result, this research also contributes to discourse that recognises the value of interdisciplinary approaches in tackling complex sustainability challenges.

7.4.2 Methodological Contributions

This research contributes to the methodological development of RtD and materials design projects. As RtD approaches can be criticised for their lack of transparency and methodologies in materials design are still emergent, this research has presented an RtD methodology that is specifically tailored to a materials-based project. When working at the convergence of multiple domains, a level of fluidity and adaptability is required alongside rigour and attention to detail. This has been built into the methodological approach.

Drawing on the work of Wensveen & Matthews (2014), three forms of prototyping were presented as the primary data collection method. These include: prototypes as vehicles for inquiry, which were iteratively conducted to develop the printing parameters, binder formulations and firing schedules (amongst other elements); prototypes as experimental components which were used to test specific hypotheses such as binder strength and circularity; and a prototype as a research archetype, which was used to demonstrate the application avenue of the research (see Chapter 3 for additional information). This research provides a clear example of how these three forms of prototyping can be integrated into materials design projects, to provide clear direction and address different objectives. This categorisation and employment of all three types of prototypes aids both the researcher and audiences in terms of traceability and reproducibility of the research.

Prototypes as research archetypes are most akin to traditional scientific experiments and were used in this research to integrate materials science and engineering methods which gave validity to decisions and outcomes of the research. For example, green strength testing was conducted to assess the appropriate binder type and a thermogravimetric analysis was conducted to validate the circularity of the final material. By integrating these types of experiments alongside more traditional design prototyping, a greater understanding of the material and process was developed, and claims were able to be substantiated. Greater integration of materials science and engineering methods into material design projects could provide greater validity generally, mitigating unfounded claims of greenwashing and giving further legitimacy to the field. This could further open dialogue between disciplines and contribute to interest from the industry due to validated claims and greater technology readiness.

A visual documentation method was also presented. All prototypes were rigorously documented in reflective experimental logs which recorded the aim, process data and reflections. Using the online platform Airtable, multiple mediums and aggregations of data can be employed, allowing for high quality photographs, text and videos to be integrated. The visual nature of this documentation method is particularly useful for materials-based projects, as it allows for clear capturing of material qualities and results. This documentation method also facilitates continued reflection on action which allows for ideas to emerge and be documented. The amalgamation of quantitative data pertaining to each prototype alongside qualitative reflections regarding the process, results, and opportunities effectively ensures the rigour

associated with scientific methods, which is essential for traceable and repeatable material development, while also highlighting the tacit knowledge or intuition that designers often utilise subconsciously. This method also allows for collaboration across teams of people with different expertise.

Furthermore, the research contributes to the expanding discussion concerning the role of designers in materials projects. Although the role of designers in finding and implementing applications for material innovations has been recognised, this research demonstrates how designers can actively engage in the material process from the outset. A variety of affordances and opportunities that may otherwise be overlooked or inadvertently mitigated can be identified and skillfully integrated into new application potentials (e.g., porosity). This approach ensures that promising materials are not discarded due to perceived limitations; rather, appropriate applications are explored and developed.

7.4.3 Empirical Contributions

This research presents a novel method for the binder jet 3D printing of recycled glass fines using a material formulation that allows for parts to remain circular. There are two key empirical contributions of this research: the material formulation and the production process, which include: the printing parameters and firing schedules. The specifics of these are outlined in Section 7.3. The material circularity has been confirmed by Thermogravimetric Analysis, presented in Chapter 6. Parts which are both waterproof and water absorbent with a porosity of approximately 14.5% can be produced. This has been validated by the ASTM standard C20-00(2022b) and opens application opportunities across a range of product applications. This represents a new method for the upcycling of glass fines, which allows for them to be used repeatedly, harnessing the inherent circularity of glass as a material. It also represents a new method of fabricating complex glass objects which cannot be produced via traditional glass manufacturing methods.

While the firing process can result in some unpredictability in the forms, a range of complex ridged geometries and single-height lattices have been printed and fired with a suitable level of predictability and repeatability. This represents a significant advancement in recycled glass 3D printing more generally, where complex lattice shapes have not yet been achieved. Only one other research group globally has presented work on 3D printing with glass fines materials (Thomsen et al., 2020; Sparre-Petersen & Hnídková, 2023), and work with BJT printing has been stagnant since publications from Marchelli et al. in 2011. This research has built on initial work from Marchelli et al. (2011) in several ways. Firstly, the research has demonstrated how BJT can be used with the specific and underutilised waste stream of glass fines rather than purer forms of recycled glass which can be recycled via traditional means. Secondly, a range of forms that can be predictably printed and fired without the use of inert powders have been presented. Parts that are both waterproof and porous have been developed and the circularity of parts has been verified. A lower percentage of binder is also utilised in this research. Finally, the extensive experimentation with the material and production process has allowed for an application avenue to be developed. This can act as a bridge to industry, allowing for the application potential to be persuasively presented.

Although the material formulation was developed specifically for BJT 3D printing, it could be employed in other production methods such as compression moulding. The green strength of the binder in combination with its ability to decompose in the kiln could provide compelling circular application opportunities for other processing methods. Similarly, the printing parameters, firing schedule and binder formulation could be applied to other powdered glass sources. This could allow for upcycling in the case of different recycled

glass streams or for new aesthetic and functional forms to be developed as a result of the BJT geometric capabilities.

7.4.4 Practical Contributions

This research presents a product application that harnesses the capabilities of the material and production method. An evaporative cooling screen that employs the inherent porosity of the BJT parts has been developed for practical application in outdoor public spaces. The screen was developed in accordance with design criteria for ceramic evaporative cooling systems, including the level of required porosity, surface area and airflow considerations. By pursuing the research beyond a proof of concept and exhibitable artefact stage (achieved in Chapter 5), to an application concept (achieved in Chapter 6), the research can be presented more persuasively and in a way that could lead to further commercialisation opportunities. This is important, as there is a need to ensure that circular materials and production methods are industrially scalable for more sustainable manufacturing and consumption practices to be achieved. Whilst still in the concept phase, a 1:1 scale demonstrator was built of an evaporative cooling screen using the circular BJT glass fines material with a porosity of approximately 15%. This has allowed for the research to more effectively address real-world constraints around designing for new materials and production methods and to be exhibited for wider dissemination of the research.

7.5 Limiting Factors

The primary limitation of this research is that the connection between circularity and other sustainability metrics has yet to be established. While attaining circularity has been the primary objective of this study, it is crucial to acknowledge that the implications of this for energy consumption or emissions has yet to be evaluated. Although energy requirements and waste management have been taken into consideration, quantification of these factors has not been conducted. For instance, the firing temperature for both waterproof and porous components is approximately half that of conventional glass forming techniques. This observation suggests the potential for reduced energy consumption, though specific measurements have not been performed as they fall outside the scope of this project. Prospective LCAs are emerging as a crucial tool for analysing and optimising the conceived environmental impact of emerging technologies and materials (Erakca et al., 2024). However, challenges related to data quality, availability, and the need to scale energy and material flows to industrial levels remain a barrier (Thonemann et al., 2020). As such, this complex analysis also sits outside the scope of the research but should be considered for future work.

As discussed previously, this research has developed a material and production method suitable for a specific application. The focus of the research has always been on finding stable, repeatable parameters rather than conducting an in-depth study of specific variables. As a result, neither the material formulation nor the production parameters are completely optimised, leaving significant scope for further development of both. Processes such as sieving the powder feedstock to achieve greater uniformity or quantitatively testing the binder level needed for optimal green strength would enable the generation of more universal rules.

Additionally, a complete analysis of the material properties has not been conducted. While porosity and water absorbency have been examined, other characteristics, such as mechanical strength and thermal conductivity, remain unquantified. This represents a limitation of the research, particularly regarding the relationship

between porosity and mechanical strength. Further efforts are needed to test and adapt the material for specific applications to be developed. Notably, many of the tools utilised in optimising BJT and quantifying material properties fall within the realm of materials science and engineering. This can pose a challenge for design researchers, as access may be restricted or costly.

7.6 Future Directions

The limitations discussed in Section 7.5 highlight several critical areas for future research. These, along with other potential avenues related to the key areas of materials, production, and application, will be discussed.

7.6.1 Material

As outlined in Section 7.4, there is considerable potential for further analysis of the material properties of the BJT glass fines. In particular, exploring the relationship between the mechanical strength and porosity of the components would be valuable for validating and enhancing evaporative applications. Investigating other properties, such as thermal conductivity and hardness, could also open new application pathways. Additionally, there is an opportunity to tailor the material's properties based on specific applications. For instance, powder preparation strategies like granulation could be used to increase the density of parts where this characteristic is necessary. Similarly, examining burnout strategies that might create additional voids within the material could help increase the porosity of components. Since access to material testing equipment can be challenging for design researchers, this could present an opportunity for cross-disciplinary collaboration.

There is also an opportunity for further exploration of colour. Considering the significant role that colour plays in product design, there is potential to investigate the incorporation of ceramic stains or virgin glass frits to modify and control the colouration. This should be approached with circularity in mind. As discussed in Chapter 5, many ceramic stains utilise minerals that do not burn away in the kiln. It is essential to examine their effects on circularity. Alternatively, coloured soda lime silica frits could be incorporated to adjust the colour and uphold circularity; however, this would necessitate using a percentage of virgin glass.

7.6.2 Production

In alignment with the proposed future work for the material, there is significant potential to further analyse and refine the production process. This encompasses all stages of production, including material preparation, printing, drying, and firing. While a workable and repeatable method has been established, the substantial body of literature on optimising BJT, along with craft-based work in glass firing schedules, highlights a wealth of knowledge and alternative approaches that could assist in fine-tuning the process. For instance, conducting more precise assessments of the binder quantity necessary for optimal green strength would be beneficial to the printing of complex geometries. Furthermore, while the unbound powder in each print can be reused, it was observed that there is a limit to the number of times this can be done. Quantification and established guidelines around the reuse and rehabilitation of the powder would also be advantageous.

Future work could also involve more accurate prediction of the slumping and shrinkage of parts in the kiln. This could be achieved through further experimentation and numerical models that scale CAD models to account for anisotropic shrinkage. Since many BJT parts are sintered during post-processing, various

research and software options have been developed to predict and compensate for the potential distortion of parts. This includes software options such as Live Sinter from Desktop Metal, which accounts for warping and shrinkage during sintering by oppositely warping parts. This process can be fine-tuned by 3D-scanning the results, allowing for further adjustment of the simulated part and reprinting (Desktop Metal, n.d.). Future work could develop or apply similar tools to the BJT glass fines material. Research is also emerging into the use of machine learning to help predict shrinkage and changes in 3D printed parts (Dritsas et al., 2023; Rossi et al., 2023). There is an opportunity for researchers in this space to apply these methods to this material and production system.

7.6.3 Application

Further work on the application should focus on assessing the evaporative and cooling capabilities of the design. While the application was designed in accordance with criteria for ceramic evaporative cooling systems, quantifying the impact of this system on a space is important. Further consideration of the ventilation strategy that drives air through the space and the surface of the material is a specific area identified by researchers as key to the evaporative potential (Chilton et al., 2017). As there are many site-specific factors that impact this, it falls outside the scope of this research. Installing a 1:1 demonstrator in a chosen space and analysing the performance would be a beneficial avenue, or conducting smaller-scale lab-based testing similar to that seen in the work of Vallejo (2018).

Furthermore, since higher porosity generally results in higher rates of evaporation, increasing the porosity of the evaporative cooling parts would likely be advantageous. This relates to the future work discussed above in terms of further quantifying and tailoring the material properties to a specific application. Regarding porosity, extensive research has been conducted on the development of glass foams, with reported porosity levels typically ranging from 85% to 95% (Scarinci et al., 2005). These foams are developed for applications such as thermal insulation or filtration. One method used to produce these foams involves incorporating foaming agents such as calcium carbonate into glass powders. Upon heating, these agents decompose, releasing gaseous CO_2 that becomes trapped within the viscous glass mass during the firing or sintering processes (Scarinci et al., 2005). This approach has been successfully applied to waste glass materials (Flood et al., 2020). There is significant potential to investigate these techniques to enhance the evaporative capacity of the BJT glass fines material.

Future work could also explore a range of other application avenues for both porous and waterproof parts. This could include an investigation of scale. As BJT printers with volumes up to $4m^2$ are commercially available and kiln sizes are virtually unlimited, there is potential for the individual 3D printed parts to be much larger. This means that fewer individual tiles would be needed to construct an evaporative screen; however, this may result in changes to the firing schedule, as larger parts may require longer soaking times. It was also found that changes to scale impacted the slumping of the glass, so this would need to be taken into account.

7.6.4 Impact

As highlighted in Section 7.5, there is scope to further assess the environmental impact of the material, production, and application components of the research beyond circularity. Future work should look to Life Cycle Analysis (LCA) tools to conduct this, as they are positioned as the most comprehensive method currently available. An LCA analyses the potential environmental impacts of energy, materials, and waste

across the entire life cycle, including the extraction and processing of raw materials, manufacturing, transportation, use, reuse, recycling, and final disposal. LCAs have been incorporated into government policies globally; in countries such as Denmark, they are now mandatory in the construction sector for new projects of a certain scale (BPIE, 2022; Sala et al., 2021). However, as noted previously, LCAs can be particularly difficult to conduct for emerging materials and manufacturing methods. While the flexibility of projects at this stage allows for sustainability potentials to be incorporated, there is also a lack of data and uncertainty (Galluccio et al., 2025). Often, the small scale of these projects must also be translated to higher levels in order to provide insights into the impact of their commercialisation (Erakca et al., 2024). Due to this complexity, a comprehensive LCA was outside the scope of this research, but should be considered an essential future direction to ensure the longevity and applicability of this research.

7.7 Conclusion

As linear models of production and consumption continue to devastate our environment, the need for designers to develop products and services that prioritise circularity has never been more urgent. This research highlights how industrial designers can engage in hands-on material development, providing greater control and opportunities to embed circularity within the material, production, and application. This is illustrated through the development of a method to transform the abundant yet underutilised waste stream of glass fines into circular product applications using binder jet 3D printing. This research has demonstrated how the material potential can be leveraged alongside the benefits of binder jet 3D printing to not just ‘use up’ the waste stream but transform it into valuable applications with industry potential. This has been made evident through the design and development of an evaporative cooling screen application, which harnesses the porosity of the material and the geometric capabilities of the production system to passively cool spaces. This research joins an emerging field of study at the intersection of design, circularity, materials, and 3D printing.

Bibliography

Bibliography

Aguiar, M. F., & Jugend, D. (2022). Circular product design maturity matrix: A guideline to evaluate new product development in light of the circular economy transition. *Journal of Cleaner Production*, *365*, 132732. https://doi.org/10.1016/j.jclepro.2022.132732

Ahluwalia, V. K. (2023). Thermogravimetric Analysis. In V. K. Ahluwalia, *Instrumental Methods of Chemical Analysis* (pp. 81–89). Springer Nature Switzerland.

Akbari, H., Cartalis, C., Kolokotsa, D., Muscio, A., Pisello, A. L., Rossi, F., Santamouris, M., Synnef, A., Wong, N. H., & Zinzi, M. (2015). Local climate change and urban heat island mitigation techniques – the state of the art. *Journal of civil engineering and management*, *22*(1), 1–16. https://doi.org/10.3846/13923730.2015.1111934

Alcalde-Calonge, A., Sáez-Martínez, F. J., & Ruiz-Palomino, P. (2022). Evolution of research on circular economy and related trends and topics. A thirteen-year review. *Ecological Informatics*, *70*, 101716. https://doi.org/10.1016/j.ecoinf.2022.101716

Alex Fraser. (2019, May 31). *An Exciting Development for Victoria's Circular Economy Victorian Minister for Environment Opens Sustainable Asphalt and Glass Recycling Plants* [Press Release]. http://www.alexfraser.com.au/article/News/Official_Opening_of_Alex_Fraser_Asphalt_and_Glass_Plants?section_id=14

Allan, P. (2019a). *Assessment of Australian recycling infrastructure—Glass packaging Updated*. Department of the Environment and Energy. https://www.awe.gov.au/sites/default/files/documents/assessment-australian-recycling-infrastructure-glass-packaging.pdf

Allan, P. (2019b). *Recycling market situation—Summary Review*. Department of the Environment and Energy. https://www.dcceew.gov.au/sites/default/files/documents/recycling-market-review-paper.pdf

Allwood, J. M. (2014). Squaring the Circular Economy. In E. Worrell & M. A. Reuter (Eds.), *Handbook of Recycling: State-of-the-art for Practitioners, Analysts, and Scientists* (pp. 445–477). Elsevier. https://doi.org/10.1016/B978-0-12-396459-5.00030-1

Amer, O., Boukhanouf, R., & Ibrahim, H. G. (2015). A Review of Evaporative Cooling Technologies. *International Journal of Environmental Science and Development*, *6*(2), 111–117. https://doi.org/10.7763/IJESD.2015.V6.571

Ant Studio. (n.d.). *CoolAnt - Natural Air Cooler*. Ant Studio. http://ant.studio/beehive

Aouf, R. S. (2017, June 13). Swarovski crystal 3D-printed, upcycled and made into gadgets by designers. *Dezeen.* https://www.dezeen.com/2017/06/13/swarovski-crystal-3d-printed-upcycled-turned-into-gadgets-emerging-designers-future/

APCO. (2019). *Glass Working Group 2018 Key Findings*. https://www.packagingcovenant.org.au/news/2018-working-groups-keyfindings-now-available.

Arlotti, J. C., & Knor, P. (2015). *Three-Dimensional Printing Glass Articles* (Patent No. US 8,991,211 B1). U.S. Patent and Trademark Office. https://patentimages.storage.googleapis.com/c2/6d/6c/06bf754c9842c2/US8991211.pdf

Arthur, R. (2017, July 12). London Store Upcycles 60,000 Plastic Bottles Into 3D-Printed Interior. *Forbes.* https://www.forbes.com/sites/rachelarthur/2017/12/07/london-store-upcycles-60000-plastic-bottles-into-3d-printed-interior/

Asadi-Eydivand, M., Solati-Hashjin, M., Farzad, A., & Abu Osman, N. A. (2016). Effect of technical parameters on porous structure and strength of 3D printed calcium sulfate prototypes. *Robotics and Computer-Integrated Manufacturing*, *37*, 57–67. https://doi.org/10.1016/j.rcim.2015.06.005

ASTM International. (2017). *Standard Test Methods for Flexural Properties of Unreinforced and Reinforced Plastics and Electrical Insulating Materials* (No. ASTM D790-17). https://compass.astm.org/document/?contentCode=ASTM%7CD0790-17%7Cen-US

ASTM International. (2020). *Test Method for Green Strength of Specimens Compacted from Metal Powders* (No. ASTM B312-20). https://doi.org/10.1520/B0312-20

ASTM International. (2022a). *Test Method for Tap Density of Metal Powders and Compounds* (No. B527 − 22). https://doi.org/10.1520/B0527-22

ASTM International. (2022b). *Test Methods for Apparent Porosity, Water Absorption, Apparent Specific Gravity, and Bulk Density of Burned Refractory Brick and Shapes by Boiling Water*. ASTM International. https://doi.org/10.1520/C0020-00R22

Australian Standards. (2020). *Ceramic tiles - Definitions, classification, characteristics and marking (AS 13006:2020).* https://www.standards.org.au/standards-catalogue/standard-details?designation=as-13006-2020

Azevedo, S., Godina, R., & Matias, J. (2017). Proposal of a Sustainable Circular Index for Manufacturing Companies. *Resources*, *6*(4), 63. https://doi.org/10.3390/resources6040063

Baca, I. M., Tur, S. M., Gonzalez, J. N., & Román, C. A. (2011). Evaporative cooling efficiency according to climate conditions. *Procedia Engineering*, *21*, 283–290. https://doi.org/10.1016/j.proeng.2011.11.2016

Baek, C. R., Kim, H. D., & Jang, Y.-C. (2024). Exploring glass recycling: Trends, technologies, and future trajectories. *Environmental Engineering Research*, *30*(3), 240241–0. https://doi.org/10.4491/eer.2024.241

Bai, Y., & Williams, C. B. (2018). The effect of inkjetted nanoparticles on metal part properties in binder jetting additive manufacturing. *Nanotechnology*, *29*(39), 395706. https://doi.org/10.1088/1361-6528/aad0bb

Bak-Andersen, M. (2021). *Reintroducing Materials for Sustainable Design: Design Process and Educational Practice*. Routledge.

Barati, B., & Karana, E. (2019). Affordances as Materials Potential: What Design Can Do for Materials Development. *International Journal of Design*, *13*(3), 105–123.

Bardzell, J., Bardzell, S., Dalsgaard, P., Gross, S., & Halskov, K. (2016). Documenting the Research Through Design Process. *Proceedings of the 2016 ACM Conference on Designing Interactive Systems*, 96–107. https://doi.org/10.1145/2901790.2901859

Barsoum, M. W. (2019). *Fundamentals of Ceramics* (2nd ed.). CRC Press.

Baudet, E., Ledemi, Y., Larochelle, P., Morency, S., & Messaddeq, Y. (2019). 3D-printing of arsenic sulfide chalcogenide glasses. *Optical Materials Express*, *9*(5), 2307-2317. https://doi.org/10.1364/OME.9.002307

Bechthold, M., Kane, A., & King, N. (2015). *Ceramic Material Systems: In Architecture and Interior Design*. Birkhauser.

Bernardo, E., Cedro, R., Florean, M., & Hreglich, S. (2007). Reutilization and stabilization of wastes by the production of glass foams. *Ceramics International*, *33*(6), 963–96. 8. https://doi.org/10.1016/j.ceramint.2006.02.010

Bernardo, E., Scarinci, G., Bertuzzi, P., Ercole, P., & Ramon, L. (2010). Recycling of waste glasses into partially crystallized glass foams. *Journal of Porous Materials*, *17*(3), 359–365. https://doi.org/10.1007/s10934-009-9286-3

Beveridge, P., Doménech, I., & Pacual, E. (2005). *Warm Glass: A Complete Guide to Kiln-forming Techniques : Fusing, Slumping, Casting*. Lark Books.

Blanchard, P. H., & Katz, F. R. (2016). Starch Hydrolysates. In Alistair M. Stephen & Glyn O. Phillips (Eds.), *Food Polysaccharides and Their Applications*. CRC Press.

Blomsma, F., & Brennan, G. (2017). The Emergence of Circular Economy: A New Framing Around Prolonging Resource Productivity. *Journal of Industrial Ecology*, *21*(3), 603–614. https://doi.org/10.1111/jiec.12603

Bocken, N. M. P., De Pauw, I., Bakker, C., & Van Der Grinten, B. (2016). Product design and business model strategies for a circular economy. *Journal of Industrial and Production Engineering*, *33*(5), 308–320. https://doi.org/10.1080/21681015.2016.1172124

Boulding, K. E. (1966). The Economics of the Coming Spaceship Earth. In H. Jarret (Ed.), *Environmental Quality in a Growing Economy* (pp. 3–14). Baltimore, MD: Resources for the Future/Johns Hopkins University Press.

Brandt, E., & Binder, T. (2007). Experimental design research: Genealogy – intervention – argument. *International Association of Societies of Design Research 2007: Emerging Trends in Design,* Hong Kong.

Bristogianni, T., & Oikonomopoulou, F. (2023). Glass up-casting: A review on the current challenges in glass recycling and a novel approach for recycling "as-is" glass waste into volumetric glass components. *Glass Structures & Engineering*, *8*(2), 255–302. https://doi.org/10.1007/s40940-022-00206-9

Buildings Performance Institute Europe (BPIE). (2022). *A life-cycle perspective on the building sector– Good practice in Europe*. https://www.bpie.eu/wp-content/uploads/2022/04/BPIE-BE_Good-Practices-in-EU-final.pdf

Bullseye Glass. (2020). *Heat & Glass: Technotes 4, Understanding the Effects of Temperature Variations on Bullseye Glass*. https://www.bullseyeglass.com/wp-content/uploads/2023/02/technotes_04.pdf

Butscher, A., Bohner, M., Hofmann, S., Gauckler, L., & Müller, R. (2011). Structural and material approaches to bone tissue engineering in powder-based three-dimensional printing. *Acta Biomaterialia*, *7*(3), 907–920. https://doi.org/10.1016/j.actbio.2010.09.039

Butscher, A., Bohner, M., Roth, C., Ernstberger, A., Heuberger, R., Doebelin, N., Rudolf von Rohr, P., & Müller, R. (2012). Printability of calcium phosphate powders for three-dimensional printing of tissue engineering scaffolds. *Acta Biomaterialia*, *8*(1), 373–385. https://doi.org/10.1016/j.actbio.2011.08.027

Cain, A., Afshar, F., Norton, J., & Daraie, M.-R. (1976). Traditional Cooling Systems in the Third World. *The Ecologist*, *6*(2), 60–64.

Calisto Friant, M., Vermeulen, W. J. V., & Salomone, R. (2020). A typology of circular economy discourses: Navigating the diverse visions of a contested paradigm. *Resources, Conservation and Recycling*, *161*, 104917. https://doi.org/10.1016/j.resconrec.2020.104917

Callister, W. D., & Rethwisch, D. G. (2018). *Materials Science and Engineering: An Introduction* (10th ed.). Wiley.

Campbell-Johnston, K., Vermeulen, W. J. V., Reike, D., & Brullot, S. (2020). The Circular Economy and Cascading: Towards a Framework. *Resources, Conservation & Recycling: X*, *7*, 100038. https://doi.org/10.1016/j.rcrx.2020.100038

Carter, C. B., & Norton, M. G. (2013). *Ceramic Materials: Science and Engineering*. Springer Science & Business Media.

Castilho, M., Gouveia, B., Pires, I., Rodrigues, J., & Pereira, M. (2015). The role of shell/core saturation level on the accuracy and mechanical characteristics of porous calcium phosphate models produced by 3Dprinting. *Rapid Prototyping Journal*, *21*(1), 43–55. https://doi.org/10.1108/RPJ-02-2013-0015

Castro, C. G., Trevisan, A. H., Pigosso, D. C. A., & Mascarenhas, J. (2022). The rebound effect of circular economy: Definitions, mechanisms and a research agenda. *Journal of Cleaner Production*, *345*, 131136. https://doi.org/10.1016/j.jclepro.2022.13113

Castro Gutierrez, N., Durrieu, V., Raynaud, C., & Rouilly, A. (2016). Influence of DE-value on the physicochemical properties of maltodextrin for melt extrusion processes. *Carbohydrate Polymers*, *144*, 464–473. https://doi.org/10.1016/j.carbpol.2016.03.004

Chen, Q., Juste, E., Lasgorceix, M., Petit, F., & Leriche, A. (2022). Binder jetting process with ceramic powders: Influence of powder properties and printing parameters. *Open Ceramics*, *9*, 100218. https://doi.org/10.1016/j.oceram.2022.100218

Cheny, T., Colin, C., & Verquin, B. (2024). Experimental evaluation of binder infiltration depth and axial overlap to control properties of green parts produced by Binder Jetting. *Additive Manufacturing*, *87*, 104231. https://doi.org/10.1016/j.addma.2024.104231

Chertow, M., & Ehrenfeld, J. (2012). Self-Organizing Systems: Toward a Theory of Industrial Symbiosis. *Journal of Industrial Ecology*, *16*. https://doi.org/10.1111/j.1530-9290.2011.00450.x

Chilton, J., Guillott, M., & Vallejo, J. (2017). Predicting Evaporative Cooling Performance of Wetted Decorative Porous Ceramic Systems in Early Design Stages. In R. Brotas, S. Roaf & F. Nicol (Eds.), *Design to Thrive: Proceedings Volume 3: PLEA International Conference* (pp. 3738–3745). NCEUB. https://plea2017.net/wp-content/themes/plea2017/docs/R_PLEA2017_proceedings_volume_III.pdf

Cho, S., Jeong, D., & Kim, H. (2020). Influence of powder characteristics on shrinkage behavior of 3D-Printed glass structures. *Ceramics International*, *46*(10), 16827–16832. https://doi.org/10.1016/j.ceramint.2020.03.259

Choong, Y. H., Krishnan, M., & Gupta, M. (2022). A printability evaluation of fine and coarse powder in binder jetting of dense and porous copper parts. *Progress in Additive Manufacturing*. https://doi.org/10.1007/s40964-022-00380-w

Chu, Y., Fu, X., Luo, Y., Canning, J., Tian, Y., Cook, K., Zhang, J., & Peng, G.-D. (2019). Silica optical fiber drawn from 3D printed preforms. *Optics Letters*, *44*(21), 5358-5361. https://doi.org/10.1364/OL.44.005358

Chumnanklang, R., Panyathanmaporn, T., Sitthiseripratip, K., & Suwanprateeb, J. (2007). 3D printing of hydroxyapatite: Effect of binder concentration in pre-coated particle on part strength. *Materials Science and Engineering: C*, *27*(4), 914–921. https://doi.org/10.1016/j.msec.2006.11.004

Clèries, L., & Rognoli, V. (2021). Materials Designers: A New Design Discipline. In *Material Designers: Boosting talent towards circular economies* (pp. 43–47). https://research.elisava.net/assets/documents/material-designers.pdf

Clèries, L., Rognoli, V., Solanki, S., & Llorach, P. (Eds.). (2020). *Material Designers: Boosting talent towards circular economies*. Elisava, Politecnico di Milano, Matter. https://research.elisava.net/assets/documents/material-designers.pdf

Close the glass loop. (2024). *Performance of Packaging Glass Recycling in Europe*. https://closetheglassloop.eu/wp-content/uploads/2025/01/Performance-of-Packaging-Glass-Recycling-in-Europe-Report_2024-compr.pdf

Colombo, P., & Franchin, G. (2021). Printing glass in the nano. *Nature Materials*, *20*(11), 1454–1456. https://doi.org/10.1038/s41563-021-01137-6

Continuum Powders. (n.d.). *Sustainable Metal Powders Fueling Advanced Manufacturing*. https://www.continuumpowders.com/

Cooperstein, I., Shukrun, E., Press, O., Kamyshny, A., & Magdassi, S. (2018). Additive Manufacturing of Transparent Silica Glass from Solutions. *ACS Applied Materials & Interfaces*, *10*(22), 18879–18885. https://doi.org/10.1021/acsami.8b03766

Corona, B., Shen, L., Reike, D., Rosales Carreón, J., & Worrell, E. (2019). Towards sustainable development through the circular economy—A review and critical assessment on current circularity metrics. *Resources, Conservation and Recycling*, *151*, 104498. https://doi.org/10.1016/j.resconrec.2019.104498

Corvellec, H., Stowell, A. F., & Johansson, N. (2022). Critiques of the circular economy. *Journal of Industrial Ecology*, *26*(2), 421–432. https://doi.org/10.1111/jiec.13187

Cross, N. (2007). From a Design Science to a Design Discipline: Understanding Designerly Ways of Knowing and Thinking. In R. Michel (Ed.), *Design Research Now: Essays and Selected Projects* (pp. 41–54). Birkhäuser. https://doi.org/10.1007/978-3-7643-8472-2_3

Cuevas, K., Chougan, M., Martin, F., Ghaffar, S. H., Stephan, D., & Sikora, P. (2021). 3D printable lightweight cementitious composites with incorporated waste glass aggregates and expanded microspheres – Rheological, thermal and mechanical properties. *Journal of Building Engineering*, *44*, 102718. https://doi.org/10.1016/j.jobe.2021.102718

Cullen, J. M. (2017). Circular Economy: Theoretical Benchmark or Perpetual Motion Machine? *Journal of Industrial Ecology*, *21*(3), 483–486. https://doi.org/10.1111/jiec.12599

Cummings, K. (2001). *Techniques of kiln-formed glass* (2nd ed.). A&C Black Publishers ; University of Pennsylvania Press.

Cummings, K. (2009). *Contemporary Kiln-formed Glass: A World Survey*.A&C Black Publishers ; University of Pennsylvania Press.

Cummings, K., & Stewart, M. (2013). Building on the past: The pâtes-de-verre sculpture of Max Stewart. *Craft Research*, *4*(2), 181–201. https://doi.org/10.1386/crre.4.2.181_1

Dalsgaard, P., & Halskov, K. (2012). Reflective design documentation. *Proceedings of the Designing Interactive Systems Conference*, 428–437. https://doi.org/10.1145/2317956.2318020

Datsiou, K. C., Saleh, E., Spirrett, F., Goodridge, R., Ashcroft, I., & Eustice, D. (2019). Additive manufacturing of glass with laser powder bed fusion. *Journal of the American Ceramic Society*, *102*(8), 4410–4414. https://doi.org/10.1111/jace.16440

Datsiou, K. C., Spirrett, F., Ashcroft, I., Magallanes, M., Christie, S., & Goodridge, R. (2021). Laser powder bed fusion of soda lime silica glass: Optimisation of processing parameters and evaluation of part properties. *Additive Manufacturing*, *39*, 101880. https://doi.org/10.1016/j.addma.2021.101880

De Los Rios, I. C., & Charnley, F. J. S. (2017). Skills and capabilities for a sustainable and circular economy: The changing role of design. *Journal of Cleaner Production*, *160*, 109–122. https://doi.org/10.1016/j.jclepro.2016.10.130

Den Hollander, M. C., Bakker, C. A., & Hultink, E. J. (2017). Product Design in a Circular Economy: Development of a Typology of Key Concepts and Terms. *Journal of Industrial Ecology*, *21*(3), 517–525. https://doi.org/10.1111/jiec.12610

Department of Agriculture, Water and the Environment. (2021). *Waste Glass Industry Standards—Snapshot of MRA Consulting Group's Report*. https://www.dcceew.gov.au/sites/default/files/documents/waste-glass-industry-standards-snapshot.pdf

Department of Environment and Energy. (2018). *Analysis of Australia's municipal recycling infrastructure capacity.* https://www.dcceew.gov.au/sites/default/files/documents/waste-stocktake-report.pdf

Desktop Metal. (n.d.). *Lidve Sinter™ – Sintering simulation software for metal binder jet 3D printing success*. Desktop Metal. https://www.desktopmetal.com/products/livesinter

Despeisse, M., Baumers, M., Brown, P., Charnley, F., Ford, S. J., Garmulewicz, A., Knowles, S., Minshall, T. H. W., Mortara, L., Reed-Tsochas, F. P., & Rowley, J. (2017). Unlocking value for a circular economy through 3D printing: A research agenda. *Technological Forecasting and Social Change*, *115*, 75–84. https://doi.org/10.1016/j.techfore.2016.09.021

Destino, J. F., Dudukovic, N. A., Johnson, M. A., Nguyen, D. T., Yee, T. D., Egan, G. C., Sawvel, A. M., Steele, W. A., Baumann, T. F., Duoss, E. B., Suratwala, T., & Dylla-Spears, R. (2018). 3D Printed Optical Quality Silica and Silica–Titania Glasses from Sol–Gel Feedstocks. *Advanced Materials Technologies*, *3*(6), 1700323. https://doi.org/10.1002/admt.201700323

Dewi, G. K., Widyorini, R., & Lukmandaru, G. (2021). Application of maltodextrin-based adhesive on particleboard made from Salacca frond. *BioResources*, *17*(1), 190–206. https://doi.org/10.15376/biores.17.1.190-206

Diener, S., Zocca, A., & Günster, J. (2021). Literature review: Methods for achieving high powder bed densities in ceramic powder bed based additive manufacturing. *Open Ceramics*, *8*, 100191. https://doi.org/10.1016/j.oceram.2021.100191

Dokter, G., Thuvander, L., & Rahe, U. (2021). How circular is current design practice? Investigating perspectives across industrial design and architecture in the transition towards a circular economy. *Sustainable Production and Consumption*, *26*, 692–708. https://doi.org/10.1016/j.spc.2020.12.032

Domínguez, S. A., & Flor, F. J. S. de la. (2016). The Effect Of Evaporative Cooling Techniques On Reducing Urban Heat. In M. Santamouris & D. Kolokotsa (Eds.), *Urban Climate Mitigation Techniques* (pp. 113-130). Routledge.

Dorula, M., Khademitab, M., Jamalkhani, M., & Mostafaei, A. (2024). Location dependency of green density and dimension variation in binder jetted parts. *The International Journal of Advanced Manufacturing Technology*, *132*(5), 2853–2861. https://doi.org/10.1007/s00170-024-13529-4

Doulos, L., Santamouris, M., & Livada, I. (2004). Passive cooling of outdoor urban spaces. The role of materials. *Solar Energy*, *77*(2), 231–249. https://doi.org/10.1016/j.solener.2004.04.005

Dritsas, S., Ravindran, R., Hoo, J. L., & Fernandez, J. G. (2023). Shrinkage prediction and correction in material extrusion of cellulose-chitin biopolymers using neural network regression. *Virtual and Physical Prototyping*, *18*(1), e2225039. https://doi.org/10.1080/17452759.2023.2225039

Du, W., Miao, G., Pei, Z., & Ma, C. (2021). Comparison of Flowability and Sinterability Among Different Binder Jetting Feedstock Powders: Nanopowder, Micropowder, and Granulated Powder. *Journal of Micro and Nano-Manufacturing, 9*(2). 021008. https://doi.org/10.1115/1.4052253

Du, W., Ren, X., Ma, C., & Pei, Z. (2017). Binder Jetting Additive Manufacturing of Ceramics: A Literature Review. *Proceedings of the ASME 2017 International Mechanical Engineering Congress and Exposition. Volume 14: Emerging Technologies; Materials: Genetics to Structures; Safety Engineering and Risk Analysis.* V014T07A006. https://doi.org/10.1115/IMECE2017-70344

Du, W., Ren, X., Pei, Z., & Ma, C. (2020). Ceramic Binder Jetting Additive Manufacturing: A Literature Review on Density. *Journal of Manufacturing Science and Engineering*, *142*(4), 040801. https://doi.org/10.1115/1.4046248

Duarte Poblete, S. S., Anselmi, L., & Rognoli, V. (2023). Emerging materials fostering interdisciplinary collaboration in Materials Design. In Y. Ghim and C. Shin (Eds.), *Proceedings of the 14th International Conference on Applied Human Factors and Ergonomics and the affiliated conferences* (pp. 119-129). AHFE Open Access. https://doi.org/10.54941/ahfe100297

Duarte Poblete, S. S., Romani, A., & Rognoli, V. (2024). Emerging materials for transition: A taxonomy proposal from a design perspective. *Sustainable Futures*, *7*, 100155. https://doi.org/10.1016/j.sftr.2024.100155

Dudukovic, N. A., Wong, L. L., Nguyen, D. T., Destino, J. F., Yee, T. D., Ryerson, F. J., Suratwala, T., Duoss, E. B., & Dylla-Spears, R. (2018). Predicting Nanoparticle Suspension Viscoelasticity for Multimaterial 3D Printing of Silica–Titania Glass. *ACS Applied Nano Materials*, *1*(8), 4038–4044. https://doi.org/10.1021/acsanm.8b00821

Dunn, K. (2017). *Prototyping Models of Climate Change: New Approaches to Modelling Climate Change Data. 3D printed models of Climate Change research created in collaboration with Climate Scientists* [Doctoral dissertation, University of Sydney]. Sydney eScholarship Repository. https://ses.library.usyd.edu.au/handle/2123/17623

Dylla-Spears, R., Yee, T. D., Sasan, K., Nguyen, D. T., Dudukovic, N. A., Ortega, J. M., Johnson, M. A., Herrera, O. D., Ryerson, F. J., & Wong, L. L. (2020). 3D printed gradient index glass optics. *Science Advances*, *6*(47), eabc7429. https://doi.org/10.1126/sciadv.abc7429

Dzhengiz, T., Miller, E. M., Ovaska, J., & Patala, S. (2023). Unpacking the circular economy: A problematizing review. *International Journal of Management Reviews*, *25*(2), 270–296. https://doi.org/10.1111/ijmr.12329

Ecovative. (n.d.). *Mushroom® Packaging is Back, and Growing*. https://shop.ecovative.com/blogs/blog/mushpack-is-back-and-growing

Elia, V., Gnoni, M. G., & Tornese, F. (2017). Measuring circular economy strategies through index methods: A critical analysis. *Journal of Cleaner Production*, *142*, 2741–2751. https://doi.org/10.1016/j.jclepro.2016.10.196

Ellen MacArthur Foundation. (2013). *Towards the circular economy Vol. 1: An economic and business rationale for an accelerated transition*. https://ellenmacarthurfoundation.org/towards-the-circular-economy-vol-1-an-economic-and-business-rationale-for-an

Ellen MacArthur Foundation. (2015). *Towards a circular economy: Business rationale for an accelerated transition*. https://www.ellenmacarthurfoundation.org/towards-a-circular-economy-business-rationale-for-an-accelerated-transition

Ellen MacArthur Foundation. (2019). *Completing the Picture: How the Circular Economy Tackles Climate Change*. https://www.ellenmacarthurfoundation.org/completing-the-picture

Envirosand (2019). Crushed Glass [Safety Data sheet].

EPA NSW. (2010). *Environmental Benefits of Recycling*. https://www.epa.nsw.gov.au/your-environment/recycling-and-reuse/business-government-recycling/recyculator/benefits-of-recycling

EPA Victoria. (2019). *Fact sheet: Use of glass fines*. https://www.epa.vic.gov.au/about-epa/publications/1748

Erakca, M., Baumann, M., Helbig, C., & Weil, M. (2024). Systematic review of scale-up methods for prospective life cycle assessment of emerging technologies. *Journal of Cleaner Production*, *451*, 142161. https://doi.org/10.1016/j.jclepro.2024.142161

Etherington, R. (2011, June 28). The Solar Sinter by Markus Kayser. *Dezeen*. https://www.dezeen.com/2011/06/28/the-solar-sinter-by-markus-kayser/

European Commission. (2015). *Closing the loop – An EU action plan for the circular economy*. https://eur-lex.europa.eu/legal-content/EN/TXT/?uri=CELEX:52015DC0614

Fardeheb, F. (2009). Examination and Review of Passive Solar Cooling Strategies in Middle Eastern and North African Vernacular Architecture. In D. Y. Goswami & Y. Zhao (Eds.), *Proceedings of ISES World Congress 2007 (Vol. I – Vol. V)* (pp. 2511–2515). Springer. https://doi.org/10.1007/978-3-540-75997-3_508

Fateri, M., & Gebhardt, A. (2014). Jewelry Fabrication via Selective Laser Melting of Glass. *Proceedings of the ASME 2014 12th Biennial Conference on Engineering Systems Design and Analysis. Volume 1: Applied Mechanics; Automotive Systems; Biomedical Biotechnology Engineering; Computational Mechanics; Design; Digital Manufacturing; Education; Marine and Aerospace Applications*, V001T06A005. https://doi.org/10.1115/ESDA2014-20380

Fateri, M., & Gebhardt, A. (2015). Selective Laser Melting of Soda-Lime Glass Powder. *International Journal of Applied Ceramic Technology*, *12*(1), 53–61. https://doi.org/10.1111/ijac.12338

Fathy, H. (1986). *Natural energy and vernacular architecture: Principles and examples with reference to hot arid climates*. University of Chicago Press.

Feng, J., Haddad, S., Gao, K., Garshasbi, S., Ulpiani, G., Santamouris, M., Ranzi, G., & Bartesaghi-Koc, C. (2023). Fighting urban climate change—State of the art of mitigation technologies. In R. Paolini & M. Santamouris (Eds.), *Urban Climate Change and Heat Islands* (pp. 227–296). Elsevier. https://doi.org/10.1016/B978-0-12-818977-1.00006-5

Fernando Laposse. (n.d.). *Corn Veneer (Totoxmotle)*. https://www.fernandolaposse.com/totomoxle

Ferreira, I. A., Godina, R., & Carvalho, H. (2021). Waste Valorization through Additive Manufacturing in an Industrial Symbiosis Setting. *Sustainability*, *13*(1), 234. https://doi.org/10.3390/su13010234

Ferreira, P., Apolinário, A., & Forman, G. (2025). Bridging Innovation in Materials Selection and Design Education. In D. Raposo, J. Neves, R. Silva, L. Correia Castilho, & R. Dias (Eds.), *Advances in Design, Music and Arts III* (Vol. 48, pp. 400–415). Springer Nature Switzerland. https://doi.org/10.1007/978-3-031-74975-9_31

Findeli, A., Brouillet, D., Martin, S., Moineau, C., & Tarrago, R. (2008). Research through Design and Transdisciplinarity: A Tentative Contribution to the Methodology of Design Research. In Swiss Design Network (Ed.), *Focused—Current Design Research Projects and Methods* (pp. 67-94). Swiss Design Network.

Flood, M., Bhat, T., Kandare, E., Fennessy, L., Lockrey, S., Avendano Franco, A., & Glover, J. (2019). *Glass fines—Final Report*. Sustainability Victoria. https://assets.sustainability.vic.gov.au/susvic/Report-Waste-Glass-Fines-RMIT.pdf

Flood, M., Fennessy, L., Lockrey, S., Avendano, A., Glover, J., Kandare, E., & Bhat, T. (2020). Glass Fines: A review of cleaning and up-cycling possibilities. *Journal of Cleaner Production*, *267*, 121875. https://doi.org/10.1016/j.jclepro.2020.121875

Ford, B. (2001). Passive downdraught evaporative cooling: Principles and practice. *Architectural Research Quarterly*, *5*(3), 271–280. https://doi.org/10.1017/S1359135501001312

Ford, S., & Despeisse, M. (2016). Additive manufacturing and sustainability: An exploratory study of the advantages and challenges. *Journal of Cleaner Production*, *137*, 1573–1587. https://doi.org/10.1016/j.jclepro.2016.04.150

Forust. (n.d.). *Forust Technology*. https://www.forust.com/technology

Francis, L. F. (2015). *Materials Processing: A Unified Approach to Processing of Metals, Ceramics and Polymers*. Academic Press.

Franklin, K., & Till, C. (2018). *Radical Matter: Rethinking Materials for a Sustainable Future*. Thames & Hudson Incorporated.

Frayling, C. (1993). Research in art and design. *Royal College of Art Research Papers*, *1*(1).

Frayling, C. (2015, June 4). *RTD 2015 Provocation by Sir Christopher Frayling Part 1: Research Through Design Evolution* [Interview]. RTD Conference Series. https://vimeo.com/129775325

Furszyfer Del Rio, D. D., Sovacool, B. K., Foley, A. M., Griffiths, S., Bazilian, M., Kim, J., & Rooney, D. (2022). Decarbonizing the glass industry: A critical and systematic review of developments, sociotechnical systems and policy options. *Renewable and Sustainable Energy Reviews*, *155*, 111885. https://doi.org/10.1016/j.rser.2021.111885

Galluccio, G., Tamke, M., Nicholas, P., Svilans, T., Gaudillière-Jami, N., & Thomsen, M. R. (2025). Material Stories: Assessing Sustainability of Digital Fabrication with Bio-Based Materials Through LCA. In M. Kioumarsi & B. Shafei (Eds.), *The 1st International Conference on Net-Zero Built Environment* (Vol. 237, pp. 25–37). Springer Nature Switzerland. https://doi.org/10.1007/978-3-031-69626-8_3

Gan, A. W. J., Guida, G., Kim, D., Shah, D., Youn, H., & Seibold, Z. (2022). Modulo Continuo—5-axis ceramic additive manufacturing applications for evaporative cooling facades modules. In B. Pak, G. Wurzer & R. Stouffs (Eds.), *Co-creating the Future: Inclusion in and through Design - Proceedings of the 40th Conference on Education and Research in Computer Aided Architectural Design in Europe (eCAADe 2022)* (Vol. 1, pp. 47-55). https://doi.org/10.52842/conf.ecaade.2022.1.047

Garmulewicz, A., Holweg, M., Veldhuis, H., & Yang, A. (2018). Disruptive Technology as an Enabler of the Circular Economy: What Potential Does 3D Printing Hold? *California Management Review*, *60*(3), 112–132. https://doi.org/10.1177/0008125617752695

Gaver, W. (2012). What should we expect from research through design? *Proceedings of the SIGCHI Conference on Human Factors in Computing Systems*, 937–946. https://doi.org/10.1145/2207676.2208538

Geissdoerfer, M., Savaget, P., Bocken, N. M. P., & Hultink, E. J. (2017). The Circular Economy – A new sustainability paradigm? *Journal of Cleaner Production*, *143*, 757–768. https://doi.org/10.1016/j.jclepro.2016.12.048

Ghisellini, P., Cialani, C., & Ulgiati, S. (2016). A review on circular economy: The expected transition to a balanced interplay of environmental and economic systems. *Journal of Cleaner Production*, *114*, 11–32. https://doi.org/10.1016/j.jclepro.2015.09.007

Gibson, I., Rosen, D., Stucker, B., & Khorasani, M. (2021). *Additive Manufacturing Technologies* (3rd ed.). Springer International Publishing.

Gildenhaar, R., Knabe, C., Gomes, C., Linow, U., Houshmand, A., & Berger, G. (2011). Calcium Alkaline Phosphate Scaffolds for Bone Regeneration 3D-Fabricated by Additive Manufacturing. *Key Engineering Materials*, *493–494*, 849–854. https://doi.org/10.4028/www.scientific.net/KEM.493-494.849

GlassCampus (n.d.). *Understanding Firing Schedules*. Glass Campus Publishing. https://www.glasscampus.com/tutorials/pdf/Understanding_Firing_Schedules.pdf

Goddin, J., Marshall, K., Pereira, A., Tuppen, C., Herrmann, S., Jones, S., Krieger, T., Lenges, C., Coleman, B., C. Jason Pierce, Iliefski-Janols, S., Veenendaal, R., Stoltz, P., Ford, L., Goodman, T., Mariagiovanna Vetere, Mistry, M., Graichen, F., Natarajan, A., … Sullens, W. (2019). *Circularity Indicators: An Approach to Measuring Circularity, Methodology*. https://doi.org/10.13140/RG.2.2.29213.84962

Gol, F., Saritas, Z. G., Cıbuk, S., Ture, C., Kacar, E., Yilmaz, A., Arslan, M., & Sen, F. (2022). Coloring effect of iron oxide content on ceramic glazes and their comparison with the similar waste containing materials. *Ceramics International*, *48*(2), 2241–2249. https://doi.org/10.1016/j.ceramint.2021.10.001

Gonzalez, J. A., Mireles, J., Lin, Y., & Wicker, R. B. (2016). Characterization of ceramic components fabricated using binder jetting additive manufacturing technology. *Ceramics International*, *42*(9), 10559–10564. https://doi.org/10.1016/j.ceramint.2016.03.079

Gordon, J. E. (2006). *The New Science of Strong Materials: Or Why You Don't Fall Through the Floor*. Princeton University Press.

Guo, P., Meng, W., Nassif, H., Gou, H., & Bao, Y. (2020). New perspectives on recycling waste glass in manufacturing concrete for sustainable civil infrastructure. *Construction and Building Materials*, *257*, 119579. https://doi.org/10.1016/j.conbuildmat.2020.119579

Haddad, S., Paolini, R., Synnefa, A., & Santamouris, M. (2018). Mitigation of urban overheating in three Australian cities (Darwin, Alice Springs and Western Sydney). In P. Rajagopalan & M. M. Andamon (Eds.), *Proceedings of 52nd International Conference of the Architectural Science Association (ANZAScA): Engaging Architectural Science: Meeting the Challenges of Higher Density* (pp. 577–583).The Architectural Science Association (ANZAScA).

Hahn, J. (2021, July 15). Asao Tokolo 3D-prints Tokyo 2020 podiums from plastic waste donated by citizens. *Dezeen*. https://www.dezeen.com/2021/07/15/podiums-tokyo-2020-olympics-asao-tokolo/

Hall, C., & Hoff, W. D. (2021). *Water transport in brick, stone and concrete* (3rd ed.). CRC Press.

Hand, R. J. (2021). Soda-Lime-Silica Glasses. In M. Pomeroy (Ed.), *Encyclopedia of Materials: Technical Ceramics and Glasses* (Vol. 1, pp. 483–495). Elsevier. https://doi.org/10.1016/B978-0-12-818542-1.00054-0

Harder, J. (2018, May). Glass recycling – Current market trends—Recovery. *Recovery: Recycling Technology Worldwide*. https://www.recovery-worldwide.com/en/artikel/glass-recycling-current-market-trends-3248774.html

He, J., & Hoyano, A. (2010). Experimental study of cooling effects of a passive evaporative cooling wall constructed of porous ceramics with high water soaking-up ability. *Building and Environment*, *45*(2), 461–472. https://doi.org/10.1016/j.buildenv.2009.07.002

He, J., & Hoyano, A. (2011). Experimental study of practical applications of a passive evaporative cooling wall with high water soaking-up ability. *Building and Environment*, *46*(1), 98–108. https://doi.org/10.1016/j.buildenv.2010.07.004

He, X., Lu, W., Sun, C., Khalesi, H., Mata, A., Andaleeb, R., & Fang, Y. (2021). Cellulose and cellulose derivatives: Different colloidal states and food-related applications. *Carbohydrate Polymers*, *255*, 117334. https://doi.org/10.1016/j.carbpol.2020.117334

Hegab, H., Khanna, N., Monib, N., & Salem, A. (2023). Design for sustainable additive manufacturing: A review. *Sustainable Materials and Technologies*, *35*, e00576. https://doi.org/10.1016/j.susmat.2023.e00576

Heimann, R. B. (2010). *Classic and Advanced Ceramics: From Fundamentals to Applications*. John Wiley & Sons.

Heinze, T., El Seoud, O. A., & Koschella, A. (2018). *Cellulose Derivatives: Synthesis, Structure, and Properties*. Springer International Publishing.

Heriyanto, Pahlevani, F., & Sahajwalla, V. (2018). From waste glass to building materials – An innovative sustainable solution for waste glass. *Journal of Cleaner Production*, *191*, 192–206. https://doi.org/10.1016/j.jclepro.2018.04.214

Herrick, F. W., Casebier, R. L., Hamilton, J. K., & Sandberg, K. R. (1983). Microfibrillated cellulose: Morphology and accessibility. *Journal of Applied Polymer Science: Applied Polymer Symposium*, *37*, 797-813.

Herriott, R. (2019). What kind of research is research through design. In M. Evans, A. Shaw & J. Na (Eds.), *Design revolutions: IASDR 2019 Conference Proceedings. Volume 1: Change, Voices, Open* (pp. 699-708). Manchester Metropolitan University Press.

Hettiarachchi, B. D., Brandenburg, M., & Seuring, S. (2022). Connecting additive manufacturing to circular economy implementation strategies: Links, contingencies and causal loops. *International Journal of Production Economics*, *246*, 108414. https://doi.org/10.1016/j.ijpe.2022.108414

Hirschberg, C., Sun, C. C., Risbo, J., & Rantanen, J. (2019). Effects of Water on Powder Flowability of Diverse Powders Assessed by Complimentary Techniques. *Journal of Pharmaceutical Sciences*, *108*(8), 2613–2620. https://doi.org/10.1016/j.xphs.2019.03.012

Hollister, P. (1988, August/September). Pâte de Verre: The French Connection. *American Craft*, *48*(4), 40-47.

Houde, S., & Hill, C. (1997). What do Prototypes Prototype? In M. Helander, T. Landauer, and P. Prabhu (Eds.), *Handbook of Human-Computer Interaction* (2nd ed., pp. 367-381). Elsevier Science.

Hubert, M. (2019). Industrial Glass Processing and Fabrication. In J. D. Musgraves, J. Hu, & L. Calvez (Eds.), *Springer Handbook of Glass* (pp. 1195–1231). Springer International Publishing. https://doi.org/10.1007/978-3-319-93728-1_34

Ibrahim, E., Shao, L., & Riffat, S. B. (2003). Performance of porous ceramic evaporators for building cooling application. *Energy and Buildings*, *35*(9), 941–949. https://doi.org/10.1016/S0378-7788(03)00019-7

Inamura, C., Stern, M., Lizardo, D., Houk, P., & Oxman, N. (2018). Additive Manufacturing of Transparent Glass Structures. *3D Printing and Additive Manufacturing*, *5*(4), 269–283. https://doi.org/10.1089/3dp.2018.0157

Ingredion. (2019). *BONDSTAR PLUS 8000 Technical Specification*.

Ingredion. (2021). *NATIONAL 208 Technical Specification*.

International Energy Agency. (2018). *The Future of Cooling: Opportunities for energy-efficient air conditioning*. https://www.iea.org/reports/the-future-of-cooling

International Resource Panel. (2018). *Re-defining Value – The Manufacturing Revolution. Remanufacturing, Refurbishment, Repair and Direct Reuse in the Circular Economy.* United Nations Environment Programme. https://www.resourcepanel.org/reports/re-defining-value-manufacturing-revolution

International Resource Panel. (2020). *Resource Efficiency and Climate Change: Material Efficiency Strategies for a Low-Carbon Future*. United Nations Environment Programme. https://www.resourcepanel.org/reports/resource-efficiency-and-climate-change

iQRenew. (2022). Crushed Glass [Safety Data Sheet].

ISO/ASTM International. (2016). *Standard Terminology for Additive Manufacturing – General Principles – Terminology* (No. ISO/ASTM52900-15). https://compass.astm.org/document/?contentCode=ASTM%7CF3177-15%7Cen-US

Jackson, B. (2016, December 9). *Micron3DP & MIT 3D printing in molten glass*. 3D Printing Industry. https://3dprintingindustry.com/newsiq/micron3dp-mit-3d-printing-molten-glass-100702/

Jaidka, S., Sharma, R., Kaur, S., & Singh, D. P. (2022). Scanning Electron Microscopy (SEM): Learning to Generate and Interpret the Topographical Aspects of Materials. In S.-K. Kamaraj, A. Thirumurugan, S. S. Dhanabalan, & S. A. Hevia (Eds.), *Microscopic Techniques for the Non-Expert* (pp. 165–185). Springer International Publishing. https://doi.org/10.1007/978-3-030-99542-3_7

Jelinski, L. W., Graedel, T. E., Laudise, R. A., McCall, D. W., & Patel, C. K. (1992). Industrial ecology: Concepts and approaches. *Proceedings of the National Academy of Sciences*, *89*(3), 793–797. https://doi.org/10.1073/pnas.89.3.793

Jernegan, J. (2009). *Dry Glazes*. A&C Black.

Jonas, W. (2007). Design Research and its Meaning to the Methodological Development of the Discipline. In R. Michel (Ed.), *Design Research Now* (pp. 187–206). Birkhäuser. https://doi.org/10.1007/978-3-7643-8472-2_11

Kääriäinen, P., Tervinen, L., Vuorinen, T., & Riutta, N. (2020). *The CHEMARTS Cookbook*. Aalto University.

Karana, E., Barati, B., & Rognoli, V. (2015). Material Driven Design (MDD): A Method to Design for Material Experiences. *International Journal of Design, 9*(2), 35-54.

Kathirvel, S., Murugesan, S., & Marathakam, A. (2022). Recent Updates on Methods, Applications, and Practical Uses of Scanning Electron Microscopy in Various Life Sciences. In S.-K. Kamaraj, A. Thirumurugan, S. S. Dhanabalan, & S. A. Hevia (Eds.), *Microscopic Techniques for the Non-Expert* (pp. 187–199). Springer International Publishing. https://doi.org/10.1007/978-3-030-99542-3_8

Kayser, M. (2011). *Solar Sinter*. Kayser Works. https://kayserworks.com/#/798817030644/

Kennedy, H. M., & Fischer, A. C. (1984). Starch and dextrins in prepared adhesives. In R. L. Whistler, J. N. Bemiller, & E. F. Paschall (Eds.), *Starch: Chemistry and Technology (Second Edition)* (pp. 593–610). Academic Press. https://doi.org/10.1016/B978-0-12-746270-7.50026-4

Kennedy, J. F., Knill, C. J., & Taylor, D. W. (1995). Maltodextrins. In M. W. Kearsley & S. Z. Dziedzic (Eds.), *Handbook of Starch Hydrolysis Products and their Derivatives* (pp. 65–82). Springer US. https://doi.org/10.1007/978-1-4615-2159-4_3

Kingery, W. D., Bowen, H. K., & Uhlmann, D. R. (1976). *Introduction to Ceramics* (2nd ed.). John Wiley & Sons.

Kirchherr, J., Reike, D., & Hekkert, M. (2017). Conceptualizing the circular economy: An analysis of 114 definitions. *Resources, Conservation and Recycling*, *127*, 221–232. https://doi.org/10.1016/j.resconrec.2017.09.005

Kirchherr, J., Yang, N.-H. N., Schulze-Spüntrup, F., Heerink, M. J., & Hartley, K. (2023). Conceptualizing the Circular Economy (Revisited): An Analysis of 221 Definitions. *Resources, Conservation and Recycling*, *194*, 107001. https://doi.org/10.1016/j.resconrec.2023.107001

Klein, J., Stern, M., Franchin, G., Kayser, M., Inamura, C., Dave, S., Weaver, J. C., Houk, P., Colombo, P., Yang, M., & Oxman, N. (2015). Additive Manufacturing of Optically Transparent Glass. *3D Printing and Additive Manufacturing*, *2*(3), 92–105. https://doi.org/10.1089/3dp.2015.0021

Kline, G. (2018). *Amazing Glaze: Techniques, Recipes, Finishing, and Firing*. Voyageur Press.

Klocke, F., McClung, A., & Ader, C. (2004). Direct Laser Sintering of Borosilicate Glass. *2004 International Solid Freeform Fabrication Symposium.* https://doi.org/10.26153/tsw/6986

Korhonen, J., Honkasalo, A., & Seppälä, J. (2018). Circular Economy: The Concept and its Limitations. *Ecological Economics*, *143*, 37–46. https://doi.org/10.1016/j.ecolecon.2017.06.041

Koskinen, I., & Frens, J. (2017). Research Prototypes. *Archives of Design Research*, *30*(3), 5–14. https://doi.org/10.15187/adr.2017.08.30.3.5

Koskinen, I., Zimmerman, J., Binder, T., Redstrom, J., & Wensveen, S. (2011). *Design Research Through Practice: From the Lab, Field, and Showroom*. Elsevier Science & Technology.

Kotz, F., Arnold, K., Bauer, W., Schild, D., Keller, N., Sachsenheimer, K., Nargang, T. M., Richter, C., Helmer, D., & Rapp, B. E. (2017). Three-dimensional printing of transparent fused silica glass. *Nature*, *544*(7650), 337–339. https://doi.org/10.1038/nature22061

Kotz, F., Quick, A. S., Risch, P., Martin, T., Hoose, T., Thiel, M., Helmer, D., & Rapp, B. E. (2021). Two-Photon Polymerization of Nanocomposites for the Fabrication of Transparent Fused Silica Glass Microstructures. *Advanced Materials*, *33*(9), 2006341. https://doi.org/10.1002/adma.202006341

Krassenstein, B. (2015, June 22). *Micron3DP Unveils Breakthrough Glass 3D Printing Technique*. 3DPrint.Com. https://3dprint.com/75286/3d-print-glass-micron3dp/

Kravchenko, M., Pigosso, D. C. A., & McAloone, T. C. (2020). Circular economy enabled by additive manufacturing: Potential opportunities and key sustainability aspects. In N. H. Mortensen, C. T. Hansen, & M. Deininger (Eds.), *Proceedings of NordDesign 2020 (Vol. DS 101).* Design Society. https://doi.org/10.35199/NORDDESIGN2020.4

Kristensen, H. S., & Mosgaard, M. A. (2020). A review of micro level indicators for a circular economy – moving away from the three dimensions of sustainability? *Journal of Cleaner Production*, *243*, 118531. https://doi.org/10.1016/j.jclepro.2019.118531

Krogh, & Koskinen, I. (2020). *Drifting by Intention: Four Epistemic Traditions from Within Constructive Design Research*. Springer International Publishing.

Krogh, P. G., Markussen, T., & Bang, A. L. (2015). Ways of Drifting. In A. Chakrabarti (Ed.), *ICoRD'15 – Research into Design Across Boundaries Volume 1: Theory, Research Methodology, Aesthetics, Human Factors and Education* (pp. 39–50). Springer.

Krogh, P., & Koskinen, I. (2015). Design Accountability: When Design Research Entangles Theory and Practice. *International Journal of Design*, *9*, 121–127.

La Londe, R. P. (2006). *Richard La Londe: Fused glass art and technique* (1st ed). Ozone Press.

Lanzetta, M., & Sachs, E. (2003). Improved surface finish in 3D printing using bimodal powder distribution. *Rapid Prototyping Journal*, *9*(3), 157–166. https://doi.org/10.1108/13552540310477463

Lebullenger, R., & Mear, F. O. (2019). Glass Recycling. In J. D. Musgraves, J. Hu, & L. Calvez (Eds.), *Springer Handbook of Glass* (pp. 1355–1377). Springer International Publishing. https://doi.org/10.1007/978-3-319-93728-1_39

Leipold, S., Petit-Boix, A., Luo, A., Helander, H., Simoens, M., Ashton, W. S., Babbitt, C. W., Bala, A., Bening, C. R., Birkved, M., Blomsma, F., Boks, C., Boldrin, A., Deutz, P., Domenech, T., Ferronato, N., Gallego-Schmid, A., Giurco, D., Hobson, K., … Xue, B. (2023). Lessons, narratives, and research directions for a sustainable circular economy. *Journal of Industrial Ecology*, *27*(1), 6–18. https://doi.org/10.1111/jiec.13346

Lim, C., Song, Y. H., Song, Y., Seo, J. H., Hwang, D. S., & Lee, D. W. (2021). Adaptive amphiphilic interaction mechanism of hydroxypropyl methylcellulose in water. *Applied Surface Science*, *565*, 150535. https://doi.org/10.1016/j.apsusc.2021.150535

Lim, Y.-K., Stolterman, E., & Tenenberg, J. (2008). The anatomy of prototypes: Prototypes as filters, prototypes as manifestations of design ideas. *ACM Transactions on Computer-Human Interaction*, *15*(2), 1–27. https://doi.org/10.1145/1375761.1375762

Lin, D., Yi, S., Heo, J., Lee, J., German, R. M., & Park, S. J. (2015). Fabrication of glass components by sintering of commercial glass powder. *Ceramics International*, *41*(3), 5057–5065. https://doi.org/10.1016/j.ceramint.2014.12.075

Liu, C., Qian, B., Liu, X., Tong, L., & Qiu, J. (2018a). Additive manufacturing of silica glass using laser stereolithography with a top-down approach and fast debinding. *RSC Advances*, *8*(29), 16344–16348. https://doi.org/10.1039/C8RA02428F

Liu, C., Qian, B., Ni, R., Liu, X., & Qiu, J. (2018b). 3D printing of multicolor luminescent glass. *RSC Advances*, *8*(55), 31564–31567. https://doi.org/10.1039/C8RA06706F

Liu, D., Tan, H.-W., & Tran, T. (2018c). Droplet impact on heated powder bed. *Soft Matter*, *14*(48), 9967–9972. https://doi.org/10.1039/C8SM01858H

Liu, J., Li, S., Gunasekara, C., Fox, K., & Tran, P. (2022a). 3D-printed concrete with recycled glass: Effect of glass gradation on flexural strength and microstructure. *Construction and Building Materials*, *314*, 125561. https://doi.org/10.1016/j.conbuildmat.2021.125561

Liu, X., Yang, Y., & Qiu, J. (2022b). Emerging techniques for customized fabrication of glass. *Journal of Non-Crystalline Solids: X*, *15*, 100114. https://doi.org/10.1016/j.nocx.2022.100114

Lotte Fine Chemical. (n.d.). *Mecellose Introduction Leaflet*. Retrieved July 18, 2023, from https://www.lotte-cellulose.com/v1/download/MECELLOSE(Industrial_HPMC,HEMC)_Introduction_Leaflet.pdf

Luo, J. (2017). *Additive manufacturing of glass using a filament fed process* [Doctoral Dissertation, Missouri University of Science and Technology]. https://scholarsmine.mst.edu/doctoral_dissertations/2565

Luo, J., Gilbert, L., Qu, C., Wilson, J., Bristow, D., Landers, R., & Kinzel, E. (2015). Wire-Fed Additive Manufacturing of Transparent Glass Parts. *Proceedings of the ASME 2015 International Manufacturing Science and Engineering Conference. Volume 1: Processing.* V001T02A108. https://doi.org/10.1115/MSEC2015-9377

Luo, J., Pan, H., & Kinzel, E. C. (2014). Additive Manufacturing of Glass. *Journal of Manufacturing Science and Engineering*, *136*(6), 061024. https://doi.org/10.1115/1.4028531

Lv, X., Ye, F., Cheng, L., Fan, S., & Liu, Y. (2019). Binder jetting of ceramics: Powders, binders, printing parameters, equipment, and post-treatment. *Ceramics International*, *45*(10), 12609–12624. https://doi.org/10.1016/j.ceramint.2019.04.012

Madden, B., & Florin, N. (2019). *Characterising the material flows through the Australian waste packaging system*. Institute for Sustainable Futures, University of Technology Sydney.

Mader, M., Hambitzer, L., Schlautmann, P., Jenne, S., Greiner, C., Hirth, F., Helmer, D., Kotz-Helmer, F., & Rapp, B. E. (2021). Melt-Extrusion-Based Additive Manufacturing of Transparent Fused Silica Glass. *Advanced Science*, *8*(23), 2103180. https://doi.org/10.1002/advs.202103180

Mäkelä, M., & Nimkulrat, N. (2018). Documentation as a practice-led research tool for reflection on experiential knowledge. *FormAcademic*, *11*(2). https://doi.org/10.7577/formakademisk.1818

Mantelli, A., Levi, M., Turri, S., & Suriano, R. (2019). Remanufacturing of end-of-life glass-fiber reinforced composites via UV-assisted 3D printing. *Rapid Prototyping Journal*, *26*(6), 981–992. https://doi.org/10.1108/RPJ-01-2019-0011

Mantelli, A., Romani, A., Suriano, R., Levi, M., & Turri, S. (2021). Direct Ink Writing of Recycled Composites with Complex Shapes: Process Parameters and Ink Optimization. *Advanced Engineering Materials*, *23*(9), 2100116. https://doi.org/10.1002/adem.202100116

Maple Glass. (2022). *Maple Glass Printing*. https://www.mapleglassprinting.com

Marchelli, G., Prabhakar, R., Storti, D., & Ganter, M. (2011). The guide to glass 3D printing: Developments, methods, diagnostics and results. *Rapid Prototyping Journal*, *17*(3), 187–194. https://doi.org/10.1108/13552541111124761

Marczyk, J., Ostrowska, K., & Hebda, M. (2022). Influence of binder jet 3D printing process parameters from irregular feedstock powder on final properties of Al parts. *Advanced Powder Technology*, *33*(11), 103768. https://doi.org/10.1016/j.apt.2022.103768

Martín Gómez, C. (2012). Constructive Development of the "Microclimate Generator Pillars" from the Pavilion of Spain in Expo Saragossa. *Architecture Research*, *2*(2), 7–13. https://doi.org/10.5923/j.arch.20120202.02

McDonough, W., & Braungart, M. (2002). *Cradle to Cradle: Remaking the Way We Make Things*. Farrar, Straus and Giroux.

Meininger, S., Mandal, S., Kumar, A., Groll, J., Basu, B., & Gbureck, U. (2016). Strength reliability and in vitro degradation of three-dimensional powder printed strontium-substituted magnesium phosphate scaffolds. *Acta Biomaterialia*, *31*, 401–411. https://doi.org/10.1016/j.actbio.2015.11.050

Menges, A., & Reichert, S. (2012). Material Capacity: Embedded Responsiveness. *Architectural Design*, *82*(2), 52–59. https://doi.org/10.1002/ad.1379

Merget, R., Bauer, T., Küpper, H., Philippou, S., Bauer, H., Breitstadt, R., & Bruening, T. (2002). Health hazards due to the inhalation of amorphous silica. *Archives of Toxicology*, *75*(11), 625–634. https://doi.org/10.1007/s002040100266

Metic, J., & Pigosso, D. C. A. (2022). Research avenues for uncovering the rebound effects of the circular economy: A systematic literature review. *Journal of Cleaner Production*, *368*, 133133. https://doi.org/10.1016/j.jclepro.2022.133133

Mewis, J., & Wagner, N. J. (2009). Thixotropy. *Advances in Colloid and Interface Science*, *147–148*, 214–227. https://doi.org/10.1016/j.cis.2008.09.005

Miao, G., Du, W., Moghadasi, M., Pei, Z., & Ma, C. (2020). Ceramic binder jetting additive manufacturing: Effects of granulation on properties of feedstock powder and printed and sintered parts. *Additive Manufacturing*, *36*, 101542. https://doi.org/10.1016/j.addma.2020.101542

Mies, A., & Gold, S. (2021). Mapping the social dimension of the circular economy. *Journal of Cleaner Production*, *321*, 128960. https://doi.org/10.1016/j.jclepro.2021.128960

Millar, N., McLaughlin, E., & Börger, T. (2019). The Circular Economy: Swings and Roundabouts? *Ecological Economics*, *158*, 11–19. https://doi.org/10.1016/j.ecolecon.2018.12.012

Mirvac. (2021, March 3). *Mirvac unveils industry-first apartment made from waste glass and textiles*. http://www.mirvac.com/about/news-and-media/mirvac-unveils-industry-first-apartment-made-from-waste-glass-and-textiles

Miyanaji, H., Orth, M., Akbar, J. M., & Yang, L. (2018). Process development for green part printing using binder jetting additive manufacturing. *Frontiers of Mechanical Engineering*, *13*(4), 504–512. https://doi.org/10.1007/s11465-018-0508-8

Miyanaji, H., Rahman, K. M., Da, M., & Williams, C. B. (2020). Effect of fine powder particles on quality of binder jetting parts. *Additive Manufacturing*, *36*, 101587. https://doi.org/10.1016/j.addma.2020.101587

Miyanaji, H., Zhang, S., Lassell, A., Zandinejad, A. A., & Yang, L. (2016a). Optimal Process Parameters for 3D Printing of Porcelain Structures. *Procedia Manufacturing*, *5*, 870–887. https://doi.org/10.1016/j.promfg.2016.08.074

Miyanaji, H., Zhang, S., Lassell, A., Zandinejad, A., & Yang, L. (2016b). Process Development of Porcelain Ceramic Material with Binder Jetting Process for Dental Applications. *JOM*, *68*(3), 831–841. https://doi.org/10.1007/s11837-015-1771-3

Moore, D. G., Barbera, L., Masania, K., & Studart, A. R. (2020). Three-dimensional printing of multicomponent glasses using phase-separating resins. *Nature Materials*, *19*(2), 212-217. https://doi.org/10.1038/s41563-019-0525-y

Moreno, M., De Los Rios, C., Rowe, Z., & Charnley, F. (2016). A Conceptual Framework for Circular Design. *Sustainability*, *8*(9), 937. https://doi.org/10.3390/su8090937

Mostafaei, A., Elliott, A. M., Barnes, J. E., Li, F., Tan, W., Cramer, C. L., Nandwana, P., & Chmielus, M. (2021). Binder jet 3D printing—Process parameters, materials, properties, modeling, and challenges. *Progress in Materials Science*, *119*, 100707. https://doi.org/10.1016/j.pmatsci.2020.100707

Mostafaei, A., Stevens, E. L., Hughes, E. T., Biery, S. D., Hilla, C., & Chmielus, M. (2016). Powder bed binder jet printed alloy 625: Densification, microstructure and mechanical properties. *Materials & Design*, *108*, 126–135. https://doi.org/10.1016/j.matdes.2016.06.067

Moultrie, J. (2015). Understanding and classifying the role of design demonstrators in scientific exploration. *Technovation*, *43–44*, 1–16. https://doi.org/10.1016/j.technovation.2015.05.002

Ngo, T. D., Kashani, A., Imbalzano, G., Nguyen, K. T. Q., & Hui, D. (2018). Additive manufacturing (3D printing): A review of materials, methods, applications and challenges. *Composites Part B: Engineering*, *143*, 172–196. https://doi.org/10.1016/j.compositesb.2018.02.012

Nguyen, D. T., Meyers, C., Yee, T. D., Dudukovic, N. A., Destino, J. F., Zhu, C., Duoss, E. B., Baumann, T. F., Suratwala, T., Smay, J. E., & Dylla-Spears, R. (2017). 3D-Printed Transparent Glass. *Advanced Materials*, *29*(26), 1701181. https://doi.org/10.1002/adma.201701181

Niaki, M. K., Torabi, S. A., & Nonino, F. (2019). Why manufacturers adopt additive manufacturing technologies: The role of sustainability. *Journal of Cleaner Production*, *222*, 381–392. https://doi.org/10.1016/j.jclepro.2019.03.019

Norris, G. (2022, October 24). Glass recycler hits wall owing $5m. *The Australian - Online*. https://www.theaustralian.com.au/subscribe/news/1/?sourceCode=TAWEB_WRE170_a_GGL&dest=https%3A%2F%2Fwww.theaustralian.com.au%2Fbusiness%2Fglass-recycler-hits-wall-owing-6m%2Fnews-story%2Fd5f80c2b1183816d62ec8a5cd77c27b0&memtype=anonymous&mode=premium&v21=dynamic-groupa-test-noscore&V21spcbehaviour=append

NSW EPA. (2020, September 8). *Paving the way for Recycled Glass* [Press Release]. https://www.epa.nsw.gov.au/news/media-releases/2020/epamedia200908-paving-the-way-for-recycled-glass

Onkaparinga Now. (2018, December 11). *First South Australian road built with plastic bags and glass.* https://www.onkaparinganow.com/News-listing/First-South-Australian-road-built-with-plastic-bags-and-glass

Ørvik, T., & Stewart, M. (2022). *Pâte de verre: The material of time*. Schiffer Publishing.

Owens Illinois. (2017). *Submission 56 on Waste and Recycling Industry in Australia to the Senate Standing Committee on Environment and Communications.* https://www.aph.gov.au/Parliamentary_Business/Committees/Senate/Environment_and_Communications/WasteandRecycling/Submissions

Oxman, N. (2010). *Material-based design computation* [Doctoral Dissertation, Massachusetts Institute of Technology]. https://dspace.mit.edu/handle/1721.1/59192

Özgün, Ö., Özkan Gülsoy, H., Yilmaz, R., & Findik, F. (2013). Injection molding of nickel based 625 superalloy: Sintering, heat treatment, microstructure and mechanical properties. *Journal of Alloys and Compounds*, *546*, 192–207. https://doi.org/10.1016/j.jallcom.2012.08.069

Pan, C., Han, Y., & Lu, J. (2020). Design and Optimization of Lattice Structures: A Review. *Applied Sciences*, *10*(18), 6374. https://doi.org/10.3390/app10186374

Paudel, B. J., & To, A. C. (2025). Spatial green density variation and its effect on distortion prediction in binder jet additive manufacturing. *Additive Manufacturing*, *98*, 104640. https://doi.org/10.1016/j.addma.2025.104640

Pearce, D. W., & Turner, R. K. (1989). *Economics of Natural Resources and the Environment*. JHU Press.

Pedgley, O. (2007). Capturing and analysing own design activity. *Design Studies*, *28*(5), 463–483. https://doi.org/10.1016/j.destud.2007.02.004

Pedgley, O., Rognoli, V., & Karana, E. (2021). Chapter 1—Expanding territories of materials and design. In O. Pedgley, V. Rognoli, & E. Karana (Eds.), *Materials Experience 2* (pp. 1–12). Butterworth-Heinemann. https://doi.org/10.1016/B978-0-12-819244-3.00028-4

Peng, T., Kellens, K., Tang, R., Chen, C., & Chen, G. (2018). Sustainability of additive manufacturing: An overview on its energy demand and environmental impact. *Additive Manufacturing*, *21*, 694–704. https://doi.org/10.1016/j.addma.2018.04.022

Petit, J.-Y., & Wirquin, E. (2013). Evaluation of various cellulose ethers performance in ceramic tile adhesive mortars. *International Journal of Adhesion and Adhesives*, *40*, 202–209. https://doi.org/10.1016/j.ijadhadh.2012.09.007

Pfeifer, M. (2009). *Materials Enabled Designs: The Materials Engineering Perspective to Product Design and Manufacturing*. Butterworth-Heinemann.

Plank, J. (2004). Applications of biopolymers and other biotechnological products in building materials. *Applied Microbiology and Biotechnology*, *66*(1), 1–9. https://doi.org/10.1007/s00253-004-1714-3

Ponis, S., Aretoulaki, E., Maroutas, T. N., Plakas, G., & Dimogiorgi, K. (2021). A Systematic Literature Review on Additive Manufacturing in the Context of Circular Economy. *Sustainability*, *13*(11), 6007. https://doi.org/10.3390/su13116007

Prasad, D., Kuru, A., Oldfield, P., Ding, L., Dave, M., Noller, C., & He, B. (2022). *Delivering on the Climate Emergency: Towards a Net Zero Carbon Built Environment*. Springer Nature Singapore. https://doi.org/10.1007/978-981-19-6371-1

Prasad, D., Santamouris, M., & Storey, M. (2017). *Cooling Western Sydney. A strategic study on the role of water in mitigating urban heat in Western Sydney.* Sydney Water, University of New South Wales, CRC for Low Carbon Living. http://nla.gov.au/nla.obj-2621166358

Prochner, I., & Godin, D. (2022). Quality in research through design projects: Recommendations for evaluation and enhancement. *Design Studies*, *78*, 101061. https://doi.org/10.1016/j.destud.2021.101061

Rabinovich, E. M. (1985). Preparation of glass by sintering. *Journal of Materials Science*, *20*(12), 4259–4297. https://doi.org/10.1007/BF00559317

Rahaman, M. N. (2007). *Sintering of Ceramics*. CRC Press. https://doi.org/10.1201/b15869

Rahimizadeh, A., Kalman, J., Henri, R., Fayazbakhsh, K., & Lessard, L. (2019). Recycled Glass Fiber Composites from Wind Turbine Waste for 3D Printing Feedstock: Effects of Fiber Content and Interface on Mechanical Performance. *Materials*, *12*(23), 3929. https://doi.org/10.3390/ma12233929

Rashad, A. M. (2014). Recycled waste glass as fine aggregate replacement in cementitious materials based on Portland cement. *Construction and Building Materials*, *72*, 340–357. https://doi.org/10.1016/j.conbuildmat.2014.08.092

Redström, J. (2011). Some Notes on Programme-Experiment Dialectics. In I. Koskinen, T. Härkäsalmi, R. Mazé!, B. Matthews & J.-J. Lee (Eds.), *Proceedings of the Nordes'11: The 4th Nordic Design Research Conference* (pp. 129-136).

Redwood, B., Schöffer, F., & Garret, B. (2017). *The 3D Printing Handbook: Technologies, design and applications*. 3D Hubs.

Reike, D., Vermeulen, W. J. V., & Witjes, S. (2018). The circular economy: New or Refurbished as CE 3.0? — Exploring Controversies in the Conceptualization of the Circular Economy through a Focus on History and Resource Value Retention Options. *Resources, Conservation and Recycling*, *135*, 246–264. https://doi.org/10.1016/j.resconrec.2017.08.027

Ribul, M., Goldsworthy, K., & Collet, C. (2021). Material-Driven Textile Design (MDTD): A Methodology for Designing Circular Material-Driven Fabrication and Finishing Processes in the Materials Science Laboratory. *Sustainability*, *13*(3), 1268. https://doi.org/10.3390/su13031268

Richerson, D. W., & Lee, W. E. (2018). *Modern Ceramic Engineering: Properties, Processing, and Use in Design*. Taylor & Francis Group.

Rishmawi, I., Salarian, M., & Vlasea, M. (2018). Tailoring green and sintered density of pure iron parts using binder jetting additive manufacturing. *Additive Manufacturing*, *24*, 508–520. https://doi.org/10.1016/j.addma.2018.10.015

Rognoli, V., Bianchini, M., Maffei, S., & Karana, E. (2015). DIY materials. *Materials & Design*, *86*, 692–702. https://doi.org/10.1016/j.matdes.2015.07.020

Romani, A., Mantelli, A., Suriano, R., Levi, M., & Turri, S. (2020). Additive Re-Manufacturing of Mechanically Recycled End-of-Life Glass Fiber-Reinforced Polymers for Value-Added Circular Design. *Materials*, *13*(16), 3545. https://doi.org/10.3390/ma13163545

Romani, A., Rognoli, V., & Levi, M. (2021). Design, Materials, and Extrusion-Based Additive Manufacturing in Circular Economy Contexts: From Waste to New Products. *Sustainability*, *13*(13), 7269. https://doi.org/10.3390/su13137269

Romani, A., Rognoli, V., & Levi, M. (2023). Speculative tinkering on circular design materials through 3D printing. In K. Vaes & J. Verlinden (Eds.), *Connectivity and creativity in times of conflict*. Academia Press. https://doi.org/10.26530/9789401496476-063

Rosa, P., Sassanelli, C., Urbinati, A., Chiaroni, D., & Terzi, S. (2020). Assessing relations between Circular Economy and Industry 4.0: A systematic literature review. *International Journal of Production Research*, *58*(6), 1662–1687. https://doi.org/10.1080/00207543.2019.1680896

Rossi, G., Chiujdea, R.-S., Hochegger, L., Lharchi, A., Harding, J., Nicholas, P., Tamke, M., & Thomsen, M. R. (2023). Statistically Modelling the Curing of Cellulose-Based 3d Printed Components: Methods for Material Dataset Composition, Augmentation and Encoding. In C. Gengnagel, O. Baverel, G. Betti, M. Popescu, M. R. Thomsen, & J. Wurm (Eds.), *Towards Radical Regeneration* (pp. 487–500). Springer International Publishing. https://doi.org/10.1007/978-3-031-13249-0_39

Roy, S. (2025). Properties and advanced applications of porous ceramic composites. *Open Ceramics*, *21*, 100714. https://doi.org/10.1016/j.oceram.2024.100714

Saadatkhah, N., Carillo Garcia, A., Ackermann, S., Leclerc, P., Latifi, M., Samih, S., Patience, G. S., & Chaouki, J. (2020). Experimental methods in chemical engineering: Thermogravimetric analysis—TGA. *The Canadian Journal of Chemical Engineering*, *98*(1), 34–43. https://doi.org/10.1002/cjce.23673

Sachs, E., Cima, M., Williams, P., Brancazio, D., & Cornie, J. (1992). Three Dimensional Printing: Rapid Tooling and Prototypes Directly from a CAD Model. *Journal of Engineering for Industry*, *114*(4), 481–488. https://doi.org/10.1115/1.2900701

Sadokierski, Z. (2020). Developing critical documentation practices for design researchers. *Design Studies*, *69*, 100940. https://doi.org/10.1016/j.destud.2020.03.002

Safe Work Australia. (2024). *Workplace exposure standards for airborne contaminants.* https://www.safeworkaustralia.gov.au/sites/default/files/2024-01/workplace_exposure_standards_for_airborne_contaminants_-_18_january_2024.pdf

Sala, S., Amadei, A. M., Beylot, A., & Ardente, F. (2021). The evolution of life cycle assessment in European policies over three decades. *The International Journal of Life Cycle Assessment*, *26*(12), 2295–2314. https://doi.org/10.1007/s11367-021-01893-2

Sand & Stone Magazine. (2018). *A stockpile of glass fines awaits recycling* [Image]. https://sandandstone.cmpavic.asn.au/alex-fraser-group/

Sander, G., Jiang, D., Wu, Y., & Birbilis, N. (2020). Exploring the possibility of a stainless steel and glass composite produced by additive manufacturing. *Materials & Design*, *196*, 109179. https://doi.org/10.1016/j.matdes.2020.109179

Santamouris, M. (2015). Analyzing the heat island magnitude and characteristics in one hundred Asian and Australian cities and regions. *Science of The Total Environment*, *512–513*, 582–598. https://doi.org/10.1016/j.scitotenv.2015.01.060

Santamouris, M. (2016a). Cooling the buildings – past, present and future. *Energy and Buildings*, *128*, 617–638. https://doi.org/10.1016/j.enbuild.2016.07.034

Santamouris, M. (2016b). Urban Warming And Mitigation: Actual status, impacts and challenges. In M. Santamouris & D. Kolokotsa, *Urban Climate Mitigation Techniques* (1st ed., pp. 1–26). Routledge.

Santamouris, M. (2020). Recent progress on urban overheating and heat island research. Integrated assessment of the energy, environmental, vulnerability and health impact. Synergies with the global climate change. *Energy and Buildings*, *207*, 109482. https://doi.org/10.1016/j.enbuild.2019.109482

Santamouris, M., Cartalis, C., Synnefa, A., & Kolokotsa, D. (2015). On the impact of urban heat island and global warming on the power demand and electricity consumption of buildings—A review. *Energy and Buildings*, *98*, 119–124. https://doi.org/10.1016/j.enbuild.2014.09.052

Santamouris, M., Ding, L., Fiorito, F., Oldfield, P., Osmond, P., Paolini, R., Prasad, D., & Synnefa, A. (2017). Passive and active cooling for the outdoor built environment – Analysis and assessment of the cooling potential of mitigation technologies using performance data from 220 large scale projects. *Solar Energy*, *154*, 14–33. https://doi.org/10.1016/j.solener.2016.12.006

Santamouris, M., & Kolokotsa, D. (2015). On the impact of urban overheating and extreme climatic conditions on housing, energy, comfort and environmental quality of vulnerable population in Europe. *Energy and Buildings*, *98*, 125–133. https://doi.org/10.1016/j.enbuild.2014.08.050

Santamouris, M., Paolini, R., Haddad, S., Synnefa, A., Garshasbi, S., Hatvani-Kovacs, G., Gobakis, K., Yenneti, K., Vasilakopoulou, K., Feng, J., Gao, K., Papangelis, G., Dandou, A., Methymaki, G., Portalakis, P., & Tombrou, M. (2020). Heat mitigation technologies can improve sustainability in cities. An holistic experimental and numerical impact assessment of urban overheating and related heat mitigation strategies on energy consumption, indoor comfort, vulnerability and heat-related mortality and morbidity in cities. *Energy and Buildings*, *217*, 110002. https://doi.org/10.1016/j.enbuild.2020.110002

Santamouris, M., Synnefa, A., & Karlessi, T. (2011). Using advanced cool materials in the urban built environment to mitigate heat islands and improve thermal comfort conditions. *Solar Energy*, *85*(12), 3085–3102. https://doi.org/10.1016/j.solener.2010.12.023

Sasan, K., Lange, A., Yee, T. D., Dudukovic, N., Nguyen, D. T., Johnson, M. A., Herrera, O. D., Yoo, J. H., Sawvel, A. M., Ellis, M. E., Mah, C. M., Ryerson, R., Wong, L. L., Suratwala, T., Destino, J. F., & Dylla-Spears, R. (2020). Additive Manufacturing of Optical Quality Germania–Silica Glasses. *ACS Applied Materials & Interfaces*, *12*(5), 6736–6741. https://doi.org/10.1021/acsami.9b21136

Sauerwein, M. (2020). *Additive Manufacturing for Design in a Circular Economy* [Doctoral Dissertation, Delft University of Technology]. TU Delft Repository. https://doi.org/10.4233/UUID:1FFE3BD6-9592-40BE-9A2A-7830778DB093

Sauerwein, M., Doubrovski, E., Balkenende, R., & Bakker, C. (2019). Exploring the potential of additive manufacturing for product design in a circular economy. *Journal of Cleaner Production*, *226*, 1138–1149. https://doi.org/10.1016/j.jclepro.2019.04.108

Scarinci, G., Brusatin, G., & Bernardo, E. (2005). Glass Foams. In M. Scheffler & P. Colombo (Eds.), *Cellular Ceramics* (1st ed., pp. 158–176). Wiley. https://doi.org/10.1002/3527606696.ch2g

Schandl, H., King, S., Walton, A., Kaksonen, A., Tapsuwan, S., & Baynes, T. (2020). *National circular economy roadmap for plastics, glass, paper and tyres* . CSIRO. https://www.csiro.au/-/media/News-releases/2021/circular-economy/20-00205_LW_CircularEconomySummary_WEB_210119.pdf

Scherer, G. W. (2001). Viscous Sintering. In K. H. J. Buschow, R. W. Cahn, M. C. Flemings, B. Ilschner, E. J. Kramer, S. Mahajan & P. Veyssière (Eds.), *Encyclopedia of Materials: Science and Technology* (pp. 9536–9540). Elsevier. https://doi.org/10.1016/B0-08-043152-6/01725-3

Schön, D. A. (1992). *The Reflective Practitioner: How Professionals Think in Action*. Routledge. https://doi.org/10.4324/9781315237473

Schroeder, P., Anggraeni, K., & Weber, U. (2019). The Relevance of Circular Economy Practices to the Sustainable Development Goals. *Journal of Industrial Ecology*, *23*(1), 77–95. https://doi.org/10.1111/jiec.12732

Seadon, J. (2019, August 14). How recycling is actually sorted, and why Australia is quite bad at it. *The Conversation*. http://theconversation.com/how-recycling-is-actually-sorted-and-why-australia-is-quite-bad-at-it-121120

Sengupta, P. (2020). Refractories for Glass Manufacturing. In P. Sengupta (Ed.), *Refractories for the Chemical Industries* (pp. 237–276). Springer International Publishing. https://doi.org/10.1007/978-3-030-61240-5_10

Shelby, J. E., & Lopes, M. (2005). *Introduction to Glass Science and Technology*. Royal Society of Chemistry.

Sher, D. (2018, September 3). MICRON3DP Co-founder discusses shift from glass to MIM-based additive manufacturing. *VoxelMatters.* https://www.voxelmatters.com/co-founder-micron3dp-mim/

Silva, I., Gurruchaga, M., Goñi, I., Fernández-Gutiérrez, M., Vázquez, B., & Román, J. S. (2013). Scaffolds based on hydroxypropyl starch: Processing, morphology, characterization, and biological behavior. *Journal of Applied Polymer Science*, *127*(3), 1475–1484. https://doi.org/10.1002/app.37551

Solanki, S. (2018). *Why Materials Matter: Responsible Design for a Better World*. Prestel Publishing.

Solis, D. M., Silva, A. V., Volpato, N., & Berti, L. F. (2019). Reaction-bonding of aluminum oxide processed by binder jetting. *Journal of Manufacturing Processes*, *41*, 267–272. https://doi.org/10.1016/j.jmapro.2019.04.008

Sparre-Petersen, M., & Hnídková, S. (2023). Developing Techniques for Closed-Loop-Recycling Soda-Lime Glass Fines through Robotic Deposition. *Arts*, *12*(4), 166. https://doi.org/10.3390/arts12040166

Spirrett, F. (2021). *Investigations into Glass Additive Manufacturing by Selective Laser Melting and Directed Energy Deposition* [Doctoral Dissertation, University of Nottingham]. https://eprints.nottingham.ac.uk/66932/1/Final_Fiona_Spirrett_14289700_Completed_Thesis.pdf

Stahel, W. R. (2010). *The Performance Economy*. Palgrave Macmillan UK. https://doi.org/10.1057/9780230288843

Standards Australia. (2009). *Workplace atmospheres - Method for sampling and gravimetric determination of inhalable dust* (AS 3640-2009). https://www.standards.org.au/standards-catalogue/standard-details?designation=as-3640-2009

Standards Australia. (2009). *Workplace atmospheres - Method for sampling and gravimetric determination of respirable dust* (AS 2985-2009). https://www.standards.org.au/standards-catalogue/standard-details?designation=as-2985-2009

Standards Australia. (2012). *Respiratory protective devices* (AS/NZS 1716-2012). https://www.standards.org.au/standards-catalogue/standard-details?designation=as-nzs-1716-2012

Stappers, P. J. (2007). Doing Design as a Part of Doing Research. In R. Michel (Ed.), *Design Research Now* (pp. 81–91). Birkhäuser. https://doi.org/10.1007/978-3-7643-8472-2_6

Stappers, P. J., & Giaccardi, E. (2017). Research through Design. In M. Soegaard & R. Friis-Dam (Eds.), *The Encyclopedia of Human-Computer Interaction* (2nd ed., pp. 1–94). The Interaction Design Foundation.

Steinert. (n.d.). *MSort AK*. https://steinertglobal.com/sorting-systems/sensor-sorting/colour-sorting-system/msort-ak/

Stevens, E., Schloder, S., Bono, E., Schmidt, D., & Chmielus, M. (2018). Density variation in binder jetting 3D-printed and sintered Ti-6Al-4V. *Additive Manufacturing*, *22*, 746–752. https://doi.org/10.1016/j.addma.2018.06.017

Stewart, M. (2010). *The Sense of My Screaming Skin. An investigation into the colouring process of Amalric Walter (1870 -1959) using metallic salts in pâtes -de-verre* [Doctoral Dissertation, Edinburgh College of Art]. ERA. https://era.ed.ac.uk/handle/1842/34102.

Suárez-Eiroa, B., Fernández, E., Méndez-Martínez, G., & Soto-Oñate, D. (2019). Operational principles of circular economy for sustainable development: Linking theory and practice. *Journal of Cleaner Production*, *214*, 952–961. https://doi.org/10.1016/j.jclepro.2018.12.271

Sumter, D., de Koning, J., Bakker, C., & Balkenende, R. (2020). Circular Economy Competencies for Design. *Sustainability*, *12*(4), 1561. https://doi.org/10.3390/su12041561

Sun, C., Tian, X., Wang, L., Liu, Y., Wirth, C. M., Günster, J., Li, D., & Jin, Z. (2017). Effect of particle size gradation on the performance of glass-ceramic 3D printing process. *Ceramics International*, 43(1, Part A), 578–584. https://doi.org/10.1016/j.ceramint.2016.09.197

Sustainability Victoria. (2018, May 28). *From trial to reality: Recycled glass and plastic in asphalt roads*. https://www.sustainability.vic.gov.au/news/news-articles/from-trial-to-reality-recycled-glass-and-plastic-in-asphalt-roads

Sustainability Victoria. (2020a). *Recovered Resources Market Bulletin: June 2020*. https://assets.sustainability.vic.gov.au/susvic/Report-Recovered-Resources-Market-Bulletin-June-2020.pdf

Sustainability Victoria. (2020b). *Recovered Resources Market Bulletin: March–May 2020*. https://assets.sustainability.vic.gov.au/susvic/Report-Recovered-Resources-Market-Bulletin-March-May-2020.pdf

Sustainability Victoria. (2021). *Recovered Resources Market Bulletin: July 2021*. https://assets.sustainability.vic.gov.au/susvic/Recovered-Resources-Market-Bulletin-July-2021.pdf

Suwanprateeb, J., Sanngam, R., & Panyathanmaporn, T. (2010). Influence of raw powder preparation routes on properties of hydroxyapatite fabricated by 3D printing technique. *Materials Science and Engineering: C*, *30*(4), 610–617. https://doi.org/10.1016/j.msec.2010.02.014

Tang, Y., Mak, K., & Zhao, Y. F. (2016). A framework to reduce product environmental impact through design optimization for additive manufacturing. *Journal of Cleaner Production*, *137*, 1560–1572. https://doi.org/10.1016/j.jclepro.2016.06.037

Tanisan, B., & Turan, S. (2011). Black ceramic pigments for porcelain tile bodies produced with chromite ores and iron oxide waste. *Journal of Ceramic Processing Research*, *12*(4), 462–467.

Tao, W., & Leu, M. C. (2016). Design of lattice structure for additive manufacturing. *2016 International Symposium on Flexible Automation (ISFA)*, 325–332. https://doi.org/10.1109/ISFA.2016.7790182

Tarafder, S., Balla, V. K., Davies, N. M., Bandyopadhyay, A., & Bose, S. (2013). Microwave-sintered 3D printed tricalcium phosphate scaffolds for bone tissue engineering: 3D Printed TCP Scaffolds for Bone Tissue Engineering. *Journal of Tissue Engineering and Regenerative Medicine*, *7*(8), 631–641. https://doi.org/10.1002/term.555

Tavares, T. M., Ganga, G. M. D., Godinho Filho, M., & Rodrigues, V. P. (2023). The benefits and barriers of additive manufacturing for circular economy: A framework proposal. *Sustainable Production and Consumption*, *37*, 369–388. https://doi.org/10.1016/j.spc.2023.03.006

Temel, D., & Fahy, L. (2024). Terracool Urban Oasis. In P. Ayres, M. R. Thomsen, B. Sheil, & M. Skavara (Eds.), *Fabricate 2024* (pp. 64–71). UCL Press. https://doi.org/10.2307/jj.11374766.12

Tessa Silva. (n.d.). *Feminised Protein: Story*. https://www.tessasilva.com/story

Thangavel, M., & Elsen Selvam, R. (2022). Review of Physical, Mechanical, and Biological Characteristics of 3D-Printed Bioceramic Scaffolds for Bone Tissue Engineering Applications. *ACS Biomaterials Science & Engineering*, *8*(12), 5060–5093. https://doi.org/10.1021/acsbiomaterials.2c00793

Tharanathan, R. N. (2005). Starch—Value Addition by Modification. *Critical Reviews in Food Science and Nutrition*, *45*(5), 371–384. https://doi.org/10.1080/10408390590967702

Thomsen, M.R., & Tamke, M. (2009). Narratives of making: Thinking practice led research in architecture. *In Communicating (by) Design 2009* (pp. 1-8).

Thomsen, M.R., Tamke, M., Sparre-Petersen, M., Buchwald, E. F., & Hnídková, S. (2020). Silica: a circular material paradigm by 3D printing and recycled glass. In L.S. Werner & D. Koering (Eds.), *Anthropologic-Architecture and Fabrication in the cognitive age: Proceedings of the 38th eCAADe Conference* (Vol. 2, pp. 613-622). http://papers.cumincad.org/cgi-bin/works/paper/ecaade2020_128

Thomsen, M. R., Ayres, P., Sheil, B., & Skavara, M. (2024). Introduction: FABRICATE 2024: Creating Resourceful Futures. In P. Ayres, M. R. Thomsen, B. Sheil, & M. Skavara (Eds.), *Fabricate 2024* (pp. 8-11). UCL Press. https://doi.org/10.2307/jj.11374766.5

Thonemann, N., Schulte, A., & Maga, D. (2020). How to Conduct Prospective Life Cycle Assessment for Emerging Technologies? A Systematic Review and Methodological Guidance. *Sustainability*, *12*(3), 1192. https://doi.org/10.3390/su12031192

Ting, G. H. A., Tay, Y. W. D., Qian, Y., & Tan, M. J. (2019). Utilization of recycled glass for 3D concrete printing: Rheological and mechanical properties. *Journal of Material Cycles and Waste Management*, *21*(4), 994–1003. https://doi.org/10.1007/s10163-019-00857-x

Ting, G. H. A., Tay, Y. W. D., & Tan, M. J. (2021). Experimental measurement on the effects of recycled glass cullets as aggregates for construction 3D printing. *Journal of Cleaner Production*, *300*, 126919. https://doi.org/10.1016/j.jclepro.2021.126919

Turbak, A. F., Snyder, F. W., & Sandberg, K. R. (1983). Microfibrillated cellulose, a new cellulose product: Properties, uses, and commercial potential. *Journal ofApplied Polymer Science : Applied Polymer Symposium*, *37*, 815–827.

United Nations Environment Programme. (2024a). *Emissions Gap Report 2024: No more hot air … please! With a massive gap between rhetoric and reality, countries draft new climate commitments*. https://doi.org/10.59117/20.500.11822/46404.

United Nations Environment Programme. (2024b). *Bend the trend: Pathways to a liveable planet as resource use spikes*. International Resource Panel. https://wedocs.unep.org/20.500.11822/44901

United Nations Environment Programme. (2022). *2022 Global Status Report for Buildings and Construction: Towards a Zero-emission, Efficient and Resilient Buildings and Construction Sector*. https://www.unep.org/resources/publication/2022-global-status-report-buildings-and-construction

United Nations Environment Programme. (2023). *Building Materials and the Climate: Constructing a New Future*. https://www.unep.org/resources/report/building-materials-and-climate-constructing-new-future

Upadhyay, M., Sivarupan, T., & El Mansori, M. (2017). 3D printing for rapid sand casting—A review. *Journal of Manufacturing Processes*, *29*, 211–220. https://doi.org/10.1016/j.jmapro.2017.07.017

Valencia, M., Bocken, N., Loaiza, C., & De Jaeger, S. (2023). The social contribution of the circular economy. *Journal of Cleaner Production*, *408*, 137082. https://doi.org/10.1016/j.jclepro.2023.137082

Vallejo, J. (2018). *Design Integration of Novel Porous Ceramic Evaporative Cooling Systems*, [Doctoral Dissertation, University of Nottingham]. Nottingham eTheses. https://eprints.nottingham.ac.uk/55217/

Van Dam, K., Simeone, L., Keskin, D., Baldassarre, B., Niero, M., & Morelli, N. (2020). Circular Economy in Industrial Design Research: A Review. *Sustainability*, *12*(24), 10279. https://doi.org/10.3390/su122410279

Vande, S. (2008). Glass: Towards an inner space—On introducing metal oxides in pate de verre making. *Glass Technology: European Journal of Glass Science and Technology Part A*, *49*(1), 17–20.

Varshneya, A. K., & Mauro, J. C. (2019). *Fundamentals of Inorganic Glasses*. Elsevier. https://doi.org/10.1016/B978-0-12-816225-5.00001-8

Victorian Parliamentary Budget Office. (2019). *State of glass recycling in Victoria: Processes, facilities and potential end product*. https://pbo.vic.gov.au/response/570

von Witzendorff, P., Pohl, L., Suttmann, O., Heinrich, P., Heinrich, A., Zander, J., Bragard, H., & Kaierle, S. (2018). Additive manufacturing of glass: CO2-Laser glass deposition printing. *Procedia CIRP*, *74*, 272–275. https://doi.org/10.1016/j.procir.2018.08.109

Voxeljet. (n.d.). *VX4000: The world's largest 3D printer for sand*. https://www.voxeljet.com/industrial-3d-printer/serial-production/vx4000/

Walzberg, J., Lonca, G., Hanes, R. J., Eberle, A. L., Carpenter, A., & Heath, G. A. (2021). Do We Need a New Sustainability Assessment Method for the Circular Economy? A Critical Literature Review. *Frontiers in Sustainability*, *1*, 620047. https://doi.org/10.3389/frsus.2020.620047

Wang, J., Meng, Q., Tan, K., & Santamouris, M. (2022). Evaporative cooling performance estimation of pervious pavement based on evaporation resistance. *Building and Environment*, *217*, 109083. https://doi.org/10.1016/j.buildenv.2022.109083

Wang, Y.-J., & Wang, L. (2000). Structures and Properties of Commercial Maltodextrins from Corn, Potato, and Rice Starches. *Starch - Stärke*, *52*(8–9), 296–304. https://doi.org/10.1002/1521-379X(20009)52:8/9<296::AID-STAR296>3.0.CO;2-A

Watt, J. (2012). *Evaporative Air Conditioning Handbook*. Springer Science & Business Media.

World Commission on Environment and Development. (1987). *Report of the World Commission on Environment and Development: Our Common Future*. United Nations.

Wensveen, S., & Matthews, B. (2014). Prototypes and prototyping in design research. In P. A. Rodgers & J. Yee (Eds.), *The Routledge Companion to Design Research* (1st ed., pp. 262–276). Routledge. https://doi.org/10.4324/9781315758466-25

Westbroek, C. D., Bitting, J., Craglia, M., Azevedo, J. M. C., & Cullen, J. M. (2021). Global material flow analysis of glass: From raw materials to end of life. *Journal of Industrial Ecology*, *25*(2), 333–343. https://doi.org/10.1111/jiec.13112

Will, J., Melcher, R., Treul, C., Travitzky, N., Kneser, U., Polykandriotis, E., Horch, R., & Greil, P. (2008). Porous ceramic bone scaffolds for vascularized bone tissue regeneration. *Journal of Materials Science: Materials in Medicine*, *19*(8), 2781–2790. https://doi.org/10.1007/s10856-007-3346-5

Wurzburg, O. B. (2016). Modified Starches. In Alistair M. Stephen & Glyn O. Phillips (Eds.), *Food Polysaccharides and Their Applications* (pp. 87–118). CRC Press.

Xin, C., Li, Z., Hao, L., & Li, Y. (2023). A comprehensive review on additive manufacturing of glass: Recent progress and future outlook. *Materials & Design*, *227*, 111736. https://doi.org/10.1016/j.matdes.2023.111736

Xu, J., Wei, Q., Huang, X., Zhu, X., & Li, G. (2010). Evaluation of human thermal comfort near urban waterbody during summer. *Building and Environment*, *45*(4), 1072–1080. https://doi.org/10.1016/j.buildenv.2009.10.025

Yamanashi, T. (2015). Innovative Façade Systems Of Japan. *Council on Tall Buildings and Urban Habitat Journal*, *2*. https://global.ctbuh.org/resources/papers/download/2340-innovative-facade-systems-of-japan.pdf

Yamanashi, T., Hatori, T., Ishihara, Y., Kawashima, N., & Niwa, K. (2011). BIO SKIN Urban Cooling Facade. *Architectural Design*, *81*(6), 100–107. https://doi.org/10.1002/ad.1326

Yegyan Kumar, A., Bai, Y., Eklund, A., & Williams, C. B. (2018). The effects of Hot Isostatic Pressing on parts fabricated by binder jetting additive manufacturing. *Additive Manufacturing*, *24*, 115–124. https://doi.org/10.1016/j.addma.2018.09.021

Yuan, Z., Bi, J., & Moriguichi, Y. (2006). The Circular Economy: A New Development Strategy in China. *Journal of Industrial Ecology*, *10*(1–2), 4–8. https://doi.org/10.1162/108819806775545321

Zago, M., Lecis, N. F. M., Vedani, M., & Cristofolini, I. (2021). Dimensional and geometrical precision of parts produced by binder jetting process as affected by the anisotropic shrinkage on sintering. *Additive Manufacturing*, *43*, 102007. https://doi.org/10.1016/j.addma.2021.102007

Zaki, R. M., Strutynski, C., Kaser, S., Bernard, D., Hauss, G., Faessel, M., Sabatier, J., Canioni, L., Messaddeq, Y., Danto, S., & Cardinal, T. (2020). Direct 3D-printing of phosphate glass by fused deposition modeling. *Materials & Design*, *194*, 108957. https://doi.org/10.1016/j.matdes.2020.108957

Zanotto, E. D., & Mauro, J. C. (2017). The glassy state of matter: Its definition and ultimate fate. *Journal of Non-Crystalline Solids*, *471*, 490–495. https://doi.org/10.1016/j.jnoncrysol.2017.05.019

Zhang, H., Huang, L., Tan, M., Zhao, S., Liu, H., Lu, Z., Li, J., & Liang, Z. (2022). Overview of 3D-Printed Silica Glass. *Micromachines*, *13*(1), 81. https://doi.org/10.3390/mi13010081

Zhang, Liu, X., & Qiu, J. (2021). 3D printing of glass by additive manufacturing techniques: A review. *Frontiers of Optoelectronics*, *14*(3), 263–277. https://doi.org/10.1007/s12200-020-1009-z

Zhao, H., Wang, A., Li, G., Hu, Q., Ye, C., Shen, M., Xiao, Y., Liu, S., & Ji, D. (2022). Improving the properties of binder jetted ceramics via nanoparticle dispersion infiltration. *Ceramics International*, *48*(22), 33580–33587. https://doi.org/10.1016/j.ceramint.2022.07.302

Zhao, H., Ye, C., Fan, Z., & Wang, C. (2017). 3D printing of CaO-based ceramic core using nanozirconia suspension as a binder. *Journal of the European Ceramic Society*, *37*(15), 5119–5125. https://doi.org/10.1016/j.jeurceramsoc.2017.06.050

Zheng, Y., Li, Y., Hou, H., Murayama, Y., Wang, R., & Hu, T. (2021). Quantifying the Cooling Effect and Scale of Large Inner-City Lakes Based on Landscape Patterns: A Case Study of Hangzhou and Nanjing. *Remote Sensing*, *13*(8), 1526. https://doi.org/10.3390/rs13081526

Ziaee, M., & Crane, N. B. (2019). Binder jetting: A review of process, materials, and methods. *Additive Manufacturing*, *28*, 781–801. https://doi.org/10.1016/j.addma.2019.05.031

Zia-ud-Din, Xiong, H., & Fei, P. (2017). Physical and chemical modification of starches: A review. *Critical Reviews in Food Science and Nutrition*, *57*(12), 2691–2705. https://doi.org/10.1080/10408398.2015.1087379

Zier, M., Stenzel, P., Kotzur, L., & Stolten, D. (2021). A review of decarbonization options for the glass industry. *Energy Conversion and Management: X*, *10*, 100083. https://doi.org/10.1016/j.ecmx.2021.100083

Zimmerman, J., Forlizzi, J., & Evenson, S. (2007). Research through design as a method for interaction design research in HCI. In *Proceedings of the 8th ACM Conference on Designing Interactive Systems (DIS '10) (pp.. Association for Computing Machinery* 493–502. https://doi.org/10.1145/1240624.1240704

Zimmerman, J., Stolterman, E., & Forlizzi, J. (2010). An analysis and critique of *Research through Design*: Towards a formalization of a research approach. In *Proceedings of the 8th ACM Conference on Designing Interactive Systems* (pp. 310–319). https://doi.org/10.1145/1858171.1858228

Zink, T., & Geyer, R. (2017). Circular Economy Rebound. *Journal of Industrial Ecology*, *21*(3), 593–602. https://doi.org/10.1111/jiec.12545

Zobel, H. F., & Stephen, A. M. (2016). Starch: Structure, Analysis, and Application. In Alistair M. Stephen & Glyn O. Phillips (Eds.), *Food Polysaccharides and Their Applications* (2nd ed., pp. 25–85). CRC Press.

Appendices

Appendix 1: Literature Review Supplementary information
Appendix 2: Preliminary Investigation Supplementary information
Appendix 3: Further Prototyping Supplementary information
Appendix 4: Application Supplementary information

Appendix 1

Literature Review Supplementary Information

1.1 Key Glass Families

Property	Silica	Soda lime silicate	Borosilicate	Pb-silicate borate	Aluminosilicate
Melting	~ 2200°C	~ 1450°C	~ 1650°C	~ 900-1400°C	~ 1650°C
Max service temp.	~ 1000°C	~ 500°C	~ 520°C	~ 270-460°C	~ 700°C
Chemical durability	Vvv good	Good	V good	Good	Vvv good
Electrical conductivity	Vvv low	Low	Low	V low	V-vvv low
Cost	High	V low	Medium	Low	Medium
Applications	Furnace tubes, crucibles for Si melting, UV windows	Container, flat, incandescent/ fluorescent lamps	Chemical labware, pharmaceutical/ cosmetics ware, auto headlamps	"Crystal" ware, art/intricate shapes, sealing glasses	Halogen lamp, fiber-reinforced plastics

Key glass families that are industrially produced.
Adapted from Varshneya & Mauro (2019).

1.2 Fused Deposition Modelling (FDM) diagram

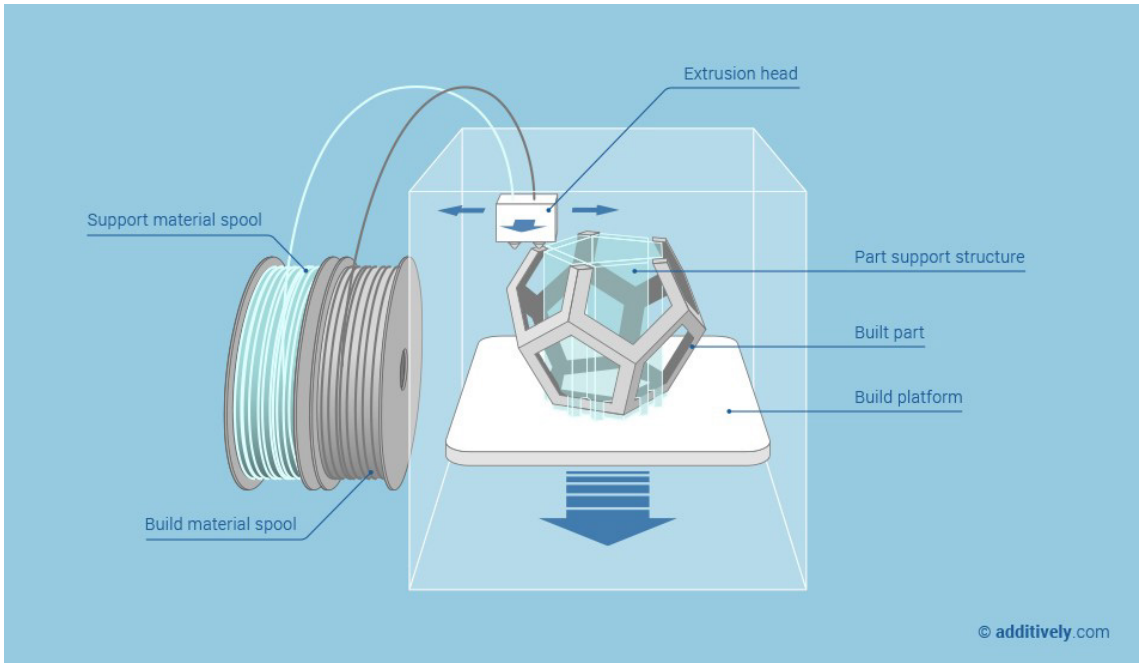

Image from additively.com (n.d.)

1.3 Vat Photopolymerisation (VAT) diagram

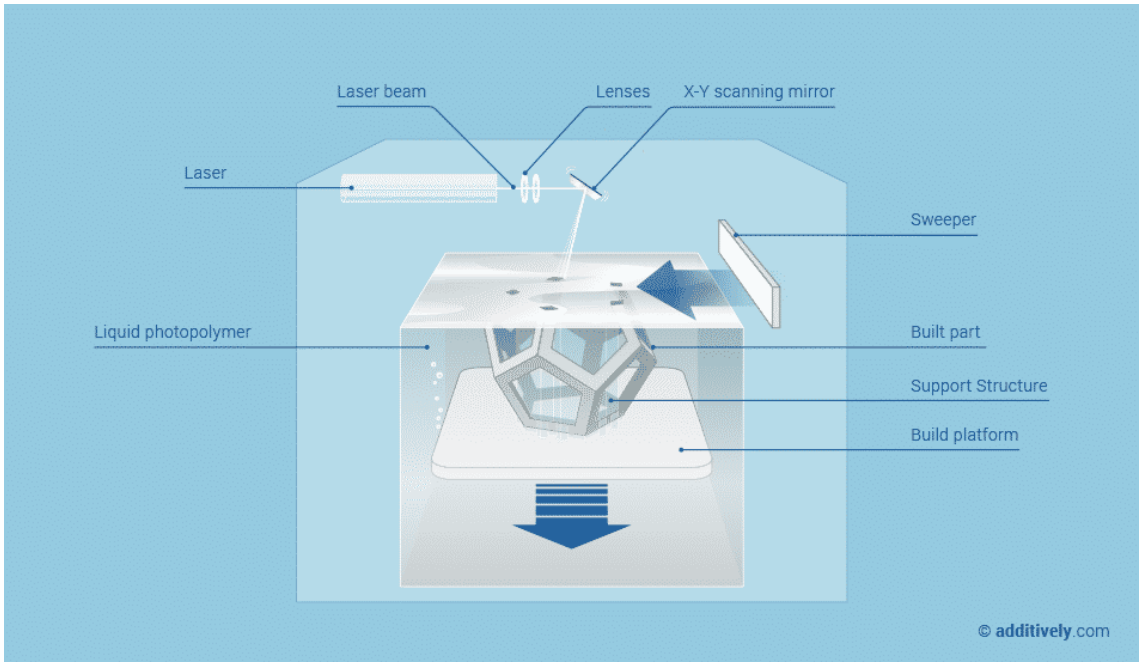

Image from additively.com (n.d.)

1.4 Powder Bed Fusion (PBF) diagram

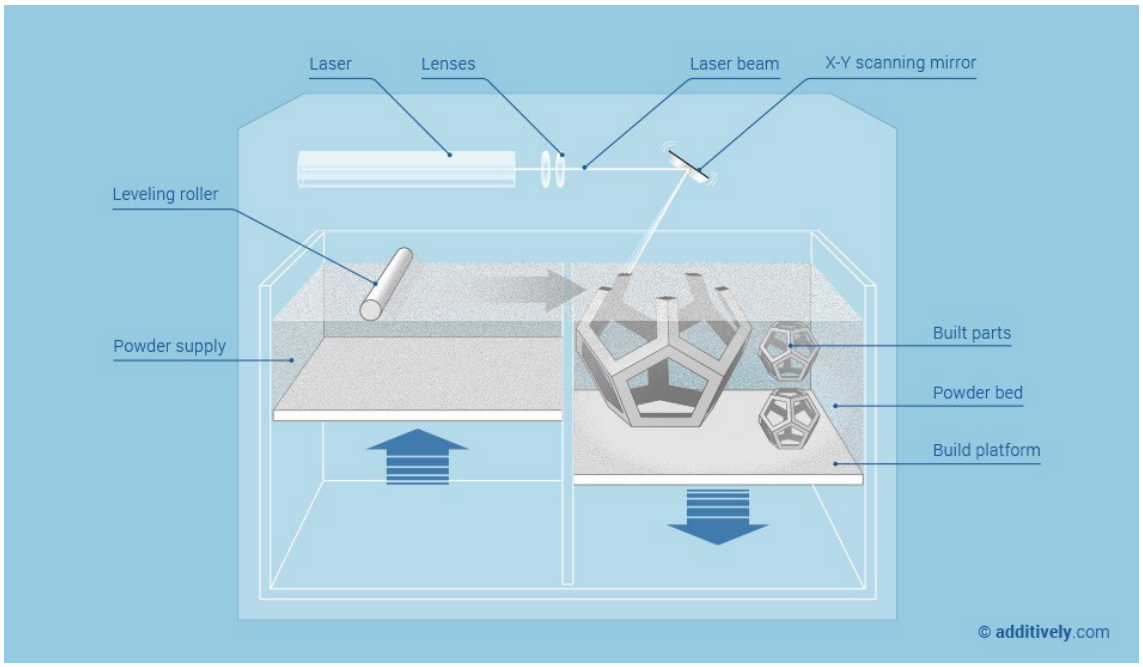

Image from additively.com (n.d.)

1.5 Binder Jetting (BJT) diagram

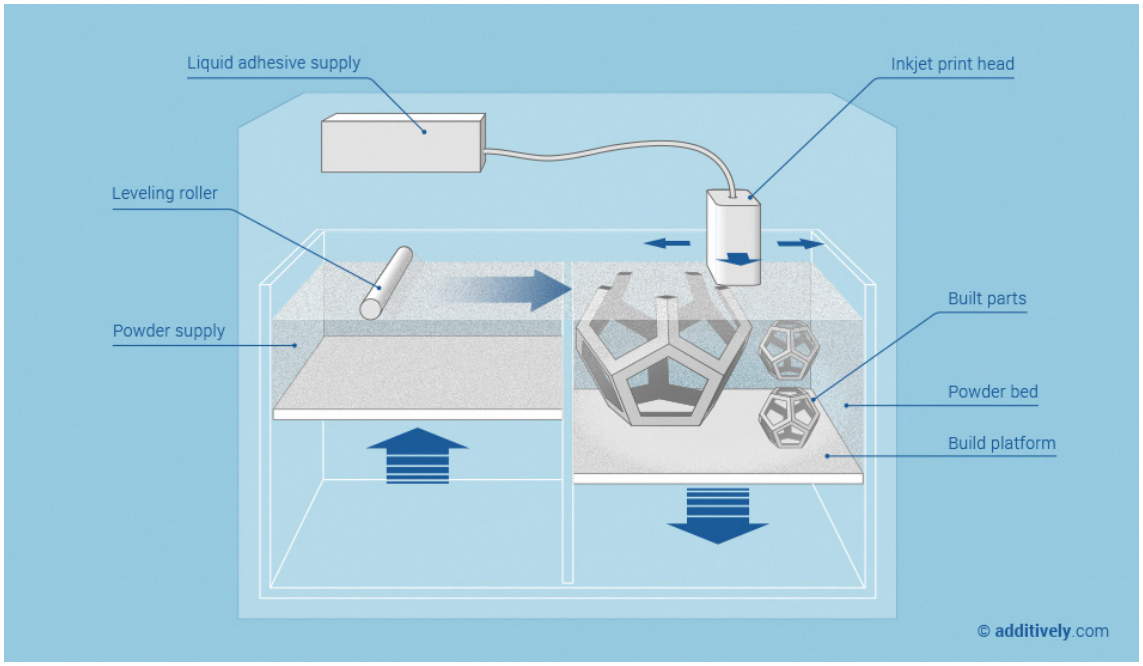

Image from additively.com (n.d.)

1.6 Further Binder Jetting Information

BJT holds significant manufacturing potential as it allows for the rapid production of complex geometries (Mostafaei et al., 2021). The surrounding powder in the print bed supports the printed part, resulting in few geometric limitations and no need for support structures (Du et al., 2020). BJT can work with virtually any powdered feedstock at an improved resolution and speed compared to other technologies (Ziaee & Crane, 2019). It is also highly scalable as parts are built at room temperature without the need for sealed chambers or laser thermal sources. This means that distortions, shrinkage or cracking resulting from thermal effects do not occur during printing (Gibson et al., 2021). As a result, BJT printers up to 4m have been commercialised, making it one of the largest 3D printing technologies available (Gibson et al., 2021;; Voxeljet, n.d.). Despite this potential, BJT has received less academic attention than other AM processes. Of approximately 31,000 papers published on AM from 1988-2019, only 610 focused on BJT (Mostafaei t al., 2021). However, there has been a recent increase in interest due to its potential for low-cost and high-speed production (Ziaee & Crane, 2019).

A wide range of metals, polymers, composites and ceramics have been used in BJT across academia, design practice and industry. Most relevant to this research is the BJT of ceramic materials. Ceramics have been used in BJT since its inception, with the first journal article published by Sachs et al. (1992) demonstrating the printing of alumina powder with a colloidal silica binder. They proposed using BJT for ceramic cores and shells in metal casting, an application which has been widely adopted by industry for its ability to rapidly and cost-effectively produce complex geometries (Upadhyay et al., 2017; Ziaee & Crane, 2019). The BJT of ceramics has also garnered attention in the biomedical field for producing implants and bone scaffolds from phosphate ceramic materials, which have a similar composition to human bones (Du et al., 2020; Thangavel & Elsen Selvam, 2022). A key challenge of BJT lies in achieving fully dense parts as the layering of the powder often results in some degree of porosity. Consequently, these current applications of BJT are ones where porosity is advantageous.

Appendix 2:

Preliminary Investigation Supplementary Information

2.1 Results from individual experiments for finding printing parameters: basic forms.

Name	Images	Binder	Saturation	Layer height	Drying time	Changes made	Notes & reflections	Print setup
Test 1.01 3.5.22		Glass 97.5% CMC 2.5% (w/w) Tap water	Core: 100% Shell: 100%	0.2 mm	Approx. 2 hrs	Initial print paramaters and method was based on estimates from the manual testing.	Excavation: Parts could not be excavated and crumbled upon being touched. Printability: Some swiping was observed in early layers during printing.	
Test 1.02 4.5.22		Glass 97.5% CMC 2.5% (w/w) Tap water	Core: 100% Shell: 100%	0.15 mm	Approx. 2 hrs	Layer height was reduced to 0.15mm. As literature reports that a thinner layer thickness can lead to higher density, it was hypothesised that this would also increase strength of the green part (Gonzalez et al., 2016; Mostafaei et al., 2021).	Excavation: Parts could not be excavated. One log was excavated but broke in half during the process. Parts further to the right seemed to be more intact. No significant difference to the previous test. Printability: Swiping occurred during printing. Swiping seems to happen more in the early layers and then peters out.	
Test 1.03 9.5.22		Glass 97.5% CMC 2.5% (w/w) Tap water	Core: 150% Shell: 150%	0.15 mm	Approx. 18 hrs	As changing the layer height had little impact, the saturation was increased. This aligns with literature indicating that low saturation leads to limited powder-binder contact, resulting in poor density and strength. (Du et al., 2017). Parts were printed in the evening and so were left overnight to cure.	Excavation: 4 of the 5 parts were excavated. The corner piece on the left, fell apart. The pieces are far stronger than previous tests although the corner piece on the right cracked upon being bumped. Printability: Swiping occurred during printing. Swiping seems to happen more in the early layers and then peters out.	
Test 1.04 10.5.22		Glass 97.5% CMC 2.5% (w/w) Tap water	Core: 150% Shell: 150%	0.175 mm	Approx. 2 hrs	Layer height was increased as it was hypothesised that the low layer height was causing the significant swiping in the previous two tests.	Excavation: Parts were excavated too early- they felt wet and crumbly and fell apart. It is hypothesised curing time is a key parameter that needs to be controlled. Printability: Swiping occurred in early layers- first approximate 20 and then petered out.	
Test 1.05 10.5.22		Glass 97.5% CMC 2.5% (w/w) Tap water	Core: 150% Shell: 150%	0.175 mm	Approx. 15 hrs	The previous test was repeated but parts were left overnight to let cure. It was hypothesised that this is key to excavating the parts.	Excavation: Parts were all excavated successfully. However, the lid on the printer suddenly closed and parts were broken. This is why no studio photos were taken. Printability: Swiping occurred in the first 20 or so layers. The results of this can be seen in the final excavated prints.	
Test 1.06 11.5.22		Glass 97.5% CMC 2.5% (w/w) Tap water	Core: 145% Shell: 145%	0.2 mm	Approx. 18 hrs	Layer height was increased in an attempt to mitigate swiping. As the layer height and saturation are linked in the ZCorp settings, the saturation was automatically reduced to 145% instead of 150%.	Excavation: All parts were excavated without breakages. Printability: Significantly less swiping. Some occurred in the early layers. The parts furthest to the right in the print bed worked really well- no swiping, crisp edges- this difference in swiping for parts on the left also happened in Marchelli et al.'s (2011) work.	

Reflective log of experimentation with basic forms in Section 4.6.1.

2.2 Results from individual experiments for finding printing parameters: geometric shapes.

Name	Images (excavation)	Images (studio)	Binder	Saturation	Layer height	Drying time	Changes made	Notes & reflections	Print setup	Images (post firing)
Test 2.01 13.5.22			Glass 97.5% CMC 2.5% (w/w) Tap water	Core: 145% Shell: 145%	0.2 mm	Approx. 64 hrs (over weekend)	Print parameters and method were based on estimates from previous set of testing with basic shapes	Excavation: Parts were very fragile, all but the furthest to the right cylinder, broke in some way. The wire frame cubes did not work at all, far too fragile at the corner joints. Printability: Significantly less swiping. Some occurred in the early layers but petered out at approx.. layer 14 and far less visible in final excavated prints.		
Test 2.02 19.5.22			Glass 97.5% CMC 2.5% (w/w) Tap water	Core: 145% Shell: 145%	0.2 mm	Approx. 18 hrs	As the cylinder print in Test 3.08 was most successful, similar geometries were tested in this print. Printing settings were kept the same.	Excavation: All but two parts were excavated without breaking. Although all were still fragile. Printability: No visible swiping occurred.		
Test 2.03 20.5.22			Glass 97.5% CMC 2.5% (w/w) Tap water	Core: 150% Shell: 150%	0.175 mm	Approx. 21 hrs	Same geometries as previous test but the layer height was decreased in an attempt to increase green strength (as curing time and saturation were already quite high).	Excavation: One part fell apart in excavation. But other parts were excavated although very fragile. Printability: Swiping occurred in the first 15 layers or so. It is hypothesised that this is due to the layer height change. The effects of this can be seen slightly on the bottom of some of the prints.		
Test 2.04 23.5.22			Glass 96.25% CMC 3.75% (w/w) Tap water	Core: 150% Shell: 150%	0.175 mm	Approx. 21 hrs	As the green strength of the parts was still a significant issue, the amount of CMC binder was increased (50% extra).	Excavation: All parts were excavated successfully and appeared stronger than previous tests. However, they are still quite fragile. Printability: Swiping occurred in first 10 layers- petered out. This can be slightly seen on excavated prints.	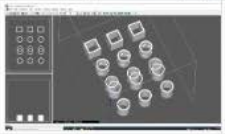	

Reflective log of experimentation with geometric shapes in Section 4.6.2.

2.3 Results from individual experiments for finding the binder formulation: Cellulose binders (CMC and (HPMC)

Name	Images	Binder	Saturation	Layer height	Drying time	Changes made	Notes & reflections	Print setup
Test 3.01 31.08.22		Glass: 97% HPMC: 3%	Core: 100% Shell: 100%	0.175 mm	Approx. 18 hrs	Initial settings for this new binder were estimated based on previous testing results.	Excavation: Parts could not be excavated. Extremely fragile, did not hold together. Printability: Bad swiping up until approx. layer 17 of 117.	
Test 3.02 01.09.22		Glass: 97% HPMC: 3%	Core: 150% Shell: 150%	0.175 mm	Approx. 18 hrs	Following the same approach as in the basic shapes testing, the saturation was increased in an attempt to increase green strength and allow for excaviation.	Excavation: Parts could not be excavated. Did not hold together- crumbled to the touch. Printability: Bad swiping occurred again- increased saturation likely exacerbated this.	
Test 3.03 06.09.22		Glass: 96% HPMC: 2% CMC: 2%	Core: 150% Shell: 150%	0.175 mm	Approx. 18 hrs	The material formulation was adjusted to include CMC. It was hypothesized that as CMC is typically more hydrophilic than HPMC, the green strength of the parts may improve. (He et al., 2021)	Excavation: More parts were able to be excavated than previous prints but they were still incredibly fragile- cracking and crumbling in hands. Printability: bad swiping occurred again, significant shifting of powder - up to layer approximately 20 of 117.	
Test 3.04 09.09.22		Glass: 96% HPMC: 2% CMC: 2%	Core: 145% Shell: 195%	0.2 mm	Approx. 18 hrs	It was hypothesised that the binders were not sufficiently "activated." So, saturation was increased. However, by increasing saturation, swiping is also likely to happen, so layer height was also increased to mitigate this. The same printed parts as 4.03 were set up, plus three solid window parts.	Excavation: Parts were able to be excavated. However, there was not enough powder left in the build platform so the prints ultimately failed. Printability: Lots of swiping- the first 20 layers of 82. The impact of this can be seen on the excavated prints. The placement of the parts is suspected to be a factor in this swiping.	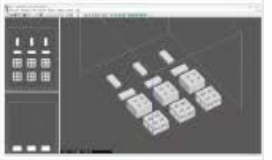
Test 3.05 13.09.22		Glass: 96% HPMC: 2% CMC: 2%	Core: 145% Shell: 195%	0.2 mm	Approx. 18 hrs	A new print placement was tested to mitigate swiping. Essentially using the logs as sacrificial parts to delay the depositing of a new layer of powder.	Excavation: Parts were excavated successfully. Some broke later as they are fairly fragile but are able to be handled. Printability: The use of sacrificial geometry worked well- only a very small amount of swiping on the first layer of the parts on the right. Swiping occurred on the logs but only for the first 4ish layers.	

Reflective log of experimentation with cellulose binders in Section 4.7.1.

2.4 Results from individual experiments for finding the binder formulation: Hydroxypropyl starch (HPS)

Name	Images	Binder	Saturation	Layer height	Drying time	Changes made	Notes & reflections	Print setup	Images (post firing)
Test 4.01 16.09.22		Glass 96% HPS 4%	Core: 145% Shell: 195%	0.2mm	Approx. 18 hrs	A new modified starch binder was tested. Ratio of binder to glass and print prameters remained the same as in the previous set of tests.	Excavation: Parts were excavated from the bed successfully however the oversaturation made it impossible to excavate the holes in the window pieces. These parts were noticeably far stronger than the CMC and HPMC mixes. Printability: Swiping on first layer and then it was totally fine. Way too much saturation. Binder leached out of the desired geometry, sticking the parts to the bottom of the printing bed.		
Test 4.02 19.09.22		Glass 96% HPS 4%	Core: 120% Shell: 145%	0.2mm	Approx. 18 hrs	The saturation settings were reduced as the binder leached out in the previous test.	Excavation: Parts were all excavated easily with no breakages. Printability: Swiping on first layer and then fine. Still some over saturation.		
Test 4.03 20.09.22		Glass 96% HPS 3%	Core: 120% Shell: 145%	0.2mm	Approx. 2 hours plus dehydrator	As there was still some oversaturation, the quantity of starch was reduced to 3% and saturation settings left the same.	Excavation: Attempted to excavate parts too early which caused one of the logs to break so all parts were put in the dehydrator. Otherwise they were successfully excavated. This binder is noticeably stronger than the CMC or HPMC mixes. Printability: No swiping occurred! Saturation settings appear to be suitable for this quantity of binder.		

Reflective log of experimentation with hydroxypropyl starch in Section 4.7.2.

Appendix 3:

Further Prototyping Supplementary Information

3.1 Results from individual experiments for Lattices 2.0 (part 1).

Name	Images (pre firing)	Binder	Saturation	Layer height	Firing	Notes & reflections	Print setup	Images (post firing)
Test 8.01 3.10.23		Glass 96% HPS 4% (w/w) Tap water	Shell 110% Core 130%	0.2 mm	780°C (no soak)	Excation: Part was excavated with no breakages. Printability: No swiping occurred. The computer logged out at layer 118 so had to restart the print from there. As a result an extra layer of powder was deposited so there was concern that the part could be weak at that layer, however it was fine. Firing, part evenly maintained its overall shape.	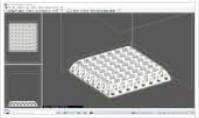	
Test 8.02 3.10.23		Glass 96% HPS 4% (w/w) Tap water	Shell 110% Core 130%	0.2 mm	780°C (no soak)	Printability: No swiping occurred. Some petering out of the powder layer on the top right edge, which led to that corner of the print breaking during excavation. Printed an extra corner piece and stuck it on using a slurry made of the feedstock powder and water. This worked well. Firing: The size of the lattice cell impacted the slumping, larger cells slumped more. Demonstrates limits of the lattice scale. Could also be an interesting effect to harness.	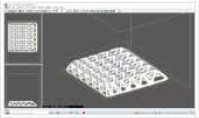	
Test 8.03 12.10.23		Glass 96% HPS 4% (w/w) Tap water	Shell 110% Core 130%	0.2 mm	Not fired	Two parts were printed together. Printability: There was some swiping on the second level print- the left wall kept shifting ofter. Moving the part further from the reservoir or rotating may help. Excavation: The binder appeared to seep between the two prints which made them difficult to separate. The bottom part broke entirely upon depowdering and was noticeably fragile. The top piece also had some breakages in the corners. Neither pieces were fired. The density of the lattice made the top piece difficult to excavate, causing breakages. Reusing the powder multiple times also may be effecting the quality.	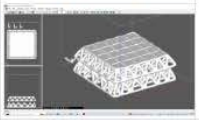	
Test 8.04 17.10.23		Glass 96% HPS 4% (w/w) Tap water	Shell 110% Core 130%	0.2 mm	780°C (no soak)	The bottom piece in the previous test was reprinted by itself and new powder was used. Printability: Some swiping occurred in early layers but self-corrected and was not evident in final excavated part. Excavation: Part was excavated without breakages but the overall form was fairly fragile due to the lack of additional square grid on the top. Firing: The scale of the lattice impacted the slumping, with larger cells slumping more. The lack of a top square grid also seemed to provide less structure.	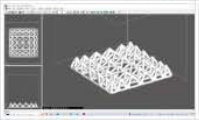	
Test 8.05 20.10.23		Glass 96% HPS 4% (w/w) Tap water	Shell 110% Core 130%	0.2 mm	780°C (no soak)	The top print from Test 8.03 was redone with a less dense lattice (5x5 cells) to allow for powder to be more easily removed. The top surface was also smoothed. Excavation: Part was excavated with no breakages. Printability: No swiping was observed. Firing: The weight of the top surface caused the lattice to largely collapse- although the outside struts maintained some shape. This could also be due to the larger cell size of the lattice. An interesting bumpy effect was created on the top surface by the lattices underneath it. The struts under the surface also appeared less fused.	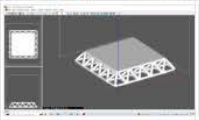	
Test 8.06 23.10.23		Glass 96% HPS 4% (w/w) Tap water	Shell 110% Core 130%	0.2 mm	Not fired	Design based on open half pyramids which decrease in height across the print - was interested to see how these would behave in kiln. However, the design was too fragile, the wall thickness of the base grid was too small and was missing radii- making it even less fragile. was created. Swiping: Lots of swiping, particularly on the horizontal edges. This eventually self corrected but likely impacted the strength of the base. Excavation: Base was too fragile and the piece crumbled apart on excavation. Piece was not fired.	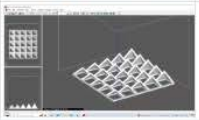	

Reflective log of Lattices 2.0 in Section 5.5.5.

3.2 Results from individual experiments for Lattices 2.0 (part 2).

Name	Images (pre firing)	Binder	Saturation	Layer height	Firing	Notes & reflections	Print setup	Images (post firing)
Test 8.07 27.10.23		Glass 96% HPS 4% (w/w) Tap water	Shell 110% Core 130%	0.2 mm	780°C (no soak)	The previous test was redesigned, using a square base that was not flat and rectangular but more like a pipe with radii. This also helps with the swiping as the early layers have less points of contact. Excavation: Part was excavated with no breakages. Printability: Some swiping on the horizontal edges but petered out and did not appear to impact final print. Firing: All open pyramids slumped down, no matter of their height. The height of the pyramid impacts the base footprint, with the overall square becoming uneven.	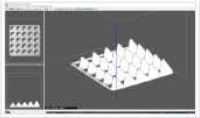	
Test 8.08 27.10.23		Glass 96% HPS 4% (w/w) Tap water	Shell 110% Core 130%	0.2 mm	780°C (no soak)	Similar design to previous test but with half closed bottom faces. Printability: It was printed once with minimal swiping, but due to a printer error it had to be redone. The second print had significantly more swiping which eventually subsided The reason for this is unclear; it may be due to layering over the first print. Excavation: Part was excavated with some small breakages, which were repaired using a slurry of the material. Firing: The pyramids slumped, with lower one showing slightly less slump. Varying height of the pyramids also slightly affected the footprint of the piece though not as much as in the previous test.	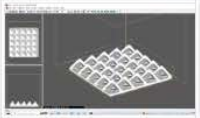	
Test 8.09 30.10.23		Glass 96% HPS 4% (w/w) Tap water	Shell 110% Core 130%	0.2 mm	780°C (no soak)	Both the bottom square grid and top square grid was removed from the design. Printability: Very minimal swiping on early layers which petered out with no noticeable impact on excavated part. Excavation: part was excavated with no breakages. The design and lack of additional square grid did make the piece quite fragile and had to be handled carefully. Firing: The lattice largely maintained its shape; however, the two outer horizontal edges were pushed outwards during firing, causing the peaks to angle outwards as those edges lacked sufficient anchor points.	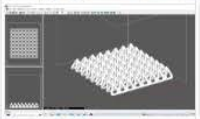	
Test 8.10 31.10.23		Glass 96% HPS 4% (w/w) Tap water	Shell 110% Core 130%	0.2 mm	780°C (no soak)	A new iteration of the pyramidal/lattice structures with more of a wave form. I was interested to see if these forms would hold their shape or create an interesting slumping effect. Printability: No swiping was observed. Excavation: Part cracked in half upon moving to dehydrator. More care should be taken. This was repaired using a slurry of the material, however, it is not seamless and can be seen in the fired part. Firing: Whilst slumping occurred, with the wave forms deflating, the form largely held its overall shape.	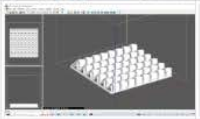	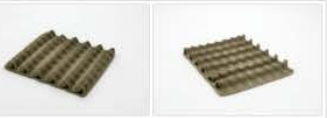
Test 8.11 2.11.23		Glass 96% HPS 4% (w/w) Tap water	Shell 110% Core 130%	0.2 mm	690°C (100 min soak)	Printability: Swiping in the early layers, particularly on the horizontal edges, This eventually petered out but likely impacted the quality of the base grid. Excavation: Part was excavated with no breakages. The quality of the print overall seemed less crisp- looked like the saturation was lower than it was supposed to be which may impact the fragility of the parts. Firing: Part was fired using a schedule which would create porosity. The waves slumped somewhat in the kiln but the points of connection provided support and created an interesting effect.	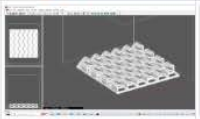	

Reflective log of Lattices 2.0 in Section 5.5.5.

3.3 Results from individual experiments with colouring.

Name	Images	Binder	Saturation	Layer height	Drying time	Changes made	Notes & reflections	Print setup	Images (post firing)
Test 9.01 19.10.22		Glass 96.5% Starch 3% iron oxide (dulux) 0.5% Tap water	ZP15E Core: 110% Shell: 130%	0.2mm	Approx. 15 hrs then dehydrated for approx. 3 hours at 45°C	Iron oxide was added to the material formulation to explore colour. Print parameters and method were determined by previous testing with vessels and lattice forms.	Excavation: All parts were excavated. Lattice shapes broke slightly at the base but this was due to a CAD error not print error. Printability: Print head showed stripes, suggesting that it needs replacement but this did not appear to impact excavated prints. Swiping on the first 3-4 layers, also not apparent in excavated prints. Firing: Dark chocolate color was achieved. Lattices mostly retained their shape. Some small vessels warped slightly at the top, while larger vessels warped significantly due to unsupported walls.		 
Test 9.02 22.11.22		Glass 96.9% Starch 2.9% iron oxide (walker) 0.2% Tap water	ZP15E Core: 110% Shell: 130%	0.2mm	Approx. 15 hrs then dehydrated for approx. 3 hours at 50°C	The lattice forms were scaled up and the CAD model adjusted to mitigate error. The Walker Ceramics grade of iron oxide was used at a lower percentage.	Excavation: All parts were excavated however the smallest piece broke signifcantly at the base and one of the big squares broke at one corner. Printability: significant swiping was observed, particularly on the smallest square in the top left. This aligns with observations from previous tests, where the majority of swiping occurs on the pieces to the left of the print bed. Firing: a milk chocolate brown colour was created in the kiln, the lattices without breakages appeared to mostly hold their shape.		 
Test 9.03 28.11.22		Glass 96.9% Starch 2.9% iron oxide (walker) 0.2% Tap water	ZP15E Core: 110% Shell: 130%	0.2mm	Approx. 60 hours then dehydrated at 50°C for approx. 3 hours	Organic lattice forms and lattices with surfaces were tested.	Excavation: Parts were initially excavated without being placed in the dehydrator, as they had been left in the print bed for two days and were expected to be dry. However, they were still damp during excavation and so were placed in the dehydrator. Corners of the top right piece broke during excavation and the bottom right part broke into pieces. Printability: negligible swiping was observed. Firing: a milk chocolate brown colour was created in the kiln, the lattices without breakages appeared to mostly hold their shape.	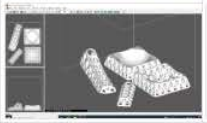	 
Test 9.04 1.12.22		Glass 94.6% Starch 5% iron oxide (walker) 0.4% Tap water	ZP15E Core: 100% Shell: 100%	0.2mm	Approx. 15 hours then dehydrated for approx. 2 hours at 50°C	Quantity of iron oxide and starch were increased for a deeper colour and green strength, respectively. It was believed that by increasing the starch content, saturation could also be reduced to speed up drying.	Excavation: Parts seemed less strong than others, lots of breakages, especially at the corners when excavating. The resolution also appeared to be lower, perhaps a result of lowering the shell saturation. Printability: Negligible swiping in the early layers. Firing: A red/brown clay colour was produced in the kiln. Surprisingly, the parts appeared to crumble apart in the kiln, but still fuse together. This has not been seen in any other tests but could be due to iron oxide being a flux.	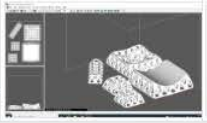	 

Reflective log of colouring experimentation in Section 5.6.

Appendix 4

Application Supplementary Information

4.1 Parametric Options from controlling the form section.

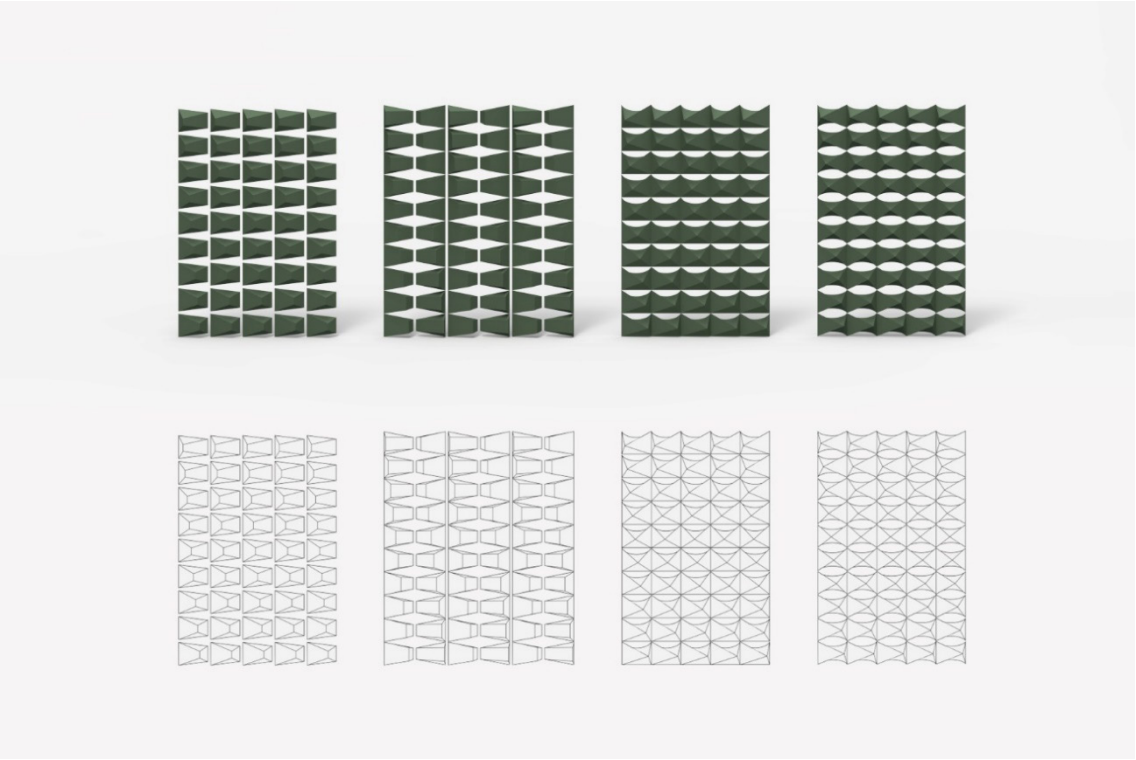

4.2 Production Parameters

The final set of production parameters and steps are outlined below.

1. Material Preparation: 4% pregelatinized HPS is combined with glass fines (particle size 75 - 150 um) in a commercial mixer for a minimum of 15 minutes. The feedstock is then placed in an oven for a minimum of 2 hours at 90°C to preheat the powder and remove any moisture. Tap water is used as the liquid activator.
2. Printing: Heated powder is placed in the feed reservoir of the BJT printer (ZCorp 310). The chosen CAD file is loaded into the ZPrint software. The printing parameters of 0.2mm layer height, core saturation of 110% and shell saturation of 130% when using propriety powder setting ZP15E are set.
3. Drying: Parts are left in print bed for a minimum of 2 hours. The whole print bed is then removed and placed in a dehydrator at approximately 75°C until fully dry. The required time in the bed and dehydrator varies on the geometry and scale of the print. Larger prints take longer to dry and it can be more difficult to remove the whole print bed from the printer- as such, larger parts may need to be left for longer to cure in the bed before placing in the dehydrator. Once dry parts are fully excavated with loose powder brushed off and reused.
4. Firing: Green parts are placed in a glass kiln on Thinfire shelf paper which stops parts sticking to the kiln. Two firing schedules have been developed; one for the production of waterproof parts, another for the production of parts with porosity of approximately 14.5%. These schedules are in Appendix 4.3 and 4.4.

4.3 Additional firing schedule used in early design development phase.

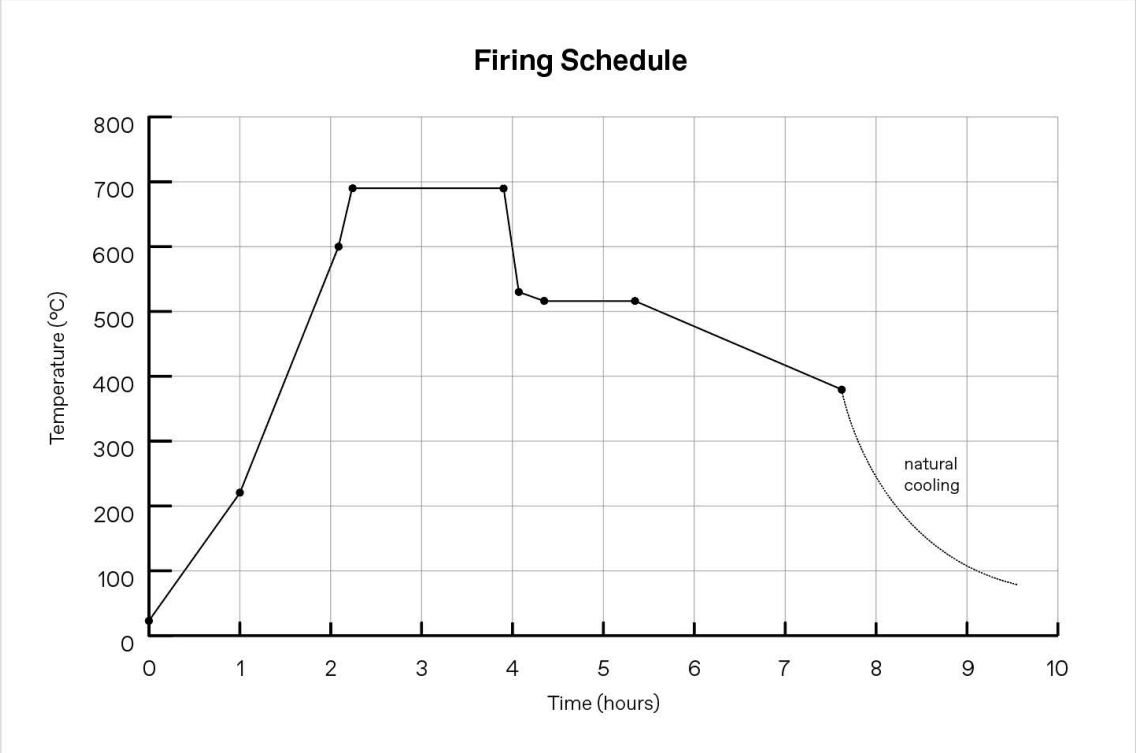

4.4 Firing Schedule for waterproof parts.

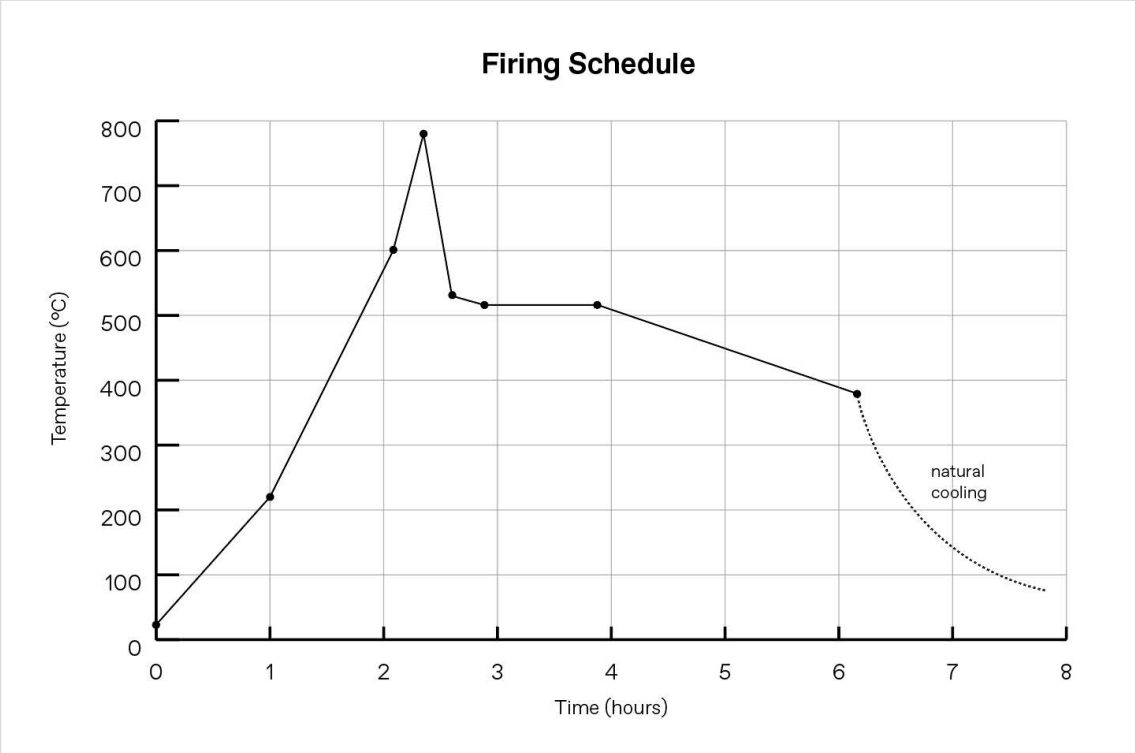

4.5 Firing Schedule for parts with an approximate porosity of 14.5%.

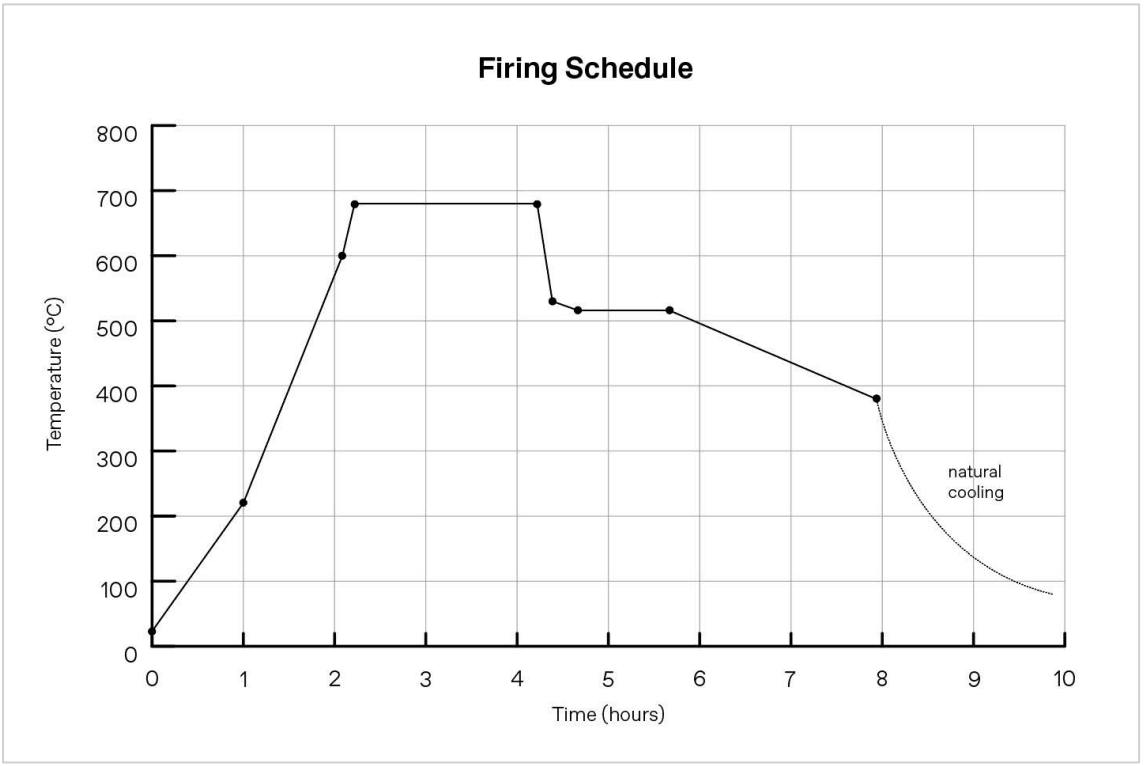

4.6 Results from individual experiments in Section 6.2.1 (early designs).

Name	Images (pre firing)	Binder	Saturation	Layer height	Firing schedule	Notes (geometries, printing, excavation, firing)	Print setup	Images (post firing)
Test 10.01 20.02.24		Glass 96% Starch 4% (w/w) Tap water	Shell: 120% Core: 140%	0.2	690°C (100 min soak)	Pyramidal design based on a water vessel supply system- where the parts would be stacked and hold water. A small amount of swiping on the first layer - could rotate the part slightly to mitigate this. Otherwise no significant issues in printing or excavating. Small printing defect- bumps on the outside surface, although these look almost intentional. During firing, part slumped significantly. The center axis largely held its shap but the unsupported walls collapsed, causing some cracking on the inside.		
Test 10.02 22.02.24		Glass 96% Starch 4% (w/w) Tap water	Shell: 120% Core: 140%	0.2	690°C (100 min soak)	Cylindrical design with high surface area. Parts stack and hold water. No swiping - likely because base is not flat, so only a small amount of liquid is deposited in early layers. Excavation took over 4 hours due to the design complexity. The powder was densely packed within each cell. This excavation time is too long so an alternative must be found for intricate designs- perhaps utilising compressed air. During firing the part slumped significantly, the surface texture created an interesting concertina effect.	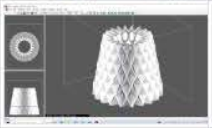	
Test 10.03 26.02.24		Glass 96% Starch 4% (w/w) Tap water	Shell: 120% Core: 140%	0.2	690°C (100 min soak)	Arc design, printed in two parts- main body and separate base, as removing powder from the internal cavity would be difficult. Parts were angled to prevent swiping. Some swiping in initial layers but was not noticeable on excavated main body. There were printing defects on the base piece, but the cause is unclear. Additionally, tolerances of the base part need to be adjusted. Part was fired using the talc method, mitigating slumping of unsupported surface. Some cracking inside and the edges warped.	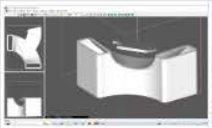	
Test 10.04 28.02.24		Glass 96% Starch 4% (w/w) Tap water	Shell: 120% Core: 140%	0.2	690°C (100 min soak)	Cube design, printed in two parts: the main body and base to ease excavation. Parts were angled to prevent swiping. No swiping was observed, but the base piece seems to have some swiping defects. Corners of the base broke during excavation; fillets should be used, and tolerances were inaccurate again. The separate base plate may not be the best option due to swiping and tolerance issues. During firing, the main body slumped significantly, separating in the middle. The unsupported surface is unsuitable.	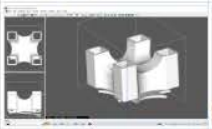	

Reflective log of experimentation with early designs of evaporative cooling components in Section 6.2.1.

4.7 Results from individual experiments in Section 6.2.2 (controlling the form).

Name	Images (pre firing)	Binder	Saturation	Layer height	Firing schedule	Notes (geometries, printing, excavation, firing)	Print setup	Images (post firing)
Test 11.01 10.5.24	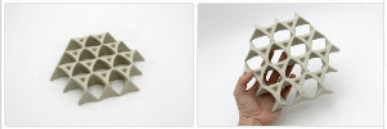	Glass 96% Starch 4% (w/w) Tap water	Shell: 120% Core: 140%	0.2	690°C (100 min soak)	The design consisted of joined upright and inverted pyramids. Corners at the edges of the part had inadequate contact points, leading to some breakages during excavation, likely worsened by some swiping in the early layers. During firing, the piece largely retained its shape, except at the edges where pyramids weren't connected. Another part was printed on top, but the small, enclosed geometries could not be excavated.	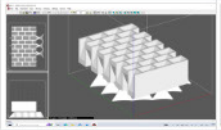	
Test 11.02 14.5.24		Glass 96% Starch 4% (w/w) Tap water	Shell: 120% Core: 140%	0.2	690°C (100 min soak)	Four irregular, curved pyramid shapes with a central rib to provide support. Some swiping on the early layers of the print could be seen in the lack of definition on the bottom edges. A small breakage occurred during excavation. During firing, the overall shape was held, and the central rib allowed for the peak to stay upright. However, the sides slumped slightly, becoming curved. May be visually overbearing in multiples.	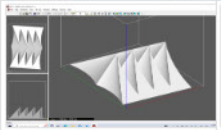	
Test 11.03 15.5.24		Glass 96% Starch 4% (w/w) Tap water	Shell: 120% Core: 140%	0.2	690°C (100 min soak)	Simplified design from previous test but with greater internal ribbing. Negative space was created between each component rather than leaving openings in the components themselves. Excavation proceeded smoothly; however, some swiping on the early layers of the print is evident, resulting in a lack of definition on the bottom edges. The ribs effectively supported the edges, but sagging occurred on the unsupported surfaces.	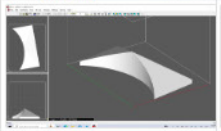	
Test 11.04 16.5.24	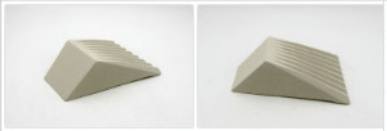	Glass 96% Starch 4% (w/w) Tap water	Shell: 120% Core: 140%	0.2	690°C (100 min soak)	Tapered trapezoidal shape with cross beam ribbing and a ridged surface. Part was excavated without issues; however some swiping on early layers can be seen in the lack of definition on the bottom edge. During firing, the ribs effectively supported the edges, but the long edge that ran down the middle of a face, caused a split in the top surface and sagging in the unsupported faces continued.	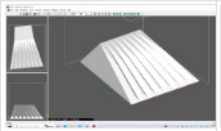	
Test 11.05 17.5.24	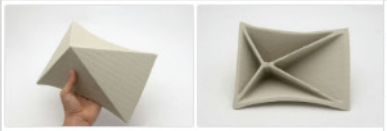	Glass 96% Starch 4% (w/w) Tap water	Shell: 120% Core: 140%	0.2	690°C (100 min soak)	Variation of design from Test 11.03 with simplified curved pyramid forms and internal ribbing. Part was excavated without issues, but the bottom edge should have a radius since the sharp edge does not print well. During firing, the ribs supported the edges, but they themselves slumped and warped, likely due to the increased height. The unsupported surfaces also sagged, resulting in cracking.	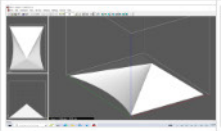	
Test 11.06 3.6.24	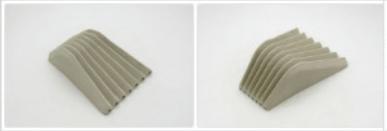	Glass 96% Starch 4% (w/w) Tap water	Shell: 120% Core: 140%	0.2	690°C (100 min soak)	Variation of design from Test 11.04 features internal slats for support. The part printed without major issues but the small gaps between ribs took considerable time and force to remove powder. This caused a crack in the side that was repaired with a glass/binder slurry. During firing, the slats themselves collapsed, likely due to the weight of the top surface and insufficient cross bracing. The ridged surface texture proved effective.	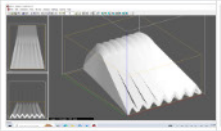	
Test 11.07 20.5.24		Glass 96% Starch 4% (w/w) Tap water	Shell: 120% Core: 140%	0.2	690°C (100 min soak)	Design based on the ridged surface texture, developing it into the overall form- incorporates a tapering effect with ridges widening as height increases. No major issues during printing or excavation; it was fast and easy. During firing, pyramidal peaks became self-supporting without collapsing or warping. However, cracking down the centre, likely caused by the change in direction of tapering elements pulling away from each other.	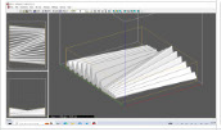	
Test 11.08 24.5.24		Glass 96% Starch 4% (w/w) Tap water	Shell: 120% Core: 140%	0.2	690°C (100 min soak)	Development of Test 11.07 but using curved ridges and rectangular overall form. The sharp edges of the ridges resulted in breakages during excavation- the tops broke off so were were lightly sanded down. Need to add a radius going forward. Fired part held its shape, although very slightly bowing and warping of outer edges. Height of the ridges could be increased as the part looks quite flat.	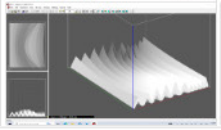	

Reflective log of controlling the form experimentation in Section 6.2.2.

4.8 Results from individual experiments with ridge design in Section 6.2.3 (part 1).

Name	Images (pre firing)	Binder	Saturation	Layer height	Firing schedule	Notes (geometries, printing, excavation, firing)	Print setup	Images (post firing)
Test 12.01 14.6.24		Glass 96% Starch 4% (w/w) Tap water	Shell: 120% Core: 140%	0.2	690°C (100 min soak)	Set of 3 tiles with 8 ridges, varying height from approx. 11-75mm. Two tiles were printed together and one separately. All printed without issues, but the combined pieces took longer to dry and were harder to separate without breaking. Minor breakages occurred during excavation; ridges need filleting, as sharp points were fragile and needed light sanding. During firing, top and bottom pieces slumped slightly but held their overall shape, while the middle piece warped significantly, resembling an open book.	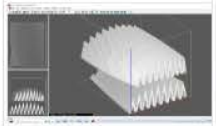	
Test 12.02 27.6.24		Glass 96% Starch 4% (w/w) Tap water	Shell: 120% Core: 140%	0.2	690°C (100 min soak)	Single tile, number of ridges was reduced to five, height tapered between approx 40-65mm. The ridges were slightly angled to encourage slumping in one direction. Some swiping during printing. Part broke down the centre upon excavation- stuck back together using slurry mix of the material. Possibly due to reusing the powder multiple times. During firing, the ridges all slumped and warped in the same direction- emulating rolling waves in the ocean. However, a greater degree of control is needed.	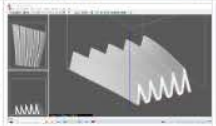	
Test 12.03 03.7.24		Glass 96% Starch 4% (w/w) Tap water	Shell: 120% Core: 140%	0.2	690°C (100 min soak)	Same design as Test 12.02 but without the angled ridges (just perpendicular). Powder was remixed. No issues during printing or excavation (possibly due to new powder). During firing, the part slumped significantly, four of the five ridges slumped in the same direction, whilst one slumped in both directions. Again, a beautiful ocean-like aesthetic, but need to have greater control over the slumping- reducing the height of the ridges will likely help.	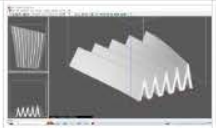	
Test 12.04 10.7.24		Glass 96% Starch 4% (w/w) Tap water	Shell: 120% Core: 140%	0.2	690°C (100 min soak)	Set of 3 tiles with 4 ridges, height varying approx. 20-65mm. Reducing ridges from 5 to 4 lowers the max base angle from about 80° in prototype 12.03 to about 73°. Parts printed individually without issues. During firing overall footprint was maintained , but slumping increased with ridge height. Ridges from 25mm-55mm best held their shape. However, 4 ridges were less visually appealing than 5. The adjoining tile edges also pulled inwards during firing, creating a gap between the ridges.	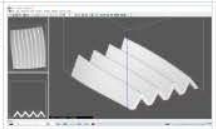	
Test 12.05 16.7.24		Glass 96% Starch 4% (w/w) Tap water	Shell: 120% Core: 140%	0.2	690°C (100 min soak)	To prevent tile edges pulling inward during firing, the middle piece from 12.05 was reprinted with chamfered edges to counteract this shrinkage. The shrinkage angle of the middle tile was approximately 5°, so the CAD file was adjusted to include a 10° chamfer. Part was printed and excavated without issues. During firing, the tile edges shrank inward, forming near-perpendicular edges. Some slight variation across the ridges exists, but this method was largely successful.	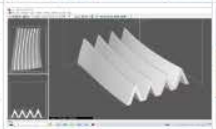	
Test 12.06 16.7.24		Glass 96% Starch 4% (w/w) Tap water	Shell: 120% Core: 140%	0.2	Not fired	Ribs were incorporated within the ridges to achieve a cactus-like appearance, which allowed the unsupported ridge walls to sag slightly. This part was printed twice but kept breaking in excavation due to the difficulty of removing the densely packed powder from the gaps between the ribs. Additionally, the wall thickness between the ridges was inadequate, leading to consistent breakage in this area. Although there is room to investigate this further, the design was abandoned.	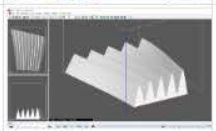	
Test 12.07 23.7.24		Glass 96% Starch 4% (w/w) Tap water	Shell: 120% Core: 140%	0.2	690°C (100 min soak)	Set of 3 tiles with 5 ridges, varying from 20-40mm. Height reduction from 12.04 accounted for the fifth ridge to keep a similar base angle. 10° chamfer was added to each edge and a wavy surface texture. Parts were printed without issues or breakages. During firing, minimal slumping occurred and parts lined up well. Slight bowing on the outer edges, but not that noticeable. Chamfered edge was too angled; the angle seems to depend on the ridge height and requires further investigation.	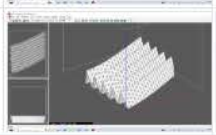	

Reflective log of experimentation with ridge design in Section 6.2.3.

4.9 Results from individual experiments with ridge design in Section 6.2.3 (part 2).

Name	Images (pre firing)	Binder	Saturation	Layer height	Firing schedule	Notes (geometries, printing, excavation, firing)	Print setup	Images (post firing)
Test 12.08 29.7.24		Glass 96% Starch 4% (w/w) Tap water	Shell: 120% Core: 140%	0.2	690°C (100 min soak)	Set of 3 tiles with 5 ridges that faded completely on the middle piece, allowing water to trickle down. Ends capped. Parts were printed separately with vertical ridges, resulting in excessive swiping on all pieces. Shell saturation was reduced to 100% to mitigate this, but was ineffective. Two of the three pieces broke. A raft was tested on the middle piece but had no noticeable effect on swiping, and this piece was too thin. One part was fired with minimal slumping, but swiping resulted in an uneven base.	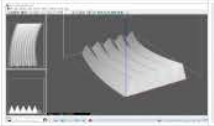	
Test 12.09 31.7.24		Glass 96% Starch 4% (w/w) Tap water	Shell: 120% Core: 140%	0.2	690°C (100 min soak)	Developed design from 12.08; added stilts for thickness and fixing holes. Adjusted edge angles based on ridge height. Parts printed separately with horizontal ridges. Swiping occurred (due to powder reuse?) but had minimal impact on final parts. Minimal slumping during firing; stilts did not affect it. Chamfer angles yielded varied results: 4 of 6 edges shrunk nearly perpendicular, while 2 shrunk inward. No correlation between ridge height and shrinkage noted. Fixing holes partially collapsed. Uncertain if ridge fa...	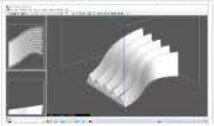	
Test 12.10 6.8.24		Glass 96% Starch 4% (w/w) Tap water	Shell: 120% Core: 140%	0.2	690°C (100 min soak)	Mounting system adjusted to use a ledge rather than a hole and remove the capped ends. Swiping occurred during printing but had minimal impact on the excavated part. During firing, part largely maintained its shape however there was some bowing on the outside curved edge. The capped ends seem to have provided some stability in other tests and may help with this bowing. The ledge worked well as a fixing point, allowing for some adjustability.	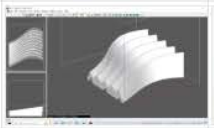	
Test 12.11 9.8.24		Glass 96% Starch 4% (w/w) Tap water	Shell: 120% Core: 140%	0.2	690°C (100 min soak)	Ends were capped again to provide stability and ledges were reduced in size. Part was printed and excavated with no major issues. Was a little difficult to excavate powder from the small gap between the ridge and ledge. During firing, part largely maintained its shape, some bowing on outside curved ridge, but not that noticeable. Fixing ledge was found to be too shallow -needs to be at least 12mm in width.	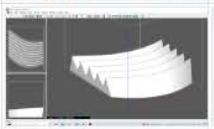	
Test 12.12 13.8.24		Glass 96% Starch 4% (w/w) Tap water	Shell: 120% Core: 140%	0.2	690°C (100 min soak)	Adding vents for air flow- 6mm flat section added between each ridge to allow for slots to be incorporated into the design. Some swiping occurred during printing but this did not impact the final part which was excvated with no issues. During firing, minimal slumping occurred. Rridges all held their shape, even the narrow, tall ones. However, the aesthetic of the slotted vents does not work that well with the more fluid, organic nature of the overall ridge design. Perhaps the slots could vary in length.	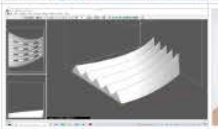	
Test 12.13 14.8.24		Glass 96% Starch 4% (w/w) Tap water	Shell: 100% Core: 140%	0.2	690°C (100 min soak)	More organic airvent design, gradually fading out. A 20mm strip at each end was left for fixings. Two tiles were printed; one broke during excavation due to fragility but was successfully reprinted. Shell saturation was reduced to mitigate swiping on early layers. During firing, the overall shape was maintained, but the vents affected shrinkage, particularly on adjacent edges, which began to shrink concavely, impacting alignment. The curvature of the outside edges on both parts was slightly warped.	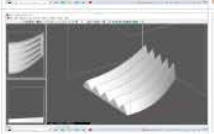	
Test 12.14 3.9.24		Glass 96% Starch 4% (w/w) Tap water	Shell: 120% Core: 140%	0.2	680°C (120 min soak)	Fixing system adjusted- ledge added to every ridge (giving adjustability during assembly) and depth increased. Experimentation with heating the powder before printing was conducted pre this experiment. This allowed for the part length to be increased and printed with the ridges oriented vertically. A label was added to test the fidelity of the print. No swiping occurred, and the part was excavated with no issues. During firing, ridges maintained their shape and the ledges and label worked well.	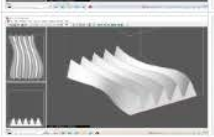	

Reflective log of experimentation with ridge design in Section 6.2.3.